UNIVERSITY OF CALIFORNIA, SAN DIEGO

Bi-functional molecular catalysts for CO_2 reduction

A dissertation submitted in partial satisfaction of the
requirements for the degree of Doctor of Philosophy

in

Chemistry

by

Alyssia Maria Lilio

Committee in charge:

Professor Clifford P. Kubiak, Chair
Professor Ralph F. Keeling
Professor Judy E. Kim
Professor Arnold L. Rheingold
Professor Michael J. Sailor

2015

The dissertation of Alyssia Maria Lilio is approved, and it is acceptable in quality and form for publication on microfilm and electronically:

_____

_____

_____

_____

_____
Chair

University of California, San Diego

2015

DEDICATION

This thesis is dedicated to my family,

to Woogi Tucker,

and Frankie and GanJah

TABLE OF CONTENTS

LIST OF FIGURES

LIST OF SCHEMES

LIST OF TABLES

ACKNOWLEDGEMENTS

I am very grateful for the constant support of my family. I would especially like to thank my parents, Loua and Sharon, for their constant love, support, and trust in me. They have always been there for me, allowing me to choose my own path and make my own decisions, but providing support when I needed it. Some people do not have the reassurance of knowing that if they make mistakes, they will have their parents behind them to help them out in every way that they can. That reassurance has given me the courage to try things that I never thought I could. My sister, Jessica, has also helped me through life in every way that she could. I really appreciate her for this and for her strength and honesty. My younger siblings, Joshua, Jacob, and Alexandra have always been there when I needed to take a break from life. They are such funny people and their companionship has helped me to gain perspective on what is most important to me in life. Regardless of what I choose to do in life, I know that they are proud of me and that makes me feel a lot better about everything else.

I also have to thank the rest of my family, Stanley Tucker, Frankie, and Jah. Stanley has given me so much support and love over the past few years. He has been there to reassure me that I am a good scientist and a good person when I needed that reassurance the most. When things get rough, he always has some random sports metaphor that I don't quite connect with, but I appreciate him anyways for listening and trying in the best way he knows how to calm me down and lift me up. I need to recognize Frankie and Jah for helping me to maintain my sanity. Besides them giving me unconditional love, our long walks together every day helped to calm me and reminded me to try to be present in the moment and appreciate the things that I have. I am excited to move onto the next part of my life with these guys.

The thing I value most about my time in graduate school is that it has allowed me to meet and work with some of the smartest, most interesting, and most hard working people I

have ever met. I so value the time I have spent getting to know the members of the Kubiak lab. I know I would have given up a long time ago if I did not have all these amazing people around me and I will miss them all. In their own way, each of them inspired me to try to be a better scientist and also just to try to be a better person. I will really miss Michael Doud. He is a talented synthetic chemist and he is always warm and positive. His kindness and positivity had a huge effect on all of us and made me think more about the kind of effect I want to have on my coworkers with my attitude. I love the way Gabe had fun with everything he did. He made sure that above everything, he was entertained and he kept us entertained and reminded me that work could be fun. I really appreciate Jane's strength and kindness. I am very thankful to have been able to work with her and I hope someday, I will learn to be as assertive and direct as she is. I respect Candace so much as a scientist and as a human. She is thoughtful in everything she does and she has always provided a shoulder to cry on when I needed it. Her encouragement through kind words and nice emails with cute animal pictures have meant so much to me. Alissa has been a strong support for me also. I appreciated our gchat meetings where we talked about our frustrations with lab, science, and life. Her kindness and optimism really helped me through these past few months. Tram is a very generous person and am and grateful for the many times she provided me with a place to stay, lab snacks, and kind words. I will miss Mark L for his sense of humor for his willingness to try to entertain me when I was feeling down. He helped me to laugh when I really needed to. I admire Jesse for his ability to do great science, but still find time to enjoy life. I appreciate Mark R for his passion for chemistry. I hope I will be able to find that kind of passion in something. His passion and his helpfulness is evident in the way he constantly tries to offer thoughtful suggestions and provide others with useful feedback. Steven is one hardest workers and one of the sweetest people I have ever met, and I appreciate him for the kindness he showed me. Daniel is a very rigorous scientist and a very sweet person. He is extremely smart, but also extremely humble and I am lucky to have been able to work

with him in Pasadena. I will also miss all the younger Kubiak group members. Since I have been working in Pasadena, I have not been able to get to know them as well as I would have liked, but every time I came down to San Diego they were welcoming and provided me with some good laughs.

I cannot forget to thank Cliff Kubiak. Cliff has a very hands off leadership style and he gives you the freedom to find your own successes and make your own mistakes. At times, this was a very frustrating way to do research and I really struggled to find my way, I but appreciate how encouraging and supportive Cliff has been through my flailing. If he ever had any doubts in my abilities to get things done, he never let me know, and the emotional support he provided was very much appreciated. While I cannot say that I accomplished all that I thought I would during my time here, I can see my growth and I know that much of it came from Cliff allowing me to figure things out myself. He is extremely generous, as shown by his willingness to encourage and support us in going to conferences and meetings, as well as his funding of many Kubiak lab get-togethers that have helped to foster the lab culture that everyone loves so much about the Kubiak group.

Lastly, I need to recognize all my friends outside of graduate school. Jennifer, Phi, Cseal, Amy, Ashley, Charbel, Johnathan, and Phillip, have all helped me in some way over the last 10 to 15 years and I am so glad that our friendships have remained intact for all this time. I love all of them dearly and am lucky to have them in my life.

Chapter 2: Much of the material in this chapter comes from a manuscript entitled "A Series of Dinuclear Copper Complexes Bridged by Phosphanylbipyridine Ligands: Synthesis, Structural Characterization and Electrochemistry," by Alyssia M. Lilio, Kyle A. Grice, and Clifford P. Kubiak. The dissertation author is the primary author of this manuscript.

Chapter 3: Much of the material in this chapter comes from a manuscript entitled "Incorporation of pendant bases into Rh(diphosphine)$_2$ complexes: Synthesis, thermodynamic studies, and catalytic CO_2 hydrogenation activity of $[Rh(P_2N_2)_2]^+$ complexes," by Alyssia M. Lilio, Mark H. Reineke, Curtis E. Moore, Arnold L Rheingold, Michael K. Takase, and Clifford P. Kubiak. The dissertation author is the primary author of this manuscript.

VITA

2008	Bachelor of Science, University of California, Irvine
2011	Master of Science, University of California, San Diego
2015	Doctor of Philosophy, University of California, San Diego

PUBLICATIONS

Lilio, A.M., Reineke, M.H., Moore, C.E., Rheingold, A.L., Takase, M.K., Kubiak, C.P. "Incorporation of Pendant Bases into Rh(diphosphine)$_2$ Complexes: Synthesis, Thermodynamic Studies, And Catalytic CO_2 Hydrogenation Activity of $[Rh(P_2N_2)_2]^+$ Complexes." *J. Am. Chem. Soc.*, **2015**, *137 (25)* 8251-8260

Lilio, A.M., Grice, K.A., Kubiak, C.P. "Series of Dinuclear Copper Complexes Bridged by Phosphanylbipyridine Ligands: Synthesis, Structural Characterization and Electrochemistry." *Eur J. Inorg. Chem.*, **2013**, *22-23*, 4016-4023.

Doud, M.D., Grice, K.A., **Lilio, A.M.**, Seu, C.S., Kubiak, C.P. "A Versatile Synthesis of $P^R{}_2N^{R'}{}_2$ Ligands for Molecular Electrocatalysts with Pendant Bases in the Second Coordination Sphere." *Organometallics*, **2012**, *31* (3), 779-782.

Roy, S.A., Blane, T.M., **Lilio, A.M.**, Kubiak, C.P. "Non-innocent ligand reservoirs for reducing or oxidizing equivalents in carbonylrhenium(I) complexes: 1,1'-bis(diphenylphosphino)ferrocene (dppf) and bis-triazinyl-pyridine (BTP)." *Inorg. Chimica Acta*, **2011**, *374*, 134-139.

ABSTRACT OF THE DISSERTATION

Bi-functional molecular catalysts for CO_2 reduction

by

Alyssia Maria Lilio

Doctor of Philosophy in Chemistry

University of California, San Diego, 2015

Professor Clifford P. Kubiak, Chair

This dissertation details efforts in designing and tuning catalysts that have the ability to engage CO_2 through a metal center and functional groups in the second coordination sphere. We attempted to improve a dinuclear copper complex that has the ability to engage CO_2 through two metal centers and was previously reported as a CO_2 reduction catalysts. Electron donating substitutions were made on the ligands in attempts to improve rates for the electrocatalytic reduction of CO_2. These modifications led to changes in the reduction potentials and the structures of the complexes, but did not produce significant improvements in turnover frequencies or overpotentials for CO_2 reduction.

We attempted to improve rhodium disphosphine catalysts for the conversion of CO_2 to $HCOO^-$ by introducing ligands with proton relays. Several $[Rh(P_2N_2)_2]^+$ complexes were

synthesized. They were structurally characterized as square planar with slight tetrahedral distortions and exhibited a reversible $2e^-$ Rh(I/–I) redox couple in voltammetric studies. We synthesized the $HRh(P_2N_2)_2$ complexes and structurally characterized them as having distorted trigonal bipyramidal geometry. The hydricities of several of the $HRh(P_2N_2)_2$ complexes were measured using equilibration experiments monitored by ^{31}P NMR. The $HRh(P_2N_2)_2$ complexes are among the most hydridic complexes the 16 e^- M(diphosphine)$_2$ class.

We compared the activity of the $[Rh(P_2N_2)_2]^+$ complexes for catalytic CO_2 hydrogenation to formate to a $[Rh(diphosphine)_2]^+$ complex of a similar hydricity that lacked pendant amines. We found that, despite the strong reducing power of the $HRh(P_2N_2)_2$ complexes, the non-pendant-amine-containing Rh complex was the best catalyst for CO_2 hydrogenation. We also tested these complexes for their electrochemical CO_2 reduction activity. While these complexes are energetic enough to react with CO_2 when reduced, they are unstable under the high potentials necessary for their reduction.

We tested Ru pincer complexes that are known to hydrogenate esters via a mechanism that involves co-operative metal-ligand interactions for their ability to reduce CO_2 and methylformate electrochemically. We also synthesized and tested an Fe analogue of these complexes for electrochemical reactivity. We found that these complexes are promising candidates for further study as CO_2 reduction catalysts.

Chapter 1

The importance of CO_2 reduction, its challenges, and lessons from nature

1.1 CO_2 as an abundant C_1 feedstock for fuels and other industrially valuable chemicals

The rise in global energy consumption is one of the biggest problems we currently face. As populations continue to grow and as economies continue to improve, the world will increasingly demand more energy and the fossil fuels that serve as our main source of energy now are finite. When fossil fuels start to run out, what we will still have in abundance is oxygen, carbon dioxide, and nitrogen, so it is critical that we continue to study the fundamental chemistry of these molecules so we can learn how to effectively utilize them to fit our needs, including helping us meet our energy demands.

Another equally concerning problem is the rising concentration of CO_2 in the atmosphere. The concentration of CO_2 in the atmosphere had remained between 210 to 300

ppm for the majority of the past 650,000 years, but has been increasing rapidly since industrial revolution because of anthropogenic CO_2 emissions.[1] Even through stringent controls of our emissions by increasing the efficiency of energy production and consumption, the CO_2 concentration is not expected to stabilize until it reaches the range of 550- to 650-ppm, with some higher estimates projected at > 750 ppm.[1] Climate models predict a variety of different responses to CO_2 levels at 550 ppm or higher. In some projections these changes are moderate, but others predict very serious environmental effects.[2] Even if our supplies of fossil fuels were not limited, the continued burning of fossil fuels at the increasing rates necessary to meet the worlds growing demands will increase the concentration of CO_2 in the atmosphere to levels significantly higher than those of the past 650,000 years, and at best we can say we do not yet fully understand how this will affect our environment and our way of life. Increasing reliance on CO_2-nuetral fuel sources is necessary to both secure our energy future and limit negative impacts on the environment. The renewable energy that we currently rely on, solar and wind, suffer from the fact that they are location dependent, intermittent, and are not readily able to be stored.

Carbon dioxide is the perfect C_1 feedstock for renewable energy. It is an abundant and growing reservoir for carbon and the products of its reduction that could be used as carbon based liquid fuels are denser in energy than hydrogen, another potential fuel. The production of fuels from CO_2 would provide a carbon neutral fuel source by taking the CO_2 from our atmosphere and recycling it into fuels that already fit well into our existing energy infrastructure. One route to carbon based fuels is to first convert CO_2 to CO and H_2O. The CO can then be used along with H_2 in well established, but expensive, Ficsher-Tröpsch processes to make hydrocarbons, including diesel and gasoline.[3] Another is to convert CO_2 to methanol, which can be used as a combustion fuel itself and can also be used in direct methanol fuel cells.[4,5] Formic acid, another product of CO_2 reduction, can also be used in fuel cells, and it has

industrial value, as it is used in the leather and tanning industries and as an animal feed additive.[6] Another potential fuel product of CO_2 reduction is methane, which is a main component in natural gas. Methane, methanol, and formic acid can also be used industrially as H_2 sources. Renewable energy sources, like wind and solar, could potentially be used to power these transformations, which would allow us to store that energy in chemical bonds for later use.

1.2 Overview of CO_2 reduction chemistry

Carbon dioxide is a linear molecule consisting of two oxygens each doubly bonded to a carbon center. It is overall, a non-polar molecule, but contains polar bonds between the carbon and oxygens due to their difference in electronegativity, which leaves a partial positive charge on the carbon and partial negative charge on the oxygens. This difference in polarity makes the carbon center susceptible to nucleophilic attack and the oxygen atoms susceptible to electrophilic attack.

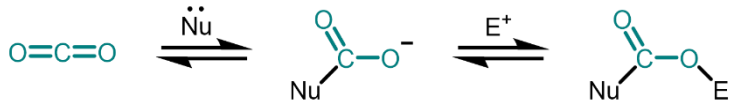

Scheme 1-1. Equation showing how CO_2 is engaged by nucleophiles and electrophiles.

CO_2 is the ultimate product of combustion and respiration, so it is very thermodynamically and kinetically stable. Its thermodynamic stability can be seen in the negative reduction potentials required to make the various CO_2 reduction products (**Table 1-1**).[7] The one electron reduction of CO_2 to its radical anion is particularly energetically costly due to the difficulty associated with taking this stable, linear molecule with a very high lying CO* LUMO and putting electrons in that orbital to bend the molecule (this energy is commonly referred to as *reorganizational energy*). The process becomes increasingly more

thermodynamically favorable when multiple protons and electrons are coupled in CO_2 reduction. The availability of protons helps to avoid high energy intermediates by neutralizing highly charged transition states and also helps to form the bonds necessary to make products. Though the more highly reduced products are increasingly more thermodynamically accessible, as one could imagine, it is challenging to manage all of these proton and electron equivalents and bring them together in the proper orientations to make more highly reduced products, which makes the production of these products kinetically costly. It is also challenging to guide multiple protons and electrons towards the production of one particular product (product selectivity) and when protons and electron are involved, it is difficult to avoid the reduction of protons, as it is thermodynamically more favorable to form H_2 than all the CO_2 reduction products. Through the use of catalysts, we can ideally overcome some of the kinetic challenges and selectivity challenges in CO_2 reduction. Unfortunately, we currently lack catalysts that are efficient enough to make the wide scale utilization of CO_2 as a raw material or fuel feedstock feasible, so there is great interest in learning how we can make better catalysts for CO_2 reduction.

Table 1-1. Reduction potentials for electrochemical half-reactions of CO_2 at pH = 7 vs. NHE in aqueous solution. Reproduced from Benson *et al*.[7]

CO_2		$+ e^- \rightarrow$	$CO_2^{\bullet -}$	$E° = -1.90$ V
CO_2	$+ 2H+$	$+ 2e^- \rightarrow$	$CO + H_2O$	$E° = -0.53$ V
CO_2	$+ 2H^+$	$+ 2e^- \rightarrow$	$HCOOH$	$E° = -0.61$ V
CO_2	$+ 4H^+$	$+ 4e^- \rightarrow$	$HCHO + H_2O$	$E° = -0.48$ V
CO_2	$+ 6H^+$	$+ 6e^- \rightarrow$	$CH_3OH + H_2O$	$E° = -0.38$ V
CO_2	$+ 8H^+$	$+ 8e^- \rightarrow$	$CH_4 + 2\ H_2O$	$E° = -0.24$ V
	H^+	$+ 2e^- \rightarrow$	H_2	$E° = 0$ V

Catalysts for CO_2 reduction can be split into 2 categories, homogeneous and heterogenous catalysts, but for this work, only homogeneous systems will be discussed. The

main argument for using homogeneous catalysts over heterogeneous is that we are able to better control and tune the active sites of homogeneous catalysts to guide them towards the formation of one desired product. These groups can both be further split into electrocatalysts and thermal hydrogenation catalysts. Homogeneous thermal hydrogenation catalysts and electrochemical CO_2 reduction catalysts both help to provide kinetically favorable pathways for bond-making and bond-breaking to speed up a normally slow chemical reaction. Both types of catalysts usually contain organometallic active sites. A major difference between the two is the source of the reducing equivalents.

In homogeneous thermal hydrogenation catalysis, the nucleophile that attacks the electrophilic carbon comes from an H_2 molecule, which is split by the catalysts into a hydride, forming a metal-hydride complex, and a proton. If the metal hydride species is sufficiently reducing, CO_2 can insert into the M–H bond to make a formate intermediate, which could potentially be further reduced through subsequent hydride transfers. The most common product for the hydrogenation of CO_2 with homogeneous catalysts is formate/formic acid, although there has recently a been report of a cascade catalysis approach for the hydrogenation of CO_2 to methanol using a panel of catalysts; one for the reduction of CO_2 to formate, one for the esterification of formate to methyl formate, and one for the hydrogenation of methyl formate to methanol.[8] There has also been a recent report of the hydrogenation of CO_2 to methanol with a single catalyst.[9] For comprehensive reviews of homogeneous CO_2 hydrogenation, interested readers should consult these recent resources.[10,11] A downside of thermal hydrogenations is that they often require elevated temperatures and pressures. Evaluation of the activity of these catalysts involves comparing their *turnover numbers* (TON), *turnover frequencies* (TOF), and the temperatures and pressures that they operate under.

Electrocatalytic CO_2 reduction is slightly more complicated. In homogeneous electrocatalytic CO_2 reduction, the nucleophile that attacks the carbon center is produced by

electrons coming from an electrode. The majority of known homogeneous CO_2 reduction electrocatalysts produce the $2e^-$ reduction products, CO and formate, with the formation of CO being much more common.[7] It seems for most catalysts, the main factor determining whether CO or formate is produced depends on if the reduced catalyst initially interacts with CO_2 or a proton. CO is produced when the reduced catalysts initially binds CO_2 to make a metallocarboxylate which is protonated at the O^- to produce CO and OH^-. The production of formate usually occurs when the reduced catalyst initially reacts with a proton to make a metal hydride. CO_2 can then insert into the metal hydride to produce a bound $HCOO^-$, similar to CO_2 hydrogenation mechanisms. Electrocatalytic CO_2 reduction is very attractive because it could ideally provide a means to convert CO_2 to fuels using solar energy, either directly with a photocathode, or by converting solar energy into electricity and then using that to drive catalysis. The next section provides a brief explanation of how electrocatalysts work and how their performance is evaluated. For comprehensive reviews of electrocatalytic CO_2 reduction, readers should consult these recent resources.[7,12-14]

1.3 Tutorial on electrocatalysis

The most common electrochemical experiments done by an organometallic chemist, and the type of experiments that will be discussed in this dissertation, are controlled potential experiments. The basics of the experiments involve driving an electrochemical half reaction by applying a potential at an electrode. The reaction being driven corresponds to the reduction or oxidation of a species in solution in which electrons are consumed or released by the species of interest, causing a change in its overall formal oxidation state. The application of this potential in the presence of a redox active species (the electrocatalyst) causes the flow of current that reflects the rate at which electrons are being transferred between the electrode and the electroactive species.

1.3.1 What is happening in homogeneous electrocatalysis?

The electro-reduction of CO_2 to any one of its reduction products requires the input of energy, as shown by the thermodynamic potentials given in **Table 1-1**. Usually, the energy required to drive these reactions with an inert electrode is considerably more than the thermodynamic potentials of the reaction because of the extra energy required to overcome the activation barriers involved in breaking and forming bonds in product formation. An electrocatalyst helps this process by providing a pathway for fast electron transfer to the substrate and a low energy pathway for the bond-making and -breaking processes involved in the chemical reaction of interest, helping to accelerate a reaction that would otherwise happen slowly. Electrocatalysts differ from thermal catalysts in that they not only directly interact with the substrate, but also acts as an electron conduit between the electrode and the substrate. They provide a means to take electrical energy and convert it to chemical energy.

Experimentally, the easiest way to identify electrocatalytic activity is from the steady-state limiting current in cyclic voltammetry (CV). In a standard experiment, the voltage dependent current response of a redox active catalyst is compared in the absence and presence of the substrate. In the absence of substrate the CV should show a redox couple corresponding to the reduction (or oxidation) of the catalyst, and in the presence of substrate a new irreversible reduction (or oxidation) event with a current that exceeds that of the original CV at given potential should be observed (**Figure 1-1**). The increase in current, referred to as *catalytic current*, occurs because of the increased number of electrons that are being transferred through the catalysts to or from the substrate as the catalyst goes through multiple catalytic cycles. The amplitude of the catalytic current at a given potential reflects the rate that reaction is being catalyzed at that potential.

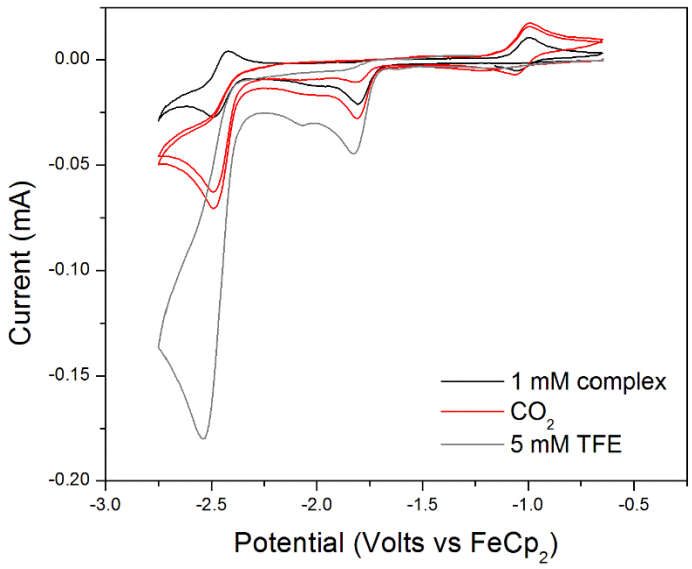

Figure 1-1. CV showing the electrochemical response of an Fe pincer complex discussed in chapter 5 under and inert atmosphere (black) and in the presence of CO_2 (red). The current further increases as a proton source is added (gray).

1.3.2 What makes a good electrocatalyst and how do we evaluate its activity?

The merits of a good electrocatalyst are that they are energy efficient, robust, and selective. The energy efficiency of an electrocatalyst is dependent on a term called *overpotential*, which is the potential beyond the thermodynamic potential for a reaction that needs to be applied to drive that reaction at a certain rate. This can be visualized on a reaction coordinate as the difference between $\Delta G^{\ddagger}$ and E°, and is essentially a measure of the height of the activation barrier for the reaction (**Figure 1-2**). In an ideal catalysts, this difference would be minimized as much as possible. The energy efficiency of a catalysts is also often discussed in terms of *turnover frequencies* for the catalytic reaction (TOFs), which can be estimated in the CV from the catalytic current. Overpotentials and TOFs are related, as the rate of an electrocatalytic reaction increases as the applied potential increases. An energy efficient electrocatalyst would show high TOFs with the lowest possible overpotential.

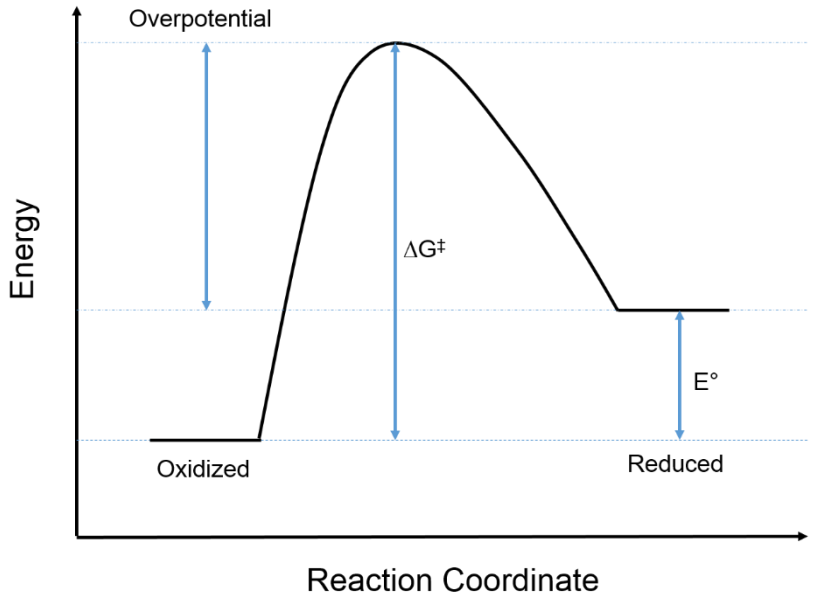

Figure 1-2. Reaction coordinate diagram showing the relationship between the standard reduction potential (E°), activation energy ($\Delta G^{\ddagger}$) and overpotential.

The selectivity of a catalyst is usually reported in terms of *faradaic efficiency*, which is a percentage showing how many electrons consumed go to the formation of particular product. Experimentally, this value is obtained by running an electrolysis experiment at the optimal potential for catalysis and comparing the electrons consumed throughout the experiment with the moles of product produced. Gas chromatography is usually used for the quantification of gaseous products, while non-volatile products are usually quantified by NMR or liquid chromatography.

The robustness of a catalyst can be discussed in terms of *turnover numbers* (TON). This value is usually obtained by running an electrolysis experiment with product quantification and determining how many times the catalysts turns over before it is deactivated. A robust catalysts would show essentially stable current and maintain the rate of product formation with the passage of time, indicating that the catalysts does not rapidly decompose or become deactivated.

1.4 A few of nature's reduction catalysts and what we have learned from them

Of all the synthetic systems reported for CO_2 reduction, none are as efficient and as selective and those found in nature. Enzymes that catalyze the reversible reduction of CO_2 to CO (CO dehydrogenases, CODHs) and the reversible reduction of CO_2 to formate (formate dehydrogenases, FDHs) have been identified and their active sites have been structurally characterized.[15-17] Similar to synthetic homogeneous catalysts, most of these enzymes contain organometallic active sites. The information obtained from these structural studies allows us to learn how they control the binding of CO_2 and the transfer of protons and electrons at an organometallic active site during their oxidation/reduction cycles and try to implement these design principles to develop better synthetic catalysts. In discussing these enzymes' active sites, the terms *first*, *second*, and *outer coordination sphere* are often used. The first coordination sphere refers to the metal center and the ligands bound directly to it and the second coordination sphere refers to functional groups on the ligand that are close enough to interact with a substrate bound to the metal, but only weakly interact or do not interact at all with the metal center. The outer coordination sphere refers to all the other parts of the enzyme. Nature has evolved such efficient and selective catalysts through billions of years of tuning all three coordination spheres to optimize them for the desired process. In this section, some of the important attributes of the first and second coordination sphere and how they enable efficient catalysis are discussed.

1.4.1 CO dehydrogenases

There are two types of CO dehydrogenases (CODHs), enzymes that catalyze the reduction of CO_2 to CO. The first type are oxygen sensitive enzymes derived from anaerobic

bacteria with [FeNi] active sites. These enzymes exhibit turnover frequencies for CO oxidation as high as 40,000 s^{-1} and up to 45 s^{-1} for CO_2 reduction and they operate near the thermodynamic potential for this conversion.[15,18] The second type are the air stable [MoCu] containing enzymes derived from aerobic bacteria. These enzymes exhibit turnover frequencies up to 100 s^{-1} for CO oxidation.[16,19] Some key findings about the structures of the active sites and the mechanisms followed by these two are discussed below.

The [FeNi] containing CODHs

The crystal structure of the CODHs from anaerobic bacteria reveals an active site containing Ni and Fe sites bridged by an Fe_3S_4 cluster that holds the two metal centers in close proximity (**Scheme 1-2**).[15,17] The first coordination sphere of the Ni(II) center contains two sulfur ligands in a T shaped geometry. The first coordination sphere of the Fe(I) center consists of a u_3-sulfido ligand, a histidine ligand, a cysteine ligand, and a fourth light ligand the sits is close proximity to the Ni center (possibly a labile hydroxide or water ligand). The crystal structures in the enzyme in two other oxidation states, one held at –320 mV, one held and –600 mV, and a third at –600 mV is the presence of CO_2 were also obtained. In both oxidation states, the geometry of the coordination sphere of both metal centers remains essentially unchanged. The similarity of the coordination geometry in both oxidation states means there is not a high reorganizational energy barrier between the two states.

When CO_2 is added to the reduced state, it binds to both Ni and Fe, with the Ni binding through the C atom at its fourth coordination site and with one of the carboxylate oxygen's bound to the Fe, replacing the labile fourth ligand. The oxygen also forms a hydrogen bond with a nearby lysine residue. The second oxygen forms a hydrogen bond to a nearby protonated histidine residue. The enzyme bi-functionally activates CO_2 at both metal centers with the Ni acting as a lewis base engaging CO_2 at its electrophilic site, while Fe acts as a lewis acid engaging the nucleophilic site. Additionally, the second coordination sphere of the enzyme

provides additional stabilization through appropriately positioned residues that are able to hydrogen bond to neutralize any built up charge, without significant changes to the structures of the active sites.

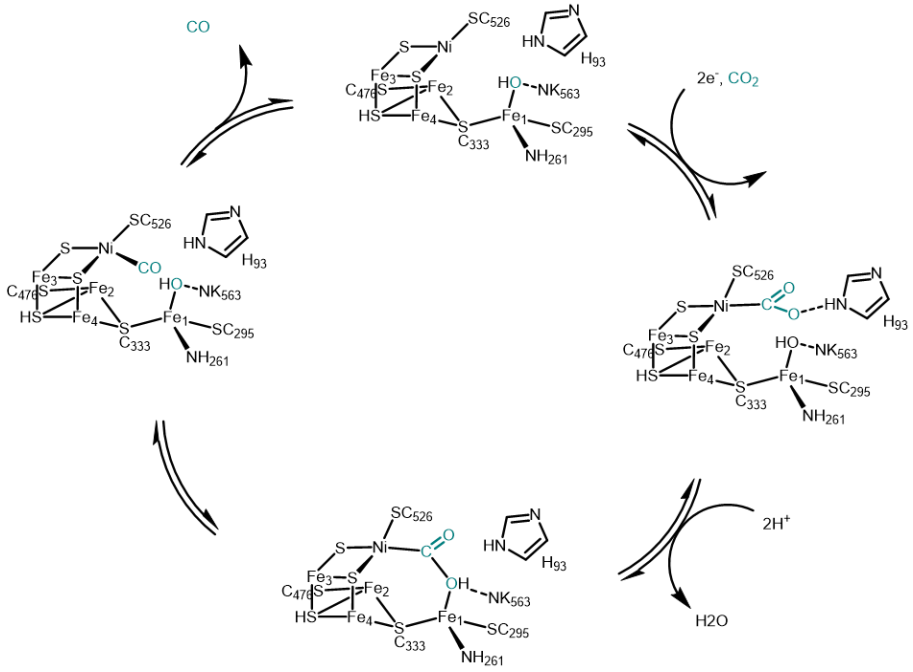

Scheme 1-2. Proposed mechanism for the reduction of CO_2 to CO by [NiFe] CODHs.

[Mo-Cu] containing CODHs

Crystal structures of the aerobic bacteria reveal a Mo-Cu active sites.[16] The main structural features of the oxidized form (**Scheme 1-3**) shows a Mo center with distorted square pyramidal geometry having a first coordination sphere consisting of an oxo group in the apical position, two sulfur atoms of a cytosine dinucleotide cofactor, a hydroxyl ligand, and a sulfide ligand that forms a bridge to the copper atom. The second coordination sphere of the molybdenum contains several residues within hydrogen bonding distance of the oxo and hydroxyl ligands. The Cu(I) center shows a linear two-coordinate geometry consisting of the

bridging sulfide ligand and a second S atom of a cysteine residue. Upon reduction, the first coordination sphere of both centers remains essentially unchanged.

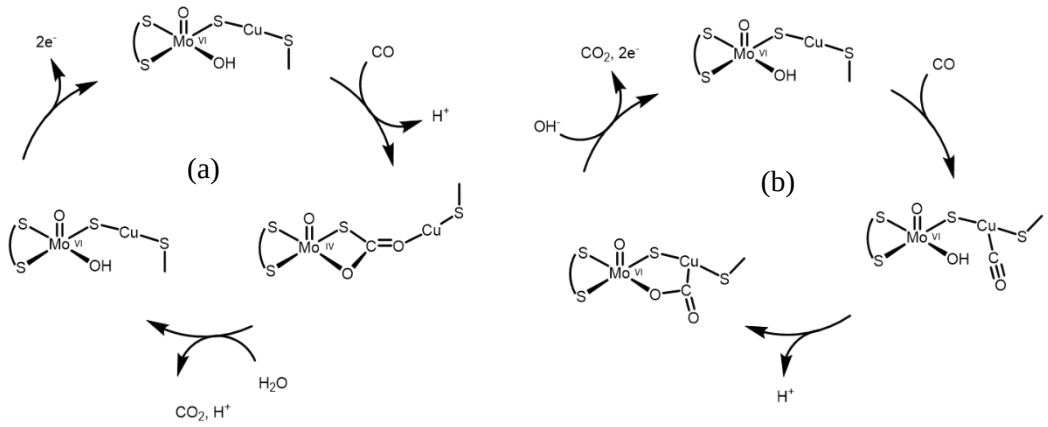

Scheme 1-3. Proposed mechanisms for the oxidation of CO to CO_2 by [MoCu] CODHs.

Based on crystal structures of the enzymes active site with an n-butylritrile ligand as an inhibitor,[16] CO is proposed to interact with the binuclear active site by inserting into the bridging sulfide ligand and the Cu and forming a C-O bond with the terminal hydroxyl ligand on the molybdenum (**Scheme 1-3)**. An additional plausible mechanism is also shown, mechanism b, where the CO binds at the Cu followed by a nucleophilic attack of the Mo-OH group on the Cu bound CO. This mechanism has been proposed based on theoretical calculations.[20,21] In both mechanisms, both metal centers are engaged in the binuclear activation of CO_2, and similar to the anaerobic CODHs, additional stabilization of charge is obtained throughout the oxidation of CO to CO_2 by strategically positioned hydrogen bonding groups in the second coordination sphere.

1.4.2 Formate dehydrogenases

Nature does not use hydrogenation as a means to reduce CO_2, but hydride transfer from formate does occur in enzymes called formate dehydrogenases (FDHs). The most prevalent type of formate dehydrogenases do not contain metals. Like hydrogenation catalyst and formate producing CO_2 electro-reduction catalysts they operate via direct hydride transfers, although in vivo, they operate irreversibly in the formate oxidation direction where a hydride is transferred from formate to a C4 atom of an NAD^+ pyridine ring that sits in close proximity for easy hydride transfer.

The other type of FDHs are metal dependent and contain Mo or W active sites. These enzymes can catalyze both the oxidation of formate to CO_2 (with rates as high as 3200 s^{-1} at pH 7.5) and the reduction of CO_2 to formate (with rates as high as 280 s^{-1}). Structural studies of several of the Mo and W enzymes reveal conserved active sites containing W(VI) or Mo(VI) metal centers showing distorted trigonal prismatic geometry in the oxidized state. The primary coordination sphere consists of 4 sulfur atoms of two pyranopterin ligands, either a sulfur atom of a cysteine residue or a selenium atom of a selenocysteine residue, and a sixth ligand that is either a sulfur or oxygen atom. As shown in the catalytic cycle in **Scheme 1-4**, there are two arginine and histidine residues that sit close to the metal center and are likely involved in stabilizing interactions through the cycle. These enzymes operate via a mechanism that involves the transfer of 2 electrons to or from the metal center along with a concerted proton transfer between the substrate and nearby residues in the second coordination sphere that are able to donate/accept a proton during catalysis.

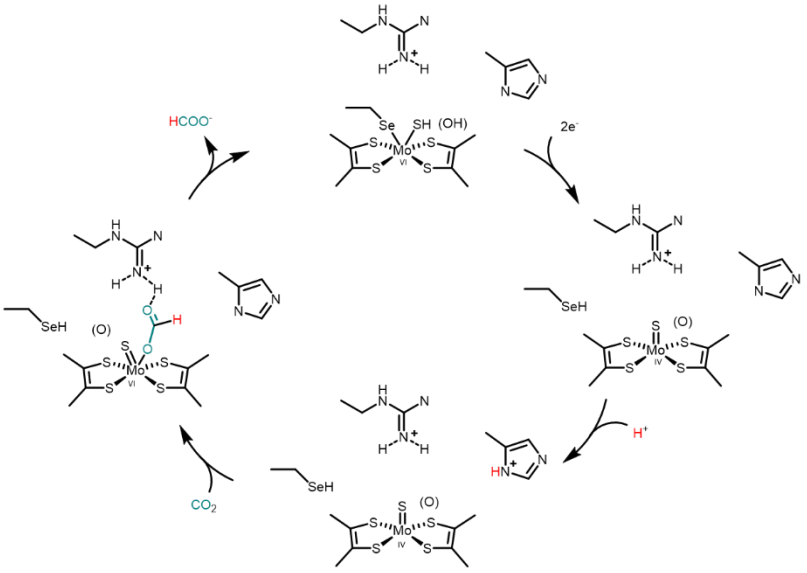

Scheme 1-4. Proposed mechanism for the reduction of CO_2 to formate by a molybdenum containing FDH.

1.4.3 Hydrogenase enzymes

Hydrogenases do not catalyze CO_2 reduction, but they do provide another example of how nature controls the movement of protons and electrons in redox processes. Hydrogenases are enzymes that catalyze the production of H_2 from two protons and two electrons, and the reverse of this reaction, the oxidation of H_2.[22-24] Structural studies of these enzymes reveal that they contain organometallic active sites containing [FeFe] or [FeNi] centers. The proposed structure of the [FeFe] enzyme is shown in **Scheme 1-5**. In the structure, the two iron centers are coordinated to CO and CN ligands and a redox active Fe_4S_4 core, and the two Fe centers are bridged by a diazathiolate ligand. The diazothiolate ligand positions an amine in the second coordination sphere over one of the Fe centers in an ideal configuration to act as a proton acceptor in the splitting of H_2 while the metal acts as a hydride acceptor. The amine is also thought to assist in proton transfer between the active site and the proton channel that leads to the exterior of the enzyme.

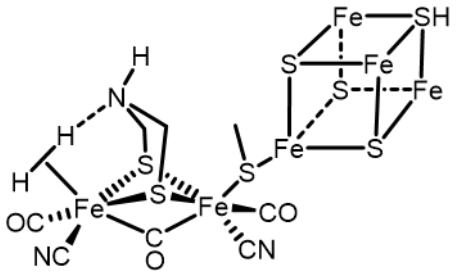

Scheme 1-5. Active site of [FeFe] hydrogenase enzymes.

1.4.4 Important lessons

CODHs, metal containing FDHs, and hydrogenase enzymes are able to reversibly catalyze their redox reactions with high turnover frequencies, which means they must operate at near the thermodynamic potentials of the reactions being catalyzed. This is an important distinguishing factor between the CO_2 reduction catalysts found in nature and the synthetic homogeneous CO_2 reduction catalysts, which all require the application of a significant overpotentials beyond the thermodynamic potentials of the reactions being driven. The way that nature is able to activate CO_2 at less forcing potentials is through strategically placed functional groups in the secondary sphere of the active site (binuclear binding sites, hydrogen bonding residues, acidic sites), which all help to make CO_2 binding more favorable without increasing the overpotential and can help the facilitate further steps in the catalytic cycle, such as the C–O bond cleavage. In the previous section the outer coordination sphere was not extensively discussed, but it also helps make these transformations more efficient through the incorporation of hydrophobic and hydrophilic tunnels that help to shuttle substrates in and products out of the active sites and additional binding sites that help control the movement of reactants during catalysis.

1.5 Bi-functional reactivity in synthetic catalysts

Nature's catalysts for these small molecule transformations are extremely complex, implementing strategically placed hydrogen bonding and proton donating groups in the second coordination sphere and complex hydrophobic and hydrophilic interactions in the outer coordination sphere which act as substrate relays into and out of the active site. Unfortunately, these catalysts are not robust enough to use them for the wide scale reduction of CO_2 so we have to focus our efforts on making better synthetic catalysts. It is difficult to imagine how a synthetic chemist would even attempt to build the same kind of complexity into a catalytic system to approach the efficiencies of nature's catalysts, which took billions of years to engineer and optimize. We have, however, with some success begun to take cues from how nature controls the binding of substrates and the movement of protons in enzymes and implement those design principles in synthetic catalysts, mainly by building functionality into the second coordination sphere of catalysts to help in bi-functional substrate activations and to provide stabilizing interactions throughout catalysis. Some examples of these successes are provided in the following section.

1.5.1 Biomimetic H_2 activation involving pendant bases

Dubois and co-workers have spent a significant amount of time developing and studying functional hydrogenase mimics that borrow from the [FeFe] hydrogenases the concept of putting a pendant amine adjacent to a vacant coordination site or a hydride ligand on a metal center. In the NiP_2N_2 hydrogenase mimics they developed, the azadithiolene ligand is mimicked through the use of cyclic diphosphine ligands containing amine functionalities which bind to the nickel center though the two phosphorous atoms leaving the amines free to act as "pendant bases" that can assist the nickel center in the cleavage and formation of H_2 and act as proton relays between the solution and the metal center (**Scheme 1-6**).[25] The activity of the

pendant amines in these complexes enables some of the highest turnover frequencies for proton reduction/H_2 oxidation known by an artificial catalyst.[26,27] The extraordinarily high activity of these complexes is attributed to the ability of the pendant amines to help in stabilizing the formation of metal dihydrogen complexes, helping in the polarization of the H–H bond, and speeding up inter- and intra-molecular proton transfers.

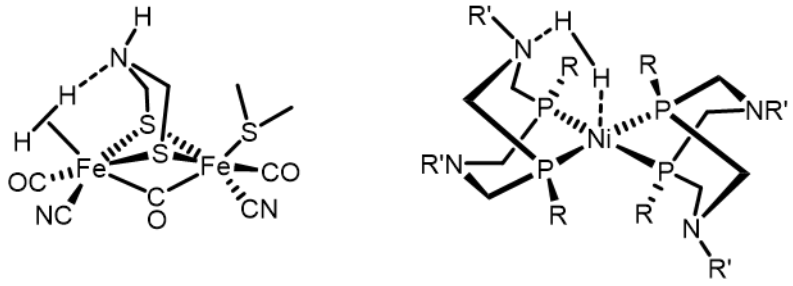

Scheme 1-6. Structure of the active site of [FeFe] hydrogenase enzymes and $Ni(P_2N_2)_2$ complexes showing how the pendant amine aids in H_2 splitting and formation.

1.5.2 Bi-functional interactions in hydrogenation chemistry

Noyori and co-workers introduced an extremely successful example of bi-functional catalysis using $RuCl_2$(diamine)(diphosphine)catalysts for the asymmetric hydrogenation of ketones.[15,16] Like CO_2 reduction, the reduction of ketones to alcohols also requires the delivery of a nucleophile and an electrophile to a polar bond. The key to the high activity of these complexes is that they contain a nucleophilic hydride and an adjacent electrophilic proton on the ligand, which are believed to be transferred to the substrate in a concerted fashion, as shown in **Scheme 1-7**. Several related ruthenium based catalysts have been developed with proton donating functionalities on the ligand that are active for the hydrogenation of polar bonds,[28-31] and progress has even been made in the preparation of non-precious metal containing catalyst for the hydrogenation of polar bonds based on iron with the implementation of bi-functional design principles.[32-34] For many of these systems, the proton donating site not only helps to provide a low energy pathway for the formation of products, but also serves as a proton acceptor

in the addition of H_2 to regenerate the catalytically active species. The participation of the ligands in the addition of H_2 allows these catalysts to operate under lower H_2 pressures and temperatures than catalysts that do not contain a proton donating/accepting functionality.

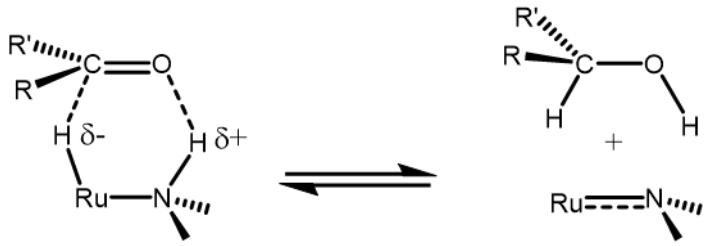

Scheme 1-7. Bi-functional activation of polar bonds by Noyori-type hydrogenation catalysts.

1.5.3 Hydrogen bonding and proton responsive ligands in CO_2 hydrogenation

In some of the best catalysts for CO_2 hydrogenation, bi-functional activity involving metal-ligand co-operation is thought to be important to their activity. Nozaki reported that an IrH_3 pincer complex was highly active for CO_2 hydrogenation and proposed that the ability of the ligand to be deprotonated plays an essential role is catalysis (**Scheme 1-8).**[35] Deprotonation of the ligand allows for facile dissociation of the coordinated formate and facile activation of H_2 to regenerate the active catalyst through the co-operative activity of the metal center and the deprotonated ligand. These two steps are thought to be two of the major bottlenecks in most other CO_2 hydrogenation catalysts. Hazari also later showed that by modifying the second coordination sphere of this type of catalyst with a proton bonding N–H group, the favorability for CO_2 insertion into $Ir(PN^HP)H_3$ trans hydride was significantly increased (**Scheme 1-8**), although the overall rates for CO_2 reduction were not improved because H_2 activation is more difficult in these complexes.[36] Despite the lack in improvement in the overall rates, this further highlights the importance of bi-functional activity in hydrogenation catalysis.

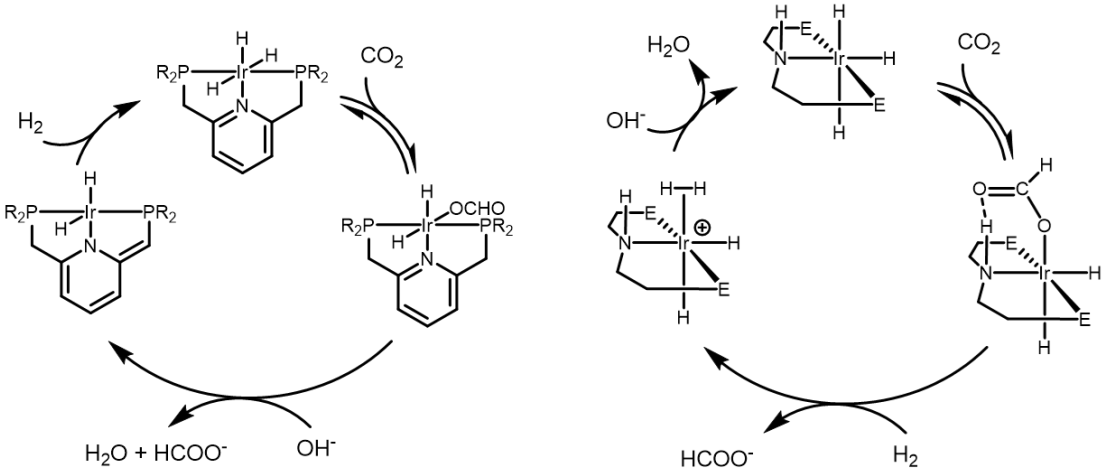

Scheme 1-8. Proposed mechanisms for CO_2 hydrogenation by Ir(PNP)H_3 (left) and Ir(PN^{H}P)H_3 (right).

Another notable example of bi-functional CO_2 hydrogenation to formate is provided in a report by Himeda and collaborators where an Ir catalyst containing bipyridine ligands with hydroxyl groups in the 2 and 2' positions was shown to exhibit high rates for hydrogenation at ambient temperatures and pressures.[37,38] This hydroxyl substituted complex shows a 16-fold increase in its rates for CO_2 hydrogenation at less forcing conditions compared to an analogous complex that does not contain hydroxyl groups. The proton responsive hydroxyl groups are thought to aid CO_2 hydrogenation by assisting in the heterolytic cleavage of H_2, and DFT calculations suggest that they also provide favorable hydrogen bonding interactions with CO_2 to assist in the insertion of CO_2 into the Ir-H bond.[39]

1.5.4 Bi-functional interactions in electrocatalytic CO_2 reduction.

While there is now great interest within both the polar bond hydrogenation community and the electrocatalytic CO_2 reduction community in the use of bi-functional catalyst, examples of the successful implementation of co-operative interactions in CO_2 hydrogenation catalysts are still limited. Examples of successful implementation of bi-functional reactivity in

electrocatalyts for CO_2 reduction are even scarcer. This section discusses some of those successes.

Co^I and Ni^I macrocyclic complexes have been extensively studied as electrocatalysts for the reduction of CO_2 to CO. These complexes show CO_2 binding constants ranging from 1 to 10^8 M^{-1}, which correlate strongly with reduction potential (complexes with more negative reduction potential bind CO_2 more readily) and are also correlated with the ability of the ligand to hydrogen bond to a coordinated CO_2 molecule (**Scheme 1-9**). The isomers of the molecule where the ligand has the protons pointed towards the same face are able to bind CO_2 several orders of magnitude more strongly than the isomers where the hydrogens are on opposite faces, despite having similar reduction potentials.[40] X-ray data and NMR studies indicate that there is hydrogen bonding between the amine hydrogens and the oxygens on the bound CO_2, contributing to the stability of the CO_2 adduct of complexes of these isomers. This example shows how strategically placed hydrogen bonding groups can help make CO_2 reduction more favorable without the application of greater overpotential.

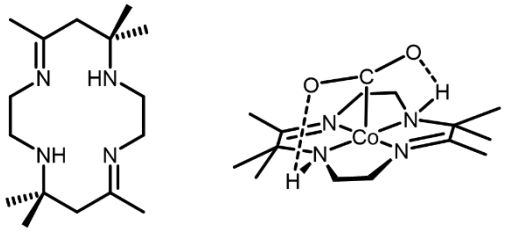

Scheme 1-9. Cobalt complex with macrocyclic ligand showing how hydrogen bonding groups on ligand stabilize CO_2 adduct.

Pd triphosphine complexes are highly active for the reduction of CO_2 to CO in acidic acetonitrile solutions. This system has been extensively studied by the Dubois group, and their kinetic studies revealed that under catalytic conditions CO_2 binding is rate limiting.[41-43 44] In attempts to make CO_2 binding more favorable, the Dubois group developed a bi-metallic analogue to facilitate the formation of the CO_2 adduct. It was thought that CO_2 could bind at

the two metal centers through the C and one of the O, as shown in **Scheme 1-10**. These studies were done before there was structural information about the active site of the [NiFe] CODHs, but the proposed scheme for CO_2 binding at the two Pd centers is very similar to how CO_2 binds in [NiFe] CODHs. Complexes of this type show very high catalytic rates for CO_2 reduction to CO ($k > 10^4$ M^{-1} s^{-1} compared to k ranging from 5 – 300 M^{-1} s^{-1} for the mononuclear systems). Although these complexes are very fast, they are not very robust, and only exhibit a few turnovers before they are deactivated. Still, this synthetic example shows how co-operative secondary interactions can make CO_2 binding more favorable and thus increase the rates of catalysis.

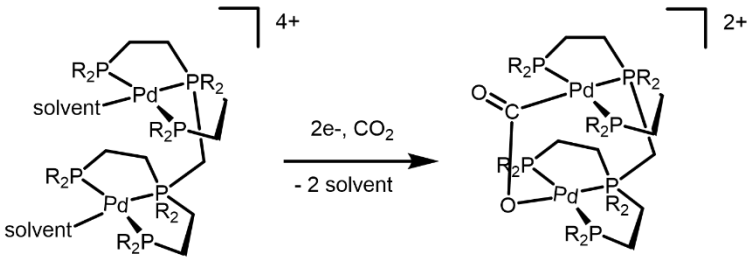

Scheme 1-10. Structure of Dubois' dinculear Pd catalyst and proposed reduced, CO_2 bound catalytic intermediate with both Pd centers binding CO_2.

A final notable example of the implementation of bi-functional catalysis design principles to improve electrocatalysis was the Saveant group's electrochemical reduction of CO_2 to CO by an Fe porphyrin with built in hydroxyl groups on the ligands to serve as proton donors while the Fe center serves as a nucleophile in the reduction of CO_2.[13] In this system, the addition of hydroxyl groups in the second coordination sphere of the porphyrin resulted in a 10 to 100-fold increase in TOF, as well as a 0.5 V decrease in overpotential.

While there has been some successful implementations of second coordination sphere interactions in the development of CO_2 reduction catalysts, this is still a relatively new field of study and we still have a great deal to learn from how we can make improvements to catalysts by adding favorable second coordination sphere interactions. The work in this dissertation was

initiated to develop electrocatalysts for CO_2 reduction that have the ability to engage CO_2 in a bi-functional manner at the metal center and through second coordination sphere interactions. We focused on trying to tune the first and second coordination sphere of complexes with bi-functional ability to optimize systems for CO_2 reduction. The primary focus of the Kubiak group is to develop homogeneous electrocatalysts, but some of the work described here deals with CO_2 hydrogenation catalysts. The first system that will be discussed is a previously reported dinuclear copper electrocatalyst that we attempted to modify to determine if we would make improvements to either the operating potential or to the rate of catalysis. Next, we synthesized Rh(diphosphine)$_2$ complexes that contain pendant amines in the second coordination sphere. We conducted thermodynamic studies, electrochemical studies, and explored how the proton-relay-containing ligands affected their ability to catalytically hydrogenate and electrochemically reduce CO_2. Last, we explored Ru and Fe pincer complexes that have bi-functional reactivity for electrochemical CO_2 reduction and methylformate reduction.

1.6 References

(1) Lewis, N. S.; Nocera, D. G. *Proc. Natl. Acad. Sci. U.S.A.*, **2006**, *103*, 15729-15735.

(2) *Climate Change 2007, Synthesis Report*: Washington, DC, 2007.

(3) Underwood, A. J. V. *Ind. Eng. Chem. Res.*, **1940**, *32*, 449-454.

(4) Surampudi, S.; Narayanan, S. R.; Vamos, E.; Frank, H.; Halpert, G.; LaConti, A.; Kosek, J.; Prakash, G. K. S.; Olah, G. A. *J. Power Sources*, **1994**, *47*, 377-385.

(5) Prakash, G. K. S.; Smart, M. C.; Wang, Q.-J.; Atti, A.; Pleynet, V.; Yang, B.; McGrath, K.; Olah, G. A.; Narayanan, S. R.; Chun, W.; Valdez, T.; Surampudi, S. *J. Fluorine Chem.*, **2004**, *125*, 1217-1230.

(6) Aresta, M.; Dibenedetto, A.; Angelini, A. *Chem. Rev.* , **2013**, *114*, 1709-1742.

(7) Benson, E. E.; Kubiak, C. P.; Sathrum, A. J.; Smieja, J. M. *Chem. Soc. Rev.* , **2009**, *38*, 89-99.

(8) Huff, C. A.; Sanford, M. S. *J. Am. Chem. Soc.* , **2011**, *133*, 18122-18125.

(9) Wesselbaum, S.; vom Stein, T.; Klankermayer, J.; Leitner, W. *Angew. Chem. Int. Ed.*, **2012**, *51*, 7499-7502.

(10) Wang, W.; Wang, S.; Ma, X.; Gong, J. *Chem. Soc. Rev.* , **2011**, *40*, 3703-3727.

(11) Jessop, P. G.; Joó, F.; Tai, C.-C. *Coord. Chem. Rev.* , **2004**, *248*, 2425-2442.

(12) Appel, A. M.; Bercaw, J. E.; Bocarsly, A. B.; Dobbek, H.; DuBois, D. L.; Dupuis, M.; Ferry, J. G.; Fujita, E.; Hille, R.; Kenis, P. J. A.; Kerfeld, C. A.; Morris, R. H.; Peden, C. H. F.; Portis, A. R.; Ragsdale, S. W.; Rauchfuss, T. B.; Reek, J. N. H.; Seefeldt, L. C.; Thauer, R. K.; Waldrop, G. L. *Chem. Rev.* , **2013**, *113*, 6621-6658.

(13) Costentin, C.; Robert, M.; Saveant, J.-M. *Chem. Soc. Rev.* , **2013**, *42*, 2423-2436.

(14) Savéant, J.-M. *Chem. Rev.* , **2008**, *108*, 2348-2378.

(15) Jeoung, J.-H.; Dobbek, H. *Science*, **2007**, *318*, 1461-1464.

(16) Dobbek, H.; Gremer, L.; Kiefersauer, R.; Huber, R.; Meyer, O. *Proc. Natl. Acad. Sci. U.S.A.*, **2002**, *99*, 15971-15976.

(17) Darnault, C.; Volbeda, A.; Kim, E. J.; Legrand, P.; Vernede, X.; Lindahl, P. A.; Fontecilla-Camps, J. C. *Nat. Struct. Mol. Biol.*, **2003**, *10*, 271-279.

(18) Svetlitchnyi, V.; Peschel, C.; Acker, G.; Meyer, O. *J. Bacteriol.*, **2001**, *183*, 5134-5144.

(19) Zhang, B.; Hemann, C. F.; Hille, R. *J. Biol. Chem.* , **2010**, *285*, 12571-12578.

(20) Hofmann, M.; Kassube, J.; Graf, T. *J. Biol. Inorg. Chem.*, **2005**, *10*, 490-495.

(21) Siegbahn, P. E. M.; Shestakov, A. F. *J. Comput. Chem.* , **2005**, *26*, 888-898.

(22) Fontecilla-Camps, J. C.; Volbeda, A.; Cavazza, C.; Nicolet, Y. *Chem. Rev.* , **2007**, *107*, 4273-4303.

(23) Fontecilla-Camps, J. C.; Amara, P.; Cavazza, C.; Nicolet, Y.; Volbeda, A. *Nature*, **2009**, *460*, 814-822.

(24) Lubitz, W.; Reijerse, E.; van Gastel, M. *Chem. Rev.* , **2007**, *107*, 4331-4365.

(25) Rakowski Dubois, M.; Dubois, D. L. *Acc. Chem. Rev.* , **2009**, *42*, 1974-1982.

(26) Wilson, A. D.; Newell, R. H.; McNevin, M. J.; Muckerman, J. T.; Rakowski DuBois, M.; DuBois, D. L. *J. Am. Chem. Soc.*, **2005**, *128*, 358-366.

(27) Wiese, S.; Kilgore, U. J.; DuBois, D. L.; Bullock, R. M. *ACS Catal.* , **2012**, *2*, 720-727.

(28) Clapham, S. E.; Hadzovic, A.; Morris, R. H. *Cood. Chem. Rev.* , **2004**, *248*, 2201-2237.

(29) Ikariya, T. *B. Chem. Soc. Jpn.*, **2011**, *84*, 1-16.

(30) O, W. W. N.; Lough, A. J.; Morris, R. H. *Chem. Comm.* , **2010**, *46*, 8240-8242.

(31) Casey, C. P.; Guan, H. *J. Am. Chem. Soc.* , **2009**, *131*, 2499-2507.

(32) Morris, R. H. *Chem. Soc. Rev.* , **2009**, *38*, 2282-2291.

(33) Junge, K.; Schroder, K.; Beller, M. *Chem. Comm.* , **2011**, *47*, 4849-4859.

(34) Sui-Seng, C.; Freutel, F.; Lough, A. J.; Morris, R. H. *Angew. Chem. Int. Ed.*, **2008**, *47*, 940-943.

(35) Tanaka, R.; Yamashita, M.; Nozaki, K. *J. Am. Chem. Soc.* , **2009**, *131*, 14168-14169.

(36) Schmeier, T. J.; Dobereiner, G. E.; Crabtree, R. H.; Hazari, N. *J. Am. Chem. Soc.* , **2011**, *133*, 9274-9277.

(37) Hull, J. F.; Himeda, Y.; Wang, W.-H.; Hashiguchi, B.; Periana, R.; Szalda, D. J.; Muckerman, J. T.; Fujita, E. *Nat. Chem.* , **2012**, *4*, 383-388.

(38) Wang, W.-H.; Hull, J. F.; Muckerman, J. T.; Fujita, E.; Himeda, Y. *Energy Environ. Sci.*, **2012**, *5*, 7923-7926.

(39) Wang, W.-H.; Muckerman, J. T.; Fujita, E.; Himeda, Y. *ACS Catal.* , **2013**, *3*, 856-860.

(40) Schmidt, M. H.; Miskelly, G. M.; Lewis, N. S. *J. Am. Chem. Soc.* , **1990**, *112*, 3420-3426.

(41) DuBois, D. L.; Miedaner, A.; Haltiwanger, R. C. *J. Am. Chem. Soc.* , **1991**, *113*, 8753-8764.

(42) Bernatis, P. R.; Miedaner, A.; Haltiwanger, R. C.; DuBois, D. L. *Organometallics*, **1994**, *13*, 4835-4843.

(43) Steffey, B. D.; Curtis, C. J.; DuBois, D. L. *Organometallics*, **1995**, *14*, 4937-4943.

(44) Dubois, D. L. *Comments Inorg. Chem.* , **1997**, *19*, 307-325.

Chapter 2

Investigation of a dinuclear copper system for CO_2 reduction

2.1 Introduction

As a starting point for my work on CO_2 reduction in the Kubiak lab, we decided to revisit a system that was previously studied in our group. The dinuclear copper complex, $[Cu_2(\mu\text{-}PPh_2bipy)_2(NCCH_3)_2](PF_6)_2$, was originally synthesized by Haines and co-workers and was later studied by the Kubiak group to explore its potential as an electrocatalyst for CO_2 reduction.[1,2] It was found that this complex exhibits 2 reductive features in its cyclic voltammogram under a nitrogen atmosphere, a quasi-reversible reduction at –1.35 V and another at –1.53 V vs SEC. Under an atmosphere of CO_2, there is an enhancement in current at the 2nd reduction and on the return scan, the re-oxidation waves for both peaks are no longer present. Bulk electrolysis at –1.7 V vs SCE followed by gas chromatography analysis (GC)

determined that one of the major products was CO. Infrared spectroelectrochemistry in the presence of CO_2 revealed that CO_3^{2-} was another product. It was concluded that this catalyst facilitates the 1-electron reduction of two CO_2 molecules that come together to make a head-to-tail dimer of CO_2 radicals and then collapse into CO and CO_3^{2-}. A thorough understanding of how CO_2 is activated by these complexes was still lacking.

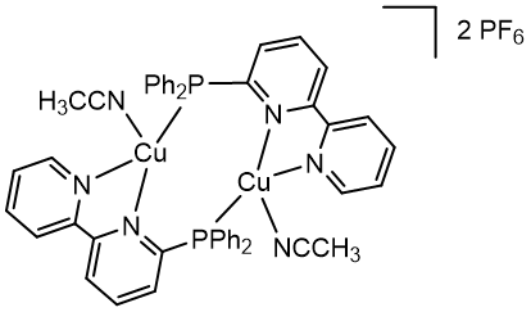

Figure 2-1. Structure of the dinuclear copper catalyst.

We were still interested in this system for a few reasons. First, copper is a very interesting metal for CO_2 reduction. As a heterogeneous catalyst, coppers CO_2 reduction activity is unique in that it is one of the few that go beyond 2-electron reductions to make more highly reduced products like CH_4 and C_2H_2.[3] Despite its unique activity as a heterogeneous electrode, this system along with another reported by Bouwman and co-workers[4] represent the only homogenous copper based electrocatalysts that have been reported for CO_2 reduction. Our interest in catalysts that are able to engage CO_2 in a bi-functional manner also made this complex interesting. This complex has the potential to engage CO_2 through two metal centers. The coordination sites occupied by two weakly coordinating acetonitrile ligands are oriented close to each other in a manner suitable for a co-operative activation of a small molecule, as is done in CO dehydrogenase enzymes. Multinuclear copper active sites are also found in several enzymes that catalyze redox reactions including the reduction of dioxygen to H_2O,[5] another

multi-electron and -proton reduction process. We hoped further study of this system might lead to improvements in catalysis or help us understand how to make other copper catalysts.

This catalyst contains phosphine and bipyridine moieties on the ligand, which are ubiquitous in transition metal chemistry. They are widely used because the electronic and steric properties of these ligands are easily controlled by changing the substituents on the ligands, which can lead to significant changes in reactivity. Additionally, bipyridines are useful ligands because they are able to act as non-innocent ligands, allowing them to serve as electron reservoirs for transition metal complexes.[6] This is important for the design of homogeneous electrocatalysts because the ability to transfer more than one electron at a time helps to avoid high energy CO_2 radical anion intermediates. This is also particularly important for the design of copper reduction catalysts because copper (I) already has a filled set of d orbitals. We wanted to explore how altering the substituents on the ligands of this system might affect catalysis; could we use more electron withdrawing ligands to make complexes that have less negative reductions, but still retain catalysis to produce catalysts that operate at lower overpotentials, or could we use more donating ligands that would make the copper centers more nucleophilic and speed up the reaction with CO_2 to produce a faster catalysts?

This chapter describes the synthesis and characterization, along with electrochemical CO_2 reactivity of four new dinuclear copper complexes with substituted 6-phosphino bipyridine ligands: $[Cu_2(\mu\text{-}PPh_2\text{-}Me_2\text{-}bipy)_2(NCCH_3)_2](PF_6)_2$ (**1**), $[Cu_2(\mu\text{-}PPh_2\text{-}t\text{Bu}_2\text{-}bipy)_2(NCCH_3)_2](PF_6)_2$ (**2**), $[Cu_2(\mu\text{-}P\textit{i}Pr_2bipy)_2(NCCH_3)](PF_6)_2$ (**3**), and $Cu_2(\mu\text{-}P\textit{i}Pr_2bipy)_2(\mu\text{-}CNCH(CH_3)_2)](PF_6)_2$ (**4**). These complexes are similar to the dinuclear copper complex previously reported by Haines and co-workers, $[Cu_2(\mu\text{-}PPh_2bipy)_2(NCCH_3)_2](PF_6)_2$ (**5**), but we have introduced slight ligand modifications to observe how changes to the electronics of the ligand affected the structures, electrochemistry, and CO_2 reactivity. We examined the effects

of substituting alkyl groups for the aryl groups on the phosphine as well as the effects of adding substituents to the bipyridine backbone.

2.2 Experimental

Materials and Methods

All chemicals were purchased from commercial sources and used as received unless otherwise specified. All manipulations were carried out using standard Schlenk and glove box techniques under an atmosphere of nitrogen. Acetonitrile, tetrahydrofuran (THF), pentane, and diethyl ether (Et_2O) were sparged with argon and dried over basic alumina in a custom dry solvent system. Tetrabutylammonium hexafluorophosphate (NBu_4PF_6) was recrystallized from methanol prior to use in electrochemical experiments. 6-bromo-2,2'-bipyridine,[7] 4,4'-dimethyl-2,2'-bipyridine N-Oxide,[8] 6-diphenylphosphino-2,2'-bipyridine (**d**),[9] and $[Cu_2(\mu\text{-}PPh_2bipy)_2(NCCH_3)_2](PF)_2$ (**5**)[1] were synthesized as previously reported. ^1H and $^{31}P\{^1H\}$NMR spectra were recorded using a 300MHz or 400MHz Varian spectrometer. ^1H NMR spectral data are referenced against the residual solvent signal and are reported in ppm downfield of tetramethylsilane ($\delta = 0$). $^{31}P\{^1H\}$ NMR spectral data are referenced against an external H_3PO_4 ($\delta=0$) reference and are reported in ppm. Mass spectrometry data was collected on a Finnagan LCQDECA in ESI positive ion mode. Elemental analyses were performed by NuMega Resonance Labs, San Diego, CA.

Electrochemical Experiments

Electrochemical experiments were performed using a BAS Epsilon potentiostat. Cyclic voltammetry experiments were performed under a nitrogen or CO_2 atmosphere in a one compartment cell with a glassy carbon working electrode, a platinum wire counter electrode and a Ag/AgCl reference electrode with ferrocence as an internal reference. For the

electrochemistry of the ligand $PiPr_2$bipy (**c**), ferrocene was not added and the couples were referenced to a Ag/AgCl pseudoreference. All experiments were performed using 0.1 M NBu_4PF_6 as the supporting electrolyte with copper complex concentrations ranging from 0.25 to 1.0 mM. IR-spectroelectrochemistry was done with a home-built sixth generation cell mounted on a specular reflectance unit. A detailed description of the cell is reported elsewhere.[10] Infrared spectra were collected on Bruker Equinox 55 FTIR spectrometer.

Crystallography

Crystals of the Cu complexes suitable for X-ray structural determinations were mounted in polybutene oil on a glass fiber and transferred on the goniometer head to the precooled instrument. Single crystal X-ray structural data was collected at 100K on either a Bruker P4 Platform or a Kappa diffractometer equipped with a Bruker Apex detector. Crystallographic measurements were carried out using Mo Kα radiation (λ = 0.71073 Å) or Cu Kα radiation (λ = 1.54178 Å). All structures were solved by direct methods using SHELXS-97 and refined with full-matrix least-squares procedures using SHELXL-97.[11] All non-hydrogen atoms were anisotropically refined unless otherwise reported; the hydrogen atoms were included in calculated positions as ridged models in the refinement. Crystallographic data collection and refinement information can be found in the Appendix section.

Synthesis of 6-chloro-4,4'-dimethyl-2,2'-bipyridine

4,4'-dimethyl-2,2'-bipyridine N-oxide (1.86 g, 10.8 mmol) was added slowly to 10 mL $POCl_3$ (16.5 g, 107 mmol) at 0 ˚C. The mixture was stirred at reflux at 100 ˚C overnight. The excess $POCl_3$ was removed under vacuum leaving a black residue. A small amount of ice water was added and the reaction was made alkaline with 25 mL 5M NaOH. The solution was extracted with CH_2Cl_2 (3 x 20 mL) and the organic fractions were collected and dried over Na_2SO_4. The solvent was evaporated leaving a brown residue. The residue was purified via

column chromatography on silica (20% EtOAc/hexanes) to obtain a white powder (0.907 g, 45.0%). ^{1}H NMR ($CDCl_3$): δ = 2.42 (s, 3H, C*H*$_3$), 2.46 (s, 3H , C*H*$_3$), 7.17 (s, 1H, Ar*H*) 7.20 (d, $J_{H\text{-}H}$ = 5.1 Hz, 1H, Ar*H*), 8.26 (s, 1H, Ar*H*), 8.208 (s, 1H, Ar*H*), 8.51 (d, $J_{H\text{-}H}$ = 5.1 Hz, 1H, Ar*H*). ESI-MS (m/z): 219.0 $[M+H]^+$. Anal Calculated for $C_{12}H_{11}N_2Cl$: C, 65.91, H, 5.07, N, 12.81. Found: C, 65.51, H, 5.43, N, 13.06.

Synthesis of 6-(diphenylphosphino)-4,4'-dimethyl-2,2'-bipyridine (a)

6-chloro-4,4'-dimethyl-2,2'-bipyridine (0.382 g, 1.75 mmol) was dissolved in 10 mL THF and the solution was cooled to –78˚C. Potassium diphenylphosphide (0.5 M in THF, 4.2 mL, 2.1 mmol) was added slowly via cannula. The dark red mixture was allowed to warm to room temperature and stirred overnight. 6M HCl was added to the reaction followed by a solution of 10% ammonium hydroxide until the mixture was basic. This was extracted with diethyl ether (3 x 20 mL) and the organic fractions were dried over Na_2SO_4. The solvent was removed under vacuum to yield a yellow oily solid. The product was precipitated from acetonitrile to obtain 0.305 g of a white powder (47 %). ^{1}H NMR (CD_2Cl): δ = 2.33 (s, 3H, C*H*$_3$), 2.36 (s, 3H, C*H*$_3$), 7.01 (s, 1H, Ar*H*), 7.11 (d, $J_{H\text{-}H}$ = 5.0 Hz, 1H, Ar*H*), 7.33–7.48 (10H, Ar*H*), 8.09 (s, 1H, Ar*H*), 8.17 (s, 1H, Ar*H*), 8.47 (d, $J_{H\text{-}H}$ = 4.9 Hz, 1H, Ar*H*). ^{31}P{^{1}H} NMR (CD_2Cl_2): δ = –3.70. ESI-MS (m/z): 269.1 $[M+H]^+$. Anal Calculated for $C_{24}H_{21}N_2P$: C, 78.24, H, 5.75, N, 7.60. Found: C, 78.11, H, 6.23, N, 8.00.

Synthesis of 4,4'-di-tert-butyl-2,2'-bipyridine N-oxide

4,4'-di-*tert*-butyl-2,2'-bipyridine (3.00 g, 1.12 mmol) was dissolved in 10 mL of $CHCl_3$. The solution was cooled to 0 ˚C and 3-chloroperoxybezoic acid (3.19 g of 77% max) in 20 mL of $CHCl_3$ was added dropwise over a period of 2 h. The mixture was allowed to come to room temperature and was stirred overnight. The solvent was removed under vacuum leaving a yellow oily residue. This was purified via column chromatography on a basic alumina (20% EtOAc/Hexanes) to obtain an off white powder (1.95 g, 61%). ^{1}H NMR ($CDCl_3$): δ = 1.34 (s,

9H, CH_3), 1.35 (s, 9H, CH_3), 7.22 (d, $J_{H\text{-}H}$ = 2.9 Hz, 1H, Ar*H*), 7.31 (d, $J_{H\text{-}H}$ = 5.2 Hz, 1H, Ar*H*), 8.05 (s, 1H, Ar*H*), 8.21 (d, *J* = 6.9 Hz, 1H, Ar*H*), 8.61 (d, *J* = 5.2 Hz, 1H, Ar*H*), 8.87 (s, 1H, Ar*H*). ESI-MS (m/z): 285.28 $[M+H]^+$. Anal Calculated for $C_{18}H_{24}N_2O$: C, 76.02, H, 8.51, N, 9.85. Found: C, 75.68, H, 8.79, N, 10.12.

Synthesis of 6-chloro-4,4'-di-tert-butyl-2,2'-bipyridine

6-chloro-4,4'-di-*tert*-butyl-2,2'-bipyridine was synthesized analogously to 6-chloro-4,4'-dimethyl-2,2'-bipyridine. The crude product was purified via column chromatography on silica (30% EtOAc/hexane). The major fraction was collected and evaporated to yield a white solid (35%). ^{1}H NMR ($CDCl_3$): δ 1.36 (s, 9H, CH_3), 1.37 (s, 9H, CH_3), 7.27–7.37 (m, 2H, Ar*H*), 8.32 (s, 2H, 2 Ar*H*), 8.57 (d, $J_{H\text{-}H}$ = 5.3, 1H, Ar*H*). ESI-MS(m/z): 303.26 $[M+H]^+$. Anal Calculated for $C_{18}H_{23}ClN_2$: C, 71.39, H, 7.66, N, 9.25. Found: C, 71.00, H, 7.36, N, 9.25.

Synthesis of 6-(diphenylphosphino)-4,4'-di-tert-butyl-2,2'-bipyridine (b)

6-(diphenylphosphino)-4,4'-di-*tert*-butyl-2,2'-bipyridine was synthesized following the same procedure used to synthesize 6-(diphenylphosphino)-4,4'-dimethyl-2,2'-bipyridine (62%). ^{1}H NMR (CD_2Cl_2): δ = 1.32 (s, 9H, CCH_3), 1.33 (s, 9H, CCH_3), 7.29 (m, 2H, Ar*H*), 7.40 (m, 9H, Ar*H*), 7.55 (m, 5H, Ar*H*), 8.26 (s, 1H, Ar*H*), 8.35 (s, 1H, Ar*H*), 8.59 (d, $J_{H\text{-}H}$ = 5.22 Hz, 1H, Ar*H*). ^{31}P{^{1}H} NMR ($CHCl_3$):δ = –1.62 ESI-MS(m/z): 453.31$[M+H]^+$. Anal Calculated for $C_{30}H_{33}N_2P$: C, 79.62, H, 7.35, N, 6.19. Found: C, 78.88, H, 7.67, N, 6.94.

Synthesis of 6-(diisopropylphosphino)-2,2'-bipyridine (c)

6-bromo-2,2'-bipyridine (1.00 g, 4.25 mmol) was dissolved in Et_2O (20 mL) and cooled to –78 ˚C with a acetone/dry ice bath. *n*-BuLi in hexanes (1.6M, 2.67 mL,4.27 mmol) was added dropwise, producing a dark orange solution. The solution was stirred at –78˚ C for 2 h, after which a solution of chlorodiisopropyl phosphine (0.68 mL, 4.27 mmol) in 10mL Et_2O was added slowly to the reaction. The mixture was allowed to come to room temperature slowly and was stirred at room temperature overnight. The resulting yellow solution was filtered and

the filtrate was evaporated under vacuum to obtain a bright orange oil. This was dissolved in hexanes and filtered. The filtrate was evaporated to yield 1.12 g (96%) of an viscous orange oil. ^{1}H NMR ($CDCl_3$): δ = 0.97 (dd, $J_{P\text{-}H}$ = 11.8 Hz, $J_{H\text{-}H}$ = 7.0 Hz, 6H, CHC*H*$_3$), 1.15(dd, $J_{P\text{-}H}$ = 14.5 Hz, $J_{H\text{-}H}$ = 7.0 Hz, 6H, CHC*H*$_3$), 2.36-2.28(sept. of d, $J_{P\text{-}H}$ = 2.5 Hz, $J_{H\text{-}H}$ = 7.0 Hz, 2H, C*H*CH$_3$), 7.23 (m, 1H, Ar*H*), 7.46 (m, 1H, Ar*H*), 7.69 (m, 1H, Ar*H*), 7.78 (m, 1H, Ar*H*), 8.30 (m, 1H, Ar*H*), 8.46 (m, 1H, Ar*H*), 8.64 (m, 1H, Ar*H*) . ^{31} P^{12} NMR ($CDCl_3$): δ = 15.15. ESI-MS (m/z): 273.11 $[M+H]^+$.

Synthesis of $[Cu_2(\mu\text{-}PPh_2\text{-}Me_2\text{-}bipy)_2(NCCH_3)_2]\ (PF_6)_2$ (1)

A solution of 6-(diphenylphosphino)-2,2'-bypyridine (0.301 g, 0.860 mmol) in acetonitrile (20 mL) was added to a solution of $[Cu(CH_3CN)_4]PF_6$ (0.320 mg, 0.860 mol) in 50mL acetonitrile, producing a yellow solution which was stirred overnight. The solvent was reduced under vacuum and Et_2O was added to precipitate the product. The solution was filtered to collect 0.296 g (58%) of **1** as a yellow solid. ^{1}H NMR (CD_2Cl_2): δ = 1.91 (s, 6H, C*H*$_3$CN) , 2.53 (s, 6H, C*H*$_3$), 2.56 (s, 6H, C*H*$_3$), 7.00–7.10 (m, 8H, Ar*H*), 7.16 (s, 2H, Ar*H*), 7.26 (d, $J_{H\text{-}H}$ = 5.1 Hz, 2H, Ar*H*), 7.35 (t, *J* = 7.6 Hz, 8H, Ar*H*), 7.49 (d, *J* = 7.5 Hz, 4H, Ar*H*), 7.91 (d, *J* = 5.3 Hz, 2H, Ar*H*), 8.19 (s, 2H, Ar*H*), 8.29 (s, 2H, Ar*H*). ^{31} P^{12} NMR (CD_2Cl_2): δ = 10.04. Anal Calculated for $C_{52}H_{48}Cu_2F_{12}N_6P_4$: C, 50.53, H, 3.91, N, 6.80. Found: C, 50.59, H, 3.98, 6.64.

Synthesis of $[Cu_2(\mu\text{-}PPh_2\text{-}t\text{Bu}_2\text{-}bipy)_2(NCCH_3)_2](PF_6)_2$ (2)

Complex **2** was synthesized analogously to **1**. (79%) ^{1}H NMR ($CDCl_3$): δ = 1.31 (s, 18H, C*H*$_3$), 1.39 (s, 18H, C*H*$_3$), 1.88 (s, 6H, C*H*$_3$CN), 7.00–7.05 (m, 8H, Ar*H*), 7.19 (s, 2H, Ar*H*), 7.30–7.49 (m, 14H, Ar*H*), 8.02 (d, $J_{H\text{-}H}$ = 5.5 Hz 2H, Ar*H*), 8.21 (s, 2H, Ar*H*), 8.28 (s, 2H, Ar*H*). ^{31}P{^{1}H} NMR (CD_2Cl_2): δ = 10.11. Anal Calculated for $C_{64}H_{72}Cu_2F_{12}N_6P_4$: C, 54.70, H, 5.17, N, 5.98. Found: C, 54.36, H, 5.30, N, 5.60.

Synthesis of $[Cu_2(\mu\text{-}P\textit{i}Pr_2bipy)_2(NCCH_3)](PF_6)_2$ (3)

Complex **3** was synthesized analogously to **1** (77%). ^{1}H NMR (CD_2Cl_2): δ = 0.96-1.02 (m, 24H, CHC*H*$_3$), 2.09 (s, 3H, NCC*H*$_3$), 2.51 (m, 4H, C*H*CH$_3$), 7.80-7.80 (m, 4H, Ar*H*), 8.24 (t, *J* = 8.1 Hz, 2H, Ar*H*), 8.33 (t, *J* = 8.1 Hz, 2H, Ar*H*), 8.40 (d, *J* = 8.1 Hz, 2H, Ar*H*), 8.45 (d, *J* = 8.3 Hz, 2H, Ar*H*), 8.85 (d, *J* = 5.2 Hz, 2H, Ar*H*). ^{31}P{^{1}H} NMR (CD_2Cl_2): δ = 34.11. Anal Calculated for $C_{36}H_{48}Cu_2F_{12}N_6P_4$: C, 41.43, H, 4.64, N, 5.83. Found: C, 39.97, H, 4.76, N, 6.20

Synthesis of [Cu$_2$(μ-P*i*Pr$_2$bipy)$_2$(μ-CNCH(CH$_3$)$_2$)](PF$_6$)$_2$ (4)

Complex **3** (0.130g; 0.128 mmol) was dissolved in 10 mL CH_2Cl_2. Isopropylisocyanide (8.8 mg, 0.127 mmol) dissolved in 1 mL CH_2Cl_2 was added via syringe. The yellow solution was allowed to stir overnight. The solvent was reduced and a yellow powder was precipitated by the addition of THF. The product was collected by filtration and dried to yield 0.079g (62%) of a yellow powder. ^{1}H NMR (CD_2Cl_2): δ = 0.54 (dd, 6H, J_{P-H} = 17.6 Hz, J_{H-H} = 7.0 Hz, CHC*H*$_3$), 0.69 (dd, 6H, J_{P-H} = 16.0 Hz, J_{H-H} = 6.8 Hz, CHC*H*$_3$), 1.00–1.27 (m, 18H, overlaid isopropyl CHC*H*$_3$), 2.38 (m, 2H, C*H*CH$_3$), 2.53 (m, 2H, C*H*CH$_3$), 3.99 (septet, 1H, *J* = 6.6 Hz, C*H*CH$_3$), 7.84–7.88 (m, 4H, Ar*H*), 8.23–8.38 (m, 4H, Ar*H*), 8.43–8.60 (m, 4H, Ar*H*), 8.89 (d, 2*H*, ArH); ^{31}P{^{1}H} NMR (CD_2Cl_2): δ = 35.18. Anal Calculated for $C_{37}H_{50}Cu_2F_{12}N_5P_4$: C, 41.95, H, 4.79, N, 6.79. Found: C, 41.95, H, 5.20, N, 6.52.

2.3 Results and Discussion

2.3.1 Synthesis

The ligands 6-(diphenylphosphino)-4,4'-dimethy-2,2'-bipyridine (PPh$_2$-Me$_2$-bipy, **a**) and 6-(diphenylphosphino)-4,4'-di-*tert*-butyl-2,2'-bipyridine (PPh$_2$-*t*Bu$_2$-bipy, **b**) were synthesized as shown in **Scheme 1**. The synthesis of the ligands was performed according to modified literature procedures for similar ligands.[9] The substituted bipyridines 4,4'-dimethyl-2,2'-bipyridine and 4,4'-di-*tert*-butyl-2,2'-bipyridine were first converted to their mono N-oxides by reaction with *m*-chloroperoxybenzoic acid. The N-oxides were then converted to the

6-chloro-substituted bipyridines by refluxing in neat $POCl_3$ under nitrogen. The ligands **a** and **b** were then obtained by the reaction of potassium diphenylphosphide with the corresponding substituted 6-chloro bipyridines. The ligand 6-(diisopropylphosphino)-2,2'-bipyridine (P*i*Pr$_2$bipy, **c**) was synthesized by lithiation of 6-bromo-2,2'-bipyridine with *n*-BuLi followed by addition of chlorodiisopropylphosphine. All ligands were characterized by ^{1}H NMR and ^{31}P{^{1}H} NMR when relevant as well as mass spectrometry and elemental analysis.

The ligand modifications above all represent the addition of electron donating substituents, which are expected to make the reduction potentials of the resulting copper complexes more negative, and potentially increase the rates of catalytic CO_2 reduction. We also attempted to make electron withdrawing substitutions on the ligands, but this proved to be much more difficult. Attempts were made to make the 4,4'-cyano and 4,4'-trifluoromethyl substituted bipyridines with orthro phosphine groups, but we were unable to make the starting 4,4' substituted bipyridines in good yields to proceed through the ligand synthesis.

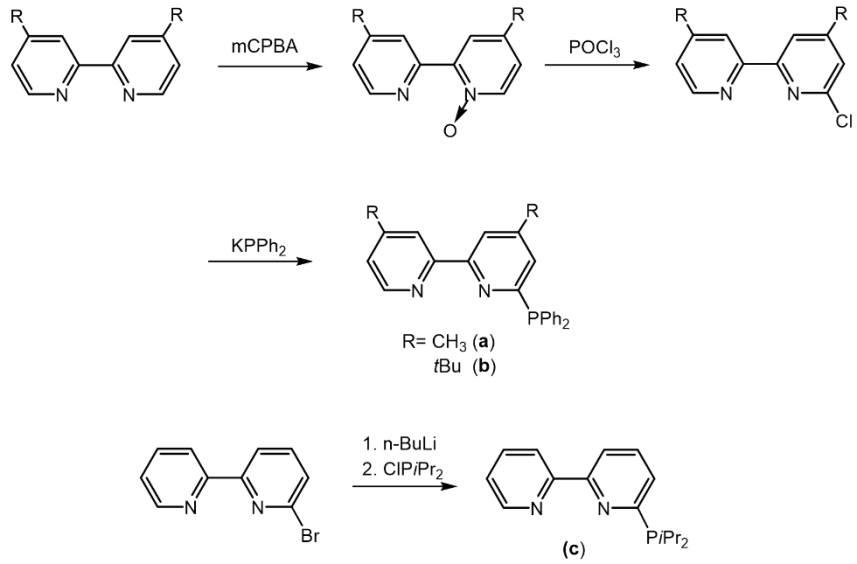

Scheme 2-1. Synthesis of ligands **a**, **b**, and **c**.

Complexes **1–4** were synthesized as shown is **Scheme 2**. Addition of 1 equivalent of ligands **a**–**c** to acetonitrile solutions of $[Cu(NCCH_3)_4]PF_6$ produced yellow solutions, which were stirred overnight. The solvents were reduced and the complexes **1**–**3** were precipitated as yellow powders with the addition of diethyl ether. Complex **4** was synthesized by adding 1 equivalent of isopropyl isocyanide to a solution of $[Cu_2(\mu\text{-}PiPr_2bipy)_2(NCCH_3)](PF_6)_2$ (**3**) in CH_2Cl_2. After stirring the solution overnight, the solvent was reduced and the product was precipitated by the addition of THF. All copper complexes were characterized by elemental analysis $^{31}P\{^1H\}$ NMR, ^1H NMR, and X-ray crystallography.

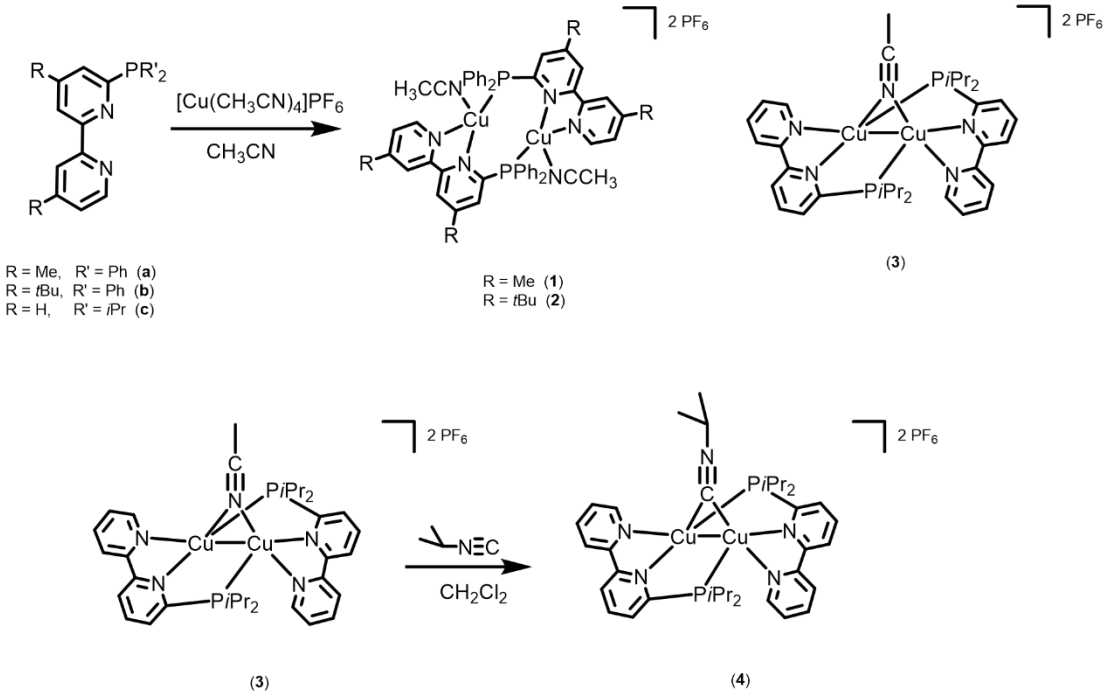

Scheme 2-2. Synthesis of complexes copper complexes **1**–**4**

2.3.2 Structural characterization

To verify that the complexes were dinuclear similar to complex **5**, they were characterized by X-ray crystallography. Suitable crystals for X-ray diffraction of **1** were obtained by layering hexanes over a methylene chloride solution of **1**. Crystals for X-ray diffraction of **2** and **3** were obtained through the slow diffusion of ether into acetonitrile solutions of the complexes. Suitable crystals for **4** were obtained through the vapor diffusion of hexanes into a concentrated CH_2Cl_2 solution. Molecular structures of the cations of **1**–**4** are shown in **Figures 2–5** and relevant bond lengths and angles are provided in the figure captions.

$[Cu_2(\mu\text{-}PPh_2Me_2bipy)_2(NCCH_3)_2](PF_6)_2$ (**1**) crystallized in the spacegroup $P\bar{1}$ along with two solvent molecules (CH_2Cl_2). Crystallographic analysis of **1** indicates that the cation is dinuclear containing two copper (I) ions, two PPh_2-Me_2-bipy ligands, and two coordinated acetonitrile molecules. The asymmetric unit contains half a molecule of **2**, an uncoordinated hexafluorophosphate anion, and an uncoordinated methylene chloride molecule. The molecular structure contains a crystallographic inversion point at the center of each dimer that generates the other half of the dimer, the second counter ion, and a second methylene chloride molecule. Similar to the compound reported by Haines and co-workers (**5**), the ligands coordinate the two copper centers in a head-to-tail manner so that each copper atom is coordinated to the phosphorus atom of one bridging ligand and the chelating bipyridine of the other. An acetonitrile molecule occupies the fourth coordination site on each copper and shows a Cu–$NCCH_3$ distance of 2.002(3) Å. The coordination geometry of each copper atom is best described as tetrahedral. The distance between the two copper atoms is 3.7244(6) Å. This is slightly contracted compared to the Cu–Cu distance in the original compound structure (3.941 Å).

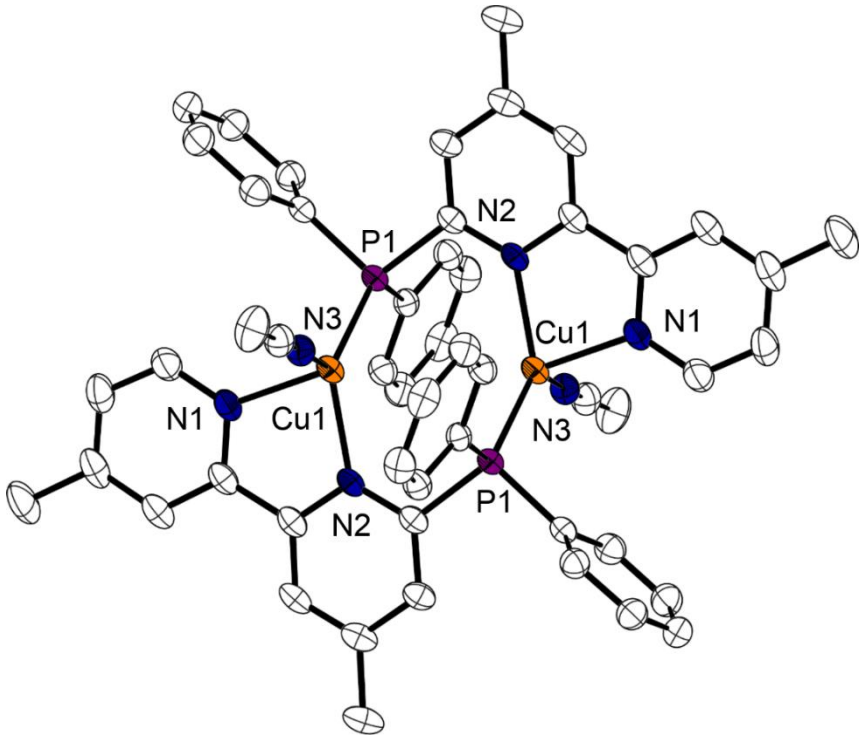

Figure 2-2. Thermal ellipsoid plots of $[Cu_2(\mu\text{-}PPh_2Me_2bipy)_2(NCCH_3)_2](PF_6)_2$ (**1**) shown at the 50 % probability level. The hydrogen atoms, uncoordinated counter ions, and solvent molecules have been omitted for clarity. Selected bond lengths [Å] and angles [°]: Cu(1)···Cu(2) 3.7244(6), Cu(1)–N(3) 2.003(2), Cu(1)–N(1) 2.091(2), Cu(1)–N(2) 2.087(2), Cu(1)–P(1) 2.1917(7), N(3)–C(26) 1.135(3), N(3)–Cu(1)–N(2) 108.95(8), N(3)–Cu(1)–P(1) 119.67(7), N(3)–Cu(1)–N(1) 98.91(9), N(3)–Cu(1)–N(2) 108.95(8).

$[Cu_2(\mu\text{-}PPh_2\text{-}t\text{Bu}_2\text{-bipy})_2(NCCH_3)_2](PF_6)_2$ (**2**) crystallized in the spacegroup $P2_1/c$ and has a dinuclear structure similar to **1**. The asymmetric unit contains half a molecule of **2** and an uncoordinated hexafluorophosphate anion. This structure of the cation contains a crystallographic inversion point in the center of the dimer that generates the other half of the molecule and a second hexafluorophosphate. Complex **2** also shows tetrahedral geometry with the ligand binding the copper centers in a head-to-tail fashion and an acetonitrile ligand in the apical position on the four-coordinate copper ion ($Cu–NCCH_3$ distance of 1.977(3) Å). The distance between the two copper atoms is 3.6809(7) Å, which is slightly contracted compared to the Cu–Cu distance in **1**.

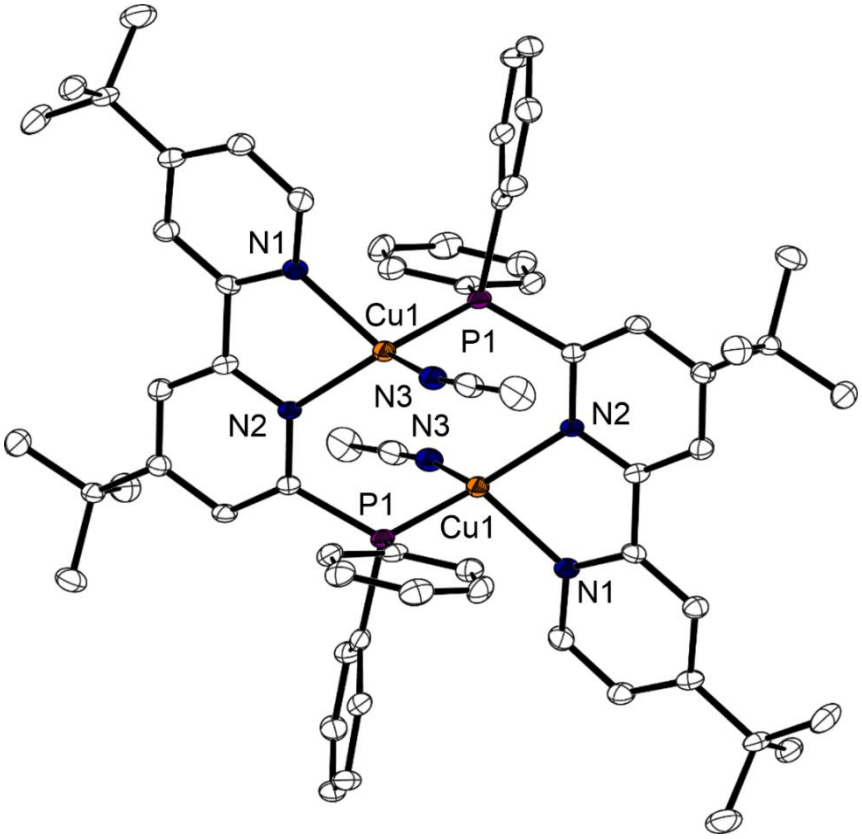

Figure 2-3. Thermal ellipsoid plots of $[Cu_2(\mu\text{-}PPh_2\text{-}t\text{Bu}_2\text{-bipy})_2(NCCH_3)_2](PF_6)_2$ (**2**) shown at the 50 % probability level. The hydrogen atoms and uncoordinated counter ions have been omitted for clarity. Selected bond lengths [Å] and angles [°]for one of the molecules in the unit cell: Cu(1)···Cu(1') 3.6809(7), Cu(1)–N(3) 1.377(3), Cu(1)–N(1) 2.062(2), Cu(1)–N(2) 2.054(2), Cu(1)–(P1#) 2.2074(10), N(3)–(C31) 1.140(4), N(3)–Cu(1)–N(1) 108.87(11), N(3)–Cu(1)–P(1#) 106.62(8), N(3)–Cu(1)–N(1) 79.81(9), N(2)–Cu(1)–(P1#) 124.49(11).

$[Cu_2(\mu\text{-P}i\text{Pr}_2\text{bipy})_2(NCCH_3)](PF_6)_2$ (**3**) crystallized in the spacegroup $P2_1/c$. The asymmetric unit contains two independent dinuclear complexes with slightly different bond lengths and angles, as well as two free acetonitrile molecules and four uncoordinated hexafluorphosphate anions . Similar to the previous compounds, this structure is dinuclear with the phosphino-bipyridine ligand coordinating the two copper centers in a head-to-tail fashion. However, in the structure of **3**, the copper ions are considerably closer to each other (2.6969(5)

Å in one of independent dinuclear molecules and 2.7067(5) Å in the other). The distances between the copper centers are slightly shorter than the sum of the van der Waals radii of Cu, which is 2.80 Å[13], indicative of weak cuprophillic interactions.[14-16] Another significant difference in the structure of **3** is that there is only one acetonitrile ligand that is coordinated to one of coppers showing tetrahedral coordination while the other copper is three coordinate . The distances between the coppers and the acetonitrile ligand are 2.008 and 2.533 in one of the dimers and 2.015 and 2.494 Å in the other dimer, showing that the acetonitrile is coordinated to only one copper center and is not acting as a bridging ligand between the coppers. In complex **3** it appears that the larger steric bulk of the isopropylphosphine ligand forces the coppers in a configuration where it would be difficult to fit two acentonitrile ligands in the pocket the coordinate both copper centers. Despite the structural differences between the structures of **1**, **2** and **5**, and structure of **3**, the overall difference in energy between the complexes appears to be small, as the spectroscopic and electrochemical features of all four complexes are very similar when they are dissolved in acetonitrile solutions (vide infra).

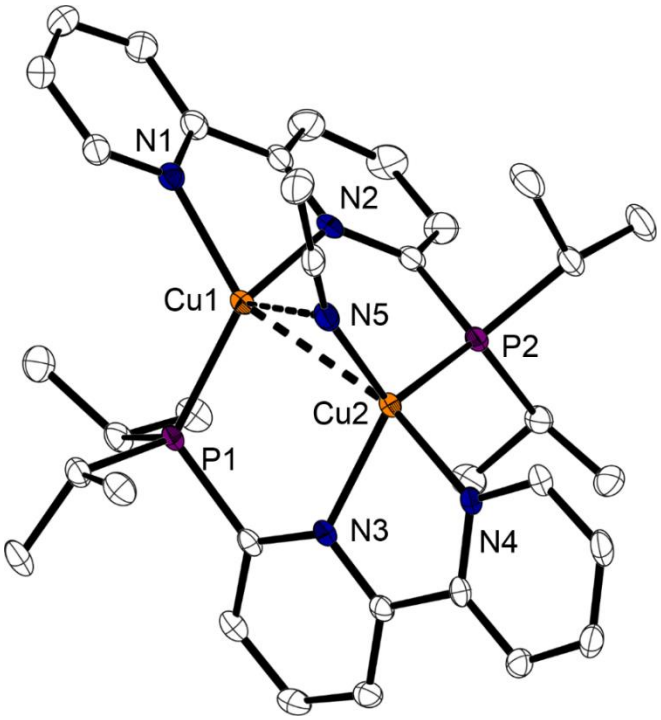

Figure 2-4. Thermal ellipsoid plots of $[Cu_2(\mu\text{-}P\textit{i}Pr_2bipy)_2(NCCH_3)](PF_6)_2$ (**3**) shown at the 50 % probability level. The hydrogen atoms and uncoordinated counter anion have been omitted for clarity, and only one of the dimers in the asymmetric unit is shown. Selected bond lengths [Å] and angles [°] for one of the molecules in the unit cell: Cu(1)–Cu(2) 2.7067(5), Cu(1)–N(1) 2.042(2), Cu(1)–N(2) 2.066(2), Cu(1)–N(5) 2.533(2), Cu(1)–P(1) 2.1848(6), Cu(2)–N(3) 2.090(2), Cu(2)–N(4) 2.068(2), Cu(2)–N(5) 2.008(2), Cu(2)–P(2) 2.2247(7), N(1)–Cu(1)–N(2) 79.85(8), N(1)–Cu(1)–N(5) 108.89(7), N(1)–Cu(1)–P(1) 122.40(6), N(2)–Cu(1)–N(5) 106.91(7), N(2)–Cu(1)–P(1) 127.44(6), N(5)–Cu(1)–P(1) 108.09(5), N(3)–Cu(2)–N(4) 78.68(7), N(3)–Cu(2)–N(5) 119.74(8), N(3)–Cu(2)–P(2) 115.33(5), N(4)–Cu(2)–N(5) 108.67(8), N(4)–Cu(2)–P(2) 110.02(5), N(5)–Cu(2)–P(2) 116.90(6).

It has previously been shown that d^{10}–d^{10} metal interactions can be strengthened by π-accepting bridging ligands.[17,18] This can be understood in terms of dπ* to bridging ligand π* backbonding effectively depopulating a metal–metal antibonding interaction to leave a net metal-metal bonding interaction. In complex **4**, we replaced the acetonitrile ligand with an isocyanide to observe how it changed the structure of the copper dimer. Complex **4** crystalized in the spacegroup *P*c. It is structurally very similar to **3**, except the acetonitrile ligand has been replaced with isopropyl isocyanide, which acts as bridge between the two copper centers in a

3 centered $2e^-$ bond, as has previously been seen in similar copper complexes.[19] Complex **4** is one of few Cu(I) dimers bridged by isocyanides.[19,20,21] Analogous to **3**, the asymmetric unit also contains two independent dinuclear complexes that have slightly different bond lengths and angles, as well as four uncoordinated hexafluorophosphate anions. The isocyanide ligand asymmetrically bonds to the copper centers of the dimers, as shown by the unequal copper cabon bond lengths (Cu(3)–C(37) 1.960(6) Å and Cu(4)–C(37) 2.165(6) Å). The bridging ligand tilts slightly towards one of the Cu centers in each dimer, suggesting the involvement of the nitrile π system in bonding.[22] The separation of the Cu(I)–Cu(I) centers in these two dimers is decreased by approximately 0.18 Å in comparison to **3,** with the dimeric copper cations in **4** having distances of 2.513(1) Å and 2.526(1) Å. We believe that the strong π-acceptor ability of isopropyl isocyanide results in more of the copper dπ* electron density donating to the π-acceptor bridging ligand, which increases the cuprophillic interactions.

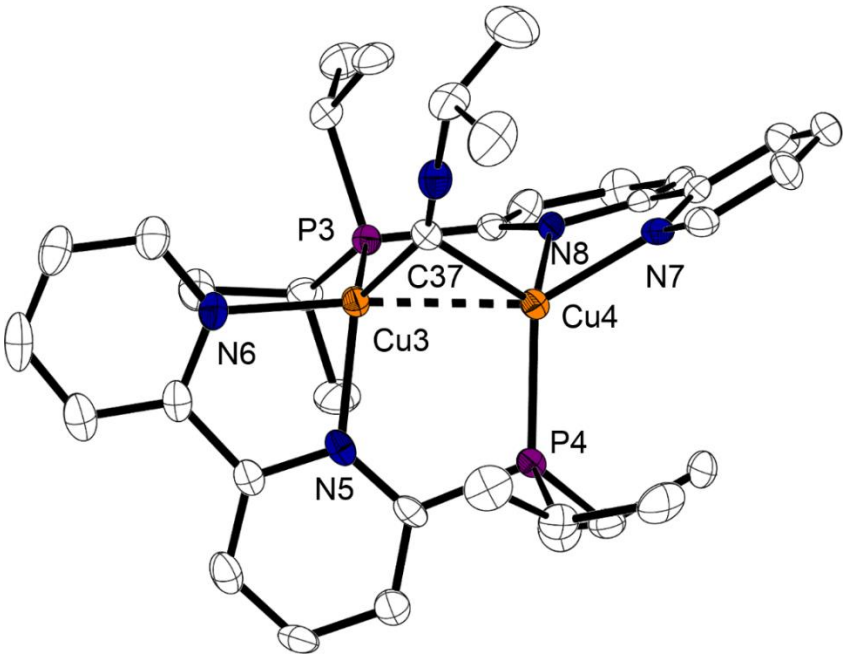

Figure 2-5. Thermal ellipsoid plots of $[Cu_2(\mu\text{-}P\textit{i}Pr_2bipy)_2(\mu\text{-}CNCH(CH_3)_2](PF_6)_2$ (**4**) shown at the 50 % probability level. The hydrogen atoms and uncoordinated counter ions have been omitted for clarity, and only one dimers of the unit cell is shown. Selected bond lengths [Å] and angles [°] for one of the molecules in the unit cell: Cu(3)…Cu(4) 2.526(1), Cu(3)–P(3) 2.268(2), Cu(3)–N(5) 2.062(6), Cu(3)–N(6) 2.050(5), Cu(3)–C(37) 1.960(6), Cu(4)–P(4) 2.225(2), Cu(4)–N(7) 2.054(5), Cu(4)–N(8) 2.100(5), Cu(4)–N(37) 2.165(6), P(3)–Cu(3)–N(5) 115.1(2), P(3)–Cu(3)–N(6) 106.8(2), P(3)–Cu(3)–C(37) 115.9(2), N(5)–Cu(3)–N(6) 80.0(2), N(5)–Cu(3)–C(37) 120.0(2), N(6)–Cu(3)–C(37) 121.2(1), P(4)–Cu(4)–N(7) 121.0(1), P(4)–Cu(4)–C(37) 116.0(2), N(7)–Cu(4)–N(8) 79.2(2), N(7)–Cu(4)–C(37) 104.8(2), N(8)–Cu(4)–C(37) 108.2(2)

2.3.3 Electrochemistry

The electrochemistry of the free ligands was examined in order to compare the reduction potentials to those of the metal complexes. The reduction potentials of the ligands are given in **Table 2-1**. The ligands **a**–**c** show a quasi-reviserible 1 e^- reduction followed by an irreversible reduction. The electrochemistry of the original phosphino-bipyridine ligand, Ph_2Pbipy (**d**), was also examined, and it showed similar reductions. As expected, these potentials are more positive than the potentials for ligands **a**, **b**, and **c**, which have more donating substituents. The two reductions observed in these ligands are attributed to the formation of the bipyridine radical anion and dianion species.[23]

Table 2-1. Reduction potentials of ligands and copper complexes

Compound	$E_{1/2}$	$E_{1/2}$	$E_{1/2}$	$E_{1/2}$
PPh_2-Me_2-bipy (**a**)	–2.20	–2.69[a]	—	—
PPh_2-*t*Bu_2-bipy (**b**)	–2.23	–2.75	—	—
P*i*Pr_2-bipy (**c**)	–2.00	–2.60[a,b]	—	—
PPh_2-bipy (**d**)	–2.02	–2.51[a]	—	—
1	–1.40	–1.65	–1.98	–2.21
2	–1.46	–1.66	–1.97	–2.11
3	–1.47	–1.66	–1.96	–2.14
4	–1.43	–1.64	–2.27[a]	—
5	–1.38	–1.56	–1.88	–2.03[c]

Potentials reported as V vs SCE, [a] Peaks are irreversible and reported as E cathodic, [b] Potentials are referenced to Ag/AgCl, [c] Potentials for the 4 reductions in the original complex, 5, were determined in this work.

Complexes **1–3** exhibit four quasi-reversible 1 e^- reductions in acetonitrile under an inert atmosphere (**Figure 2-5**). The reductions appear similar to the two bipyridine reductions seen in the ligand electrochemistry and are assigned to the formation of the bipyridine radical anion and dianion for both of the ligands in the dinuclear cation. This electrochemistry is different than that reported for the parent compound (**5**), where only two quasi-reversible 1 e^- reductions were described. Our re-examination of the electrochemistry of **5** revealed that it also had two more reductions in the cathodic region after the reported reductions (**Figure 2-6**). The reduction potentials of all complexes are given in **Table 2-1**. In the three new acetonititrile-coordinated complexes reported in this paper (**1**–**3**), the reductions occur at potentials that are slightly more negative compared to the original complex (**5**). This is expected because the methyl and *tert*-butyl substituents on the modified bipyridine ligands of **1** and **2** and the isopropyl groups in the phosphine of **3** make the ligands more electron-donating compared to the PPh_2bipy ligands on **5**. The electrochemistry of complex **4** in acetonitrile shows 2 quasi-reversible reductions. Scanning further negative, there is one more irreversible reduction. When scanning out to the third reduction, the reversibility of the first 2 peaks is lost on the

return scan, indicative of an irreversible chemical process happening at the third reduction. The cyclic voltammograms of complex **4** can be seen in **Figure 2-7**.

In the ligand electrochemistry, the peak separation between the first (bipyridine radical anion) and the second (bipyridinedianion) reductions is *ca.* 500 mV. The approximate peak separation between the first two reductions in the electrochemistry of **1**–**3** and **5** is *ca.* 200 mV and the separation between the first peaks and the third peaks are *ca.* 500 mV. In **4**, the peak separation between the first two reductions is also *ca. 200* mV. We conclude, on this basis that the reductions of the copper complexes are bipyridine-based and that 1 e^- sequentially goes into each bipyridine ring before the third and fourth electrons produce the bipyridine dianions in **1**–**3** and **5**. The *ca.* 200 mV separations between the first and second reductions of the complexes also indicates that there is some electronic communication between the two ligands, otherwise the first reduction would be a single 2 e^- reduction due to simultaneous 1e^- reductions of the two bipyridine ligands.

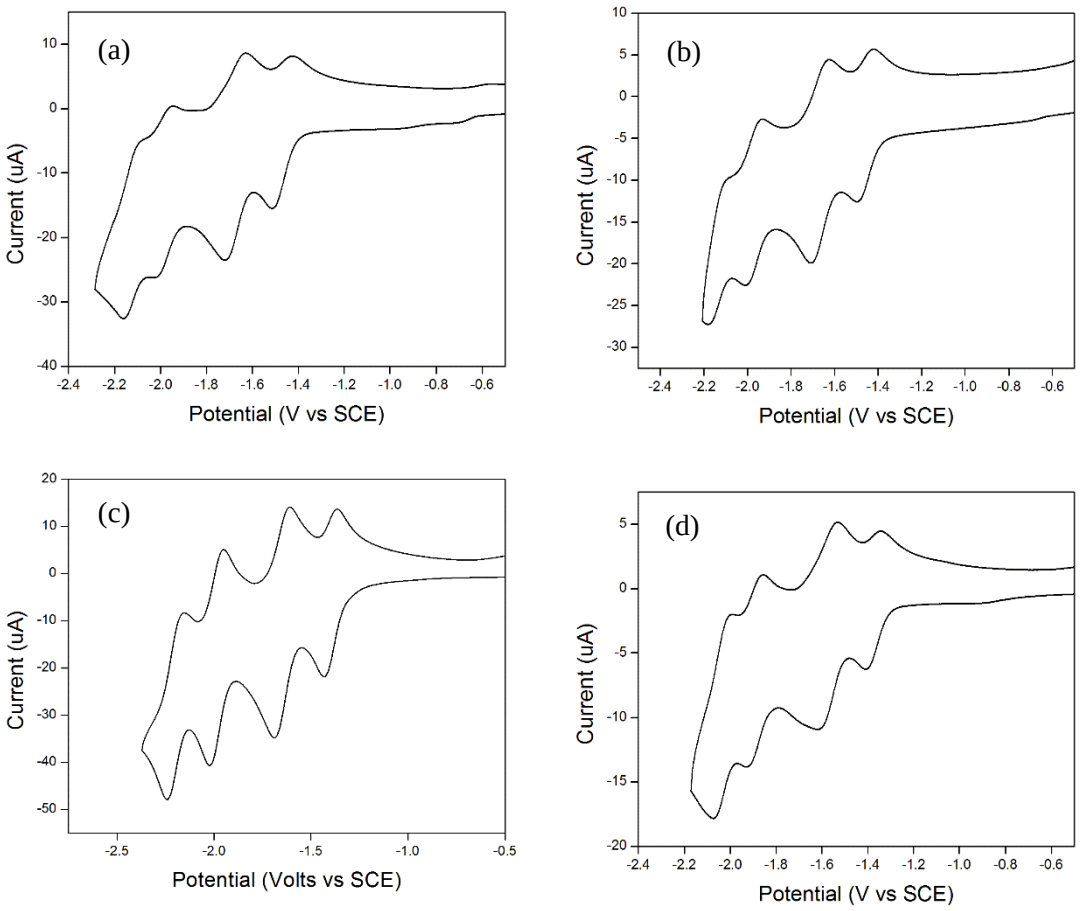

Figure 2-6. Cyclic voltammograms of $[Cu_2(\mu\text{-}PPh_2\text{-}Me_2\text{-}bipy)_2(NCCH_3)_2]$ $(PF_6)_2$ (a), $[Cu_2(\mu\text{-}PPh_2\text{-}t\text{Bu}_2\text{-}bipy)_2(NCCH_3)_2]$ $(PF_6)_2$ (b), $[Cu_2(\mu\text{-}P\textit{i}Pr_2bipy)_2(\mu\text{-}NCCH_3)](PF_6)_2$ (c), and of $[Cu_2(\mu\text{-}PPh_2\text{-}bipy)_2(NCCH_3)_2]$ $(PF_6)_2$ (d) in acetonitrile.

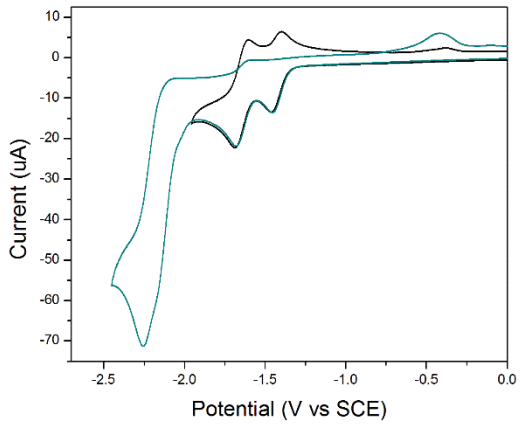

Figure 2-7. Cyclic voltammogram $Cu_2(\mu\text{-}PiPr_2bipy)_2(\mu\text{-}CNCH(CH_3)_2)](PF_6)_2$ (**4**) in acetonitrile.

Reactivity of CO_2

Under an atmosphere of CO_2, complexes **1**–**3** exhibit increases in current at the second reduction and the disappearance of the returning oxidation waves (**Figure 2-8**). After re-sparging with nitrogen, the original CV responses are restored. This behavior is indicative of a reduction of CO_2. The amount of current enhancement is similar for complexes **1**, **2**, and **3** as well as for the original complex **5**. It is notable that all of the complexes catalyze the reduction of CO_2 with similar current enhancements (1.5 to 1.7 x increase at the peak current) and at similar potentials (–1.56 to –1.66 V vs SCE). Under an atmosphere of CO_2, **4** shows no current enhancement at the second reduction. This is attributed to the fact that the loss of the labile acetonitrile ligand is necessary for CO_2 to bind to the copper center. With the more strongly binding isocyanide ligand, CO_2 is likely unable to coordinate to the copper centers.

In order to assess the products of CO_2 reduction and determine the faradaic efficiencies of their formations, attemps were made to do bulk electrolysis experiments with GC analysis. In bulk electrolysis experiments, we did observe the formation of CO as current was passed, but we were never able to obtain faradaic efficiences anywhere near those that had been

reported for the origional complex, **5** (the previous publication reported 50% faradaic efficiency for CO formation). Attempts to repeat bulk electrolysis experiments with **5** also produced similar results; formation of CO at low current efficiencies (*ca*. 20%).

We aslo did spectroelectrochemical experiments with complex **5** and with some of the newly synthesized complexes to monitor the formation of carbonate, but these experiments did not conclusively tell us if the complexes were catalyzing CO_2 reduction to CO and CO_3^{2-}. In the IR spectroelectrochemistry experiments done previously, the working electrode used was a platinum coin, which can act as a catalyst for CO_2 reduction itself to form CO and carbonate.[24] Control experiments using an IR spectroelectrochemical cell similar to the one used in the previous publication[2] with a platinum working electrode, CO_2 saturated acetonitrile solution, and no complex also lead to the production of carbonate, as was seen in the previously published experiments. In the previous publication the formation of carbonate was attributed to the reduction of CO_2 to CO and CO_3^{2-} by the copper complex, but it is very likely that the carbonate was produced from CO_2 reduction by the electrode.

Based on these results, it is clear that the copper complexes **1**–**3** and the previously reported complex **5** do catalyze the reduction of CO_2 to CO, albeit with low efficiences. Whether the other oxygen from CO_2 is going to the formation of carbonate or water is still unclear. In light of the low efficiencies for the formation of CO by these complexes, and the lack of improvements to catalysis by making ligand substitutions, we decided to move on from studying this system for CO_2 redution.

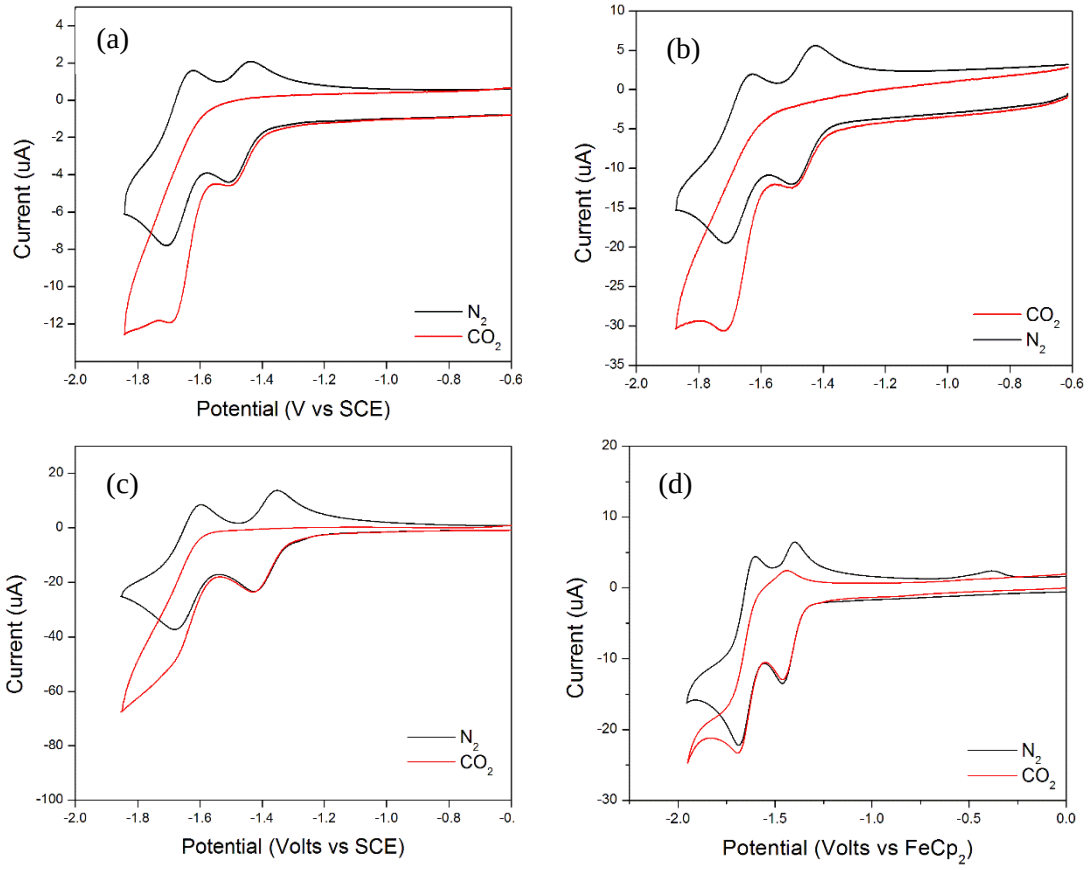

Figure 2-8. Cyclic voltammograms of $[Cu_2(\mu\text{-}PPh_2\text{-}Me_2\text{-}bipy)_2(NCCH_3)_2]$ $(PF_6)_2$ (a), $[Cu_2(\mu\text{-}PPh_2\text{-}t\text{Bu}_2\text{-}bipy)_2(NCCH_3)_2]$ $(PF_6)_2$ (b), $[Cu_2(\mu\text{-}P\textit{i}Pr_2bipy)_2(NCCH_3)](PF_6)_2$ (c), and of $Cu_2(\mu\text{-}P\textit{i}Pr_2bipy)_2(\mu\text{-}CNCH(CH_3)_2)](PF_6)_2$ (d) in acetonitrile under N_2 and CO_2 atmospheres.

2.4 Conclusions

In this chapter, we attempted to make improvements in and gain a better understanding of how the previously reported dinuclear copper complex catalyzed the two electron reduction of CO_2 to CO and CO_3-. We made ligand modifications in attempts to make these complexes more powerful reductants, hoping that that would help to speed up rates for CO_2 reduction.

The stuctures of the new 4,4‘ dimethyl and 4,4‘ ditertbutyl copper complexes **1** and **2** are very similar to the previously reported complex **5**. The structure of complex **3** is

significantly different. The coppers in the dimers in complex **3** show close copper copper distances, indicative of cuprophilic interactions, and contain one copper center that is four coordinate with an acetonitrile ligand with the other copper being three coordinate. The acetonitrile ligand can be replaced with and isocyanide ligand to form a rare isocyanide bridged copper core showing increased cuprophillic interactions. This platform could potentially be used to study the interaction of small molecules with dinuclear copper centers.

Complexes **1**–**3** show increases in current under CO_2 indicative of electrocatalytic CO_2 reduction and bulk electrolysis studies reveal CO is a major product. The current efficiencies for the formation of CO are low (20%) and no enhancements in activity were observed by increasing the reducing power of the copper dianions with electron donating substituents. With these findings, we decided to to end further studies of the CO_2 reduction by these complexes, although these complexes are still notable despite their low efficincies for CO_2 reduction, as only one other electrocatalytic copper based system has been reported.

2.5 References

(1) Field, J. S.; Haines, R. J.; Parry, C. J.; Sookraj, S. H. *Polyhedron*, **1993**, *12*, 2425-2428.

(2) Haines, R. J.; Wittrig, R. E.; Kubiak, C. P. *Inorg. Chem.* , **1994**, *33*, 4723-4728.

(3) Hori, Y.; Wakebe, H.; Tsukamoto, T.; Koga, O. *Electrochim. Acta.*, **1994**, *39*, 1833-1839.

(4) Angamuthu, R.; Byers, P.; Lutz, M.; Spek, A. L.; Bouwman, E. *Science* **2010**, *327*, 313-315.

(5) Solomon, E. I.; Sundaram, U. M.; Machonkin, T. E. *Chem. Rev.* , **1996**, *96*, 2563-2606.

(6) Scarborough, C. C.; Wieghardt, K. *Inorg. Chem.* , **2011**, *50*, 9773-9793.

(7) Shin, D.; Switzer, C. *Chem. Comm.* , **2007**, 4401-4403.

(8) Della Ciana, L.; Hamachi, I.; Meyer, T. J. *J. Org. Chem.* , **1989**, *54*, 1731-1735.

(9) Field, J. S. H.; Haines, R., J.; Parry, C. J.; Sookraj, S. H. *S. Africa. J. Chem.*, **1993**, *46*, 70.

(10) Zavarine, I. S.; Kubiak, C. P. *J. Electroanal. Chem.* , **2001**, *495*, 106-109.

(11) Sheldrick, G. M. *Acta Crystallogr., Sect. A: Found. Crystallogr.* , **2008**, *64*, 112-122.

(12) Yang, L.; Powell, D. R.; Houser, R. P. *Dalton Trans.* , **2007**, 955-964.

(13) Bondi, A. *J. Phys. Chem.* , **1964**, *68*, 441-451.

(14) Merz, K. M.; Hoffmann, R. *Inorg. Chem.* , **1988**, *27*, 2120-2127.

(15) Mehrotra, P. K.; Hoffmann, R. *Inorg. Chem.* , **1978**, *17*, 2187-2189.

(16) Pyykkö, P. *Chem. Rev.* , **1997**, *97*, 597-636.

(17) Ratliff, K. S.; Delaet, D. L.; Gao, J.; Fanwick, P. E.; Kubiak, C. P. *Inorg. Chem.*, **1990**, *29*, 4022-4027.

(18) Bera, J. K.; Nethaji, M.; Samuelson, A. G. *Inorg. Chem.* , **1998**, *38*, 218-228.

(19) Davenport, T. C.; Tilley, T. D. *Angew. Chem. Int. Ed.*, **2011**, *50*, 12205-12208.

(20) Diez, J.; Gamasa, M. P.; Gimeno, J.; Aguirre, A.; Garcia-Granda, S. *Organometallics*, **1991**, *10*, 380-382.

(21) Fournier, É.; Lebrun, F.; Drouin, M.; Decken, A.; Harvey, P. D. *Inorg. Chem.* , **2004**, *43*, 3127-3135.

(22) Germain, M. E.; Temprado, M.; Castonguay, A.; Kryatova, O. P.; Rybak-Akimova, E. V.; Curley, J. J.; Mendiratta, A.; Tsai, Y.-C.; Cummins, C. C.; Prabhakar, R.; McDonough, J. E.; Hoff, C. D. *J. Am. Chem. Soc.* , **2009**, *131*, 15412-15423.

(23) Gore-Randall, E.; Irwin, M.; Denning, M. S.; Goicoechea, J. M. *Inorg. Chem.* , **2009**, *48*, 8304-8316.

(24) Christensen, P. A.; Hamnett, A.; Muir, A. V. G.; Freeman, N. A. *J. Electroanal. Chem.* , **1990**, *288*, 197-215.

2.6 Appendix

2.6.1 Crystal data for $[Cu_2(\mu\text{-}PPh_2\text{-}Me_2\text{-}bipy)_2(NCCH_3)_2](PF_6)_2$ (1)

Crystals of $[Cu_2(\mu\text{-}PPh_2\text{-}Me_2\text{-}bipy)_2(NCCH_3)_2](PF_6)_2$ were found to have crystalized in the P-1 space group with half a molecule per asymmetric unit (Z' = 0.5). The rest of the molecule is generated by a crystallographic inversion center in the middle of the dication. The asymmetric unit also contains one uncoordinated hexafluorophosphate counter ion and one uncoordinated methylene chloride molecule. The hexafluorophosphate ion showed positional disorder and was modeled. The data set was modeled to 3.35% (2Θ)

Table 2-2. Crystal data and structure refinement for $[Cu_2(\mu\text{-}PPh_2\text{-}Me_2\text{-}bipy)_2(NCCH_3)_2](PF_6)_2$ (**1**)

Identification code	Work
Empirical formula	C54 H52 Cl4 Cu2 F12 N6 P4
Formula weight	1405.78
Temperature	100(2) K
Wavelength	0.71073 Å
Crystal system	Triclinic
Space group	P-1
Unit cell dimensions	a = 10.5600(10) Å α= 78.9710(10)°. b = 10.5675(10) Å β= 70.9080(10)°. c = 14.2924(13) Å γ = 85.8240(10)°.
Volume	1479.3(2) $Å^3$
Z	1
Density (calculated)	1.578 Mg/m^3
Absorption coefficient	1.088 mm^{-1}
F(000)	712
Crystal size	0.40 x 0.20 x 0.20 mm^3
Theta range for data collection	1.96 to 25.43°.
Index ranges	-12<=h<=12, -12<=k<=12, -17<=l<=17
Reflections collected	18640
Independent reflections	5470 [R(int) = 0.0316]
Completeness to theta = 25.00°	99.9 %
Absorption correction	Semi-empirical from equivalents
Max. and min. transmission	0.8117 and 0.6700
Refinement method	Full-matrix least-squares on F^2
Data / restraints / parameters	5470 / 72 / 428
Goodness-of-fit on F^2	1.030
Final R indices [I>2sigma(I)]	R1 = 0.0335, wR2 = 0.0804
R indices (all data)	R1 = 0.0390, wR2 = 0.0846
Extinction coefficient	not measured
Largest diff. peak and hole	0.435 and -0.395 $e.Å^{-3}$

Table 2-3. Bond lengths [Å] and angles [°] for $[Cu_2(\mu\text{-}PPh_2\text{-}Me_2\text{-}bipy)_2(NCCH_3)_2](PF_6)_2$ (**1**)

Cu(1)-N(3)	2.003(2)	Cu(1)-N(2)	2.087(2)
Cu(1)-N(1)	2.091(2)	Cu(1)-P(1)	2.1991(7)
P(1)-C(1)	1.0817(2)	P(1)-C(7)	1.830(2)
P(1)-C(22)	1.844(2)	N(1)-C(14)	1.342(3)
N(1)-C(15)	1.348(3)	N(2)-C(16)	1.352(3)
N(2)-C(22)#1	1.353(3)	N(3)-C(26)	1.135(3)
C(1)-C(2)	1.391(4)	C(1)-C(3)	1.396(3)
C(2)-C(4)	1.384(4)	C(2)-H(2)	0.9500
C(3)-C(5)	1.382(4)	C(3)-H(3)	0.9500
C(4)-C(6)	1.385(4)	C(4)-H(4)	0.9500
C(5)-C(6)	1.379(4)	C(5)-H(5)	0.9500
C(6)-H(6)	0.9500	C(7)-C(9)	1.390(3)
C(7)-C(8)	1.395(4)	C(8)-C(12)	1.387(4)
C(8)-H(8)	0.9500	C(9)-C(10)	1.387(4)
C(9)-H(9)	0.9500	C(10)-C(11)	1.376(4)
C(10)-H(10)	0.9500	C(11)-C(12)	1.380(4)
C(11)-H(11)	0.9500	C(12)-H(12)	0.9500
C(14)-C(19)	1.378(4)	C(14)-H(14)	0.9500
C(15)-C(18)	1.391(4)	C(15)-C(16)	1.488(4)
C(16)-C(17)	1.393(4)	C(17)-C(24)	1.386(4)
C(17)-H(17)	0.9500	C(18)-C(20)	1.391(4)
C(18)-H(18)	0.9500	C(19)-C(20)	1.382(4)
C(19)-H(19)	0.9500	C(20)-C(21)	1.505(4)
C(21)-H(21A)	0.9800	C(21)-H(21B)	0.9800
C(21)-H(21C)	0.9800	C(22)-N(2)#1	1.353(3)
C(22)-C(23)	1.379(3)	C(23)-C(24)#1	1.393(4)
C(23)-H(23)	0.9500	C(24)-C(23)#1	1.393(4)
C(24)-C(25)	1.501(4)	C(25)-H(25A)	0.9800
C(25)-H(25B)	0.9800	C(25)-H(25C)	0.9800
C(26)-C(27)	1.457(4)	C(27)-H(27A)	0.9800
C(27)-H(27B)	0.9800	C(27)-H(27C)	0.9800
Cl(1S)-C(1S)	1.770(3)	Cl(2S)-C(1S)	1.747(4)
C(1S)-H(1SA)	0.9900	C(1S)-H(1SB)	0.9900
P(2)-F(4B)	1.385(7)	P(2)-F(5)	1.506(4)
P(2)-F(6)	1.519(4)	P(2)-F(2)	1.540(8)
P(2)-F(2B)	1.544(10)	P(2)-F(3B)	1.550(7)
P(2)-F(5B)	1.560(9)	P(2)-F(1)	1.562(5)
P(2)-F(3)	1.586(4)	P(2)-F(1B)	1.610(7)

Table 2-3. (cont'd)

P(2)-F(4)	1.615(4)	P(2)-F(6B)	1.677(7)
N(3)-Cu(1)-N(2)	108.95(8)	N(3)-Cu(1)-N(1)	98.81(9)
N(2)-Cu(1)-N(1)	79.10(8)	N(3)-Cu(1)-P(1)	119.67(7)
N(2)-Cu(1)-P(1)	127.09(6)	N(1)-Cu(1)-P(1)	110.89(6)
C(1)-P(1)-C(7)	103.32(11)	C(1)-P(1)-C(22)	102.07(11)
C(7)-P(1)-C(22)	102.05(11)	C(1)-P(1)-Cu(1)	116.03(8)
C(7)-P(1)-Cu(1)	109.91(8)	C(22)-P(1)-Cu(1)	121.24(8)
C(14)-N(1)-C(15)	117.7(2)	C(14)-N(1)-Cu(1)	127.33(18)
C(15)-N(1)-Cu(1)	114.95(17)	C(16)-N(2)-C(22)#1	118.1(2)
C(16)-N(2)-Cu(1)	114.45(16)	C(22)#1-N(2)-Cu(1)	127.32(16)
C(26)-N(3)-Cu(1)	176.0(2)	C(2)-C(1)-C(3)	119.4(2)
C(2)-C(1)-P(1)	122.64(19)	C(3)-C(1)-P(1)	117.76(19)
C(4)-C(2)-C(1)	120.1(2)	C(4)-C(2)-H(2)	119.9
C(1)-C(2)-H(2)	119.9	C(5)-C(3)-C(1)	120.1(3)
C(5)-C(3)-H(3)	120.0	C(1)-C(3)-H(3)	120.0
C(2)-C(4)-C(6)	119.9(3)	C(2)-C(4)-H(4)	120.1
C(6)-C(4)-H(4)	120.1	C(6)-C(5)-C(3)	120.1(3)
C(6)-C(5)-H(5)	120.0	C(3)-C(5)-H(5)	120.0
C(5)-C(6)-C(4)	120.4(3)	C(5)-C(6)-H(6)	119.8
C(4)-C(6)-H(6)	119.8	C(9)-C(7)-C(8)	118.8(2)
C(9)-C(7)-P(1)	123.5(2)	C(8)-C(7)-P(1)	117.70(19)
C(12)-C(8)-C(7)	120.5(2)	C(12)-C(8)-H(8)	119.7
C(7)-C(8)-H(8)	119.7	C(10)-C(9)-C(7)	120.3(3)
C(10)-C(9)-H(9)	119.8	C(7)-C(9)-H(9)	119.8
C(11)-C(10)-C(9)	120.4(3)	C(11)-C(10)-H(10)	119.8
C(9)-C(10)-H(10)	119.8	C(10)-C(11)-C(12)	120.1(3)
C(10)-C(11)-H(11)	120.0	C(12)-C(11)-H(11)	120.0
C(11)-C(12)-C(8)	119.9(3)	C(11)-C(12)-H(12)	120.0
C(8)-C(12)-H(12)	120.0	N(1)-C(14)-C(19)	123.4(3)
N(1)-C(14)-H(14)	118.3	C(19)-C(14)-H(14)	118.3
N(1)-C(15)-C(18)	121.8(2)	N(1)-C(15)-C(16)	115.3(2)
C(18)-C(15)-C(16)	122.9(2)	N(2)-C(16)-C(17)	121.7(2)
N(2)-C(16)-C(15)	116.2(2)	C(17)-C(16)-C(15)	122.1(2)
C(24)-C(17)-C(16)	120.3(2)	C(24)-C(17)-H(17)	119.8
C(16)-C(17)-H(17)	119.8	C(20)-C(18)-C(15)	120.1(3)
C(20)-C(18)-H(18)	119.9	C(15)-C(18)-H(18)	119.9
C(14)-C(19)-C(20)	119.6(3)	C(14)-C(19)-H(19)	120.2
C(20)-C(19)-H(19)	120.2	C(19)-C(20)-C(18)	117.5(2)

Table 2-3. (cont'd)

C(19)-C(20)-C(21)	121.4(3)	C(18)-C(20)-C(21)	121.2(3)
C(20)-C(21)-H(21A)	109.5	C(20)-C(21)-H(21B)	109.5
H(21A)-C(21)-H(21B)	109.5	C(20)-C(21)-H(21C)	109.5
H(21A)-C(21)-H(21C)	109.5	H(21B)-C(21)-H(21C)	109.5
N(2)#1-C(22)-C(23)	122.3(2)	N(2)#1-C(22)-P(1)	114.87(17)
C(23)-C(22)-P(1)	122.79(19)	C(22)-C(23)-C(24)#1	120.2(2)
C(22)-C(23)-H(23)	119.9	C(24)#1-C(23)-H(23)	119.9
C(17)-C(24)-C(23)#1	117.3(2)	C(17)-C(24)-C(25)	121.6(2)
C(23)#1-C(24)-C(25)	121.0(2)	C(24)-C(25)-H(25A)	109.5
C(24)-C(25)-H(25B)	109.5	H(25A)-C(25)-H(25B)	109.5
C(24)-C(25)-H(25C)	109.5	H(25A)-C(25)-H(25C)	109.5
H(25B)-C(25)-H(25C)	109.5	N(3)-C(26)-C(27)	179.4(3)
C(26)-C(27)-H(27A)	109.5	C(26)-C(27)-H(27B)	109.5
H(27A)-C(27)-H(27B)	109.5	C(26)-C(27)-H(27C)	109.5
H(27A)-C(27)-H(27C)	109.5	H(27B)-C(27)-H(27C)	109.5
Cl(2S)-C(1S)-Cl(1S)	111.74(19)	Cl(2S)-C(1S)-H(1SA)	109.3
Cl(1S)-C(1S)-H(1SA)	109.3	Cl(2S)-C(1S)-H(1SB)	109.3
Cl(1S)-C(1S)-H(1SB)	109.3	H(1SA)-C(1S)-H(1SB)	107.9
F(4B)-P(2)-F(5)	126.7(8)	F(4B)-P(2)-F(6)	126.8(9)
F(5)-P(2)-F(6)	96.4(4)	F(4B)-P(2)-F(2)	113.3(7)
F(5)-P(2)-F(2)	89.9(4)	F(6)-P(2)-F(2)	93.9(4)
F(4B)-P(2)-F(2B)	97.8(8)	F(5)-P(2)-F(2B)	104.3(6)
F(6)-P(2)-F(2B)	99.9(4)	F(2)-P(2)-F(2B)	16.4(7)
F(4B)-P(2)-F(3B)	96.1(9)	F(5)-P(2)-F(3B)	131.3(7)
F(6)-P(2)-F(3B)	34.9(5)	F(2)-P(2)-F(3B)	93.2(4)
F(2B)-P(2)-F(3B)	89.5(5)	F(4B)-P(2)-F(5B)	98.0(9)
F(5)-P(2)-F(5B)	34.4(5)	F(6)-P(2)-F(5B)	130.6(7)
F(2)-P(2)-F(5B)	84.7(5)	F(2B)-P(2)-F(5B)	92.4(6)
F(3B)-P(2)-F(5B)	165.3(8)	F(4B)-P(2)-F(1)	60.8(6)
F(5)-P(2)-F(1)	92.5(4)	F(6)-P(2)-F(1)	91.6(3)
F(2)-P(2)-F(1)	173.8(5)	F(2B)-P(2)-F(1)	158.3(6)
F(3B)-P(2)-F(1)	89.6(3)	F(5B)-P(2)-F(1)	94.0(4)
F(4B)-P(2)-F(3)	52.5(7)	F(5)-P(2)-F(3)	177.9(4)
F(6)-P(2)-F(3)	85.3(3)	F(2)-P(2)-F(3)	88.8(4)
F(2B)-P(2)-F(3)	74.2(5)	F(3B)-P(2)-F(3)	50.5(5)
F(5B)-P(2)-F(3)	143.7(6)	F(1)-P(2)-F(3)	88.6(4)
F(4B)-P(2)-F(1B)	92.1(6)	F(5)-P(2)-F(1B)	70.2(4)
F(6)-P(2)-F(1B)	73.0(4)	F(2)-P(2)-F(1B)	154.2(4)

Table 2-3. (cont'd)

F(2B)-P(2)-F(1B)	170.0(5)	F(3B)-P(2)-F(1B)	88.3(5)
F(5B)-P(2)-F(1B)	87.3(5)	F(1)-P(2)-F(1B)	31.4(3)
F(3)-P(2)-F(1B)	111.5(4)	F(4B)-P(2)-F(4)	47.3(7)
F(5)-P(2)-F(4)	87.8(3)	F(6)-P(2)-F(4)	173.9(3)
F(2)-P(2)-F(4)	90.4(4)	F(2B)-P(2)-F(4)	83.2(4)
F(3B)-P(2)-F(4)	140.6(6)	F(5B)-P(2)-F(4)	54.0(6)
F(1)-P(2)-F(4)	83.9(3)	F(3)-P(2)-F(4)	90.5(3)
F(1B)-P(2)-F(4)	104.6(4)	F(4B)-P(2)-F(6B)	173.8(8)
F(5)-P(2)-F(6B)	55.1(5)	F(6)-P(2)-F(6B)	48.1(5)
F(2)-P(2)-F(6B)	72.0(5)	F(2B)-P(2)-F(6B)	87.0(6)
F(3B)-P(2)-F(6B)	80.0(7)	F(5B)-P(2)-F(6B)	85.6(7)
F(1)-P(2)-F(6B)	114.1(5)	F(3)-P(2)-F(6B)	126.0(5)
F(1B)-P(2)-F(6B)	83.0(5)	F(4)-P(2)-F(6B)	137.7(5)

2.6.2 Crystal data for $[Cu_2(\mu\text{-}PPh_2\text{-}t\text{Bu}_2\text{-bipy})_2(NCCH_3)_2](PF_6)_2$ (2)

Crystals of $[Cu_2(\mu\text{-}PPh_2\text{-}tBu_2\text{-bipy})_2(NCCH_3)_2](PF_6)_2$ were found to have crystalized in the P2(1)/c space group with half a molecule per asymmetric unit (Z' = 0.5). The rest of the molecule is generated by a crystallographic inversion center in the middle of the dication. The asymmetric unit also contains one uncoordinated counter anion. The data was modeled to 5.27% (2Θ)

Table 2-4. Crystal data and structure refinement for $[Cu_2(\mu\text{-}PPh_2\text{-}t\text{Bu}_2\text{-bipy})_2(NCCH_3)_2](PF_6)_2$ (**2**)

Identification code	alyssia03_0m	
Empirical formula	C64 H72 Cu2 F12 N6 P4	
Formula weight	1404.24	
Temperature	100(2) K	
Wavelength	0.71073 Å	
Crystal system	Monoclinic	
Space group	P2(1)/c	
Unit cell dimensions	a = 11.3120(16) Å	α= 90°.
	b = 14.811(2) Å	β= 100.230(2)°.
	c = 19.456(3) Å	γ = 90°.
Volume	3207.7(8) Å^3	
Z	2	
Density (calculated)	1.454 Mg/m^3	
Absorption coefficient	0.843 mm^{-1}	
F(000)	1448	
Crystal size	0.40 x 0.20 x 0.20 mm^3	
Theta range for data collection	1.74 to 28.33°.	
Index ranges	-14<=h<=15, -18<=k<=19, -24<=l<=25	
Independent reflections	7114 [R(int) = 0.0678]	
Completeness to theta = 25.00°	99.5 %	
Absorption correction	Semi-empirical from equivalents	
Max. and min. transmission	0.8495 and 0.7292	
Refinement method	Full-matrix least-squares on F^2	
Data / restraints / parameters	7114 / 0 / 404	
Goodness-of-fit on F^2	1.002	
Final R indices [I>2sigma(I)]	R1 = 0.0529, wR2 = 0.1202	
R indices (all data)	R1 = 0.0884, wR2 = 0.1370	
Extinction coefficient	not measured	
Largest diff. peak and hole	1.189 and -0.830 e.Å^{-3}	

Table 2-5. Bond lengths [Å] and angles [°] for $[Cu_2(\mu\text{-}PPh_2\text{-}t\text{Bu}_2\text{-bipy})_2(NCCH_3)_2](PF_6)_2$ (**2**)

Cu(1)-N(3)	1.977(3)	Cu(1)-N(2)	2.054(2)
Cu(1)-N(1)	2.062(2)	Cu(1)-P(1)#1	2.2074(10)
P(1)-C(25)	1.810(4)	P(1)-C(18)	1.833(3)
P(1)-C(19)	1.842(3)	P(1)-Cu(1)#1	2.2074(10)
N(1)-C(1)	1.344(4)	N(1)-C(9)	1.345(4)
N(2)-C(10)	1.349(4)	N(2)-C(18)	1.360(3)
N(3)-C(31)	1.140(4)	C(1)-C(2)	1.377(4)
C(1)-H(1)	0.9500	C(2)-C(3)	1.386(4)
C(2)-H(2)	0.9500	C(3)-C(8)	1.396(4)
C(3)-C(4)	1.534(4)	C(4)-C(7)	1.523(4)
C(4)-C(5)	1.531(5)	C(4)-C(6)	1.531(5)
C(5)-H(5A)	0.9800	C(5)-H(5B)	0.9800
C(5)-H(5C)	0.9800	C(6)-H(6A)	0.9800
C(6)-H(6B)	0.9800	C(6)-H(6C)	0.9800
C(7)-H(7A)	0.9800	C(7)-H(7B)	0.9800
C(7)-H(7C)	0.9800	C(8)-C(9)	1.389(4)
C(8)-H(8)	0.9500	C(9)-C(10)	1.495(4)
C(10)-C(11)	1.388(4)	C(11)-C(12)	1.391(4)
C(11)-H(11)	0.9500	C(12)-C(17)	1.399(4)
C(12)-C(13)	1.521(4)	C(13)-C(15)	1.522(5)
C(13)-C(14)	1.530(4)	C(13)-C(16)	1.543(4)
C(14)-H(14A)	0.9800	C(14)-H(14B)	0.9800
C(14)-H(14C)	0.9800	C(15)-H(15A)	0.9800
C(15)-H(15B)	0.9800	C(15)-H(15C)	0.9800
C(16)-H(16A)	0.9800	C(16)-H(16B)	0.9800
C(16)-H(16C)	0.9800	C(17)-C(18)	1.382(4)
C(17)-H(17)	0.9500	C(19)-C(24)	1.382(5)
C(19)-C(20)	1.390(5)	C(20)-C(21)	1.390(4)
C(20)-H(20)	0.9500	C(21)-C(22)	1.377(5)
C(21)-H(21)	0.9500	C(22)-C(23)	1.370(5)
C(22)-H(22)	0.9500	C(23)-C(24)	1.395(4)
C(23)-H(23)	0.9500	C(24)-H(24)	0.9500
C(25)-C(26)	1.391(5)	C(25)-C(30)	1.396(4)
C(26)-C(27)	1.373(5)	C(26)-H(26)	0.9500
C(27)-C(28)	1.400(5)	C(27)-H(27)	0.9500
C(28)-C(29)	1.383(5)	C(28)-H(28)	0.9500
C(29)-C(30)	1.381(5)	C(29)-H(29)	0.9500
C(30)-H(30)	0.9500	C(31)-C(32)	1.459(5)

Table 2-5. (cont'd)

C(32)-H(32A)	0.9800	C(32)-H(32B)	0.9800
C(32)-H(32C)	0.9800	P(2)-F(4)	1.587(2)
P(2)-F(6)	1.593(2)	P(2)-F(2)	1.593(2)
P(2)-F(1)	1.597(2)	P(2)-F(3)	1.599(2)
P(2)-F(5)	1.600(2)	N(3)-Cu(1)-N(2)	124.49(11)
N(3)-Cu(1)-N(1)	108.87(11)	N(2)-Cu(1)-N(1)	79.81(9)
N(3)-Cu(1)-P(1)#1	106.62(8)	N(2)-Cu(1)-P(1)#1	121.75(8)
N(1)-Cu(1)-P(1)#1	110.25(8)	C(25)-P(1)-C(18)	104.38(15)
C(25)-P(1)-C(19)	101.95(14)	C(18)-P(1)-C(19)	104.50(12)
C(25)-P(1)-Cu(1)#1	122.07(10)	C(18)-P(1)-Cu(1)#1	112.27(11)
C(19)-P(1)-Cu(1)#1	109.93(11)	C(1)-N(1)-C(9)	118.2(2)
C(1)-N(1)-Cu(1)	127.3(2)	C(9)-N(1)-Cu(1)	113.92(18)
C(10)-N(2)-C(18)	117.7(2)	C(10)-N(2)-Cu(1)	113.78(18)
C(18)-N(2)-Cu(1)	127.98(19)	C(31)-N(3)-Cu(1)	169.9(3)
N(1)-C(1)-C(2)	122.2(3)	N(1)-C(1)-H(1)	118.9
C(2)-C(1)-H(1)	118.9	C(1)-C(2)-C(3)	120.7(3)
C(1)-C(2)-H(2)	119.7	C(3)-C(2)-H(2)	119.7
C(2)-C(3)-C(8)	116.7(3)	C(2)-C(3)-C(4)	120.4(3)
C(8)-C(3)-C(4)	122.9(3)	C(7)-C(4)-C(5)	108.2(3)
C(7)-C(4)-C(6)	108.5(3)	C(5)-C(4)-C(6)	109.5(3)
C(7)-C(4)-C(3)	112.7(3)	C(5)-C(4)-C(3)	108.5(3)
C(6)-C(4)-C(3)	109.3(3)	C(4)-C(5)-H(5A)	109.5
C(4)-C(5)-H(5B)	109.5	H(5A)-C(5)-H(5B)	109.5
C(4)-C(5)-H(5C)	109.5	H(5A)-C(5)-H(5C)	109.5
H(5B)-C(5)-H(5C)	109.5	C(4)-C(6)-H(6A)	109.5
C(4)-C(6)-H(6B)	109.5	H(6A)-C(6)-H(6B)	109.5
C(4)-C(6)-H(6C)	109.5	H(6A)-C(6)-H(6C)	109.5
H(6B)-C(6)-H(6C)	109.5	C(4)-C(7)-H(7A)	109.5
C(4)-C(7)-H(7B)	109.5	H(7A)-C(7)-H(7B)	109.5
C(4)-C(7)-H(7C)	109.5	H(7A)-C(7)-H(7C)	109.5
H(7B)-C(7)-H(7C)	109.5	C(9)-C(8)-C(3)	120.0(3)
C(9)-C(8)-H(8)	120.0	C(3)-C(8)-H(8)	120.0
N(1)-C(9)-C(8)	122.1(3)	N(1)-C(9)-C(10)	115.0(2)
C(8)-C(9)-C(10)	122.9(3)	N(2)-C(10)-C(11)	122.3(3)
N(2)-C(10)-C(9)	115.3(2)	C(11)-C(10)-C(9)	122.4(3)
C(10)-C(11)-C(12)	120.8(3)	C(10)-C(11)-H(11)	119.6
C(12)-C(11)-H(11)	119.6	C(11)-C(12)-C(17)	116.0(3)
C(11)-C(12)-C(13)	122.9(3)	C(17)-C(12)-C(13)	120.9(3)

Table 2-5. (cont'd)

C(12)-C(13)-C(15)	107.3(3)	C(12)-C(13)-C(14)	112.1(2)
C(15)-C(13)-C(14)	110.3(3)	C(12)-C(13)-C(16)	110.5(3)
C(15)-C(13)-C(16)	108.6(3)	C(14)-C(13)-C(16)	108.0(3)
C(13)-C(14)-H(14A)	109.5	C(13)-C(14)-H(14B)	109.5
H(14A)-C(14)-H(14B)	109.5	C(13)-C(14)-H(14C)	109.5
H(14A)-C(14)-H(14C)	109.5	H(14B)-C(14)-H(14C)	109.5
C(13)-C(15)-H(15A)	109.5	C(13)-C(15)-H(15B)	109.5
H(15A)-C(15)-H(15B)	109.5	C(13)-C(15)-H(15C)	109.5
H(15A)-C(15)-H(15C)	109.5	H(15B)-C(15)-H(15C)	109.5
C(13)-C(16)-H(16A)	109.5	C(13)-C(16)-H(16B)	109.5
H(16A)-C(16)-H(16B)	109.5	C(13)-C(16)-H(16C)	109.5
H(16A)-C(16)-H(16C)	109.5	H(16B)-C(16)-H(16C)	109.5
C(18)-C(17)-C(12)	121.1(3)	C(18)-C(17)-H(17)	119.5
C(12)-C(17)-H(17)	119.5	N(2)-C(18)-C(17)	121.9(3)
N(2)-C(18)-P(1)	114.1(2)	C(17)-C(18)-P(1)	123.5(2)
C(24)-C(19)-C(20)	119.1(3)	C(24)-C(19)-P(1)	122.3(3)
C(20)-C(19)-P(1)	118.4(3)	C(19)-C(20)-C(21)	120.4(3)
C(19)-C(20)-H(20)	119.8	C(21)-C(20)-H(20)	119.8
C(22)-C(21)-C(20)	119.6(3)	C(22)-C(21)-H(21)	120.2
C(20)-C(21)-H(21)	120.2	C(23)-C(22)-C(21)	120.6(3)
C(23)-C(22)-H(22)	119.7	C(21)-C(22)-H(22)	119.7
C(22)-C(23)-C(24)	119.9(3)	C(22)-C(23)-H(23)	120.1
C(24)-C(23)-H(23)	120.1	C(19)-C(24)-C(23)	120.3(3)
C(19)-C(24)-H(24)	119.8	C(23)-C(24)-H(24)	119.8
C(26)-C(25)-C(30)	119.0(3)	C(26)-C(25)-P(1)	123.0(2)
C(30)-C(25)-P(1)	117.7(3)	C(27)-C(26)-C(25)	121.0(3)
C(27)-C(26)-H(26)	119.5	C(25)-C(26)-H(26)	119.5
C(26)-C(27)-C(28)	119.9(3)	C(26)-C(27)-H(27)	120.1
C(28)-C(27)-H(27)	120.1	C(29)-C(28)-C(27)	119.5(3)
C(29)-C(28)-H(28)	120.3	C(27)-C(28)-H(28)	120.3
C(30)-C(29)-C(28)	120.5(3)	C(30)-C(29)-H(29)	119.7
C(28)-C(29)-H(29)	119.7	C(29)-C(30)-C(25)	120.2(3)
C(29)-C(30)-H(30)	119.9	C(25)-C(30)-H(30)	119.9
N(3)-C(31)-C(32)	178.2(4)	C(31)-C(32)-H(32A)	109.5
C(31)-C(32)-H(32B)	109.5	H(32A)-C(32)-H(32B)	109.5
C(31)-C(32)-H(32C)	109.5	H(32A)-C(32)-H(32C)	109.5
H(32B)-C(32)-H(32C)	109.5	F(4)-P(2)-F(6)	178.82(13)
F(4)-P(2)-F(2)	90.24(12)	F(6)-P(2)-F(2)	90.60(13)

Table 2-5. (cont'd)

F(4)-P(2)-F(1)	89.87(12)	F(6)-P(2)-F(1)	90.95(13)
F(2)-P(2)-F(1)	90.51(13)	F(4)-P(2)-F(3)	89.58(12)
F(6)-P(2)-F(3)	89.59(13)	F(2)-P(2)-F(3)	90.21(13)
F(1)-P(2)-F(3)	179.10(14)	F(4)-P(2)-F(5)	90.46(12)
F(6)-P(2)-F(5)	88.70(12)	F(2)-P(2)-F(5)	179.22(13)
F(1)-P(2)-F(5)	89.83(12)	F(3)-P(2)-F(5)	89.46(12)

2.6.3 Crystal data for $[Cu_2(\mu\text{-}P\textit{i}Pr_2bipy)_2(NCCH_3)](PF_6)_2$ **(3)**

Crystals of $[Cu_2(\mu\text{-}P\textit{i}Pr_2bipy)_2(NCCH_3)](PF_6)_2$ were found to have crystalized in the P2(1)/c space group with two molecule per asymmetric unit (Z' = 2) along with 4 uncoordinated counter ions and two uncoordinated acetonitrile molecules. The data was modeled to 3.83% (2Θ).

Table 2-6. Crystal data and structure refinement for $[Cu_2(\mu\text{-}P\textit{i}Pr_2bipy)_2(NCCH_3)](PF_6)_2$ (**3**)

Identification code	alyssia_11_0m	
Empirical formula	C36 H48 Cu2 F12 N6 P4	
Formula weight	1043.78	
Temperature	100(2) K	
Wavelength	1.54184 Å	
Crystal system	Monoclinic	
Space group	P2(1)/c	
Unit cell dimensions	a = 25.1774(8) Å	α= 90°.
	b = 11.7439(4) Å	β= 106.3850(10)°.
	c = 31.1195(10) Å	γ = 90°.
Volume	8827.7(5) $Å^3$	
Z	8	
Density (calculated)	1.571 Mg/m^3	
Absorption coefficient	3.330 mm^{-1}	
F(000)	4256	
Crystal size	0.41 x 0.40 x 0.37 mm^3	
Theta range for data collection	4.05 to 67.36°.	
Index ranges	-29<=h<=28, -14<=k<=13, -33<=l<=36	
Reflections collected	45573	
Independent reflections	15465 [R(int) = 0.0371]	
Completeness to theta = 67.37°	97.6 %	
Absorption correction	Semi-empirical from equivalents	
Max. and min. transmission	0.3722 and 0.3422	
Refinement method	Full-matrix least-squares on F^2	
Data / restraints / parameters	15465 / 0 / 1101	
Goodness-of-fit on F^2	1.020	
Final R indices [I>2sigma(I)]	R1 = 0.0383, wR2 = 0.0989	
R indices (all data)	R1 = 0.0429, wR2 = 0.1023	
Extinction coefficient	not measured	
Largest diff. peak and hole	0.842 and -0.594 $e.Å^{-3}$	

Table 2-7. Bond lengths [Å] and angles [°] for $[Cu_2(\mu\text{-}P\textit{i}Pr_2bipy)_2(NCCH_3)](PF_6)_2$ (**3**)

Cu(1)-N(1)	2.0421(19)	Cu(1)-N(2)	2.0665(18)
Cu(1)-P(1)	2.1848(6)	Cu(1)-Cu(2)	2.7067(4)
Cu(2)-N(5)	2.008(2)	Cu(2)-N(4)	2.0681(18)
Cu(2)-N(3)	2.0906(18)	Cu(2)-P(2)	2.2247(6)
P(1)-C(11)	1.836(2)	P(1)-C(29)	1.840(2)
P(1)-C(32)	1.849(2)	P(2)-C(10)	1.836(2)
P(2)-C(23)	1.843(2)	P(2)-C(26)	1.860(2)
N(1)-C(1)	1.336(3)	N(1)-C(5)	1.351(3)
N(2)-C(6)	1.346(3)	N(2)-C(10)	1.348(3)
N(3)-C(15)	1.347(3)	N(3)-C(11)	1.355(3)
N(4)-C(20)	1.341(3)	N(4)-C(16)	1.351(3)
N(5)-C(21)	1.133(3)	C(1)-C(2)	1.384(3)
C(1)-H(1)	0.9500	C(2)-C(3)	1.381(4)
C(2)-H(2)	0.9500	C(3)-C(4)	1.389(4)
C(3)-H(3)	0.9500	C(4)-C(5)	1.391(3)
C(4)-H(4)	0.9500	C(5)-C(6)	1.488(3)
C(6)-C(7)	1.390(3)	C(7)-C(8)	1.386(4)
C(7)-H(7)	0.9500	C(8)-C(9)	1.382(4)
C(8)-H(8)	0.9500	C(9)-C(10)	1.392(3)
C(9)-H(9)	0.9500	C(11)-C(12)	1.386(3)
C(12)-C(13)	1.383(3)	C(12)-H(12)	0.9500
C(13)-C(14)	1.379(3)	C(13)-H(13)	0.9500
C(14)-C(15)	1.398(3)	C(14)-H(14)	0.9500
C(15)-C(16)	1.484(3)	C(16)-C(17)	1.388(3)
C(17)-C(18)	1.388(3)	C(17)-H(17)	0.9500
C(18)-C(19)	1.385(4)	C(18)-H(18)	0.9500
C(19)-C(20)	1.383(3)	C(19)-H(19)	0.9500
C(20)-H(20)	0.9500	C(21)-C(22)	1.462(3)
C(22)-H(22A)	0.9800	C(22)-H(22B)	0.9800
C(22)-H(22C)	0.9800	C(23)-C(24)	1.529(3)
C(23)-C(25)	1.530(3)	C(23)-H(23)	1.0000
C(24)-H(24A)	0.9800	C(24)-H(24B)	0.9800
C(24)-H(24C)	0.9800	C(25)-H(25A)	0.9800
C(25)-H(25B)	0.9800	C(25)-H(25C)	0.9800
C(26)-C(27)	1.523(3)	C(26)-C(28)	1.533(3)
C(26)-H(26)	1.0000	C(27)-H(27A)	0.9800
C(27)-H(27B)	0.9800	C(27)-H(27C)	0.9800
C(28)-H(28A)	0.9800	C(28)-H(28B)	0.9800

Table 2-7. (cont'd)

C(28)-H(28C)	0.9800	C(29)-C(31)	1.525(3)
C(29)-C(30)	1.534(3)	C(29)-H(29)	1.0000
C(30)-H(30A)	0.9800	C(30)-H(30B)	0.9800
C(30)-H(30C)	0.9800	C(31)-H(31A)	0.9800
C(31)-H(31B)	0.9800	C(31)-H(31C)	0.9800
C(32)-C(34)	1.531(3)	C(32)-C(33)	1.537(3)
C(32)-H(32)	1.0000	C(33)-H(33A)	0.9800
C(33)-H(33B)	0.9800	C(33)-H(33C)	0.9800
C(34)-H(34A)	0.9800	C(34)-H(34B)	0.9800
C(34)-H(34C)	0.9800	Cu(3)-N(6)	2.0413(19)
Cu(3)-N(7)	2.0715(19)	Cu(3)-P(4)	2.1899(6)
Cu(3)-Cu(4)	2.6969(4)	Cu(4)-N(10)	2.014(2)
Cu(4)-N(9)	2.0681(19)	Cu(4)-N(8)	2.0778(18)
Cu(4)-P(3)	2.2205(6)	P(3)-C(44)	1.838(2)
P(3)-C(60)	1.844(2)	P(3)-C(57)	1.856(2)
P(4)-C(45)	1.839(2)	P(4)-C(63)	1.841(2)
P(4)-C(66)	1.851(2)	N(6)-C(35)	1.334(3)
N(6)-C(39)	1.358(3)	N(7)-C(40)	1.347(3)
N(7)-C(44)	1.347(3)	N(8)-C(49)	1.349(3)
N(8)-C(45)	1.351(3)	N(9)-C(54)	1.345(3)
N(9)-C(50)	1.351(3)	N(10)-C(55)	1.139(3)
C(35)-C(36)	1.387(3)	C(35)-H(35)	0.9500
C(36)-C(37)	1.384(4)	C(36)-H(36)	0.9500
C(37)-C(38)	1.382(4)	C(37)-H(37)	0.9500
C(38)-C(39)	1.388(3)	C(38)-H(38)	0.9500
C(39)-C(40)	1.482(3)	C(40)-C(41)	1.393(4)
C(41)-C(42)	1.375(4)	C(41)-H(41)	0.9500
C(42)-C(43)	1.389(4)	C(42)-H(42)	0.9500
C(43)-C(44)	1.390(4)	C(43)-H(43)	0.9500
C(45)-C(46)	1.387(3)	C(46)-C(47)	1.385(3)
C(46)-H(46)	0.9500	C(47)-C(48)	1.382(3)
C(47)-H(47)	0.9500	C(48)-C(49)	1.399(3)
C(48)-H(48)	0.9500	C(49)-C(50)	1.480(3)
C(50)-C(51)	1.389(3)	C(51)-C(52)	1.390(3)
C(51)-H(51)	0.9500	C(52)-C(53)	1.384(4)
C(52)-H(52)	0.9500	C(53)-C(54)	1.383(3)
C(53)-H(53)	0.9500	C(54)-H(54)	0.9500
C(55)-C(56)	1.449(4)	C(56)-H(56A)	0.9800

Table 2-7. (cont'd)

C(56)-H(56B)	0.9800	C(56)-H(56C)	0.9800
C(57)-C(59)	1.526(4)	C(57)-C(58)	1.534(4)
C(57)-H(57)	1.0000	C(58)-H(58A)	0.9800
C(58)-H(58B)	0.9800	C(58)-H(58C)	0.9800
C(59)-H(59A)	0.9800	C(59)-H(59B)	0.9800
C(59)-H(59C)	0.9800	C(60)-C(61)	1.527(3)
C(60)-C(62)	1.528(3)	C(60)-H(60)	1.0000
C(61)-H(61A)	0.9800	C(61)-H(61B)	0.9800
C(61)-H(61C)	0.9800	C(62)-H(62A)	0.9800
C(62)-H(62B)	0.9800	C(62)-H(62C)	0.9800
C(63)-C(65)	1.526(3)	C(63)-C(64)	1.534(3)
C(63)-H(63)	1.0000	C(64)-H(64A)	0.9800
C(64)-H(64B)	0.9800	C(64)-H(64C)	0.9800
C(65)-H(65A)	0.9800	C(65)-H(65B)	0.9800
C(65)-H(65C)	0.9800	C(66)-C(68)	1.530(3)
C(66)-C(67)	1.535(3)	C(66)-H(66)	1.0000
C(67)-H(67A)	0.9800	C(67)-H(67B)	0.9800
C(67)-H(67C)	0.9800	C(68)-H(68A)	0.9800
C(68)-H(68B)	0.9800	C(68)-H(68C)	0.9800
P(5)-F(6)	1.5812(18)	P(5)-F(3)	1.5844(17)
P(5)-F(1)	1.5864(16)	P(5)-F(4)	1.5881(16)
P(5)-F(2)	1.5935(17)	P(5)-F(5)	1.5966(16)
P(6)-F(10)	1.5964(15)	P(6)-F(9)	1.6029(15)
P(6)-F(11)	1.6042(15)	P(6)-F(8)	1.6049(15)
P(6)-F(7)	1.6053(16)	P(6)-F(12)	1.6082(16)
P(7)-F(15)	1.5707(19)	P(7)-F(16)	1.5790(19)
P(7)-F(13)	1.5822(19)	P(7)-F(17)	1.5908(17)
P(7)-F(14)	1.5950(18)	P(7)-F(18)	1.5979(19)
P(8)-F(19)	1.5912(16)	P(8)-F(22)	1.5999(18)
P(8)-F(24)	1.6012(16)	P(8)-F(20)	1.6016(16)
P(8)-F(21)	1.6055(16)	P(8)-F(23)	1.6060(16)
N(11)-C(69)	1.138(4)	C(69)-C(70)	1.455(4)
C(70)-H(70A)	0.9800	C(70)-H(70B)	0.9800
C(70)-H(70C)	0.9800	N(12)-C(71)	1.145(4)
C(71)-C(72)	1.457(5)	C(72)-H(72A)	0.9800
C(72)-H(72B)	0.9800	C(72)-H(72C)	0.9800
N(1)-Cu(1)-N(2)	79.85(7)	N(1)-Cu(1)-P(1)	122.40(6)
N(2)-Cu(1)-P(1)	127.44(6)	N(1)-Cu(1)-Cu(2)	148.59(5)

Table 2-7. (cont'd)

N(2)-Cu(1)-Cu(2)	91.35(5)	P(1)-Cu(1)-Cu(2)	86.849(18)
N(5)-Cu(2)-N(4)	108.67(8)	N(5)-Cu(2)-N(3)	119.74(7)
N(4)-Cu(2)-N(3)	78.68(7)	N(5)-Cu(2)-P(2)	116.90(6)
N(4)-Cu(2)-P(2)	110.02(5)	N(3)-Cu(2)-P(2)	115.34(5)
N(5)-Cu(2)-Cu(1)	62.96(6)	N(4)-Cu(2)-Cu(1)	162.66(5)
N(3)-Cu(2)-Cu(1)	92.28(5)	P(2)-Cu(2)-Cu(1)	87.186(19)
C(11)-P(1)-C(29)	104.90(11)	C(11)-P(1)-C(32)	101.95(10)
C(29)-P(1)-C(32)	106.08(11)	C(11)-P(1)-Cu(1)	115.95(7)
C(29)-P(1)-Cu(1)	111.15(8)	C(32)-P(1)-Cu(1)	115.68(8)
C(10)-P(2)-C(23)	103.98(11)	C(10)-P(2)-C(26)	102.36(11)
C(23)-P(2)-C(26)	104.73(11)	C(10)-P(2)-Cu(2)	114.96(8)
C(23)-P(2)-Cu(2)	117.26(8)	C(26)-P(2)-Cu(2)	111.98(8)
C(1)-N(1)-C(5)	118.6(2)	C(1)-N(1)-Cu(1)	128.20(16)
C(5)-N(1)-Cu(1)	111.77(15)	C(6)-N(2)-C(10)	120.3(2)
C(6)-N(2)-Cu(1)	109.59(15)	C(10)-N(2)-Cu(1)	125.22(15)
C(15)-N(3)-C(11)	119.32(19)	C(15)-N(3)-Cu(2)	112.31(14)
C(11)-N(3)-Cu(2)	125.29(14)	C(20)-N(4)-C(16)	118.56(19)
C(20)-N(4)-Cu(2)	126.78(15)	C(16)-N(4)-Cu(2)	113.92(15)
C(21)-N(5)-Cu(2)	162.93(19)	N(1)-C(1)-C(2)	122.9(2)
N(1)-C(1)-H(1)	118.5	C(2)-C(1)-H(1)	118.5
C(3)-C(2)-C(1)	118.5(2)	C(3)-C(2)-H(2)	120.7
C(1)-C(2)-H(2)	120.7	C(2)-C(3)-C(4)	119.3(2)
C(2)-C(3)-H(3)	120.4	C(4)-C(3)-H(3)	120.4
C(3)-C(4)-C(5)	118.9(2)	C(3)-C(4)-H(4)	120.5
C(5)-C(4)-H(4)	120.5	N(1)-C(5)-C(4)	121.7(2)
N(1)-C(5)-C(6)	115.0(2)	C(4)-C(5)-C(6)	123.3(2)
N(2)-C(6)-C(7)	121.2(2)	N(2)-C(6)-C(5)	115.0(2)
C(7)-C(6)-C(5)	123.7(2)	C(8)-C(7)-C(6)	118.6(2)
C(8)-C(7)-H(7)	120.7	C(6)-C(7)-H(7)	120.7
C(9)-C(8)-C(7)	119.9(2)	C(9)-C(8)-H(8)	120.1
C(7)-C(8)-H(8)	120.1	C(8)-C(9)-C(10)	119.0(2)
C(8)-C(9)-H(9)	120.5	C(10)-C(9)-H(9)	120.5
N(2)-C(10)-C(9)	120.8(2)	N(2)-C(10)-P(2)	113.32(17)
C(9)-C(10)-P(2)	125.89(18)	N(3)-C(11)-C(12)	121.3(2)
N(3)-C(11)-P(1)	112.99(16)	C(12)-C(11)-P(1)	125.63(17)
C(13)-C(12)-C(11)	119.3(2)	C(13)-C(12)-H(12)	120.4
C(11)-C(12)-H(12)	120.4	C(14)-C(13)-C(12)	119.6(2)
C(14)-C(13)-H(13)	120.2	C(12)-C(13)-H(13)	120.2

Table 2-7. (cont'd)

C(13)-C(14)-C(15)	118.7(2)	C(13)-C(14)-H(14)	120.6
C(15)-C(14)-H(14)	120.6	N(3)-C(15)-C(14)	121.6(2)
N(3)-C(15)-C(16)	115.15(19)	C(14)-C(15)-C(16)	123.3(2)
N(4)-C(16)-C(17)	121.8(2)	N(4)-C(16)-C(15)	115.17(19)
C(17)-C(16)-C(15)	123.0(2)	C(18)-C(17)-C(16)	119.1(2)
C(18)-C(17)-H(17)	120.5	C(16)-C(17)-H(17)	120.5
C(19)-C(18)-C(17)	119.1(2)	C(19)-C(18)-H(18)	120.4
C(17)-C(18)-H(18)	120.4	C(20)-C(19)-C(18)	118.7(2)
C(20)-C(19)-H(19)	120.7	C(18)-C(19)-H(19)	120.7
N(4)-C(20)-C(19)	122.8(2)	N(4)-C(20)-H(20)	118.6
C(19)-C(20)-H(20)	118.6	N(5)-C(21)-C(22)	178.5(3)
C(21)-C(22)-H(22A)	109.5	C(21)-C(22)-H(22B)	109.5
H(22A)-C(22)-H(22B)	109.5	C(21)-C(22)-H(22C)	109.5
H(22A)-C(22)-H(22C)	109.5	H(22B)-C(22)-H(22C)	109.5
C(24)-C(23)-C(25)	111.2(2)	C(24)-C(23)-P(2)	110.98(16)
C(25)-C(23)-P(2)	109.85(17)	C(24)-C(23)-H(23)	108.2
C(25)-C(23)-H(23)	108.2	P(2)-C(23)-H(23)	108.2
C(23)-C(24)-H(24A)	109.5	C(23)-C(24)-H(24B)	109.5
H(24A)-C(24)-H(24B)	109.5	C(23)-C(24)-H(24C)	109.5
H(24A)-C(24)-H(24C)	109.5	H(24B)-C(24)-H(24C)	109.5
C(23)-C(25)-H(25A)	109.5	C(23)-C(25)-H(25B)	109.5
H(25A)-C(25)-H(25B)	109.5	C(23)-C(25)-H(25C)	109.5
H(25A)-C(25)-H(25C)	109.5	H(25B)-C(25)-H(25C)	109.5
C(27)-C(26)-C(28)	111.4(2)	C(27)-C(26)-P(2)	115.29(18)
C(28)-C(26)-P(2)	110.36(16)	C(27)-C(26)-H(26)	106.4
C(28)-C(26)-H(26)	106.4	P(2)-C(26)-H(26)	106.4
C(26)-C(27)-H(27A)	109.5	C(26)-C(27)-H(27B)	109.5
H(27A)-C(27)-H(27B)	109.5	C(26)-C(27)-H(27C)	109.5
H(27A)-C(27)-H(27C)	109.5	H(27B)-C(27)-H(27C)	109.5
C(26)-C(28)-H(28A)	109.5	C(26)-C(28)-H(28B)	109.5
H(28A)-C(28)-H(28B)	109.5	C(26)-C(28)-H(28C)	109.5
H(28A)-C(28)-H(28C)	109.5	H(28B)-C(28)-H(28C)	109.5
C(31)-C(29)-C(30)	110.7(2)	C(31)-C(29)-P(1)	109.13(16)
C(30)-C(29)-P(1)	109.39(17)	C(31)-C(29)-H(29)	109.2
C(30)-C(29)-H(29)	109.2	P(1)-C(29)-H(29)	109.2
C(29)-C(30)-H(30A)	109.5	C(29)-C(30)-H(30B)	109.5
H(30A)-C(30)-H(30B)	109.5	C(29)-C(30)-H(30C)	109.5
H(30A)-C(30)-H(30C)	109.5	H(30B)-C(30)-H(30C)	109.5

Table 2-7. (cont'd)

C(29)-C(31)-H(31A)	109.5	C(29)-C(31)-H(31B)	109.5
H(31A)-C(31)-H(31B)	109.5	C(29)-C(31)-H(31C)	109.5
H(31A)-C(31)-H(31C)	109.5	H(31B)-C(31)-H(31C)	109.5
C(34)-C(32)-C(33)	111.01(19)	C(34)-C(32)-P(1)	110.05(16)
C(33)-C(32)-P(1)	114.60(17)	C(34)-C(32)-H(32)	106.9
C(33)-C(32)-H(32)	106.9	P(1)-C(32)-H(32)	106.9
C(32)-C(33)-H(33A)	109.5	C(32)-C(33)-H(33B)	109.5
H(33A)-C(33)-H(33B)	109.5	C(32)-C(33)-H(33C)	109.5
H(33A)-C(33)-H(33C)	109.5	H(33B)-C(33)-H(33C)	109.5
C(32)-C(34)-H(34A)	109.5	C(32)-C(34)-H(34B)	109.5
H(34A)-C(34)-H(34B)	109.5	C(32)-C(34)-H(34C)	109.5
H(34A)-C(34)-H(34C)	109.5	H(34B)-C(34)-H(34C)	109.5
N(6)-Cu(3)-N(7)	79.70(8)	N(6)-Cu(3)-P(4)	122.81(6)
N(7)-Cu(3)-P(4)	125.87(6)	N(6)-Cu(3)-Cu(4)	148.80(6)
N(7)-Cu(3)-Cu(4)	91.13(5)	P(4)-Cu(3)-Cu(4)	86.712(18)
N(10)-Cu(4)-N(9)	107.86(8)	N(10)-Cu(4)-N(8)	119.04(8)
N(9)-Cu(4)-N(8)	79.00(7)	N(10)-Cu(4)-P(3)	117.25(6)
N(9)-Cu(4)-P(3)	110.47(5)	N(8)-Cu(4)-P(3)	115.68(5)
N(10)-Cu(4)-Cu(3)	61.92(6)	N(9)-Cu(4)-Cu(3)	161.81(5)
N(8)-Cu(4)-Cu(3)	92.78(5)	P(3)-Cu(4)-Cu(3)	87.707(19)
C(44)-P(3)-C(60)	103.81(11)	C(44)-P(3)-C(57)	102.42(11)
C(60)-P(3)-C(57)	104.42(11)	C(44)-P(3)-Cu(4)	114.74(8)
C(60)-P(3)-Cu(4)	118.19(8)	C(57)-P(3)-Cu(4)	111.59(9)
C(45)-P(4)-C(63)	104.97(11)	C(45)-P(4)-C(66)	101.79(10)
C(63)-P(4)-C(66)	105.82(11)	C(45)-P(4)-Cu(3)	115.91(7)
C(63)-P(4)-Cu(3)	111.36(8)	C(66)-P(4)-Cu(3)	115.80(8)
C(35)-N(6)-C(39)	118.7(2)	C(35)-N(6)-Cu(3)	128.49(16)
C(39)-N(6)-Cu(3)	111.25(16)	C(40)-N(7)-C(44)	119.9(2)
C(40)-N(7)-Cu(3)	109.40(15)	C(44)-N(7)-Cu(3)	125.77(15)
C(49)-N(8)-C(45)	119.58(19)	C(49)-N(8)-Cu(4)	112.29(14)
C(45)-N(8)-Cu(4)	125.40(15)	C(54)-N(9)-C(50)	118.7(2)
C(54)-N(9)-Cu(4)	127.02(16)	C(50)-N(9)-Cu(4)	113.16(15)
C(55)-N(10)-Cu(4)	159.23(19)	N(6)-C(35)-C(36)	122.6(2)
N(6)-C(35)-H(35)	118.7	C(36)-C(35)-H(35)	118.7
C(37)-C(36)-C(35)	118.5(2)	C(37)-C(36)-H(36)	120.8
C(35)-C(36)-H(36)	120.8	C(38)-C(37)-C(36)	119.6(2)
C(38)-C(37)-H(37)	120.2	C(36)-C(37)-H(37)	120.2
C(37)-C(38)-C(39)	118.9(2)	C(37)-C(38)-H(38)	120.6

Table 2-7. (cont'd)

C(39)-C(38)-H(38)	120.6	N(6)-C(39)-C(38)	121.6(2)
N(6)-C(39)-C(40)	115.3(2)	C(38)-C(39)-C(40)	123.0(2)
N(7)-C(40)-C(41)	121.3(2)	N(7)-C(40)-C(39)	114.9(2)
C(41)-C(40)-C(39)	123.8(2)	C(42)-C(41)-C(40)	118.7(2)
C(42)-C(41)-H(41)	120.6	C(40)-C(41)-H(41)	120.6
C(41)-C(42)-C(43)	119.9(3)	C(41)-C(42)-H(42)	120.1
C(43)-C(42)-H(42)	120.1	C(42)-C(43)-C(44)	118.8(2)
C(42)-C(43)-H(43)	120.6	C(44)-C(43)-H(43)	120.6
N(7)-C(44)-C(43)	121.1(2)	N(7)-C(44)-P(3)	113.07(17)
C(43)-C(44)-P(3)	125.84(19)	N(8)-C(45)-C(46)	121.3(2)
N(8)-C(45)-P(4)	113.14(16)	C(46)-C(45)-P(4)	125.46(17)
C(47)-C(46)-C(45)	119.2(2)	C(47)-C(46)-H(46)	120.4
C(45)-C(46)-H(46)	120.4	C(48)-C(47)-C(46)	119.6(2)
C(48)-C(47)-H(47)	120.2	C(46)-C(47)-H(47)	120.2
C(47)-C(48)-C(49)	118.7(2)	C(47)-C(48)-H(48)	120.6
C(49)-C(48)-H(48)	120.6	N(8)-C(49)-C(48)	121.4(2)
N(8)-C(49)-C(50)	115.24(19)	C(48)-C(49)-C(50)	123.4(2)
N(9)-C(50)-C(51)	121.7(2)	N(9)-C(50)-C(49)	115.39(19)
C(51)-C(50)-C(49)	122.9(2)	C(50)-C(51)-C(52)	119.0(2)
C(50)-C(51)-H(51)	120.5	C(52)-C(51)-H(51)	120.5
C(53)-C(52)-C(51)	119.1(2)	C(53)-C(52)-H(52)	120.4
C(51)-C(52)-H(52)	120.4	C(54)-C(53)-C(52)	118.9(2)
C(54)-C(53)-H(53)	120.6	C(52)-C(53)-H(53)	120.6
N(9)-C(54)-C(53)	122.5(2)	N(9)-C(54)-H(54)	118.7
C(53)-C(54)-H(54)	118.7	N(10)-C(55)-C(56)	178.3(3)
C(55)-C(56)-H(56A)	109.5	C(55)-C(56)-H(56B)	109.5
H(56A)-C(56)-H(56B)	109.5	C(55)-C(56)-H(56C)	109.5
H(56A)-C(56)-H(56C)	109.5	H(56B)-C(56)-H(56C)	109.5
C(59)-C(57)-C(58)	110.5(2)	C(59)-C(57)-P(3)	115.0(2)
C(58)-C(57)-P(3)	110.74(17)	C(59)-C(57)-H(57)	106.7
C(58)-C(57)-H(57)	106.7	P(3)-C(57)-H(57)	106.7
C(57)-C(58)-H(58A)	109.5	C(57)-C(58)-H(58B)	109.5
H(58A)-C(58)-H(58B)	109.5	C(57)-C(58)-H(58C)	109.5
H(58A)-C(58)-H(58C)	109.5	H(58B)-C(58)-H(58C)	109.5
C(57)-C(59)-H(59A)	109.5	C(57)-C(59)-H(59B)	109.5
H(59A)-C(59)-H(59B)	109.5	C(57)-C(59)-H(59C)	109.5
H(59A)-C(59)-H(59C)	109.5	H(59B)-C(59)-H(59C)	109.5
C(61)-C(60)-C(62)	111.2(2)	C(61)-C(60)-P(3)	110.70(16)

Table 2-7. (cont'd)

C(62)-C(60)-P(3)	110.20(17)	C(61)-C(60)-H(60)	108.2
C(62)-C(60)-H(60)	108.2	P(3)-C(60)-H(60)	108.2
C(60)-C(61)-H(61A)	109.5	C(60)-C(61)-H(61B)	109.5
H(61A)-C(61)-H(61B)	109.5	C(60)-C(61)-H(61C)	109.5
H(61A)-C(61)-H(61C)	109.5	H(61B)-C(61)-H(61C)	109.5
C(60)-C(62)-H(62A)	109.5	C(60)-C(62)-H(62B)	109.5
H(62A)-C(62)-H(62B)	109.5	C(60)-C(62)-H(62C)	109.5
H(62A)-C(62)-H(62C)	109.5	H(62B)-C(62)-H(62C)	109.5
C(65)-C(63)-C(64)	110.6(2)	C(65)-C(63)-P(4)	109.34(16)
C(64)-C(63)-P(4)	109.38(17)	C(65)-C(63)-H(63)	109.2
C(64)-C(63)-H(63)	109.2	P(4)-C(63)-H(63)	109.2
C(63)-C(64)-H(64A)	109.5	C(63)-C(64)-H(64B)	109.5
H(64A)-C(64)-H(64B)	109.5	C(63)-C(64)-H(64C)	109.5
H(64A)-C(64)-H(64C)	109.5	H(64B)-C(64)-H(64C)	109.5
C(63)-C(65)-H(65A)	109.5	C(63)-C(65)-H(65B)	109.5
H(65A)-C(65)-H(65B)	109.5	C(63)-C(65)-H(65C)	109.5
H(65A)-C(65)-H(65C)	109.5	H(65B)-C(65)-H(65C)	109.5
C(68)-C(66)-C(67)	111.32(19)	C(68)-C(66)-P(4)	109.83(16)
C(67)-C(66)-P(4)	114.77(17)	C(68)-C(66)-H(66)	106.8
C(67)-C(66)-H(66)	106.8	P(4)-C(66)-H(66)	106.8
C(66)-C(67)-H(67A)	109.5	C(66)-C(67)-H(67B)	109.5
H(67A)-C(67)-H(67B)	109.5	C(66)-C(67)-H(67C)	109.5
H(67A)-C(67)-H(67C)	109.5	H(67B)-C(67)-H(67C)	109.5
C(66)-C(68)-H(68A)	109.5	C(66)-C(68)-H(68B)	109.5
H(68A)-C(68)-H(68B)	109.5	C(66)-C(68)-H(68C)	109.5
H(68A)-C(68)-H(68C)	109.5	H(68B)-C(68)-H(68C)	109.5
F(6)-P(5)-F(3)	179.27(12)	F(6)-P(5)-F(1)	89.73(11)
F(3)-P(5)-F(1)	89.58(11)	F(6)-P(5)-F(4)	90.47(12)
F(3)-P(5)-F(4)	90.23(11)	F(1)-P(5)-F(4)	178.87(11)
F(6)-P(5)-F(2)	90.13(11)	F(3)-P(5)-F(2)	89.64(11)
F(1)-P(5)-F(2)	89.65(10)	F(4)-P(5)-F(2)	91.46(10)
F(6)-P(5)-F(5)	90.96(11)	F(3)-P(5)-F(5)	89.28(10)
F(1)-P(5)-F(5)	90.96(9)	F(4)-P(5)-F(5)	87.93(10)
F(2)-P(5)-F(5)	178.75(11)	F(10)-P(6)-F(9)	89.90(8)
F(10)-P(6)-F(11)	90.77(8)	F(9)-P(6)-F(11)	89.72(9)
F(10)-P(6)-F(8)	90.32(8)	F(9)-P(6)-F(8)	90.49(8)
F(11)-P(6)-F(8)	178.89(9)	F(10)-P(6)-F(7)	178.70(10)
F(9)-P(6)-F(7)	91.03(9)	F(11)-P(6)-F(7)	90.14(9)

Table 2-7. (cont'd)

F(8)-P(6)-F(7)	88.76(9)	F(10)-P(6)-F(12)	89.69(8)
F(9)-P(6)-F(12)	179.02(9)	F(11)-P(6)-F(12)	89.39(9)
F(8)-P(6)-F(12)	90.41(9)	F(7)-P(6)-F(12)	89.39(9)
F(15)-P(7)-F(16)	92.02(14)	F(15)-P(7)-F(13)	89.91(13)
F(16)-P(7)-F(13)	177.98(15)	F(15)-P(7)-F(17)	91.92(10)
F(16)-P(7)-F(17)	90.26(11)	F(13)-P(7)-F(17)	90.27(12)
F(15)-P(7)-F(14)	89.06(11)	F(16)-P(7)-F(14)	90.20(11)
F(13)-P(7)-F(14)	89.24(12)	F(17)-P(7)-F(14)	178.90(12)
F(15)-P(7)-F(18)	179.80(16)	F(16)-P(7)-F(18)	87.78(13)
F(13)-P(7)-F(18)	90.28(11)	F(17)-P(7)-F(18)	88.08(10)
F(14)-P(7)-F(18)	90.94(12)	F(19)-P(8)-F(22)	178.61(12)
F(19)-P(8)-F(24)	89.71(9)	F(22)-P(8)-F(24)	91.24(11)
F(19)-P(8)-F(20)	90.91(8)	F(22)-P(8)-F(20)	90.11(10)
F(24)-P(8)-F(20)	90.13(9)	F(19)-P(8)-F(21)	89.70(9)
F(22)-P(8)-F(21)	89.36(11)	F(24)-P(8)-F(21)	179.01(9)
F(20)-P(8)-F(21)	89.08(9)	F(19)-P(8)-F(23)	90.34(9)
F(22)-P(8)-F(23)	88.63(10)	F(24)-P(8)-F(23)	90.37(9)
F(20)-P(8)-F(23)	178.65(10)	F(21)-P(8)-F(23)	90.43(9)
N(11)-C(69)-C(70)	178.9(4)	C(69)-C(70)-H(70A)	109.5
C(69)-C(70)-H(70B)	109.5	H(70A)-C(70)-H(70B)	109.5
C(69)-C(70)-H(70C)	109.5	H(70A)-C(70)-H(70C)	109.5
H(70B)-C(70)-H(70C)	109.5	N(12)-C(71)-C(72)	179.6(4)
C(71)-C(72)-H(72A)	109.5	C(71)-C(72)-H(72B)	109.5
H(72A)-C(72)-H(72B)	109.5	C(71)-C(72)-H(72C)	109.5
H(72A)-C(72)-H(72C)	109.5	H(72B)-C(72)-H(72C)	109.5

2.6.4 Crystal data for $[Cu_2(\mu\text{-P}i\text{Pr}_2\text{bipy})_2(\mu\text{-CNCH}(CH_3)_2)](PF_6)$ (**4**)

Crystals of $[Cu_2(\mu\text{-P}i\text{Pr}_2\text{bipy})_2(\mu\text{-CNCH}(CH_3)_2)](PF_6)_2$ were found to have crystalized in the Pc space group with two molecules per asymmetric unit (Z' = 2) along with 4 uncoordinated counter ions. One of the bridging isopropyl isocyanide ligands and shows positional distortion, which was modeled. The data was modeled to 4.65% (2Θ)

2-8. Crystal data and structure refinement for $[Cu_2(\mu\text{-}P\textit{i}Pr_2bipy)_2(\mu\text{-}CNCH(CH_3)_2)](PF_6)_2$ (**4**)

Identification code	alyssia15_0m	
Empirical formula	C36 H49 Cu2 F12 N5 P4	
Formula weight	1030.76	
Temperature	100(2) K	
Wavelength	0.71073 Å	
Crystal system	Monoclinic	
Space group	Pc	
Unit cell dimensions	a = 12.2695(8) Å	α= 90°.
	b = 24.4640(16) Å	β= 92.8070(10)°.
	c = 14.6092(10) Å	γ = 90°.
Volume	4379.9(5) $Å^3$	
Z	4	
Density (calculated)	1.563 Mg/m^3	
Absorption coefficient	1.202 mm^{-1}	
F(000)	2104	
Crystal size	0.2 x 0.4 x 0.1 mm^3	
Theta range for data collection	1.62 to 25.55°.	
Index ranges	-14<=h<=14, -29<=k<=29, -17<=l<=17	
Reflections collected	31782	
Independent reflections	14710 [R(int) = 0.0585]	
Completeness to theta = 25.00°	99.9 %	
Absorption correction	Semi-empirical from equivalents	
Max. and min. transmission	0.9881 and 0.9881	
Refinement method	Full-matrix least-squares on F^2	
Data / restraints / parameters	14710 / 2 / 1065	
Goodness-of-fit on F^2	1.013	
Final R indices [I>2sigma(I)]	R1 = 0.0465, wR2 = 0.0920	
R indices (all data)	R1 = 0.0623, wR2 = 0.0994	
Extinction coefficient	not measured	
Largest diff. peak and hole	0.726 and -0.447 $e.Å^{-3}$	

Table 2-9. Bond lengths [Å] and angles [°] for $[Cu_2(\mu\text{-}PiPr_2bipy)_2(\mu\text{-}CNCH(CH_3)_2)](PF_6)_2$ (**4**)

Cu(1)-N(1)	2.053(4)	Cu(1)-C(1)	2.054(6)
Cu(1)-N(2)	2.089(4)	Cu(1)-P(1)	2.2430(16)
Cu(1)-Cu(2)	2.5127(9)	Cu(2)-N(4)	2.058(4)
Cu(2)-N(3)	2.061(4)	Cu(2)-C(1)	2.062(6)
Cu(2)-P(2)	2.2392(16)	P(1)-C(28)	1.852(5)
P(1)-C(15)	1.855(5)	P(1)-C(25)	1.859(6)
P(2)-C(31)	1.831(6)	P(2)-C(14)	1.841(5)
P(2)-C(34)	1.856(5)	N(1)-C(5)	1.341(7)
N(1)-C(9)	1.364(7)	N(2)-C(10)	1.351(6)
N(2)-C(14)	1.356(6)	N(3)-C(15)	1.342(6)
N(3)-C(19)	1.356(6)	N(4)-C(24)	1.327(7)
N(4)-C(20)	1.350(6)	N(9)-C(1)	1.119(7)
N(9)-C(2A)	1.448(12)	N(9)-C(2B)	1.610(19)
C(2A)-C(3A)	1.525(17)	C(2A)-C(4A)	1.57(2)
C(2A)-H(8)	1.0000	C(2B)-C(4B)	1.36(4)
C(2B)-C(3B)	1.53(3)	C(2B)-H(8A)	1.0000
C(3A)-H(5A)	0.9800	C(3A)-H(35A)	0.9800
C(3A)-H(5C)	0.9800	C(3B)-H(70A)	0.9800
C(3B)-H(70B)	0.9800	C(3B)-H(70C)	0.9800
C(4A)-H(70D)	0.9800	C(4A)-H(70E)	0.9800
C(4A)-H(70F)	0.9800	C(4B)-H(76A)	0.9800
C(4B)-H(76B)	0.9800	C(4B)-H(76C)	0.9800
C(5)-C(6)	1.375(7)	C(5)-H(04)	0.9500
C(6)-C(7)	1.402(8)	C(6)-H(6)	0.9500
C(7)-C(8)	1.362(8)	C(7)-H(0A)	0.9500
C(8)-C(9)	1.399(7)	C(8)-H(1B)	0.9500
C(9)-C(10)	1.486(7)	C(10)-C(11)	1.388(7)
C(11)-C(12)	1.367(7)	C(11)-H(7)	0.9500
C(12)-C(13)	1.391(7)	C(12)-H(0Z)	0.9500
C(13)-C(14)	1.384(7)	C(13)-H(06)	0.9500
C(15)-C(16)	1.394(7)	C(16)-C(17)	1.382(7)
C(16)-H(0)	0.9500	C(17)-C(18)	1.374(8)
C(17)-H(13)	0.9500	C(18)-C(19)	1.387(7)
C(18)-H(48E)	0.9500	C(19)-C(20)	1.489(7)
C(20)-C(21)	1.383(7)	C(21)-C(22)	1.379(8)
C(21)-H(1H)	0.9500	C(22)-C(23)	1.379(8)
C(22)-H(0B)	0.9500	C(23)-C(24)	1.375(7)
C(23)-H(11)	0.9500	C(24)-H(10)	0.9500

Table 2-9. (cont'd)

C(25)-C(27)	1.532(8)	C(25)-C(26)	1.542(8)
C(25)-H(000)	1.0000	C(26)-H(40D)	0.9800
C(26)-H(40E)	0.9800	C(26)-H(40F)	0.9800
C(27)-H(03A)	0.9800	C(27)-H(03B)	0.9800
C(27)-H(03C)	0.9800	C(28)-C(29)	1.521(8)
C(28)-C(30)	1.550(7)	C(28)-H(1I)	1.0000
C(29)-H(0JA)	0.9800	C(29)-H(0JB)	0.9800
C(29)-H(0JC)	0.9800	C(30)-H(0RA)	0.9800
C(30)-H(0RB)	0.9800	C(30)-H(0RC)	0.9800
C(31)-C(32)	1.534(8)	C(31)-C(33)	1.548(7)
C(31)-H(232)	1.0000	C(32)-H(23D)	0.9800
C(32)-H(23E)	0.9800	C(32)-H(23F)	0.9800
C(33)-H(23A)	0.9800	C(33)-H(23B)	0.9800
C(33)-H(23C)	0.9800	C(34)-C(36)	1.529(8)
C(34)-C(35)	1.529(7)	C(34)-H(400)	1.0000
C(35)-H(40A)	0.9800	C(35)-H(40B)	0.9800
C(35)-H(40C)	0.9800	C(36)-H(1GA)	0.9800
C(36)-H(1GB)	0.9800	C(36)-H(1GC)	0.9800
Cu(3)-C(37)	1.964(5)	Cu(3)-N(6)	2.046(4)
Cu(3)-N(5)	2.066(4)	Cu(3)-P(3)	2.2658(16)
Cu(3)-Cu(4)	2.5256(9)	Cu(4)-N(7)	2.057(4)
Cu(4)-N(8)	2.099(4)	Cu(4)-C(37)	2.162(5)
Cu(4)-P(4)	2.2246(15)	P(3)-C(61)	1.830(5)
P(3)-C(60)	1.841(5)	P(3)-C(64)	1.864(5)
P(4)-C(41)	1.848(5)	P(4)-C(70)	1.853(5)
P(4)-C(67)	1.859(6)	N(5)-C(41)	1.330(7)
N(5)-C(45)	1.352(6)	N(6)-C(50)	1.345(7)
N(6)-C(46)	1.366(7)	N(7)-C(55)	1.346(6)
N(7)-C(51)	1.348(7)	N(8)-C(60)	1.333(7)
N(8)-C(56)	1.343(6)	N(10)-C(37)	1.142(6)
N(10)-C(38)	1.461(7)	C(38)-C(40)	1.485(9)
C(38)-C(39)	1.541(9)	C(38)-H(0L)	1.0000
C(39)-H(60A)	0.9800	C(39)-H(60B)	0.9800
C(39)-H(60C)	0.9800	C(40)-H(50A)	0.9800
C(40)-H(50B)	0.9800	C(40)-H(50C)	0.9800
C(41)-C(42)	1.381(7)	C(42)-C(43)	1.384(7)
C(42)-H(3)	0.9500	C(43)-C(44)	1.395(8)
C(43)-H(2)	0.9500	C(44)-C(45)	1.379(8)

Table 2-9. (cont'd)

C(44)-H(09)	0.9500	C(45)-C(46)	1.479(8)
C(46)-C(47)	1.384(7)	C(47)-C(48)	1.372(9)
C(47)-H(1K)	0.9500	C(48)-C(49)	1.380(9)
C(48)-H(1A)	0.9500	C(49)-C(50)	1.373(8)
C(49)-H(0G)	0.9500	C(50)-H(1)	0.9500
C(51)-C(52)	1.397(7)	C(51)-H(0T)	0.9500
C(52)-C(53)	1.367(8)	C(52)-H(0@)	0.9500
C(53)-C(54)	1.371(8)	C(53)-H(406)	0.9500
C(54)-C(55)	1.392(7)	C(54)-H(1F)	0.9500
C(55)-C(56)	1.489(7)	C(56)-C(57)	1.393(7)
C(57)-C(58)	1.380(8)	C(57)-H(0N)	0.9500
C(58)-C(59)	1.378(7)	C(58)-H(407)	0.9500
C(59)-C(60)	1.391(7)	C(59)-H(408)	0.9500
C(61)-C(62)	1.521(7)	C(61)-C(63)	1.538(7)
C(61)-H(222)	1.0000	C(62)-H(22G)	0.9800
C(62)-H(22H)	0.9800	C(62)-H(22I)	0.9800
C(63)-H(22A)	0.9800	C(63)-H(22B)	0.9800
C(63)-H(22C)	0.9800	C(64)-C(65)	1.513(8)
C(64)-C(66)	1.527(7)	C(64)-H(226)	1.0000
C(65)-H(22J)	0.9800	C(65)-H(22K)	0.9800
C(65)-H(22L)	0.9800	C(66)-H(22D)	0.9800
C(66)-H(22E)	0.9800	C(66)-H(22F)	0.9800
C(67)-C(68)	1.519(8)	C(67)-C(69)	1.538(8)
C(67)-H(94)	1.0000	C(68)-H(95A)	0.9800
C(68)-H(95B)	0.9800	C(68)-H(95C)	0.9800
C(69)-H(96A)	0.9800	C(69)-H(96B)	0.9800
C(69)-H(96C)	0.9800	C(70)-C(71)	1.525(8)
C(70)-C(72)	1.538(7)	C(70)-H(90)	1.0000
C(71)-H(93A)	0.9800	C(71)-H(93B)	0.9800
C(71)-H(93C)	0.9800	C(72)-H(91A)	0.9800
C(72)-H(91B)	0.9800	C(72)-H(91C)	0.9800
P(5)-F(3)	1.542(5)	P(5)-F(2)	1.563(4)
P(5)-F(5)	1.582(4)	P(5)-F(4)	1.596(4)
P(5)-F(6)	1.611(3)	P(5)-F(1)	1.638(5)
P(6)-F(7)	1.591(4)	P(6)-F(9)	1.590(4)
P(6)-F(8)	1.591(4)	P(6)-F(12)	1.595(4)
P(6)-F(10)	1.596(3)	P(6)-F(11)	1.607(4)
P(7)-F(13)	1.583(4)	P(7)-F(17)	1.597(4)

Table 2-9. (cont'd)

P(7)-F(14)	1.605(3)	P(7)-F(15)	1.607(4)
P(7)-F(16)	1.609(3)	P(7)-F(18)	1.620(3)
P(8)-F(21)	1.584(4)	P(8)-F(19)	1.590(4)
P(8)-F(20)	1.601(3)	P(8)-F(23)	1.606(4)
P(8)-F(24)	1.610(4)	P(8)-F(22)	1.614(3)
N(1)-Cu(1)-C(1)	103.8(2)	N(1)-Cu(1)-N(2)	78.73(17)
C(1)-Cu(1)-N(2)	113.05(19)	N(1)-Cu(1)-P(1)	122.02(13)
C(1)-Cu(1)-P(1)	118.69(16)	N(2)-Cu(1)-P(1)	113.95(13)
N(1)-Cu(1)-Cu(2)	149.44(13)	C(1)-Cu(1)-Cu(2)	52.52(17)
N(2)-Cu(1)-Cu(2)	92.70(12)	P(1)-Cu(1)-Cu(2)	88.34(4)
N(4)-Cu(2)-N(3)	80.28(17)	N(4)-Cu(2)-C(1)	107.7(2)
N(3)-Cu(2)-C(1)	108.4(2)	N(4)-Cu(2)-P(2)	111.39(13)
N(3)-Cu(2)-P(2)	125.45(13)	C(1)-Cu(2)-P(2)	116.75(16)
N(4)-Cu(2)-Cu(1)	156.52(13)	N(3)-Cu(2)-Cu(1)	94.17(12)
C(1)-Cu(2)-Cu(1)	52.24(17)	P(2)-Cu(2)-Cu(1)	90.50(4)
C(28)-P(1)-C(15)	102.7(2)	C(28)-P(1)-C(25)	108.2(3)
C(15)-P(1)-C(25)	103.4(3)	C(28)-P(1)-Cu(1)	117.54(19)
C(15)-P(1)-Cu(1)	111.70(18)	C(25)-P(1)-Cu(1)	112.02(19)
C(31)-P(2)-C(14)	107.3(3)	C(31)-P(2)-C(34)	104.2(3)
C(14)-P(2)-C(34)	100.7(2)	C(31)-P(2)-Cu(2)	118.98(19)
C(14)-P(2)-Cu(2)	112.64(17)	C(34)-P(2)-Cu(2)	111.14(18)
C(5)-N(1)-C(9)	118.6(5)	C(5)-N(1)-Cu(1)	127.4(4)
C(9)-N(1)-Cu(1)	113.9(4)	C(10)-N(2)-C(14)	118.9(4)
C(10)-N(2)-Cu(1)	112.8(3)	C(14)-N(2)-Cu(1)	125.7(3)
C(15)-N(3)-C(19)	119.6(4)	C(15)-N(3)-Cu(2)	126.2(3)
C(19)-N(3)-Cu(2)	114.2(3)	C(24)-N(4)-C(20)	118.9(5)
C(24)-N(4)-Cu(2)	126.3(4)	C(20)-N(4)-Cu(2)	114.0(3)
C(1)-N(9)-C(2A)	170.1(8)	C(1)-N(9)-C(2B)	161.9(9)
C(2A)-N(9)-C(2B)	26.5(7)	N(9)-C(1)-Cu(1)	139.6(5)
N(9)-C(1)-Cu(2)	144.6(5)	Cu(1)-C(1)-Cu(2)	75.2(2)
N(9)-C(2A)-C(3A)	106.1(10)	N(9)-C(2A)-C(4A)	103.8(9)
C(3A)-C(2A)-C(4A)	116.0(13)	N(9)-C(2A)-H(8)	110.2
C(3A)-C(2A)-H(8)	110.2	C(4A)-C(2A)-H(8)	110.2
C(4B)-C(2B)-C(3B)	112(2)	C(4B)-C(2B)-N(9)	111.3(16)
C(3B)-C(2B)-N(9)	106.1(13)	C(4B)-C(2B)-H(8A)	109.2
C(3B)-C(2B)-H(8A)	109.2	N(9)-C(2B)-H(8A)	109.2
C(2A)-C(3A)-H(5A)	109.5	C(2A)-C(3A)-H(35A)	109.5
H(5A)-C(3A)-H(35A)	109.5	C(2A)-C(3A)-H(5C)	109.5

Table 2-9. (cont'd)

H(5A)-C(3A)-H(5C)	109.5	H(35A)-C(3A)-H(5C)	109.5
C(2A)-C(4A)-H(70D)	109.5	C(2A)-C(4A)-H(70E)	109.5
H(70D)-C(4A)-H(70E)	109.5	C(2A)-C(4A)-H(70F)	109.5
H(70D)-C(4A)-H(70F)	109.5	H(70E)-C(4A)-H(70F)	109.5
N(1)-C(5)-C(6)	123.1(6)	N(1)-C(5)-H(04)	118.5
C(6)-C(5)-H(04)	118.5	C(5)-C(6)-C(7)	118.2(5)
C(5)-C(6)-H(6)	120.9	C(7)-C(6)-H(6)	120.9
C(8)-C(7)-C(6)	119.6(5)	C(8)-C(7)-H(0A)	120.2
C(6)-C(7)-H(0A)	120.2	C(7)-C(8)-C(9)	119.6(5)
C(7)-C(8)-H(1B)	120.2	C(9)-C(8)-H(1B)	120.2
N(1)-C(9)-C(8)	120.9(5)	N(1)-C(9)-C(10)	115.6(5)
C(8)-C(9)-C(10)	123.4(5)	N(2)-C(10)-C(11)	121.7(5)
N(2)-C(10)-C(9)	113.5(5)	C(11)-C(10)-C(9)	124.7(5)
C(12)-C(11)-C(10)	119.3(5)	C(12)-C(11)-H(7)	120.4
C(10)-C(11)-H(7)	120.4	C(11)-C(12)-C(13)	119.4(5)
C(11)-C(12)-H(0Z)	120.3	C(13)-C(12)-H(0Z)	120.3
C(14)-C(13)-C(12)	119.2(5)	C(14)-C(13)-H(06)	120.4
C(12)-C(13)-H(06)	120.4	N(2)-C(14)-C(13)	121.2(5)
N(2)-C(14)-P(2)	110.9(4)	C(13)-C(14)-P(2)	127.3(4)
N(3)-C(15)-C(16)	121.9(5)	N(3)-C(15)-P(1)	114.0(4)
C(16)-C(15)-P(1)	124.0(4)	C(17)-C(16)-C(15)	117.5(5)
C(17)-C(16)-H(0)	121.2	C(15)-C(16)-H(0)	121.2
C(18)-C(17)-C(16)	121.4(5)	C(18)-C(17)-H(13)	119.3
C(16)-C(17)-H(13)	119.3	C(17)-C(18)-C(19)	118.2(5)
C(17)-C(18)-H(48E)	120.9	C(19)-C(18)-H(48E)	120.9
N(3)-C(19)-C(18)	121.4(5)	N(3)-C(19)-C(20)	115.2(5)
C(18)-C(19)-C(20)	123.4(5)	N(4)-C(20)-C(21)	120.4(5)
N(4)-C(20)-C(19)	115.7(5)	C(21)-C(20)-C(19)	123.8(5)
C(22)-C(21)-C(20)	120.5(5)	C(22)-C(21)-H(1H)	119.7
C(20)-C(21)-H(1H)	119.8	C(21)-C(22)-C(23)	118.2(5)
C(21)-C(22)-H(0B)	120.9	C(23)-C(22)-H(0B)	120.9
C(24)-C(23)-C(22)	118.7(5)	C(24)-C(23)-H(11)	120.6
C(22)-C(23)-H(11)	120.6	N(4)-C(24)-C(23)	123.2(5)
N(4)-C(24)-H(10)	118.4	C(23)-C(24)-H(10)	118.4
C(27)-C(25)-C(26)	110.0(5)	C(27)-C(25)-P(1)	111.6(4)
C(26)-C(25)-P(1)	116.4(4)	C(27)-C(25)-H(000)	106.0
C(26)-C(25)-H(000)	106.0	P(1)-C(25)-H(000)	106.0
C(25)-C(26)-H(40D)	109.5	C(25)-C(26)-H(40E)	109.5

Table 2-9. (cont'd)

H(40D)-C(26)-H(40E)	109.5	C(25)-C(26)-H(40F)	109.5
H(40D)-C(26)-H(40F)	109.5	H(40E)-C(26)-H(40F)	109.5
C(25)-C(27)-H(03A)	109.5	C(25)-C(27)-H(03B)	109.5
H(03A)-C(27)-H(03B)	109.5	C(25)-C(27)-H(03C)	109.5
H(03A)-C(27)-H(03C)	109.5	H(03B)-C(27)-H(03C)	109.5
C(29)-C(28)-C(30)	108.0(5)	C(29)-C(28)-P(1)	111.1(4)
C(30)-C(28)-P(1)	110.3(4)	C(29)-C(28)-H(1I)	109.1
C(30)-C(28)-H(1I)	109.1	P(1)-C(28)-H(1I)	109.1
C(28)-C(29)-H(0JA)	109.5	C(28)-C(29)-H(0JB)	109.5
H(0JA)-C(29)-H(0JB)	109.5	C(28)-C(29)-H(0JC)	109.5
H(0JA)-C(29)-H(0JC)	109.5	H(0JB)-C(29)-H(0JC)	109.5
C(28)-C(30)-H(0RA)	109.5	C(28)-C(30)-H(0RB)	109.5
H(0RA)-C(30)-H(0RB)	109.5	C(28)-C(30)-H(0RC)	109.5
H(0RA)-C(30)-H(0RC)	109.5	H(0RB)-C(30)-H(0RC)	109.5
C(32)-C(31)-C(33)	110.1(5)	C(32)-C(31)-P(2)	111.2(4)
C(33)-C(31)-P(2)	109.1(4)	C(32)-C(31)-H(232)	108.8
C(33)-C(31)-H(232)	108.8	P(2)-C(31)-H(232)	108.8
C(31)-C(32)-H(23D)	109.5	C(31)-C(32)-H(23E)	109.5
H(23D)-C(32)-H(23E)	109.5	C(31)-C(32)-H(23F)	109.5
H(23D)-C(32)-H(23F)	109.5	H(23E)-C(32)-H(23F)	109.5
C(31)-C(33)-H(23A)	109.5	C(31)-C(33)-H(23B)	109.5
H(23A)-C(33)-H(23B)	109.5	C(31)-C(33)-H(23C)	109.5
H(23A)-C(33)-H(23C)	109.5	H(23B)-C(33)-H(23C)	109.5
C(36)-C(34)-C(35)	111.2(5)	C(36)-C(34)-P(2)	110.0(4)
C(35)-C(34)-P(2)	115.0(4)	C(36)-C(34)-H(400)	106.7
C(35)-C(34)-H(400)	106.7	P(2)-C(34)-H(400)	106.7
C(34)-C(35)-H(40A)	109.5	C(34)-C(35)-H(40B)	109.5
H(40A)-C(35)-H(40B)	109.5	C(34)-C(35)-H(40C)	109.5
H(40A)-C(35)-H(40C)	109.5	H(40B)-C(35)-H(40C)	109.5
C(34)-C(36)-H(1GA)	109.5	C(34)-C(36)-H(1GB)	109.5
H(1GA)-C(36)-H(1GB)	109.5	C(34)-C(36)-H(1GC)	109.5
H(1GA)-C(36)-H(1GC)	109.5	H(1GB)-C(36)-H(1GC)	109.5
C(37)-Cu(3)-N(6)	112.4(2)	C(37)-Cu(3)-N(5)	120.0(2)
N(6)-Cu(3)-N(5)	80.04(18)	C(37)-Cu(3)-P(3)	115.87(16)
N(6)-Cu(3)-P(3)	106.76(14)	N(5)-Cu(3)-P(3)	115.13(12)
C(37)-Cu(3)-Cu(4)	55.89(16)	N(6)-Cu(3)-Cu(4)	162.65(14)
N(5)-Cu(3)-Cu(4)	94.84(12)	P(3)-Cu(3)-Cu(4)	90.45(4)
N(7)-Cu(4)-N(8)	79.39(17)	N(7)-Cu(4)-C(37)	104.67(18)

Table 2-9. (cont'd)

N(8)-Cu(4)-C(37)	108.27(18)	N(7)-Cu(4)-P(4)	121.06(13)
N(8)-Cu(4)-P(4)	121.22(12)	C(37)-Cu(4)-P(4)	116.10(15)
N(7)-Cu(4)-Cu(3)	148.20(12)	N(8)-Cu(4)-Cu(3)	92.18(12)
C(37)-Cu(4)-Cu(3)	48.79(15)	P(4)-Cu(4)-Cu(3)	89.61(4)
C(61)-P(3)-C(60)	105.9(2)	C(61)-P(3)-C(64)	104.2(2)
C(60)-P(3)-C(64)	101.4(2)	C(61)-P(3)-Cu(3)	121.19(19)
C(60)-P(3)-Cu(3)	111.52(18)	C(64)-P(3)-Cu(3)	110.67(17)
C(41)-P(4)-C(70)	105.8(2)	C(41)-P(4)-C(67)	97.7(2)
C(70)-P(4)-C(67)	105.4(3)	C(41)-P(4)-Cu(4)	112.90(18)
C(70)-P(4)-Cu(4)	116.97(19)	C(67)-P(4)-Cu(4)	115.94(19)
C(41)-N(5)-C(45)	120.2(5)	C(41)-N(5)-Cu(3)	125.8(3)
C(45)-N(5)-Cu(3)	113.7(4)	C(50)-N(6)-C(46)	118.2(5)
C(50)-N(6)-Cu(3)	126.7(4)	C(46)-N(6)-Cu(3)	114.2(3)
C(55)-N(7)-C(51)	118.6(4)	C(55)-N(7)-Cu(4)	113.7(3)
C(51)-N(7)-Cu(4)	127.7(4)	C(60)-N(8)-C(56)	120.9(5)
C(60)-N(8)-Cu(4)	125.6(3)	C(56)-N(8)-Cu(4)	110.3(3)
C(37)-N(10)-C(38)	173.5(6)	N(10)-C(37)-Cu(3)	153.7(5)
N(10)-C(37)-Cu(4)	129.7(4)	Cu(3)-C(37)-Cu(4)	75.31(19)
N(10)-C(38)-C(40)	109.8(5)	N(10)-C(38)-C(39)	106.3(5)
C(40)-C(38)-C(39)	112.5(6)	N(10)-C(38)-H(0L)	109.4
C(40)-C(38)-H(0L)	109.4	C(39)-C(38)-H(0L)	109.4
C(38)-C(39)-H(60A)	109.5	C(38)-C(39)-H(60B)	109.5
H(60A)-C(39)-H(60B)	109.5	C(38)-C(39)-H(60C)	109.5
H(60A)-C(39)-H(60C)	109.5	H(60B)-C(39)-H(60C)	109.5
C(38)-C(40)-H(50A)	109.5	C(38)-C(40)-H(50B)	109.5
H(50A)-C(40)-H(50B)	109.5	C(38)-C(40)-H(50C)	109.5
H(50A)-C(40)-H(50C)	109.5	H(50B)-C(40)-H(50C)	109.5
N(5)-C(41)-C(42)	121.6(5)	N(5)-C(41)-P(4)	114.8(4)
C(42)-C(41)-P(4)	123.2(4)	C(41)-C(42)-C(43)	119.3(5)
C(41)-C(42)-H(3)	120.3	C(43)-C(42)-H(3)	120.3
C(42)-C(43)-C(44)	118.5(5)	C(42)-C(43)-H(2)	120.7
C(44)-C(43)-H(2)	120.7	C(45)-C(44)-C(43)	119.5(5)
C(45)-C(44)-H(09)	120.2	C(43)-C(44)-H(09)	120.2
N(5)-C(45)-C(44)	120.7(5)	N(5)-C(45)-C(46)	115.8(5)
C(44)-C(45)-C(46)	123.5(5)	N(6)-C(46)-C(47)	120.5(5)
N(6)-C(46)-C(45)	115.0(5)	C(47)-C(46)-C(45)	124.5(5)
C(48)-C(47)-C(46)	120.4(6)	C(48)-C(47)-H(1K)	119.8
C(46)-C(47)-H(1K)	119.8	C(47)-C(48)-C(49)	118.9(6)

Table 2-9. (cont'd)

C(47)-C(48)-H(1A)	120.6	C(49)-C(48)-H(1A)	120.6
C(50)-C(49)-C(48)	118.9(6)	C(50)-C(49)-H(0G)	120.5
C(48)-C(49)-H(0G)	120.5	N(6)-C(50)-C(49)	123.0(6)
N(6)-C(50)-H(1)	118.5	C(49)-C(50)-H(1)	118.5
N(7)-C(51)-C(52)	121.8(5)	N(7)-C(51)-H(0T)	119.1
C(52)-C(51)-H(0T)	119.1	C(53)-C(52)-C(51)	119.1(6)
C(53)-C(52)-H(0@)	120.4	C(51)-C(52)-H(0@)	120.4
C(52)-C(53)-C(54)	119.3(5)	C(52)-C(53)-H(406)	120.3
C(54)-C(53)-H(406)	120.3	C(53)-C(54)-C(55)	119.6(6)
C(53)-C(54)-H(1F)	120.2	C(55)-C(54)-H(1F)	120.2
N(7)-C(55)-C(54)	121.5(5)	N(7)-C(55)-C(56)	115.2(4)
C(54)-C(55)-C(56)	123.3(5)	N(8)-C(56)-C(57)	120.9(5)
N(8)-C(56)-C(55)	115.0(5)	C(57)-C(56)-C(55)	124.0(5)
C(58)-C(57)-C(56)	118.3(5)	C(58)-C(57)-H(0N)	120.8
C(56)-C(57)-H(0N)	120.8	C(59)-C(58)-C(57)	119.9(5)
C(59)-C(58)-H(407)	120.1	C(57)-C(58)-H(407)	120.1
C(58)-C(59)-C(60)	119.3(5)	C(58)-C(59)-H(408)	120.4
C(60)-C(59)-H(408)	120.4	N(8)-C(60)-C(59)	120.4(5)
N(8)-C(60)-P(3)	112.2(4)	C(59)-C(60)-P(3)	127.0(4)
C(62)-C(61)-C(63)	110.7(5)	C(62)-C(61)-P(3)	111.4(4)
C(63)-C(61)-P(3)	109.7(4)	C(62)-C(61)-H(222)	108.3
C(63)-C(61)-H(222)	108.3	P(3)-C(61)-H(222)	108.3
C(61)-C(62)-H(22G)	109.5	C(61)-C(62)-H(22H)	109.5
H(22G)-C(62)-H(22H)	109.5	C(61)-C(62)-H(22I)	109.5
H(22G)-C(62)-H(22I)	109.5	H(22H)-C(62)-H(22I)	109.5
C(61)-C(63)-H(22A)	109.5	C(61)-C(63)-H(22B)	109.5
H(22A)-C(63)-H(22B)	109.5	C(61)-C(63)-H(22C)	109.5
H(22A)-C(63)-H(22C)	109.5	H(22B)-C(63)-H(22C)	109.5
C(65)-C(64)-C(66)	110.3(5)	C(65)-C(64)-P(3)	115.2(4)
C(66)-C(64)-P(3)	109.9(4)	C(65)-C(64)-H(226)	107.0
C(66)-C(64)-H(226)	107.0	P(3)-C(64)-H(226)	107.0
C(64)-C(65)-H(22J)	109.5	C(64)-C(65)-H(22K)	109.5
H(22J)-C(65)-H(22K)	109.5	C(64)-C(65)-H(22L)	109.5
H(22J)-C(65)-H(22L)	109.5	H(22K)-C(65)-H(22L)	109.5
C(64)-C(66)-H(22D)	109.5	C(64)-C(66)-H(22E)	109.5
H(22D)-C(66)-H(22E)	109.5	C(64)-C(66)-H(22F)	109.5
H(22D)-C(66)-H(22F)	109.5	H(22E)-C(66)-H(22F)	109.5
C(68)-C(67)-C(69)	110.0(5)	C(68)-C(67)-P(4)	110.1(4)

Table 2-9. (cont'd)

C(69)-C(67)-P(4)	112.0(4)	C(68)-C(67)-H(94)	108.2
C(69)-C(67)-H(94)	108.2	P(4)-C(67)-H(94)	108.2
C(67)-C(68)-H(95A)	109.5	C(67)-C(68)-H(95B)	109.5
H(95A)-C(68)-H(95B)	109.5	C(67)-C(68)-H(95C)	109.5
H(95A)-C(68)-H(95C)	109.5	H(95B)-C(68)-H(95C)	109.5
C(67)-C(69)-H(96A)	109.5	C(67)-C(69)-H(96B)	109.5
H(96A)-C(69)-H(96B)	109.5	C(67)-C(69)-H(96C)	109.5
H(96A)-C(69)-H(96C)	109.5	H(96B)-C(69)-H(96C)	109.5
C(71)-C(70)-C(72)	109.3(5)	C(71)-C(70)-P(4)	111.8(4)
C(72)-C(70)-P(4)	108.7(4)	C(71)-C(70)-H(90)	109.0
C(72)-C(70)-H(90)	109.0	P(4)-C(70)-H(90)	109.0
C(70)-C(71)-H(93A)	109.5	C(70)-C(71)-H(93B)	109.5
H(93A)-C(71)-H(93B)	109.5	C(70)-C(71)-H(93C)	109.5
H(93A)-C(71)-H(93C)	109.5	H(93B)-C(71)-H(93C)	109.5
C(70)-C(72)-H(91A)	109.5	C(70)-C(72)-H(91B)	109.5
H(91A)-C(72)-H(91B)	109.5	C(70)-C(72)-H(91C)	109.5
H(91A)-C(72)-H(91C)	109.5	H(91B)-C(72)-H(91C)	109.5
F(3)-P(5)-F(2)	95.7(3)	F(3)-P(5)-F(5)	90.1(3)
F(2)-P(5)-F(5)	90.4(3)	F(3)-P(5)-F(4)	89.7(3)
F(2)-P(5)-F(4)	174.6(3)	F(5)-P(5)-F(4)	90.0(3)
F(3)-P(5)-F(6)	91.2(2)	F(2)-P(5)-F(6)	89.7(2)
F(5)-P(5)-F(6)	178.6(3)	F(4)-P(5)-F(6)	89.7(2)
F(3)-P(5)-F(1)	175.4(3)	F(2)-P(5)-F(1)	88.6(3)
F(5)-P(5)-F(1)	91.6(3)	F(4)-P(5)-F(1)	86.0(3)
F(6)-P(5)-F(1)	87.1(2)	F(7)-P(6)-F(9)	178.8(2)
F(7)-P(6)-F(8)	90.0(2)	F(9)-P(6)-F(8)	91.0(2)
F(7)-P(6)-F(12)	90.9(2)	F(9)-P(6)-F(12)	89.8(2)
F(8)-P(6)-F(12)	90.2(2)	F(7)-P(6)-F(10)	89.7(2)
F(9)-P(6)-F(10)	89.3(2)	F(8)-P(6)-F(10)	179.2(2)
F(12)-P(6)-F(10)	90.6(2)	F(7)-P(6)-F(11)	88.5(2)
F(9)-P(6)-F(11)	90.7(2)	F(8)-P(6)-F(11)	90.0(2)
F(12)-P(6)-F(11)	179.4(3)	F(10)-P(6)-F(11)	89.21(19)
F(13)-P(7)-F(17)	91.1(2)	F(13)-P(7)-F(14)	90.60(19)
F(17)-P(7)-F(14)	90.57(19)	F(13)-P(7)-F(15)	178.9(2)
F(17)-P(7)-F(15)	90.0(2)	F(14)-P(7)-F(15)	89.42(18)
F(13)-P(7)-F(16)	90.50(19)	F(17)-P(7)-F(16)	90.2(2)
F(14)-P(7)-F(16)	178.6(2)	F(15)-P(7)-F(16)	89.47(19)
F(13)-P(7)-F(18)	90.1(2)	F(17)-P(7)-F(18)	178.8(2)

Table 2-9. (cont'd)

F(14)-P(7)-F(18)	89.59(18)	F(15)-P(7)-F(18)	88.83(18)
F(16)-P(7)-F(18)	89.58(18)	F(21)-P(8)-F(19)	178.5(2)
F(21)-P(8)-F(20)	89.47(19)	F(19)-P(8)-F(20)	89.3(2)
F(21)-P(8)-F(23)	90.0(2)	F(19)-P(8)-F(23)	89.0(2)
F(20)-P(8)-F(23)	89.87(19)	F(21)-P(8)-F(24)	91.1(2)
F(19)-P(8)-F(24)	89.9(2)	F(20)-P(8)-F(24)	90.19(18)
F(23)-P(8)-F(24)	178.9(2)	F(21)-P(8)-F(22)	90.4(2)
F(19)-P(8)-F(22)	90.8(2)	F(20)-P(8)-F(22)	179.7(2)
F(23)-P(8)-F(22)	89.90(19)	F(24)-P(8)-F(22)	90.04(19)

2.6.5 Copyright note

Chapter 3

Synthesis and characterization of $[Rh(P_2N_2)_2]^+$ and $HRh(P_2N_2)_2$ complexes and investigation of second coordination sphere interactions on CO_2 hydrogenation

3.1 Introduction

The incorporation of functional groups in the second coordination sphere of molecular catalysts has been studied as a strategy to produce simple functional mimics of nature's most active catalysts.[1] Nickel complexes with cyclic diphosphine P_2N_2 (1,5-diaza-3,7-diphosphacyclooctane) ligands[2,3] are a prominent example of this approach. The development of these complexes by Daniel Dubois and co-workers was inspired by the prevalence of proton containing amino acid functional groups in the active sites of many enzymes. P_2N_2 ligands contain pendant nitrogen base arms that help to shuttle protons to and from the metal center. In

$Ni(P_2N_2)_2$ complexes this proton shuttling activity of the amine groups enables some of the highest turnover frequencies for proton reduction/H_2 oxidation known by an artificial catalyst.[4,5] The presumed mechanism involves a transient Ni–H species and protonated pendant bases.[6,7]

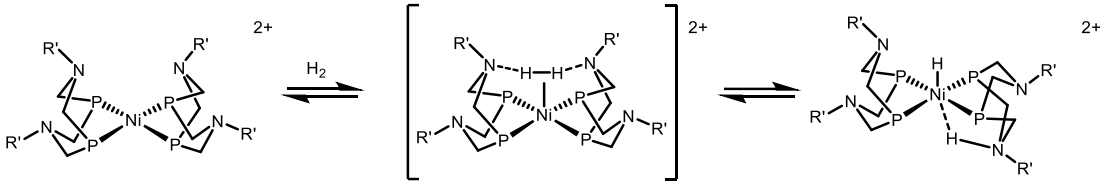

Figure 3-1. Proposed intermediates in the mechanism for proton reduction/ H_2 oxidation in $Ni(P_2N_2)_2$ complexes.

We became interested in the use of $Ni(P_2N_2)_2$ complexes for CO_2 reduction because of their potential to deliver both a proton and a hydride to CO_2. It has been demonstrated that these complexes have the ability to hold a hydride and a proton in close proximity, suggesting they might be suitable to simultaneously engage CO_2 at its electrophilic and nucleophilic sites, as is done in nature's CO_2 reduction catalysts. We quickly found that they thermodynamically favor the reverse reaction, the oxidative decomposition of formic acid to CO_2 and H_2.[8,9] In these studies the participation of the pendant base in the mechanism was found to be necessary for catalysts, lending support to the idea that the participation of a base in the second coordination sphere can lead to unique CO_2/formate reactivity.

The formate decomposition reactivity of the Ni complexes makes sense when the thermodynamic parameter known as the "hydricity" of the $Ni(P_2N_2)_2$ complexes is compared to the hydricity of formate. Hydricity is a measure of hydride donor ability, analogous to how acidity is a measure of proton donor ability (**Scheme 3-1**). A smaller hydricity indicates that the compound is a better hydride donor and a larger hydricity indicates the compound (in the conjugate non-hydride state) is a better hydride acceptor. The hydricity of formate is 44

kcal/mol,[10,11] so if a metal complex has a hydricity that is higher, it is not thermodynamically favorable to for that complex to donate a hydride to CO_2 to make formate (the reverse reaction is favored). The $Ni(P_2N_2)_2$ complexes extensively studied by the Dubois group have hydricities that range from 55 to 60 kcal/mol, so they are not nearly hydridic enough for CO_2 hydrogenation, and even under elevated pressures of H_2 and CO_2 hydrogenation does not occur.[8]

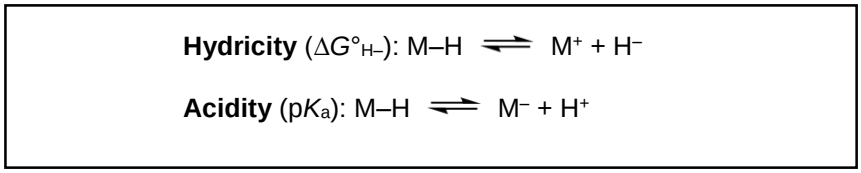

Scheme 3-1. Chemical equations demonstrating the hydride and proton donor ability, respectively, of a generic metal hydride.

The hydricity of complexes of this type can be increased by increasing the electron donating ability of the ligands[6,12,13] to potentially make the reverse reaction more favorable. The increase can be understood from a simple molecular orbital perspective, as the energy of the anti-bonding d orbitals would be destabilized by increased mixing of the metal d orbitals and the ligand sigma orbitals, resulting in an increase the energy of the $dx^2–y^2$ LUMO acceptor orbital. This would cause a destabilized $Ni(d_x^2–y^2)–H(1s)$ interaction in the resulting hydride complex and an increased hydride donor ability (**Figure 3-2**). In our lab, Prof. Kyle Grice and Michael Doud made efforts to increase the electron donating ability of P_2N_2 ligands through the development of a new ligand synthesis that allowed various alkyl phosphine substituted P_2N_2 ligands to be made (the previous synthesis protocol only allowed for the synthesis of phenyl and cyclohexyl phosphine substituted ligands).[3] The Dubois group measured the hydricity of the newly synthesized $[HNi(P^{Me}{}_2N^{Ph}{}_2)_2]^+$ complex to be 54 kcal/mol, which was still not sufficiently hydridic to reduce CO_2.[5]

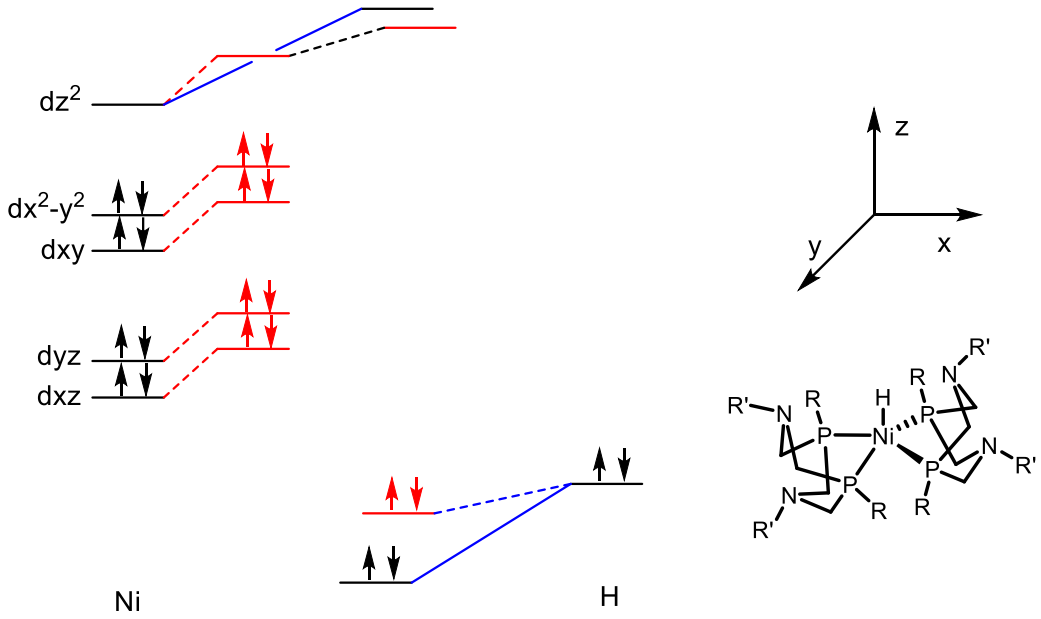

Figure 3-2. MO diagram showing the interaction between a Ni^{2+}-ligand fragment and a hydride. An increase in the overlap between the Ni and its phosphine ligands results in destabilization of the Ni d orbitals and the Ni-H bonding orbital (red lines).

We also decided to explore the synthesis of other transition metal complexes with P_2N_2 ligands that would make more hydricic metal hydride complexes. Experimental data of the 16-e^- $[M(diphosphine)_2]^{n+}$ class show the hydricities of the metal complexes with the same ligand set generally tend to increase as you move to the left or down the periodic table[11,13-15] and the trends are also supported by computational studies.[16-18] This is consistent with the destabilization of d orbital energies arising from a decrease in Z_{eff} as you move down a row a or to the left of the periodic table, resulting in destabilization of the M–H bonding orbital (similar to the molecular orbital situation shown in **Figure 3-2**). Dr. Candace Seu worked on the synthesis of a series of $Pd(P_2N_2)_2$ for CO_2 reduction, as it was reasoned that these complexes might be just hydric enough to reduce CO_2; Comparisons of $[M(diphosphine)_2]^{2+}$ complexes (M = Ni and Pd diphosphine = PNP) show that the Pd complex was 15 kcal/mol more hydricic than the Ni complex.[15,19] A similar increase in hydricity in the $Pd(P_2N_2)_2$ complexes compared to nickel would put the hydricities close to that of formate. The series of $Pd(P_2N_2)_2$ complexes

were tested for their ability to electrochemically reduce CO_2, but these complexes do not show any electrochemical reactivity with CO_2 in the absence of protons and in the presence of an excess of protons, they preferentially produce H_2.[20] Experimental measurements of the hydricities failed, but the absence of electrochemical reactivity with CO_2 may indicate that these complexes are also not hydridic enough to donate a hydride to CO_2.

Given its rich hydrogenation chemistry,[21,22] Rh(I) was a natural choice to make sufficiently hydridic $M(P_2N_2)_2$ complexes for CO_2 reduction to study the effects adding functional groups to the second coordination sphere of a CO_2 reduction catalyst. CO_2 hydrogenation with rhodium bis-diphosphine complexes has previously been reported[23,24] and there was also a report of electrochemical reduction of CO_2 to formate by a rhodium bis-diphosphine complex.[25] The hydricities of a few $[Rh(diphosphine)_2]^+$ complexes have been measured and the values measured range from 28–34 kcal/mol.[14,26] The hydricties of several other $[Rh(diphosphine)_2]^+$ complexes have been calculated[12] and for all complexes, it would be thermodynamically favorable for hydride transfer to CO_2 to occur.

Tuning of the second coordination sphere of rhodium bis-diphosphine CO_2 reduction catalysts could potentially lead to rate enhancements in their electrochemical and/or thermal hydrogenation activity, as has been observed in other CO_2 hydrogenation[27-29] and electrochemical reduction catalysts.[30] Recently, pendant bases have been incorporated into this type of catalyst through PNP diphosphine ligands which contain amines in the second coordination sphere and mono- and dipeptides in the outer coordination sphere and studies of the influence of the added substituents on the thermal hydrogenation of CO_2 were conducted. It was found that the addition of an amine in the second coordination sphere increased catalytic rates for CO_2 hydrogenation by increasing electron density at the metal center, increasing the hydricity of the Rh complexes, but electron withdrawing substituents in the outer coordination

sphere decreased activity.[31] What was unclear after this study is whether the addition of the pendant base had any effect on catalysis beyond just changing the electron density at the metal center.

We set out to synthesize rhodium diphosphine complexes with P_2N_2 ligands to extend the chemistry of the P_2N_2 platform to rhodium, map out thermodynamic properties of these complexes relevant to catalysis, and to explore the effects of the pendant base containing ligands on the hydrogenation of CO_2. Herein we report the synthesis and characterization of these complexes and the corresponding rhodium hydrides, as well as thermodynamic measurements of K_{eq} for oxidative H_2 addition, and hydricities and acidities of the monohydride species. We also report the relative CO_2 hydrogenation activity of these complexes and $[Rh(depe)_2]^+$, a complex that has a hydricity in the range of the values measured for the $[Rh(P_2N_2)_2]^+$ complexes in this report, but no pendant base, and discuss how substituent effects may be changing the rates for CO_2 hydrogenation.

3.2 Experimental

Materials and Methods

Unless otherwise noted, all reactions were carried out under a N_2 atmosphere using standard Schlenk and glovebox techniques. Acetone was dried over 4Å molecular sieves and degassed prior to use. All other solvents used were dried over activated molecular sieves and alumina and degassed prior to use. The diphosphine ligands $P^{Ph}{}_2N^{Ph}{}_2$, $P^{Cy}{}_2N^{Ph}{}_2$, $P^{Ph}{}_2N^{PhOMe}{}_2$, $P^{Cy}{}_2N^{PhOMe}{}_2$, and $P^{Ph}{}_2N^{Bn}{}_2$ were synthesized as previously reported.[8,32] Tetrabutylammonium hexafluorophosphate (NBu_4PF_6) was recrystallized from methanol prior to use. All other chemicals were obtained from commercial suppliers and used without further purification. ^1H and $^{31}P\{^1H\}$ NMR spectra were recorded using 300MHz or 500MHz Varian spectrometers. ^1H

NMR chemical shifts were referenced against the residual solvent signal and are reported in ppm downfield of tetramethylsilane ($\delta = 0$). $^{31}P\{^{1}H\}$ NMR chemical shifts were externally referenced to 85 % phosphoric acid ($\delta = 0$). Mass spectrometry data was collected on a Finnagan LCQDECA in ESI positive ion mode. Elemental analyses were performed by Midwest Microlabs, LLC. in Indianapolis, Indiana.

Electrochemical Experiments

Electrochemical experiments were performed using a BAS Epsilon potentiostat. Cyclic voltammograms (CV's) were performed under nitrogen in a one compartment cell using a glassy carbon BASi working electrode, a glassy carbon rod counter electrode, and a non-aqueous Ag reference electrode from BASi that contained an acetonitrile solution of 0.2 M NBu_4PF_6 and 1mM $AgNO_3$. All experiments were performed in dry acetonitrile using 0.2 M NBu_4PF_6 as the supporting electrolyte. After taking initial CV's, Cp_2Co^+ was added as an internal reference. Then, a clean electrolyte solution was made and another CV of Cp_2Co^+ was taken to confirm that the reference electrode was stable. The position of the Cp_2Co^+ couple was then used to reference the reduction potentials of the complexes to the Cp_2Fe^+/Cp_2Fe couple in acetonitrile.

Crystallography

Crystals of the Rh complexes suitable for X-ray structural determinations were mounted in polybutene oil on a glass fiber and transferred on the goniometer head to the precooled instrument (100 K). Data was collected on either a Bruker P4, Platform, D8 Venture, or Kappa Apex II diffractometer. Crystallographic measurements were carried out using Mo Kα radiation ($\lambda = 0.71073$ Å) or Cu Kα radiation ($\lambda = 1.54178$ Å). All structures were solved by direct methods using OLEX2 and refined with full-matrix least-squares procedures using SHELXL-97. All non-hydrogen atoms were anisotropically refined unless otherwise reported.

The hydrogen atoms were included in calculated positions as ridged models in the refinement, unless otherwise reported.

Synthesis of $[Rh(P^{Ph}{}_2N^{Ph}{}_2)_2]BF_4$ (1)

In a 10 mL schlenk flask, Chloro(1,5-cyclooctadiene)rhodium(I) dimer (0.228 g, 0.462 mmol) and silver tetrafluoroborate (0.180 g, 0.925 mmol) were slurried in 5 mL acetone. The mixture was allowed to stir for 1 hour. In a 100 mL schlenk flask, $P^{Ph}{}_2N^{Ph}{}_2$ (0.834 g, 1.85 mmol) was dissolved in 50 mL methylene chloride. The AgCl that precipitated out in the first flask was filtered out and the yellow filtrate was added to the 100 mL flask containing the ligand, producing an orange solution. The solution was allowed to stir overnight. The solution was reduced and diethyl ether was added, forming a yellow precipitate. The precipitate was collected to obtain 0.783 g (61%) of a yellow powder. ^{1}H NMR (500 MHz, CD_3CN): δ 7.46–7.40 (m, 8H, Ar*H*), 7.30–7.14 (m, 12H, Ar*H*), 7.10 (t, *J* = 7.6 Hz, 8H, Ar*H*), 7.04–6.88 (m, 12H, Ar*H*), 4.05 (s, 18H, PC*H*$_2$N).^{31}P{^{1}H} NMR (121 MHz, CD_3CN): δ 5.38 (d, $J_{Rh\text{-}P}$ = 123.7 Hz). HRMS (ESI-TOF) m/z: $[M–BF_4]^+$ Calc. for $C_{56}H_{56}N_4P_4Rh$: 1011.2505; Found: 1011.2501, 100%. Elemental Anal. Calc. for $C_{56}H_{56}N_4P_4Rh$: C, 61.22%; H, 5.14%; N, 5.10%; Found: C, 61.28%; H, 5.10 %; N, 5.06%.

Synthesis of $[Rh(P^{Ph}{}_2N^{Bn}{}_2)_2]BF_4$ (2)

This complex was synthesized using a procedure similar to that for $Rh(P^{Ph}{}_2N^{Ph}{}_2)_2BF_4$ in 70% yield. ^{1}H NMR (500 MHz, CD_3CN): δ 7.50–7.24 (m, 20H, Ar*H*), 7.12–7.06 (m, H, Ar*H*), 6.97–6.84 (m, 16H, Ar*H*), 4.30 (s, 8H, C*H*$_2$benzyl), 3.62 (d, *J* = 13.1 Hz, 8H, PC*H*$_2$), 3.31 (d, *J* = 13.1 Hz, 8H, PC*H*$_2$).^{31}P{^{1}H} NMR (121 MHz, CD_3CN): δ –2.71 (d, $J_{Rh\text{-}P}$ = 120.3 Hz). HRMS (ESI-TOF) m/z: $[M–BF_4]^+$ Calc. for $C_{60}H_{64}N_4P_4Rh$: 1067.3131; Found: 1067.3128, 100%. Elemental Anal. Calc. for $C_{60}H_{64}BF_4N_4P_4Rh$: C, 62.41%, H, 5.59%; N, 4.85%; Found, C, 62.21%; H, 5.56%; N, 4.97 %.

Synthesis of $[Rh(P^{Ph}{}_2N^{PhOMe}{}_2)_2]BF_4$ (3)

This complex was synthesized using a procedure similar to that for $Rh(P^{Ph}_2N^{Ph}_2)_2BF_4$ in 94% yield. ^{1}H NMR (500 MHz, CD_3CN): δ 7.29–7.21 (m, 8H, Ar*H*), 7.21–7.12 (m, 4H, Ar*H*), 7.10–6.98 (m, 16H, Ar*H*), 6.95–6.87 (m, 8H, Ar*H*), 3.97 (s, 16H, PCH_2), 3.75 (s, 12H, OCH_3). ^{31}P{^{1}H} NMR (121 MHz, CD_3CN): δ 3.87 (d, J_{Rh-P} = 123.5 Hz). HRMS (ESI-TOF) m/z: $[M–BF_4]^+$ Calc. for $C_{60}H_{64}N_4O_4P_4Rh$: 1131.2928; Found: 1131.2924, 100% Elemental Anal. Calc. For $C_{60}H_{64}BF_4N_4O_4P_4Rh$: C, 59.13%; H, 5.29%; N, 4.60%; Found: C, 59.23%; H, 5.55%, N, 4.60%.

Synthesis of $[Rh(P^{Cy}_2N^{Ph}_2)_2]BF_4$ (4)

This complex was synthesized using a procedure similar to that for $Rh(P^{Ph}_2N^{Ph}_2)_2BF_4$ in 82% yield. ^{1}H NMR (500 MHz, CD_3CN): δ 7.23–7.18 (m, 8H, Ar*H*), 7.08–7.03(m, 8H, Ar*H*), 6.88–6.83 (m, 4H), 3.80 (s, br, 16H, CH_2P), 1.95–0.99 (m, 40H, CH_2 cyclohexyl). ^{31}P{^{1}H} NMR (121 MHz, CD_3CN): δ 9.6 (d, J_{Rh-P} = 122.4 Hz). HRMS (ESI-TOF) m/z: $[M–BF_4]^+$ Calc. for $C_{56}H_{80}N_4P4Rh$: 1035.4383; Found: 1035.4381, 100%. Elemental Anal. Calc. for $C_{56}H_{80}BF_4N_4P_4Rh$: C, 59.90%; H, 7.18%; 4.99%. Found: C, 58.99%; H, 7.12%; N, 4.94%.

Synthesis of $[Rh(P^{Cy}_2N^{PhOMe}_2]_2BF_4$ (5)

This complex was synthesized using a procedure similar to that for $Rh(P^{Ph}_2N^{Ph}_2)_2BF_4$ in 59% yield. ^{1}H NMR (500 MHz, CD_3CN): δ 7.09 (d, J = 9.0 Hz, 8H, Ar*H*), 6.78 (d, J = 9.0 Hz, 8H, Ar*H*), 3.67 (s, 16H, OCH_3), 1.97–0.70 (m, 40H, CH_2 cycohexyl). ^{31}P{^{1}H} NMR (121 MHz, CD_3CN): δ 8.09 (d, J_{Rh-P} = 122.6 Hz). HRMS (ESI-TOF) m/z: $[M–BF_4]^+$ Calc. for $C_{60}H_{88}N_4O_4P_4Rh$: 1155.4806; Found: 1155.4803, 100%. Elemental Anal. Calc. for $C_{60}H_{88}N_4O_4P_4Rh$: C, 57.98%; H, 7.14%; N, 4.51%; Found: C, 57.54%; H, 6.97%; N, 4.28%.

Synthesis of $HRh(P^{Ph}_2N^{Ph}_2)_2$ (6)

0.113 g (0.103 mmol) $[Rh(P^{Ph}_2N^{Ph}_2)_2]BF_4$ was added to a vial with a stir bar along with 10 mL toluene. 124 µL of a solution of 1M $NaHBEt_3$ in toluene (0.145 mmol) was added to the stirring solution via syringe. The yellow solution began to turn orange and formed an orange

precipitate. The solution was stirred overnight and the toluene was then removed. The orange product was dissolved in 10 mL THF and filtered to remove the $NaBF_4$. The THF solution was layered with 10 mL pentane and cooled to –35 ^{0}C. The next day the orange precipitate was collected and dried in vacuum to yield 0.058 g product (56%). ^{1}H NMR (500 MHz, C_6D_6): δ 7.55 (broad s, 8H, Ar*H*), 7.14–7.05 (m, 8H, Ar*H*), 7.04–6.94 (m, 12H, Ar*H*), 6.88–6.73 (m, 12H, Ar*H*), 3.91 (d, *J* = 13.0 Hz, 8H, PCH_2), 3.57 (d, *J* = 13.0 Hz, 8H, PCH_2), –8.43 (pd, *J* = 27.3, 14.5 Hz, 1H, Rh*H*).^{31}P{^{1}H} NMR (121 MHz, C_6D_6): δ 16.06 (d, $J_{Rh\text{-}P}$ = 129.2 Hz). ESI-MS (m/z): (1012.3, $[M]^+$, 63%, 1011.3, $[M–H]^+$, 100%. Elemental Anal. Calc. for $C_{56}H_{57}N_4P_4Rh$: C, 66.40%; H, 5.67%; N, 5.53%. Found: C, 66.17%; H, 5.58%; N, 5.51%.

Synthesis of HRh($P^{Ph}_2N^{Bn}_2$)$_2$ (7)

Complex was synthesized using a procedure similar to that for HRh($P^{Ph}_2N^{Ph}_2$)$_2$ in 50% yield. ^{1}H NMR (500 MHz, C_6D_6): δ 7.95–7.50 (m, 8H, Ar*H*), 7.28–7.19 (m, 8H, Ar*H*), 7.18–6.91 (m, 24H, Ar*H*), 3.67 (s, 8H, CH_2benzyl), 3.33 (d, *J* = 11.8 Hz, 8H, PCH_2), 2.78 (d, *J* = 11.8 Hz, 8H, PCH_2), –7.66 (pd, *J* = 26.2, 17.6 Hz, 1H, Rh*H*). ^{31}P{^{1}H} NMR (121 MHz, C_6D_6): δ 9.05 (d, $J_{Rh\text{-}P}$ = 129.4 Hz). ESI-MS (m/z): (10168.3, $[M]^+$, 66%, 1067.3, $[M–H]^+$, 100%. Elemental Anal. Calc. for $C_{60}H_{65}N_4P_4Rh$: C, 67.41%, H, 6.13%; N, 5.42%. Found: C, 67.33%; H, 6.20%; N, 5.20%.

Synthesis of HRh($P^{Ph}_2N^{PhOMe}_2$)$_2$ (8)

This complex was synthesized using a procedure similar to that for HRh($P^{Ph}_2N^{Ph}_2$)$_2$ in 75% yield. ^{1}H NMR (500 MHz, C_6D_6): δ 7.61 (broad s, 8H, Ar*H*), 7.07–7.00 (m, 12H, Ar*H*), 6.91–6.83 (m, 8H, Ar*H*), 6.83–6.72 (m, 8H, Ar*H*), 3.94 (d, *J* = 12.7 Hz, 8H, PCH_2), 3.59 (d, *J* = 12.7 Hz, 8H, PCH_2), 3.36 (s, 12H, CH_3O), –8.32 (pd, *J* = 26.8, 14.1 Hz, 1H, Rh*H*). ^{31}P{^{1}H} NMR (121 MHz, C_6D_6): δ 13.79 (d, $J_{Rh\text{-}P}$ = 128.6 Hz). ESI-MS (m/z): (1132.2, $[M]^+$, 57%, 1131.2, $[M–H]^+$, 100%. Elemental Anal. Calc. for $C_{60}H_{65}N_4P_4Rh$: C, 63.61%; H, 5.78%, 4.95%. Found: C, 62.80%; H, 5.81%; N, 5.00%.

Synthesis of $HRh(P^{Cy}_2N^{Ph}_2)_2$ (9)

This complex was synthesized using a procedure similar to that for $HRh(P^{Ph}_2N^{Ph}_2)_2$ in 60% yield. ^{1}H NMR (500 MHz, C_6D_6) δ 7.27–7.21 (m, 8H, Ar*H*), 7.10–7.04 (m, 8H, Ar*H*), 6.88–6.82 (m, 4H, Ar*H*), 3.44 (q, *J* = 12.5 Hz, 16H, PCH_2), –10.27 (pd, *J* = 23.5, 12.1 Hz, 1H). ^{31}P{^{1}H} NMR (121 MHz, C_6D_6): δ 21.72 (d, J_{Rh-P} = 128.2 Hz). ESI-MS (m/z): (1036.4, $[M]^+$, 63%, 1035.4, $[M–H]^+$. Elemental Anal. Calc. for $C_{60}H_{81}N_4P_4Rh$: C, 64.86%; H, 7.87%; N, 5.40%. Found: C, 64.21%; H, 7.72%; N, 5.45%.

Synthesis of $HRh(P^{Cy}_2N^{PhOMe}_2)_2$ (10)

This complex was synthesized using a procedure similar to that for $HRh(P^{Ph}_2N^{Ph}_2)_2$ in 72% yield. ^{1}H NMR (500 MHz, C_6D_6): δ 7.10–7.03 (m, 8H, Ar*H*), 6.92–6.80 (m, 8H, Ar*H*), 3.45 (d, *J* = 12.2 Hz, 8H, PCH_2), 3.42 – 3.35 (s (OCH_3, 12H) overlayed by d (PCH_2, 8H), 1.94 –0.73 (m, 40H, Cy*H*), –10.20 (dp, *J* = 23.3, 12.1 Hz, 1H). ^{31}P{^{1}H} NMR (121 MHz, C_6D_6): δ 21.67 (d, J_{Rh-P} = 131.5 Hz). ESI-MS (m/z): (1156.4, $[M]^+$, 59%, 1055.4, $[M–H]^+$, Elemental Anal. Calc. for $C_{60}H_{89}N_4O_4P_4Rh$: C, 62.28%; H, 7.75%, N, 4.48%. Found: C, 62.21%; H, 7.80%; N, 4.48%.

General Procedure for Hydricity Determination by Heterolytic H_2 Cleavage:

$[Rh(P^{Ph}_2N^{PhOMe}_2)_2]BF_4$. In a typical experiment, $[Rh(P^{Ph}_2N^{PhOMe}_2)_2]BF_4$ (10–16 mg, 0.009–0.013 mmol) and 2,8,9-triisopropyl-2,5,8,9-tetraaza-1-phosphabicyclo[3,3,3]undecane (7.5–16 mg, 0.02–0.04mmol) were weighed into 3 J. Young NMR tubes and dissolved in 0.5 mL benzonitrile. The tubes were evacuated and an atmosphere of H_2 was introduced. After 2 weeks an equilibrium was reached indicated by a constant ratio of products. Integration of each of the peaks of the 4 species in the ^{31}P NMR spectra allowed for the determination of the relative ratios and these were used to determine the equilibrium constant. Equilibrium constants were calculated using the average of data obtained from 3 experiments.

General Procedure for the reaction of H_2 gas with $[Rh(P_2N_2)_2]BF_4$ complexes:

An NMR tube capped with a rubber septa containing 0.043 M THF-d_8 was purged with H_2 for 10 min using a needle. ^{31}P NMR spectra were recorded and integrated to determine the relative ratios of $[Rh(P_2N_2)_2]^+$ to $[H_2Rh(P_2N_2)_2]^+$. Equilibrium constants were calculated using the average of data obtained from 3 experiments.

General Procedure for Catalysis.

In a glovebox, ~400 mg of Verkade's base (2,8,9-triisobutyl-2,5,8,9-tetraaza-1-phosphabicyclo[3.3.3]undecane) was dissolved in 2 mL of THF-d_8 to make the base concentration ~ 500 mM. The appropriate amount of catalysts was added to make catalysts concentration ~1mM. 4 µL benzene was added as an internal standard for the quantification of formate. 400 µL of this solution was added to 3 J. Young NMR tubes. The tubes were freeze-pump-thawed to remove N_2 and then backfilled with 1 atm CO_2. They were then frozen with liquid N_2 just up to the solvent line to condense the CO_2 and then an atmosphere of H_2 was introduced to the headspace to make the overall pressure ~ 2 atm of 1:1 CO_2/H_2. The tube was brought to room temperature and briefly placed in a vortex mixer to allow for gas mixing and quantitative ^1H NMR and $^{31}P\{^1H\}$ were collected between 2 to 5 min apart for 1 hour. The amount of conversion at each point was measured by comparing the integral of the benzene peak with the formate peak. Turnover frequencies were calculated from the slope of the linear portions of the plots of time verses the amount of formate. The turnover frequencies given are an average for three experiments.

3.3 Results and Discussion

3.3.1 Synthesis

Synthesis of $[Rh(P_2N_2)_2]BF_4$ complexes

A series of P_2N_2 ligands was chosen in order to systematically vary the hydricities of the rhodium compounds and the basicities of the pendant amines. The ligands $P^{Cy}{}_2N^{Ph}{}_2$,

$P^{Ph}{}_2N^{Ph}{}_2$, $P^{Ph}{}_2N^{Bn}{}_2$, $P^{Ph}{}_2N^{PhOMe}{}_2$, and $P^{Cy}{}_2N^{PhOMe}{}_2$ were synthesized as previously reported.[8,32] Procedures for the synthesis of Rh(I) complexes **1**–**5** were adapted from previously reported methods.[14] Stoichiometric amounts of rhodium(I) chloride 1,5-cyclooctadiene dimer and $AgBF_4$ were dissolved in acetone, the precipitated AgCl was filtered out, and the filtrate was added to a methylene chloride solution containing two equivalents of ligand per Rh and allowed to react overnight. The solvent was reduced in volume and the product was precipitated with the addition of diethyl ether to yield complexes **1**–**5**, isolated as yellow powders. All complexes were characterized by elemental analysis, mass spectroscopy, and ^1H and $^{31}P\{^1H\}$ NMR spectroscopy. The ^{31}P NMR of each shows a characteristic doublet in the range of –3 to 10 ppm with a $^1J_{P\text{-}Rh}$ coupling constant of 121–124 Hz. The ^{31}P shifts and coupling constants are consistent with a chelating phosphine bound to Rh(I).[14,33] The single sharp $^{31}P\{^1H\}$ resonance is indicative of all four phosphorus atoms being magnetically equivalent. The $^{31}P\{^1H\}$ NMR data is provided in **Table 3-1** for comparison and the rest of the spectroscopic data is given in the Experimental section.

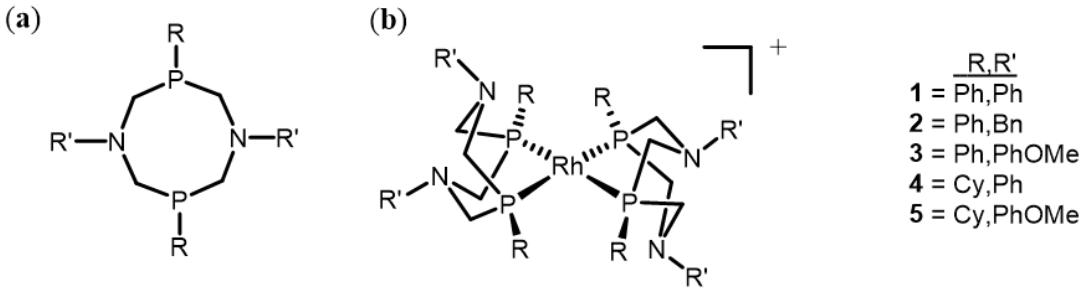

Figure 3-3. Structure of a P_2N_2 ligand (a) and a $[Rh(P_2N_2)_2]^+$ complex (b).

Synthesis of $HRh(P_2N_2)_2$ complexes

$HRh(P_2N_2)_2$ complexes **6**–**10** were synthesized by reacting the $[Rh(P_2N_2)_2]BF_4$ complexes with 1.2 equivalents of $NaHBEt_3$ in toluene. The solutions were stirred overnight and then filtered to remove any precipitated $NaBF_4$. The filtrates were evaporated and the

residues were dissolved in a minimum of THF and layered with pentane to induce precipitation of the products, which were isolated as yellow to red-orange powders and were characterized by elemental analysis, mass spectroscopy, and ^{1}H and $^{31}P\{^{1}H\}$ NMR spectroscopy. In the ^{1}H NMR spectra, the hydride resonances appear as a doublet of quintets, consistent with splitting by one Rh and four equivalent phosphorus atoms. The $^{31}P\{^{1}H\}$ spectra contain one resonance that appears as a doublet ($^{1}J_{P-Rh}$ = 128–132 Hz) shifted downfield by about 10 ppm as compared to the parent diphosphine complex.

Table 3-1. ^{1}H and $^{31}P\{^{1}H\}$ NMR assignments for $[Rh(P_2N_2)_2]^+$, $HRh(P_2N_2)_2$ and $[H_2Rh(P_2N_2)_2]^+$ complexes.

Complex		$^{31}P\{^{1}H\}$ NMR (ppm)	^{1}H NMR Hydride peak (ppm)
1	$[Rh(P^{Ph}{}_2N^{Ph}{}_2)_2]^+$	5.38[a]	—
2	$[Rh(P^{Ph}{}_2N^{Bn}{}_2)_2]^+$	–2.71[a]	—
3	$[Rh(P^{Ph}{}_2N^{PhOMe}{}_2)_2]^+$	3.87[a]	—
4	$[Rh(P^{Cy}{}_2N^{Ph}{}_2)_2]^+$	9.6[a]	—
5	$[Rh(P^{Cy}{}_2N^{PhOMe}{}_2)_2]^+$	8.09[a]	—
6	$HRh(P^{Ph}{}_2N^{Ph}{}_2)_2$	16.06[b]	–8.43[b]
7	$HRh(P^{Ph}{}_2N^{Bn}{}_2)_2$	9.05[b]	–7.66[b]
8	$HRh(P^{Ph}{}_2N^{PhOMe}{}_2)_2$	13.79[b]	–8.32[b]
9	$HRh(P^{Cy}{}_2N^{Ph}{}_2)_2$	21.72[b]	–10.27[b]
10	$HRh(P^{Cy}{}_2N^{PhOMe}{}_2)_2$	21.67[b]	–10.20[b]
	$[H_2Rh(P^{Ph}{}_2N^{Ph}{}_2)_2]^+$	15.25, 1.79[b]	*C*
	$[H_2Rh(P^{Ph}{}_2N^{Bn}{}_2)_2]^+$	12.38, 2.97[b]	*C*
	$[H_2Rh(P^{Ph}{}_2N^{PhOMe}{}_2)_2]^+$	13.3, 1.12[b]	*C*
	$[H_2Rh(P^{Cy}{}_2N^{Ph}{}_2)_2]^+$	15.99, 16.54[b]	*C*
	$[H_2Rh(P^{Cy}{}_2N^{OMe}{}_2)_2]^+$	15.22, 14.61[b]	*C*

[a] Measured in CD_3CN. [b] Measured in C_6D_6. [c] Peak was not observed.

3.3.2 Structural Characterization

Solid-state structures of complexes **1–5** were obtained via single-crystal diffraction (**Figure 3-4** to **Figure 3-8**) and selected bond lengths, bond angles, and dihedral angles are shown in **Table 3-2**. For complex **1**, the PF_6 salt was used, as it crystallized more easily than the BF_4 salt. The two salts are indistinguishable by NMR and mass spectroscopy. Suitable crystals for X-ray diffraction of all complexes were grown from the vapor diffusion of diethyl ether into saturated acetonitrile solutions. Complexes **1–5** show very similar structures in which both P_2N_2 ligands are coordinated to the Rh through the phosphorus atoms, with nominally square planar geometries around the Rh(I) centers. The small deviations from square planar geometry can be best compared via their dihedral angles (**Table 3-2**). In **1**–**4**, the ligands consistently crystallize in alternating chair-boat-chair-boat conformations with respect to the two 6 membered metallocycles formed by each ligand clockwise around the central Rh atom. The complexes also have very similar dihedral angles, ranging from 23–26°. In complex **5**, both ligands crystallize in boat-boat conformations. The geometry of complex **5** is more distorted towards tetrahedral, with a dihedral angle of 32.3°. In all complexes, the ligands show similar bite angles (79–82°). The measured bite angles are smaller by an average of 1° when compared to the analogous Ni complexes and 0.6° smaller when compared to the Pd complexes. The Rh–P bond lengths of the five structures are on the order of 2.28 Å, which is slightly longer (0.08 Å) when compared to the analogous Ni complexes, but slightly shorter (0.05 Å) when compared to the Pd complexes.

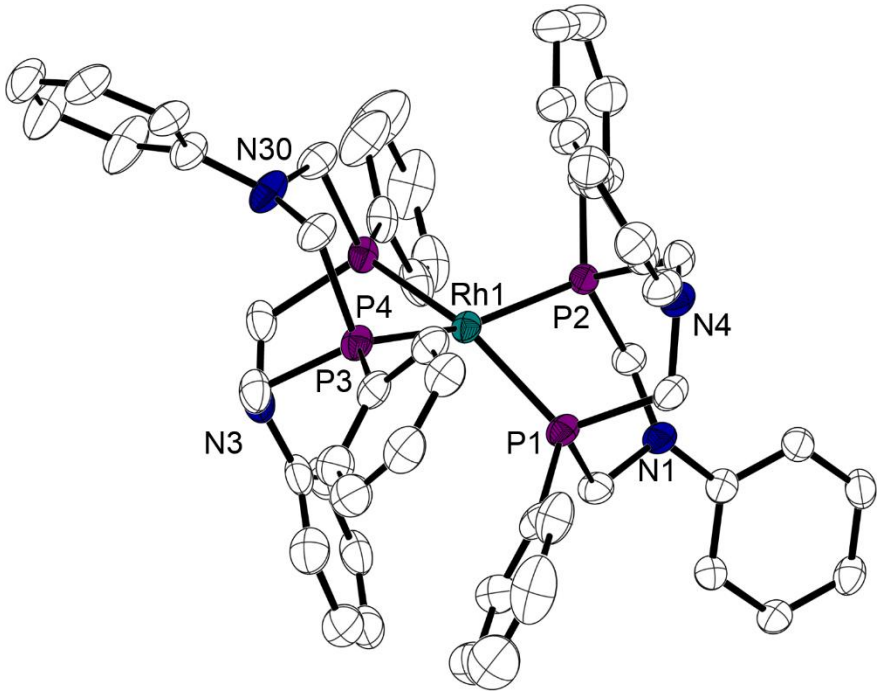

Figure 3-4. Thermal ellipsoid plots of $[Rh(P^{Ph}_2N^{Ph}_2)_2]^+$ (**1**) shown at the 50% probability level. Hydrogens, uncoordinated solvent molecules, and the counter ion has been omitted for clarity.

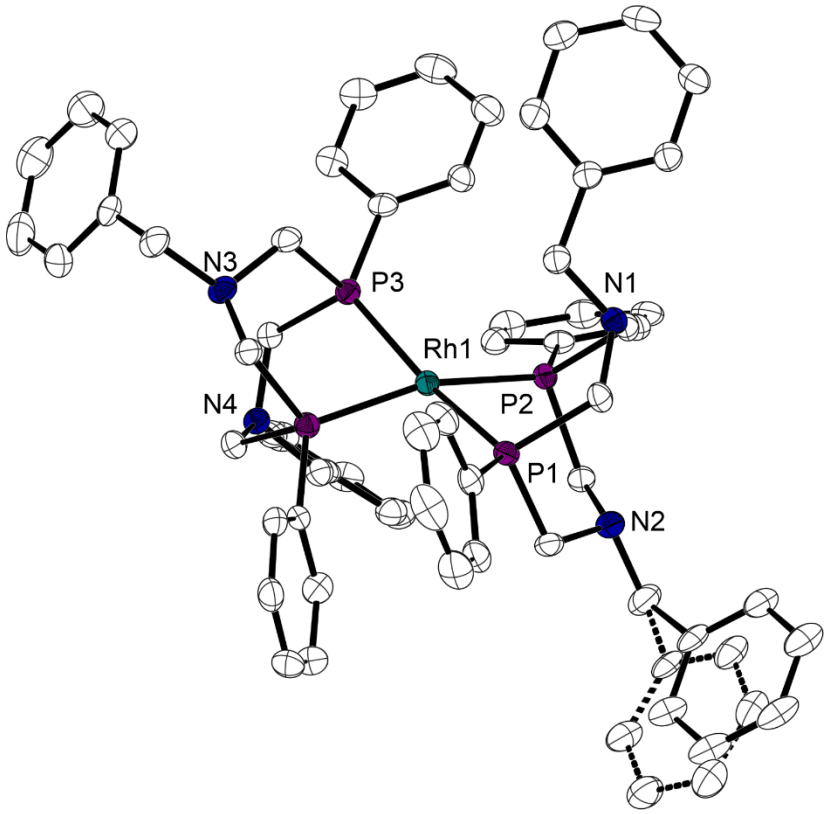

Figure 3-5. Thermal ellipsoid plots of $[Rh(P^{Ph}_2N^{Bn}_2)_2]^+$ (**2**) shown at the 50% probability level. Hydrogens, uncoordinated solvent molecules, and the counter ion has been omitted for clarity.

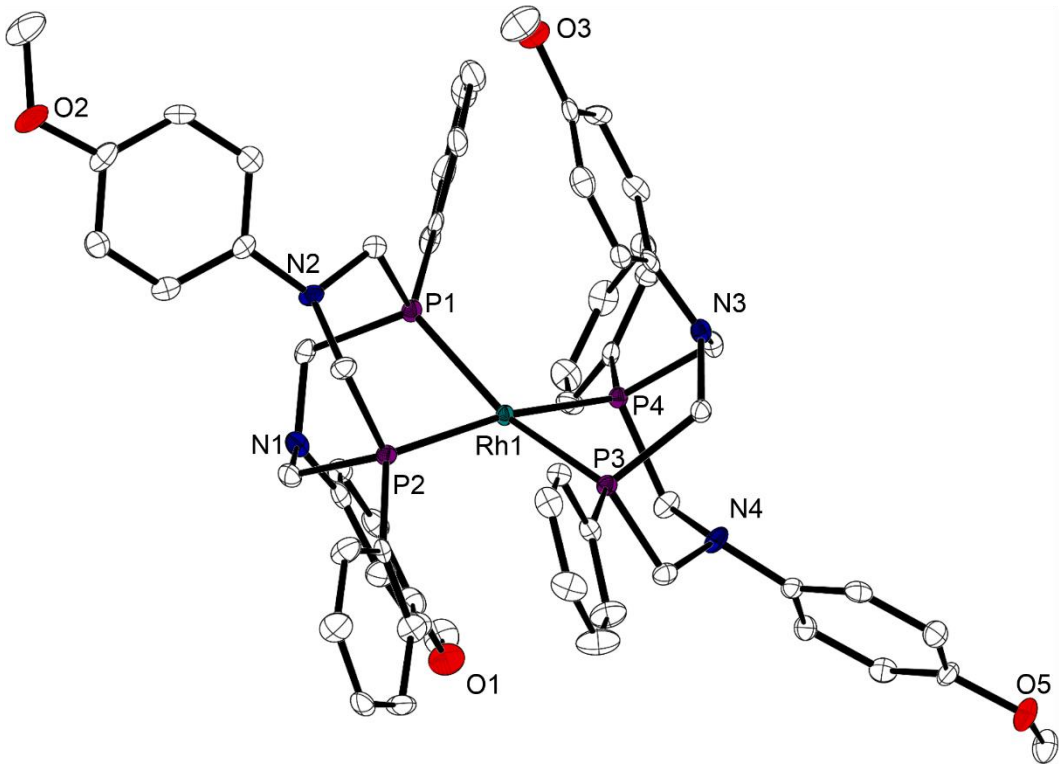

Figure 3-6. Thermal ellipsoid plots of $[Rh(P^{Ph}{}_2N^{PhOMe}{}_2)_2]^+$ (**3**) shown at the 50% probability level. Hydrogens, uncoordinated solvent molecules, and the counter ion has been omitted for clarity.

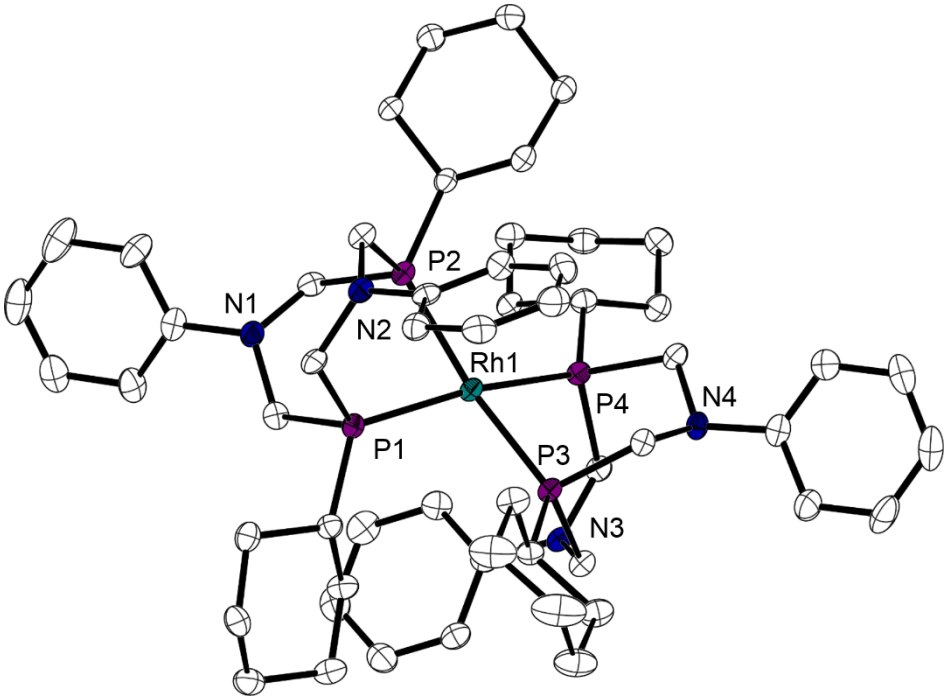

Figure 3-7. Thermal ellipsoid plots of $[Rh(P^{Cy}{}_2N^{Ph}{}_2)_2]^+$ (**4**) shown at the 50% probability level. Hydrogens and the counter ion has been omitted for clarity.

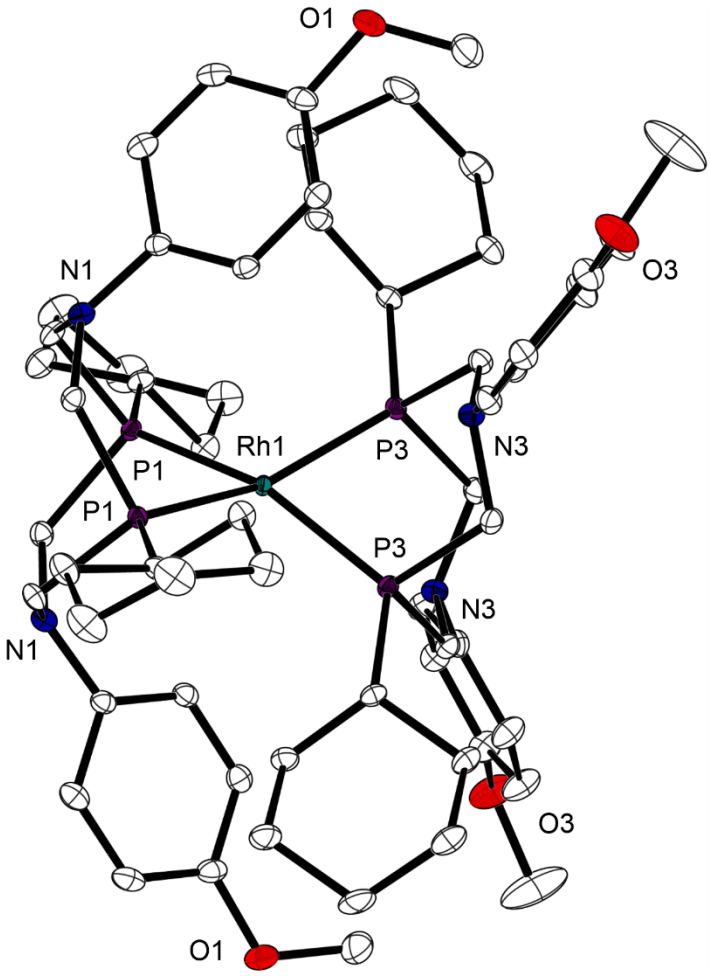

Figure 3-8. Thermal ellipsoid plots of $[Rh(P^{Cy}{}_2N^{PhOMe}{}_2)_2]^+$ (**5**) shown at the 50% probability level. Hydrogens, uncoordinated solvent molecules, and the counter ion has been omitted for clarity.

Table 3-2. Selected bond lengths [Å], bond angles [°], and dihedral angles [°] for the $[Rh(P_2N_2)_2]^+$ complexes **1–5**.

(**1**) $Rh(P^{Ph}_2N^{Ph}_2)_2PF_6$		(**2**) $Rh(P^{Ph}_2N^{Bn}_2)_2BF_4$ a		$Rh(P^{Ph}_2N^{Bn}_2)_2BF_4$ b	
Rh1–P1	2.2863(7)	Rh1–P1	2.2877(10)	Rh1'–P1'	2.2871(10)
Rh1–P2	2.2663(7)	Rh1–P2	2.2724(9)	Rh1'–P2'	2.2718(9)
Rh1–P3	2.2706(7)	Rh1–P3	2.2669(10)	Rh1'–P3'	2.2658(9)
Rh1–P4	2.2715(7)	Rh1–P4	2.2819(9)	Rh1'–P4'	2.2793(9)
P2–Rh1–P1	81.03(2)	P1–Rh1–P2	80.02(3)	P1'–Rh1'–P2'	79.43(3)
P3–Rh1–P4	81.97(3)	P3–Rh1–P4	80.79(3)	P3'–Rh1'–P4'	79.96(3)
P1–Rh1–P4	162.17(3)	P1–Rh1–P3	165.57(4)	P3'–Rh1'–P1'	166.44(4)
P2–Rh1–P3	164.15(3)	P2–Rh1–P4	162.89(4)	P2'–Rh1'–P4'	163.16(4)
Dihedral	25.73	Dihedral	23.86	Dihedral	23.44
(**3**) $Rh(P^{Ph}_2N^{PhOMe}_2)_2BF_4$		(**4**) $Rh(P^{Cy}_2N^{Ph}_2)_2BF_4$		(**5**) $Rh(P^{Cy}_2N^{PhOMe}_2)_2BF_4$	
Rh1–P1	2.2954(9)	Rh1–P1	2.29208(9)	Rh1–P1#	2.2781(4)
Rh1–P2	2.2787(9)	Rh1–P2	2.2931(11)	Rh1–P1	2.2782(4)
Rh1–P3	2.27879(8)	Rh1–P3	2.2927(11)	Rh1–P3#	2.2829(4)
Rh1–P4	2.2879(8)	Rh1–P4	2.3166(10)	Rh1–P3	2.2828(4)
P1–Rh1–P2	81.68(3)	P1–Rh1–P2	80.70(4)	P1#–Rh1–P1	79.81(2)
P3–Rh1–P4	82.01(3)	P3–Rh1–P4	80.69(4)	P3#–Rh1–P3	79.30(2)
P1–Rh1–P3	161.97(3)	P1–Rh1–P4	164.71(4)	P1–Rh1–P3	159.494(15)
P2–Rh1–P4	169.03(3)	P2–Rh1–P4	164.83(4)	P1#–Rh1–P3#	159.493(15)
Dihedral	22.61	Dihedral	23.49	Dihedral	32.28

For complex **2**, two molecules crystallized in the asymmetric unit, molecules a and b.

Crystals of the neutral rhodium hydrides **7**–**9** were obtained (**Figure 3-9** to **Figure 3-11**) and selected bond lengths and bond angles are given in **Table 3-3**. The hydride ligands of these complexes were located in the difference maps. The geometries of the neutral hydrides can be described as distorted trigonal bipyramidal with one phosphorus atom (P4) and the hydride ligand occupying the axial positions. Complexes of the $[HM(diphosphine)_2]^{n+}$ type (M = Co, Pd, Pt) have been shown to adopt this geometry over a square pyramidal geometry.[34-36] Deviation from trigonal bipyramidal geometry is apparent in the H–Rh–P4 bond angles, which are significantly smaller than the expected 180° due to constraints imposed by the chelating ligands. The angles between the hydride ligands and the equatorial phosphorus atoms are also considerably less than the expected 90°. This bending of *cis* ligands towards hydrogen can be

attributed to both steric and electronic effects. [35,37-39] The Rh–H bond distances of 1.587(15) Å to 1.64(7) Å are in the range expected for Rh(I)–H bonds.[40-42] The Rh–P bond distances are slightly longer compared to those of the starting complexes.

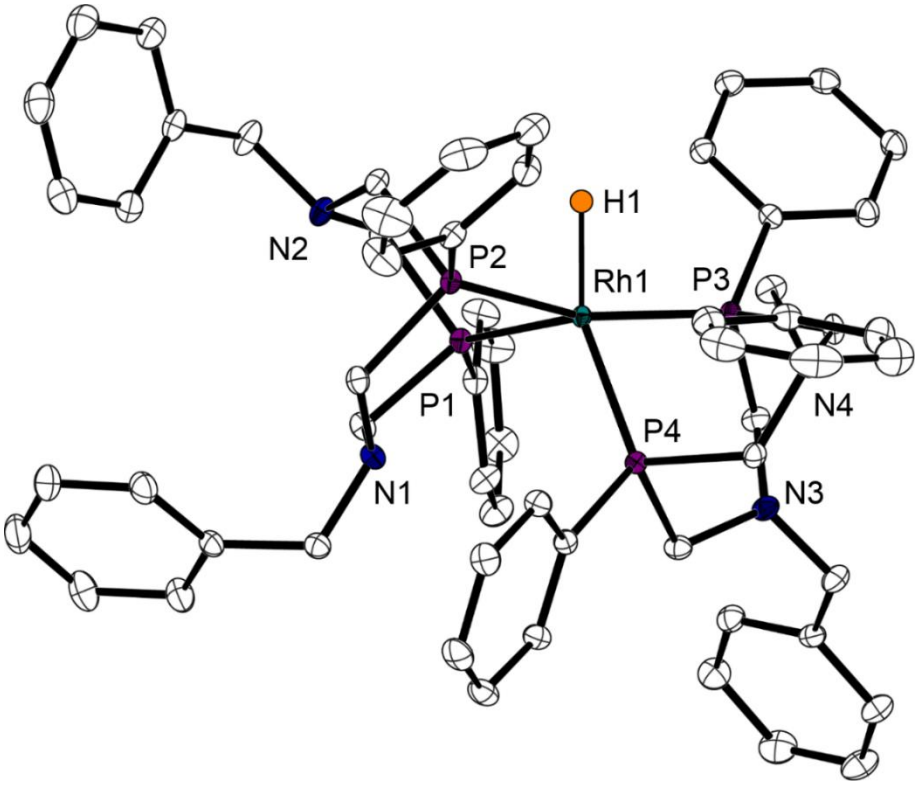

Figure 3-9. Thermal ellipsoid plots of $HRh(P^{Ph}{}_2N^{Bn}{}_2)_2$ (**7**) shown at the 50% probability level. Hydrogens, with the exception of the hydride ligand been omitted for clarity.

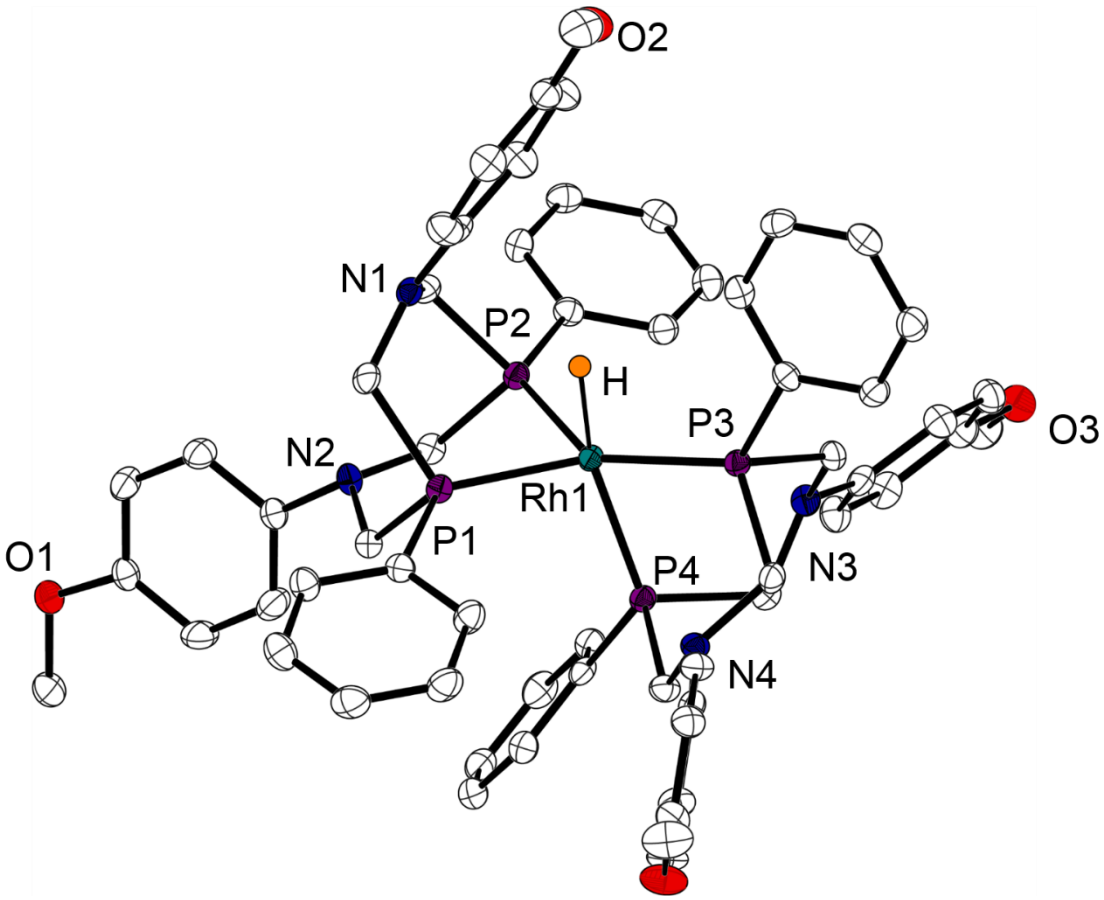

Figure 3-10. Thermal ellipsoid plots of $HRh(P^{Ph}_2N^{PhOMe}_2)_2$ (**8**) shown at the 50% probability level. Hydrogens, with the exception of the hydride ligand, and an uncoordinated solvent molecule have been omitted for clarity.

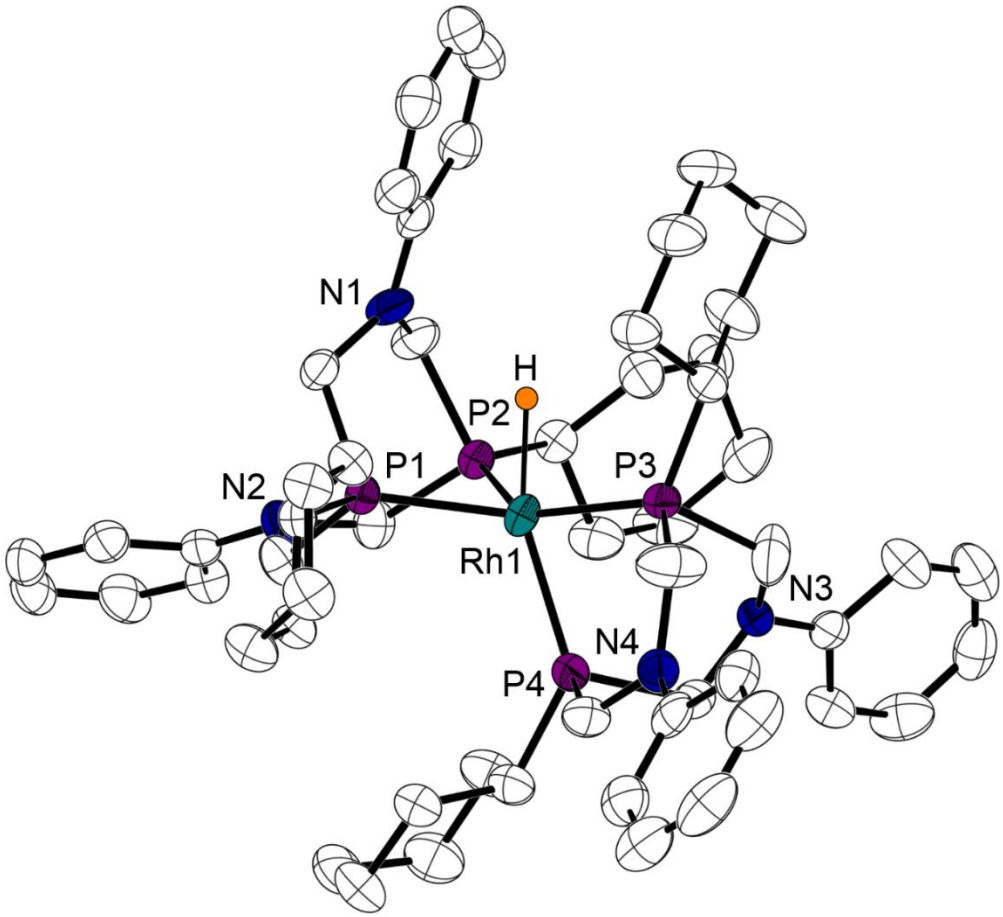

Figure 3-11. Thermal ellipsoid plots of $HRh(P^{Cy}{}_2N^{Ph}{}_2)_2$ (**9**) shown at the 50% probability level. Hydrogens, with the exception of the hydride ligand, have been omitted for clarity.

In complex **7**, both P_2N_2 ligands crystallized in chair-boat conformation with the amine arm *cis* to the hydride ligand pointing away from the metal center. Two similar molecules crystalize in the asymmetric unit of complex **8**, and in both molecules, the equatorial P_2N_2 ligands take on chair-boat conformations, with the amine in the boat conformation pointing towards the hydride ligand (average non-bonding N–H distance is 2.679 Å). The other P_2N_2 ligands take on the boat-boat conformation. In complex **9**, both P_2N_2 ligands take on chair-boat conformations. Similar to complex **8**, one of the amine arms of the P_2N_2 ligand is poised to interact with the hydride ligand (non-bonding N–H distance is 2.428 Å). Only one other

$[HM(P^{R}{}_2N^{R}{}_2)_2]^{n+}$ structure, $[HNi(P^{iPr}{}_2N^{Ph}{}_2)_2]^+$, has been previously reported, although the hydride ligand could not be resolved in this case. In this structure, one arm of the P_2N_2 ligands is also pointed towards the expected location of the hydride ligand as it is in complexes **8** and **9**, indicating a possible hydrogen bonding interaction between the pendant amine and hydride ligand.[43] In the case of the nickel complexes, this interaction has also been observed in spectroscopic and computational data.[44] It should be noted that the interaction between the amine arm and the hydride ligand in the crystal structures of complexes **8** and **9** does not necessarily indicate an interaction in solution.

Table 3-3. Selected bond lengths [Å] and bond angles [°] for the $HRh(P_2N_2)_2^+$ complexes **7**–**9**.

(**7**) $HRh(P^{Ph}{}_2N^{Bn}{}_2)_2$		(**8**) $HRh(P^{Ph}{}_2N^{PhOMe}{}_2)_2$ a		$HRh(P^{Ph}{}_2N^{PhOMe}{}_2)_2$ b	
Rh1–H1	1.587(15)	Rh1–H1	1.59(3)	Rh(1')–HA	1.61(3)
Rh1–P1	2.2538(3)	Rh1–P1	2.2839(9)	Rh(1')–P(1')	2.2812(9)
Rh1–P2	2.3186(3)	Rh1–P2	2.2879(9)	Rh(1')–P(2')	2.3024(9)
Rh1–P3	2.2246(3)	Rh1–P3	2.2420(9)	Rh(1')–P(3')	2.2389(9)
Rh1–P4	2.2803(3)	Rh1–P4	2.2841(9)	Rh(1')–P(4')	2.2779(9)
H1–Rh1–P1	80.0(5)	H1–Rh1–P1	82(2)	P(1')–Rh(1')–HA	82.4(19)
H1–Rh–P2	95.5(5)	H1–Rh–P2	87(2)	P(2')–Rh(1')–HA	84.5(19)
H1–Rh1–P3	87.3(5)	H1–Rh1–P3	85(2)	P(3')–Rh(1')–HA	88.0(19)
H1–Rh1–P4	154.4(5)	H1–Rh1–P4	162(2)	P(4')–Rh(1')–HA	166(2)
P1–Rh1–P2	80.811(10)	P1–Rh1–P2	82.89(3)	P(1')–Rh(1')–P(2')	82.07(3)
P3–Rh1–P4	81.254(11)	P3–Rh1–P4	78.94(3)	P(3')–Rh(1') –P(4')	78.34(3)
		(**9**) $HRh(P^{Cy}{}_2N^{Ph}{}_2)_2$			
Rh1–H1	1.64(7)	Rh1–P4	2.2683(14)	H –Rh1–P4	158(2)
Rh1–P1	2.2621(13)	H –Rh1–P1	83(2)	P1–Rh1–P2	81.72(5)
Rh1–P2	2.2598(14)	H –Rh1–P2	79(2)	P3–Rh1–P4	79.32(5)
Rh1–P3	2.1967(14)	H –Rh1–P2	79(2)		

For complex **2**, two molecules crystallized in the asymmetric unit, molecules a and b.

3.3.3 Electrochemical Studies

The cyclic voltammograms (CVs) of complexes **1**–**5** show single reversible 2-electron reductions (**Figure 3-12**) corresponding to the d^8/d^{10} couple, which are consistent with the electrochemistry of previously reported Rh(I) bis-diphosphine complexes.[14,25] The observed

reductions are diffusion controlled, as indicated by linear plots of the peak current against the square root of scan the rate (**Figure 3-13**). The 2-electron nature of this couple is evident in the splitting of the cathodic and anodic peaks, which fall between the 60 mV expected for a completely reversible one-electron reduction and the 30 mV expected for a completely reversible 2-electron reduction.[45] For comparison, the splitting of the II/I peaks for cobaltocene in the same set of experiments was 61 mV. Upon reduction, Rh(I) is expected to go from square planar to tetrahedral geometry based on structures of other d^8 and d^{10} complexes.[13,46,47] The reversibility of the electrochemical reduction suggests that the complexes are able to rapidly adjust their geometries on the electrochemical timescale. The ratios of the cathodic and anodic peak currents deviate somewhat from what is expected for a fully reversible process, likely due to irreversible chemical processes which occur after reduction. Reduction potentials and peak splitting are given in **Table 3-4**.

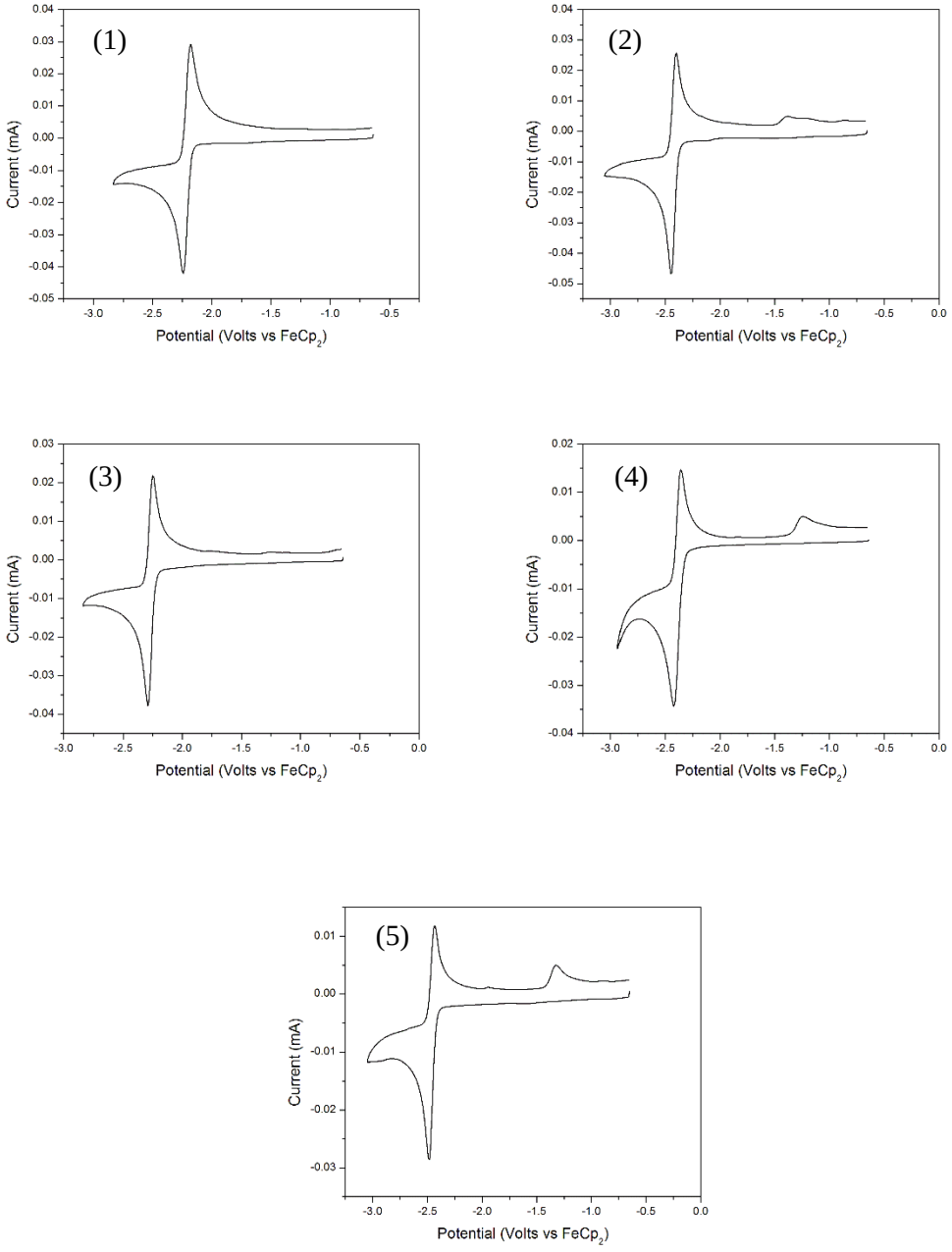

Figure 3-12. Cyclic voltammograms of $[Rh(P^{Ph}{}_2N^{Ph}{}_2)_2]^+$ (**1**), $[Rh(P^{Ph}{}_2N^{Bn}{}_2)_2]^+$ (**2**), $[Rh(P^{Ph}{}_2N^{PhOMe}{}_2)_2]^+$ (**3**), $[Rh(P^{Cy}{}_2N^{Ph}{}_2)_2]^+$ (**4**), and $[Rh(P^{Cy}{}_2N^{PhOMe}{}_2)_2]^+$ (**5**) , 0.2 M NBu_4PF_6/acetonitrile, glassy carbon working and counter electrodes, 100 mV/s.

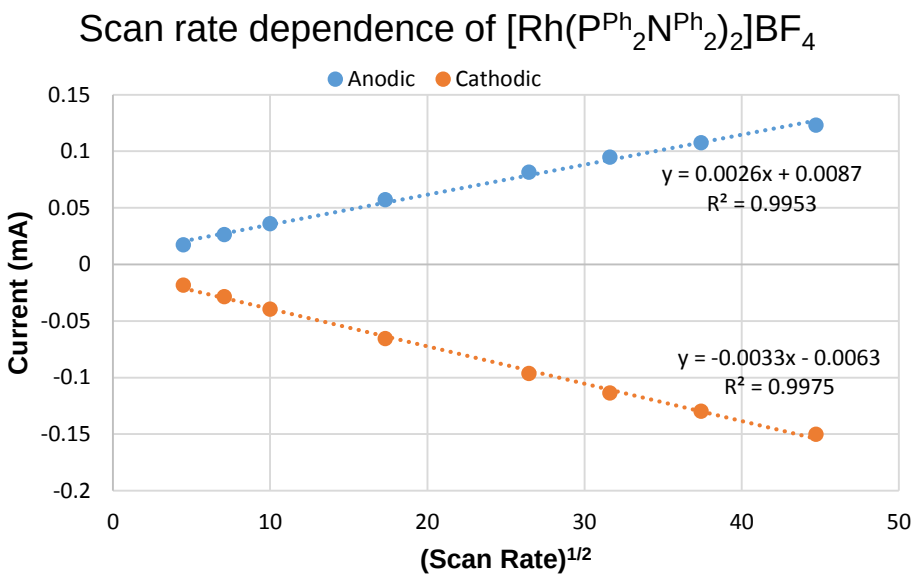

Figure 3-13. Scan rate dependence carried out on 1mM $[Rh(P^{Ph}{}_2N^{Ph}{}_2)_2]BF_4$. Conditions: 0.2M NBu_4PF_6 in acetonitrile, glassy carbon working and counter electrodes.

The reduction potentials of complexes **1**–**5** generally follow the trend that complexes with more donating cyclohexyl substituents on the phosphine have reduction potentials ~ 0.2 V more negative than those with phenyl phosphines. The electron donating ability of the amine group also influences the reduction potentials, despite its distance from the Rh center. More basic amine groups contribute to more negative reduction potentials, as can clearly be seen when the phenyl phosphine substituent is kept constant. In the case of phenyl-phosphine containing ligands, the reduction potentials span a range of 0.2 V as the amine substituent changes.

Table 3-4. Reduction potentials and peak data for the series of $[Rh(P_2N_2)_2]^+$ complexes.

Complex		$E_{1/2}(Rh^{I/-I})$ (V vs. $FeCp_2^{+/0}$)	ΔE_p	i_{pc}/i_{pa}	$E_{1/2}(Rh^{I/-I})$ (V vs. $FeCp_2^{+/0}$)
1	$[Rh(P^{Ph}{}_2N^{Ph}{}_2)_2]^+$	–2.21	50	1.1	0.05
2	$[Rh(P^{Ph}{}_2N^{Bn}{}_2)_2]^+$	–2.43	48	1.3	–0.05
3	$[Rh(P^{Ph}{}_2N^{PhOMe}{}_2)_2]^+$	–2.27	42	1.2	–0.02
4	$[Rh(P^{Cy}{}_2N^{Ph}{}_2)_2]^+$	–2.39	50	1.4	–0.04
5	$[Rh(P^{Cy}{}_2N^{PhOMe}{}_2)_2]^+$	–2.45	42	1.6	–0.13

Conditions: 1 mM complex in 0.2 M NBu_4PF_6 in acetonitrile solution, 100 mV/s scan rate, 3 mm glassy carbon working electrode.

3.3.4 Thermodynamic measurements

Reactivity of $[Rh(P_2N_2)_2]$ complexes with H_2 in the absence of a base

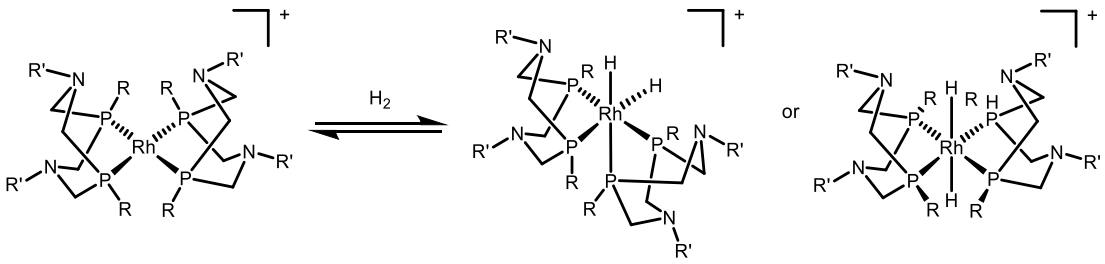

Scheme 3-2. Reaction of $[Rh(P_2N_2)_2]BF_4$ complexes with H_2.

Rhodium diphosphine complexes are known to react with H_2 in the absence of a base to form six-coordinate dihydride complexes.[31,48,49] In order to investigate the effect of the pendant base on this process, we reacted complexes **1**–**5** with 1 atm of H_2 in THF and observed the products by $^{31}P\{^1H\}$ NMR. All five complexes incompletely reacted to form what is assigned as the dihydride product, based on the appearance of two apparent doublets of triplets in the $^{31}P\{^1H\}$ NMR (**Table 3-1** and **Figure 3-14**). For the phenyl phosphine complexes, there is a large separation between the two ^{31}P peaks, indicating the molecule has two phosphorus environments that are very different; these complexes are tentatively assigned to be *cis* dihydrides. For the cyclohexyl phosphine complexes, the two triplets are very close to each

other indicating there are two similar phosphorus environments, and these complexes are tentatively assigned to be *trans* dihydrides. In this case, the added steric bulk of the cyclohexyl substituents likely disfavors the *cis* dihydride configuration. The equilibrium constants for the reaction of the $[Rh(P_2N_2)_2]^+$ complexes with H_2 were measured ($K_{eq} = [H_2Rh^+]/[Rh^+][H_2]$, where the concentration of H_2 is expressed in atmospheres) by the integration of the ^{31}P NMR spectra at 21 °C (**Table 3-5**). The dihydride resonances could not be resolved in the ^1H NMR, and likely overlap other resonances, but no peaks corresponding to a protonated amine were observed and no phosphorus peaks corresponding to the $HRh(P_2N_2)_2$ complexes were seen in the $^{31}P\{^1H\}$ NMR, indicating that the pendant amine arms are not acting as unassisted bases. In all cases, when an excess of Verkade's base is present, the dihydride species were deprotonated and an equilibrium between the monohydride and Rh^+ complexes was established (shown by the hydricity equilibration experiments discussed in the next section).

The pK_a's of the dihydride complexes were not measured, but the pK_a's of other $[H_2Rh(diphosphine)_2]^+$ complexes containing diphosphine ligands with alkyl backbones (depx,[49] dmpe, dppe, and dmdppe[16]) have been experimentally measured and calculated and the values range between 29 and 37. Given the pK_a of the free amines of the ligands ($PhNH_3^+$ = 10.6, $PhOMeNH_3^+$ = 11.9, and $BnNH_3^+$ = 16.9)[8] it is not surprising that the amine arms of the ligands would not be able to deprotonate the dihydride complexes to generate the monohydride species.

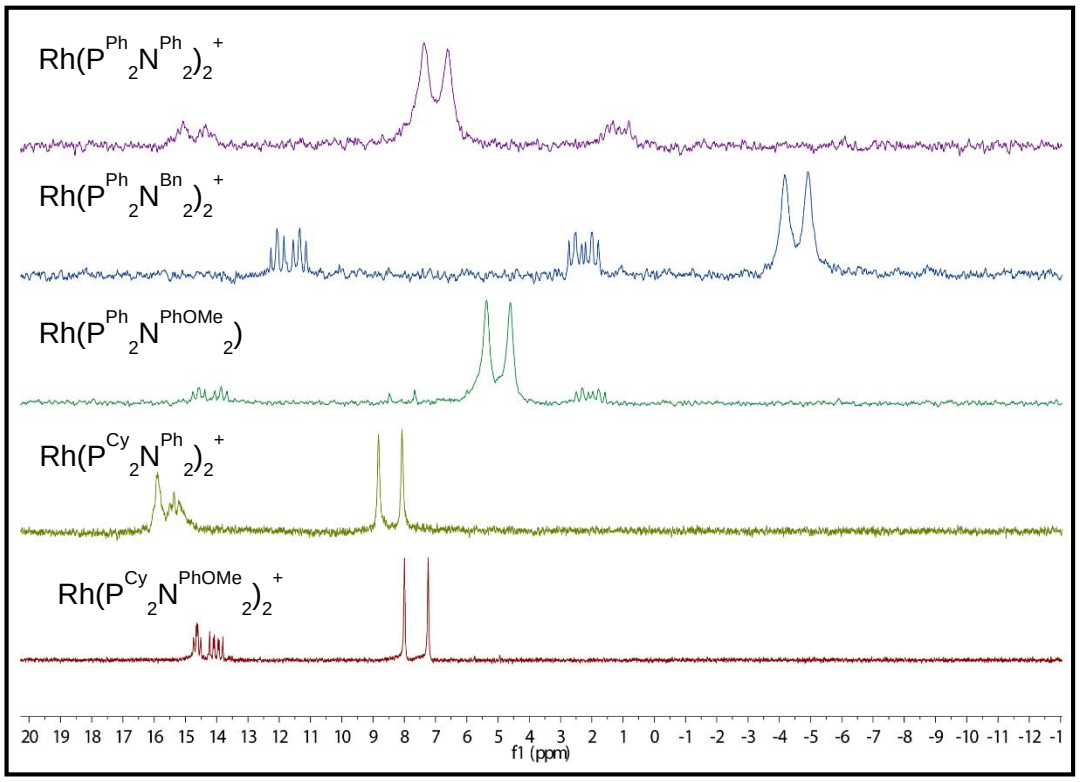

Figure 3-14. $^{31}P\{^{1}H\}$ NMR spectra of the reaction of the $[Rh(P_2N_2)_2]BF_4$ complexes with H_2.

Hydricity of and acidity of the $HRh(P_2N_2)_2$ complexes

The reaction of $[Rh(P^{Ph}{}_2N^{Bn}{}_2)_2]BF_4$ (**2**), $[Rh(P^{Ph}{}_2N^{PhOMe}{}_2)_2]BF_4$ (**3**), $[Rh(P^{Cy}{}_2N^{Ph}{}_2)_2]BF_4$ (**4**), and $[Rh(P^{Cy}{}_2N^{PhOMe}{}_2)_2]BF_4$ (**5**) with H_2 in the presence of Verkade's base (2,8,9-triisopropyl-2,5,8,9-tetraaza-1-phosphabicyclo[3,3,3]undecane) resulted in an equilibrium between the $[Rh(P_2N_2)_2]^+$ and $HRh(P_2N_2)_2$ species and the protonated and deprotonated base, as shown in **Scheme 3-3**, equation 1. If the solutions are purged with N_2 after reaching equilibrium, the spectra revert to those of the starting complex, confirming the reversibility of this activation. Verkade's base (pK_a of 33.63 in acetonitrile)[50] was convenient because it is a weakly nucleophilic phosphorus-containing base with $^{31}P\{^{1}H\}$ signals that do not overlap with those of the HRh and Rh^+ complexes, allowing for the determination of the

relative equilibrium ratios of the Rh complexes and the base and conjugate acid by integration of the ^{31}P resonances. Benzonitrile was used for solubility reasons (equilibrium values obtained in benzonitrile are expected to be a good estimate for equilibrium values in acetonitrile, which is the solvent most commonly used for these measurements).[14]

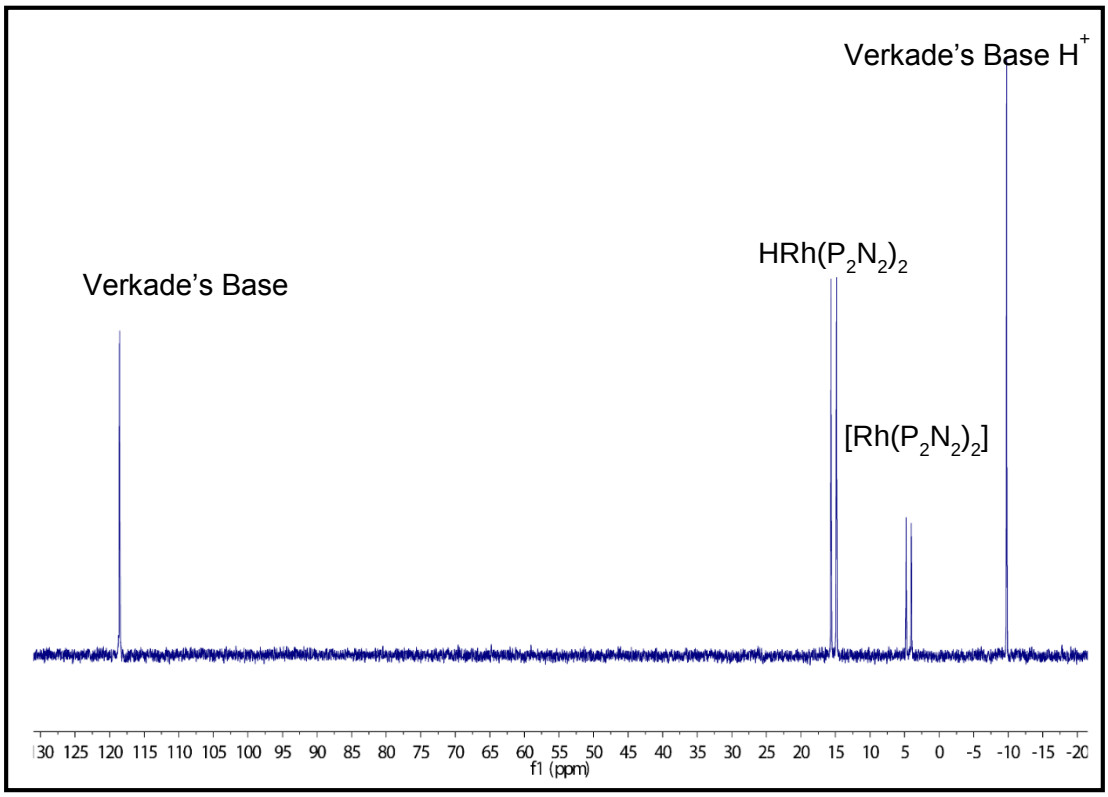

Figure 3-15. $^{31}P\{^{1}H\}$ NMR of $[Rh(P^{Ph}{}_2P^{PhOMe}{}_2)_2]^+$ (**3**) and Verkade's base under H_2 in benzonitrile showing a typical equilibration reaction.

Using the thermodynamic cycle shown in **Scheme 3-3**, the free energies associated with equations 1–3 can be used in equation 4 to calculate the hydride donor abilities, $\Delta G°_{H^-}$. Verkade's base proved to be too basic to establish an equilibrium in the reaction with complex 1 and H_2, which led to complete formation of the $HRh(P^{Ph}{}_2N^{Ph}{}_2)_2$ complex, so this hydricity was not measured. Based on the dominance of the hydride product, however, it is expected that this is the least hydridic complex in this report. With the thermodynamic cycle shown in

Scheme 3-4, the free energies associated with equations 7–9 can be used in equation 10 to calculate the pK_a of the $HRh(P_2N_2)_2$ complexes.

	$\Delta G°$ (kcal/mol)	
$HRh(P_2N_2)_2 + HB \rightleftharpoons [Rh(P_2N_2)_2]^+ + B + H_2$	$-RT \ln K_{eq}$	(1)
$B + H^+ \rightleftharpoons HB^+$	$-1.364\ pK_a$	(2)
$H_2 \rightleftharpoons H^+ + H^-$	76.0	(3)
$HRh(P_2N_2)_2 \rightleftharpoons [Rh(P_2N_2)_2]^+ + H^-$	$G°_{H^-} = -RT \ln K_{eq} - 1.364\ pK_a + 76.0$	(4)

Scheme 3-3. Determination of hydride donor abilities for $HRh(P_2N_2)_2$ complexes

	$\Delta G°$ (kcal/mol)	
$HRh(P_2N_2)_2 \rightleftharpoons [Rh(P_2N_2)_2]^+ + H^-$	$\Delta G°_{H^-}$	(5)
$[Rh(P_2N_2)_2]^+ + 2e^- \rightleftharpoons [Rh(P_2N_2)_2]^-$	$-nF[(E_{RhI/-I})]$	(6)
$H^- \rightleftharpoons H^+ + 2e^-$	79.6 kcal/mol	(7)
$HRh(P_2N_2)_2 \rightleftharpoons [Rh(P_2N_2)_2]^- + H^+$	$\Delta G°_{H^+} = \Delta G°_{H^-} - nF[(E_{RhI/-I})] - 79.6$	(8)
	$pK_a = \Delta G°_{H^+} / (2.303\ RT)$	

Scheme 3-4. Determination of pK_a of $HRh(P_2N_2)_2$ complexes

The $HRh(P_2N_2)_2$ complexes have calculated hydricities that range from 28–32 kcal/mol, where a smaller $\Delta G°_{H^-}$ indicates the complex is a better hydride donor. These hydricities are comparable to those measured for other HRh(disphosphine)$_2$ complexes[14,26,49] and are among the most hydridic values measured for the $[HM(disphosphine)_2]^{n+}$ class. Based on comparisons between previously reported hydricities for rhodium and nickel $[HM(diphoshine)_2]^{n+}$ species (diphosphine = depe, dmpe)[13,26], complexes **7–10** have a similar increase in hydricity of 24–28 kcal/mol compared with analogous $HNi(P_2N_2)_2$ complexes.[8] The estimated pK_a's for the monohydride species range from 39–50 and show that these complexes are also among the most basic of the $[M(disphosphine)_2]^+$ complexes. Their pK_a's are comparable to those measured for other Co and Rh diphosphine monohydride complexes.[14,35]

Previous studies have shown that hydride donor abilities of d^8 $[HM(diphosphine)_2]^{n+}$ complexes (M = Pd, Ni) are linearly correlated to the reduction potential of the d^8/d^9 couple, with complexes with more negative reduction potentials being better hydride donors (smaller $\Delta G°_{H^-}$ values). The d^9/d^{10} couple has been shown to be linearly correlated to the pK_a of the $[HM(diphosphine)_2]^{n+}$ complex.[32,37,51] For the $[Rh(P_2N_2)_2]^+$ complexes in this report, the d^8/d^9 couple is significantly destabilized and the complexes show one redox couple corresponding to the d^8/d^{10} couple. The reduction potentials, which are influenced by the electron-donating ability of the ligands, should be correlated with both the hydricity and pK_a of the corresponding Rh(I) hydride.

The linear correlation of the hydricity with the E^0 for the d^8/d^9 couple is robust for $[Ni(P_2N_2)_2]^{2+}$ complexes, indicating that there are no unusual thermodynamic consequences introduced by the incorporation of the pendant base into the ligand backbone in the case of nickel.[32] For the $[Rh(P_2N_2)_2]^+$ complexes in this study, the correlation between the reduction potential and the hydricity is slightly weaker. When the base is held constant, as in the complexes $[Rh(P^{Cy}{}_2N^{PhOMe}{}_2)_2]^+$ and $[Rh(P^{Ph}{}_2N^{PhOMe}{}_2)_2]^+$, the complex with the more negative reduction potential is more hydridic, consistent with trends previously seen. A disruption in this trend occurs when comparing the hydricities of $[Rh(P^{Ph}{}_2N^{Bn}{}_2)_2]^+$ to $[Rh(P^{Cy}{}_2N^{PhOMe}{}_2)_2]^+$ and $[Rh(P^{Ph}{}_2N^{PhOMe}{}_2)_2]^+$ to $[Rh(P^{Cy}{}_2N^{Ph}{}_2)_2]^+$. In both cases, even though the complex with the cyclohexyl phosphine has the more negative reduction potential, the phenyl phosphine complex with the more basic amine is more hydridic or has a similar hydricity. The pK_a of the pendant amine seems to have a significant effect on the hydricity of the $HRh(P_2N_2)_2$ complex, beyond any effect it has on the reduction potential of the Rh(I) complex.

Table 3-5. Thermodynamic and electrochemical data for $[Rh(P_2N_2)_2]BF_4$ complexes

Complex		K_{H_2} (atm^{-1})[a]	$\Delta G°_{H_2}$	$E(Rh^{I/-I})$[b]	K_{eq1}[c]	$\Delta G°_{H^-}$	pK_a
1	$[Rh(P^{Ph}_2N^{Ph}_2)_2]^+$	0.41	0.53[d]	–2.21(0.03)[e]	—	—	—
2	$[Rh(P^{Ph}_2N^{Bn}_2)_2]^+$	0.48	0.44[d]	–2.43(0.02)[e]	20.13(3.26)	28.1[d]	44.8
3	$[Rh(P^{Ph}_2N^{PhOMe}_2)_2]^+$	0.30	0.72[d]	–2.27(0.02)[e]	0.15(0.03)	31.1[d]	39.4
4	$[Rh(P^{Cy}_2N^{Ph}_2)_2]^+$	1.0	0[d]	–2.39(0.03)[e]	0.05(0.01)	31.7[d]	46.0
5	$[Rh(P^{Cy}_2N^{PhOMe}_2)_2]^+$	0.67	0.42[d]	–2.45(0.02)[e]	0.91(0.19)	30.0[d]	49.9
	$[Rh(depe)_2]^+$	0.25[f]	0.82[f]	—	—	28.1[f]	—

[a]Values measured in d_8-THF. [b]Values measured in acetonitrile [c]Values measured in benzonitrile. [d] Units of kcal/mol. [e] Units of volts vs $FeCp_2$. Previously reported.[26,48]

3.3.5 Catalytic hydrogenation of CO_2

Complexes **1-5** were active for CO_2 hydrogenation to formate at room temperature under two atmospheres of 1:1 CO_2/H_2 in the presence of Verkade's base (2,8,9-triisobutyl-2,5,8,9-tetraaza-1-phosphabicyclo[3.3.3]undecane. Catalytic studies were performed in a J. Young NMR tube, and the formation of formate over one hour was quantified by measuring the ^1H NMR signal for formate (8.7 ppm) relative to a benzene internal standard. ^1H and ^{31}P NMR were recorded every 2 to 5 minutes and between scans, the tube was briefly placed in a vortex mixer to allow for gas mixing. The CO_2 hydrogenation activity of a rhodium diphosphine complex without pendant amines, $[Rh(depe)_2]^+$, was also measured to see how its activity compared to $[Rh(P_2N_2)_2]^+$ complexes. $[Rh(depe)_2]^+$ was chosen because its $\Delta G°_{H^-}$ was previously measured to be 28.1 kcal/mol,[26] which is in a similar range to that of the $[Rh(P_2N_2)_2]^+$ complexes. In the ^1H and $^{31}P\{^1H\}$ NMR spectra, only the starting material ($[Rh(P_2N_2)_2]^+$) was observed during catalysis, suggesting that H_2 addition is likely the slow step in catalysis.

Table 3-6. Rates of hydrogenation of CO_2 for $[Rh(P_2N_2)_2]^+$ and $[Rh(depe)_2]^+$ in THF

Complex		$[M^+]$ (mM)	[base] (mM)	TOF (h^{-1})
1	$[Rh(P^{Ph}{}_2N^{Ph}{}_2)_2]^+$	0.98	494	590 ± 20
2	$[Rh(P^{Ph}{}_2N^{PhOMe}{}_2)_2]^+$	1.0	498	460 ± 70
3	$[Rh(P^{Ph}{}_2N^{Bn}{}_2)_2]^+$	0.92	520	240 ± 30
4	$[Rh(P^{Cy}{}_2N^{Ph}{}_2)_2]^+$	1.1	500	720 ± 60
5	$[Rh(P^{Cy}{}_2N^{PhOMe}{}_2)_2]^+$	0.90	494	630 ± 40
	$[Rh(depe)_2]^+$	1.0	500	1070 ± 60

Conditions: 400 µL d_8-THF, 1:1 CO_2/H_2, 2 atm at 21°. [a]BF_4 salts were used for all complexes. [b]TON in this case is the turnovers after running the reaction for 1 hour.

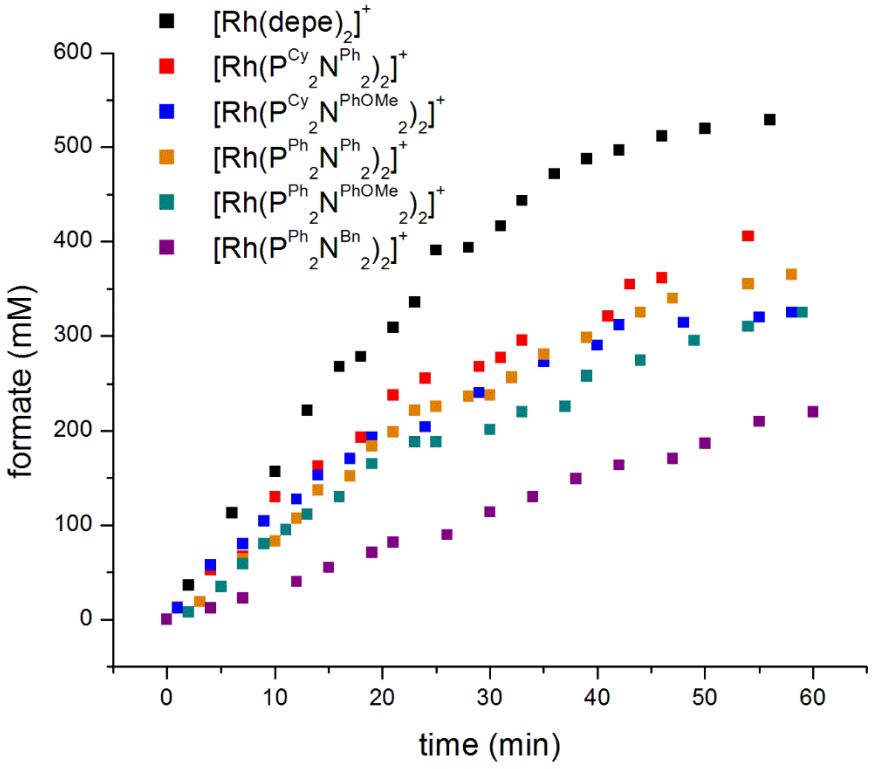

Figure 3-16. Formate vs time for each metal complex over an hour.

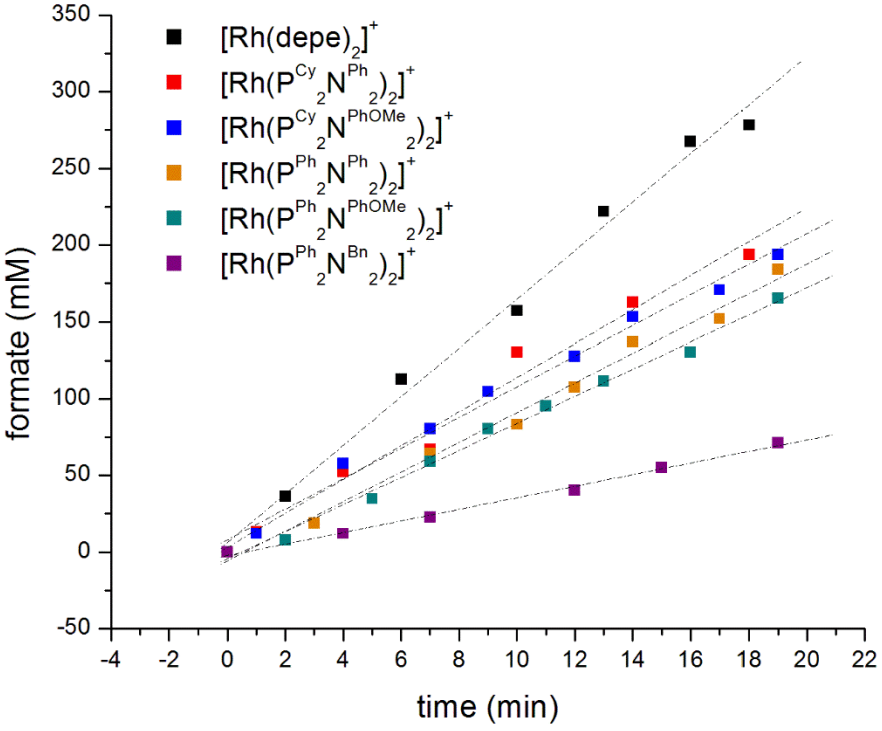

Figure 3-17. Formate vs time for each metal complex for 20 min showing regions fitted to obtain kinetic rates.

3.3.6 Effect of pendant amine on catalysis

The typical proposed mechanism for CO_2 hydrogenation by rhodium bis-diphosphine complexes includes the following steps: (1) H_2 addition to Rh(I) cation to make the dihydride complex, (2) deprotonation of the dihydride to make the HRh(I) complex, and (3) hydride transfer to CO_2/formate loss.[31,52] Incorporation of P_2N_2 ligands into catalysts for this process could potentially affect any of the above steps via increased electron density at the metal center as well as the action of the pendant base during both hydrogen activation and deprotonation of the dihydride.

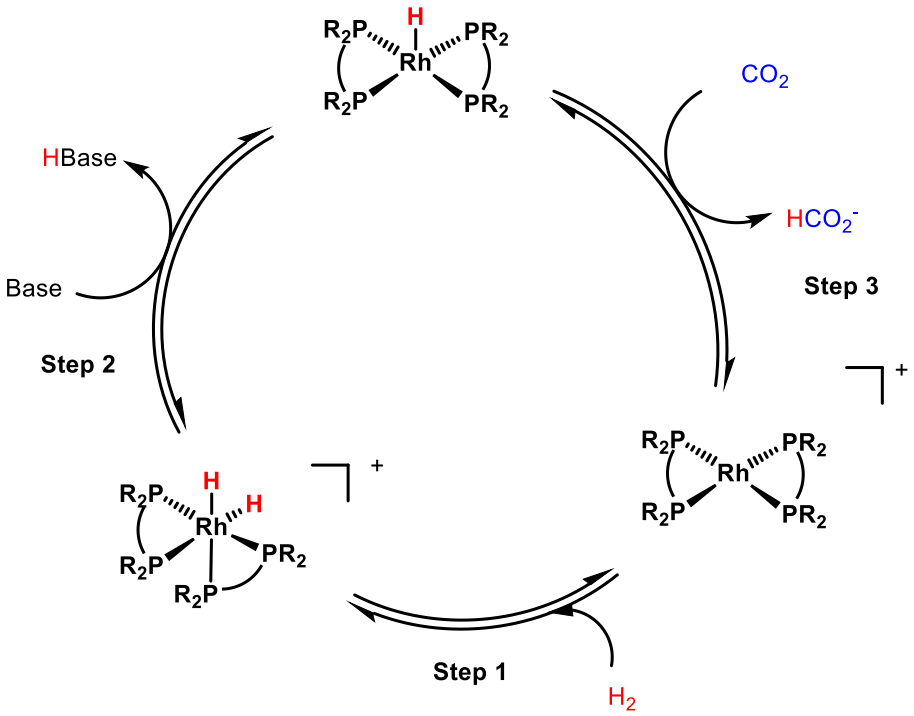

Figure 3-18. Proposed catalytic mechanism for the hydrogenation of CO_2.

Increasing the electron donating ability of the diphosphine ligand could lead to changes in the rates for CO_2 hydrogenation by destabilizing the monohydride species that reacts with CO_2. However, during catalysis no monohydride species were observed on the NMR timescale, indicating that the hydricity of the monohydride species is not the most prominent factor controlling the relative rates for CO_2 hydrogenation. This is further highlighted by the difference in rates of CO_2 hydrogenation by $[Rh(P^{Ph}{}_2N^{Bn}{}_2)_2]^+$ and $[Rh(depe)_2]^+$. These complexes have similar hydricities, but $[Rh(P^{Ph}{}_2N^{Bn}{}_2)_2]^+$ is a much slower catalyst than $[Rh(depe)_2]^+$.

The NMR timescale observation of only starting Rh(I) starting cation during catalysis seems to indicate that H_2 addition is the slow step in catalysis, with all subsequent steps being comparatively facile. The pendant amine itself could be affecting catalytic rates by influencing H_2 addition or aiding in the deprotonation of dihydride species. Given that no monohydride is

seen upon H_2 activation by the Rh(I) complexes in the absence of an external base, we can rule out direct deprotonation of this species by the pendant base. Also, there is no clear trend between the pK_a of the pendant amine and the favorability of H_2 addition, and there is no clear trend between ΔG_{H2} and the rates of catalysis either.

The fact that H_2 addition seems to be rate limiting, despite the lack of a strong correlation between the $\Delta G°_{H2}$ values in the absence of an external base and the catalytic rates, may indicate that the dominant factor in catalysis is the ability of the external base to come close enough to the metal center to assist in the oxidative addition of H_2. $[Rh(depe)_2]^+$, which is the least sterically hindered, shows the fastest rate, with all of the P_2N_2 complexes being significantly slower. The rates also seem to trend with the increased bulk of the pendant amine more generally, decreasing as the amine becomes bulkier. In effect, because the pendant base cannot directly deprotonate the dihydride species, its presence can only improve catalysis by increasing the electron density at the metal center. However, because initial activation of H_2 by the combined action of the Rh(I) center and the external base appears to be the rate-determining step, the added steric bulk of the P_2N_2 ligand outweighs any benefit conferred by increasing the donation of the ligand. A conclusive study on this matter would ideally use an equally strong, less sterically hindered external base, but it is difficult to find a base in this pK_a range that is smaller and non-nucleophilic. When catalysis was attempted with a weaker base, triethylamine, no formate production was observed under the conditions used.

The lack of any benefit to catalysis due to the addition of the pendant base highlights the importance of assuring that no steps in a catalytic cycle are substantially mismatched in energy. We initially hoped that the addition of the pendant amine would help to increase the rates for H_2 splitting, and that by using a strongly basic metal, we would see increased rates in CO_2 hydrogenation. However, while the use of such a strong hydride forming metal with very donating ligands produced an extremely strong Rh(I) hydride donor for CO_2 hydrogenation, it

also produced a strongly basic dihydride precursor that could not be deprotonated by the pendant amine, negating any benefit from having the pendant base in the second coordination sphere. As noted by others, the best catalysts of this type would have a monohydride strong enough to activate CO_2, but such an intermediate would not be so basic that the dihydride species could not be easily deprotonated.[52]

3.4 Summary and Conclusions

In this work, we introduce pendant amines in the form of 1,5-diaza-3,7-diphosphacyclooctane P_2N_2 ligands to the $[Rh(disphosphine)_2]^+$ platform, extending the rich chemistry of these proton-relay-containing ligands to rhodium. Along with the synthesis and characterization of the $[Rh(P_2N_2)_2]^+$ complexes, we were able to synthesize and characterize the corresponding $HRh(P_2N_2)_2$ complexes, as well as obtain structural data for the $HRh(P^{Ph}_2N^{Bn}_2)_2$, $HRh(P^{Ph}_2N^{PhOMe}_2)_2$ and $HRh(P^{Cy}_2N^{Ph}_2)_2$ complexes. These structures represent only the second examples of X-ray structures of $[HM(P_2N_2)_2]^{n+}$ complexes, and the first where the hydride ligands could explicitly be resolved in the difference maps. These structures show possible hydrogen bonding interactions between the pendant amine and the hydride ligands, as has previously been proposed based on structural, NMR, and computational studies for $[HNi(P_2N_2)]^+$ complexes.

We also studied the possibility of enhancing CO_2 reduction activity of the rhodium diphosphine platform through the addition of functionality into the second coordination sphere, as has been fruitfully explored in the design of hydrogenase mimics, but is only starting to be investigated in CO_2 hydrogenation catalysis.[27-29,31] To gain a better understanding of how the series of pendant amine containing disphosphine ligands affect catalytic activity, we measured the hydricities of several of the complexes, estimated their pK_a's, measured their relative affinities for H_2 addition, and measured their rates for CO_2 hydrogenation.

The P_2N_2 complexes in this study are catalytically active for CO_2 hydrogenation, but their CO_2 hydrogenation activity was lower than a non-pendant-amine-containing Rh diphosphine complex with a hydricity in the same range as the P_2N_2 complexes. The data suggest that the added steric bulk of the P_2N_2 ligands hinders catalysis despite the strong reducing power of the relevant monohydride intermediates. In order to see improved catalysis with the addition of pendant bases to this type of complex, it is likely necessary that either the pendant bases used needs to be more basic or the hydricity of the monohydride complex should be reduced in order lower the basicity of the dihydride precursor.

3.5 References

(1) Tard, C.; Pickett, C. J. *Chem. Rev.* , **2009**, *109*, 2245-2274.

(2) G. Märkl, V.; Jin, G. Y.; Schoerner, C. *Tetrahedron Lett.*, **1980**, *21*, 1409-1412.

(3) Doud, M. D.; Grice, K. A.; Lilio, A. M.; Seu, C. S.; Kubiak, C. P. *Organometallics*, **2012**, *31*, 779-782.

(4) Wilson, A. D.; Newell, R. H.; McNevin, M. J.; Muckerman, J. T.; Rakowski DuBois, M.; DuBois, D. L. *J. Am. Chem. Soc.*, **2005**, *128*, 358-366.

(5) Wiese, S.; Kilgore, U. J.; DuBois, D. L.; Bullock, R. M. *ACS Catal.* , **2012**, *2*, 720-727.

(6) Rakowski DuBois, M.; DuBois, D. L. *Chem. Soc. Rev.*, **2009**, *38*, 62-72.

(7) Yang, J. Y.; Bullock, R. M.; Shaw, W. J.; Twamley, B.; Fraze, K.; DuBois, M. R.; DuBois, D. L. *J. Am. Chem. Soc.* , **2009**, *131*, 5935-5945.

(8) Galan, B. R.; Schöffel, J.; Linehan, J. C.; Seu, C.; Appel, A. M.; Roberts, J. A. S.; Helm, M. L.; Kilgore, U. J.; Yang, J. Y.; DuBois, D. L.; Kubiak, C. P. *J. Am. Chem. Soc.*, **2011**, *133*, 12767-12779.

(9) Seu, C. S.; Appel, A. M.; Doud, M. D.; DuBois, D. L.; Kubiak, C. P. *Energy Enviorn. Sci.*, **2012**, *5*, 6480-6490.

(10) DuBois, D. L.; Berning, D. E. *Appl. Organomet. Chem.*, **2000**, *14*, 860-862.

(11) Curtis, C. J.; Miedaner, A.; Ellis, W. W.; DuBois, D. L. *J. Am. Chem. Soc.* , **2002**, *124*, 1918-1925.

(12) Qi, X.-J.; Fu, Y.; Liu, L.; Guo, Q.-X. *Organometallics*, **2007**, *26*, 4197-4203.

(13) Berning, D. E.; Noll, B. C.; DuBois, D. L. *J. Am. Chem. Soc.* , **1999**, *121*, 11432-11447.

(14) Price, A. J.; Ciancanelli, R.; Noll, B. C.; Curtis, C. J.; DuBois, D. L.; DuBois, M. R. *Organometallics*, **2002**, *21*, 4833-4839.

(15) Curtis, C. J.; Miedaner, A.; Raebiger, J. W.; DuBois, D. L. *Organometallics*, **2004**, *23*, 511-516.

(16) Qi, X.-J.; Liu, L.; Fu, Y.; Guo, Q.-X. *Organometallics*, **2006**, *25*, 5879-5886.

(17) Kovács, G.; Pápai, I. *Organometallics*, **2006**, *25*, 820-825.

(18) Nimlos, M. R.; Chang, C. H.; Curtis, C. J.; Miedaner, A.; Pilath, H. M.; DuBois, D. L. *Organometallics*, **2008**, *27*, 2715-2722.

(19) Curtis, C. J.; Miedaner, A.; Ciancanelli, R.; Ellis, W. W.; Noll, B. C.; Rakowski DuBois, M.; DuBois, D. L. *Inorg. Chem.* , **2003**, *42*, 216-227.

(20) Seu, C. S.; Ung, D.; Doud, M. D.; Moore, C. E.; Rheingold, A. L.; Kubiak, C. P. *Organometallics*, **2013**, *32*, 4556-4563.

(21) Rossen, K. *Angew. Chem. Int. Ed.*, **2001**, *40*, 4611-4613.

(22) Schrock, R. R.; Osborn, J. A. *J. Am. Chem. Soc.*, **1976**, *98*, 2134-2143.

(23) Jessop, P. G.; Joó, F.; Tai, C.-C. *Coord. Chem. Rev.* , **2004**, *248*, 2425-2442.

(24) Leitner, W. *Angew. Chem. Int. Ed.*, **1995**, *34*, 2207-2221.

(25) Slater, S.; Wagenknecht, J. H. *J. Am. Chem. Soc.* , **1984**, *106*, 5367-5368.

(26) Mock, M. T.; Potter, R. G.; Camaioni, D. M.; Li, J.; Dougherty, W. G.; Kassel, W. S.; Twamley, B.; DuBois, D. L. *J. Chem. Soc., Chem. Commun.*, **2009**, *131*, 14454-14465.

(27) Schmeier, T. J.; Dobereiner, G. E.; Crabtree, R. H.; Hazari, N. *J. Am. Chem. Soc.* , **2011**, *133*, 9274-9277.

(28) Wang, W.-H.; Hull, J. F.; Muckerman, J. T.; Fujita, E.; Himeda, Y. *Energy Environ. Sci.*, **2012**, *5*, 7923-7926.

(29) Fujita, E.; Muckerman, J. T.; Himeda, Y. *Biochim. Biophys. Acta.*, **2013**, *1827*, 1031-1038.

(30) Costentin, C.; Drouet, S.; Robert, M.; Savéant, J.-M. *Science*, **2012**, *338*, 90-94.

(31) Bays, J. T.; Priyadarshani, N.; Jeletic, M. S.; Hulley, E. B.; Miller, D. L.; Linehan, J. C.; Shaw, W. J. *ACS Catal.*, **2014**, *4*, 3663-3670.

(32) Fraze, K.; Wilson, A. D.; Appel, A. M.; Rakowski DuBois, M.; DuBois, D. L. *Organometallics*, **2007**, *26*, 3918-3924.

(33) Garrou, P. E. *Chem. Rev.*, **1981**, *81*, 229-266.

(34) Aresta, M.; Dibenedetto, A.; Amodio, E.; Pápai, I.; Schubert, G. *Inorg. Chem.*, **2002**, *41*, 6550-6552.

(35) Ciancanelli, R.; Noll, B. C.; DuBois, D. L.; DuBois, M. R. *J. Am. Chem. Soc.*, **2002**, *124*, 2984-2992.

(36) Miedaner, A.; DuBois, D. L.; Curtis, C. J.; Haltiwanger, R. C. *Organometallics*, **1993**, *12*, 299-303.

(37) Wander, S. A.; Miedaner, A.; Noll, B. C.; Barkley, R. M.; DuBois, D. L. *Organometallics*, **1996**, *15*, 3360-3373.

(38) Albright, T. A.; Hoffmann, R.; Thibeault, J. C.; Thorn, D. L. *J. Am. Chem. Soc.*, **1979**, *101*, 3801-3812.

(39) Elian, M.; Hoffmann, R. *Inorg. Chem.*, **1975**, *14*, 1058-1076.

(40) Pruchnik, F. P.; Smoleński, P.; Gałdecka, E.; Gałdecki, Z. *Inorg. Chem. Acta*, **1999**, *293*, 110-114.

(41) Ball, R. G.; James, B. R.; Mahajan, D.; Trotter, J. *Inorg. Chem.*, **1981**, *20*, 254-261.

(42) McLean, M. R.; Stevens, R. C.; Bau, R.; Koetzle, T. F. *Inorg. Chim. Acta*, **1989**, *166*, 173-175.

(43) Das, P.; Stolley, R. M.; van der Eide, E. F.; Helm, M. L. *Inorg. Chem.*, **2014**, *2014*, 4611-4618.

(44) O'Hagan, M.; Shaw, W. J.; Raugei, S.; Chen, S.; Yang, J. Y.; Kilgore, U. J.; DuBois, D. L.; Bullock, R. M. *J. Am. Chem. Soc.* , **2011**, *133*, 14301-14312.

(45) Faulkner, A. J. B. L. R.: *Electrochemical Methods: Fundamentals and Applications*; John Wiley & Sons Inc, 2000.

(46) Longato, B.; Riello, L.; Bandoli, G.; Pilloni, G. *Inorg. Chem.*, **1999**, *38*, 2818-2823.

(47) Berning, D. E.; Miedaner, A.; Curtis, C. J.; Noll, B. C.; Rakowski DuBois, M. C.; DuBois, D. L. *Organometallics*, **2001**, *20*, 1832-1839.

(48) DuBois, D. L.; Blake, D. M.; Miedaner, A.; Curtis, C. J.; DuBois, M. R.; Franz, J. A.; Linehan, J. C. *Organometallics*, **2006**, *25*, 4414-4419.

(49) Raebiger, J. W.; DuBois, D. L. *Organometallics*, **2004**, *24*, 110-118.

(50) Kisanga, P. B.; Verkade, J. G.; Schwesinger, R. *J. Org. Chem.*, **2000**, *65*, 5431-5432.

(51) Raebiger, J. W.; Miedaner, A.; Curtis, C. J.; Miller, S. M.; Anderson, O. P.; DuBois, D. L. *J. Chem. Soc., Chem. Commun.*, **2004**, *126*, 5502-5514.

(52) Jeletic, M. S.; Mock, M. T.; Appel, A. M.; Linehan, J. C. *J. Am. Chem. Soc.*, **2013**, *135*, 11533-11536.

3.6 Appendix

3.6.1 Crystal data for $[Rh(P^{Ph}_2N^{Ph}_2)_2]PF_6$ (1)

The systematic absences in the diffraction data were consistent with the monoclinic space group P21/n with Z = 4 and Z' = 1. The asymmetric unit also contains a PF_6^- and half of an uncoordinated acetonitrile molecule. The acetonitrile molecule is distorted over two positions that share the position of the nitrogen atom. All non-hydrogen atoms were refined anisotropically. All hydrogen atoms were included into the model at geometrically calculated positions and refined using a riding model. The goodness of fit on F^2 was 0.945 with R1(wR2) = 0.0435(0.0896) for [I>2sigma(I)] and with a largest difference peak and hole of 0.99 and -0.65(e.Å-3).

Table 3-7. Crystal data and structure refinement for $Rh(P^{Ph}{}_2N^{Ph}{}_2)_2BF_4$ (**1**)

Identification code	Alyssia27_0m	
Empirical formula	C57 H57.5 F6 N4.5 P5 Rh	
Formula weight	1177.34	
Temperature	100.0 K	
Wavelength	1.54178 Å	
Crystal system	Monoclinic	
Space group	P21/n	
Unit cell dimensions	a = 16.0883(4) Å	α = 90°.
	b = 17.7264(5) Å	β = 98.3280(10)°.
	c = 18.4436) Å	γ = 90°.
Volume	5204.4(2) $Å^3$	
Z	4	
Density (calculated)	1.503 Mg/m^3	
Absorption coefficient	0.466 mm^{-1}	
F(000)	2420	
Crystal size	0.05 x 0.05 x 0.05 mm^3	
Theta range for data collection	0.934 to 25.410°.	
Index ranges	-19<=h<=19, -20<=k<=20, -22<=l<=19	
Reflections collected	30889	
Independent reflections	9249 [R(int) = 0.0308]	
Completeness to theta = 25.000°	99.9 %	
Absorption correction	Semi-empirical from equivalents	
Max. and min. transmission	0.8004 and 0.8004	
Refinement method	Full-matrix least-squares on F^2	
Data / restraints / parameters	9249 / 0 / 678	
Goodness-of-fit on F^2	1.035	
Final R indices [I>2sigma(I)]	R1 = 0.0396, wR2 = 0.1031	
R indices (all data)	R1 = 0.0402, wR2 = 0.1037	
Extinction coefficient	not measured	
Largest diff. peak and hole	0.989 and -0.693 e.Å-3	

Table 3-8. Bond lengths [Å] and angles [°] for $Rh(P^{Ph}_2N^{Ph}_2)_2BF_4$ (**1**)

Rh(1)-P(2)	2.2662(7)	Rh(1)-P(3)	2.2705(7)
Rh(1)-P(4)	2.2716(7)	Rh(1)-P(1)	2.2863(7)
P(1)-C(21)	1.824(3)	P(1)-C(1)	1.875(3)
P(1)-C(2)	1.876(3)	P(2)-C(27)	1.821(3)
P(2)-C(3)	1.853(3)	P(2)-C(4)	1.893(3)
P(3)-C(45)	1.824(3)	P(3)-C(6)	1.874(3)
P(3)-C(7)	1.888(3)	P(4)-C(51)	1.826(3)
P(4)-C(8)	1.862(3)	P(4)-C(5)	1.890(3)
N(1)-C(9)	1.432(3)	N(1)-C(1)	1.456(3)
N(1)-C(3)	1.465(3)	N(2)-C(15)	1.413(4)
N(2)-C(4)	1.443(4)	N(2)-C(2)	1.450(4)
N(3)-C(33)	1.399(4)	N(3)-C(6)	1.453(4)
N(3)-C(5)	1.454(4)	N(4)-C(39)	1.416(4)
N(4)-C(7)	1.454(4)	N(4)-C(8)	1.464(4)
C(1)-H(1A)	0.9900	C(1)-H(1B)	0.9900
C(2)-H(2A)	0.9900	C(2)-H(2B)	0.9900
C(3)-H(3A)	0.9900	C(3)-H(3B)	0.9900
C(4)-H(4A)	0.9900	C(4)-H(4B)	0.9900
C(5)-H(5A)	0.9900	C(5)-H(5B)	0.9900
C(6)-H(6A)	0.9900	C(6)-H(6B)	0.9900
C(7)-H(7A)	0.9900	C(7)-H(7B)	0.9900
C(8)-H(8A)	0.9900	C(8)-H(8B)	0.9900
C(9)-C(14)	1.396(4)	C(9)-C(10)	1.396(4)
C(10)-C(11)	1.386(4)	C(10)-H(10)	0.9500
C(11)-C(12)	1.385(4)	C(11)-H(11)	0.9500
C(12)-C(13)	1.387(4)	C(12)-H(12)	0.9500
C(13)-C(14)	1.384(4)	C(13)-H(13)	0.9500
C(14)-H(14)	0.9500	C(15)-C(20)	1.389(4)
C(15)-C(16)	1.407(4)	C(16)-C(17)	1.385(5)
C(16)-H(16)	0.9500	C(17)-C(18)	1.391(5)
C(17)-H(17)	0.9500	C(18)-C(19)	1.372(5)
C(18)-H(18)	0.9500	C(19)-C(20)	1.400(4)
C(19)-H(19)	0.9500	C(20)-H(20)	0.9500
C(21)-C(22)	1.392(5)	C(21)-C(26)	1.394(5)
C(22)-C(23)	1.394(5)	C(22)-H(22)	0.9500
C(23)-C(24)	1.362(6)	C(23)-H(23)	0.9500
C(24)-C(25)	1.370(7)	C(24)-H(24)	0.9500
C(25)-C(26)	1.402(6)	C(25)-H(25)	0.9500

Table 3-8. (cont'd)

C(26)-H(26)	0.9500	C(27)-C(32)	1.393(4)
C(27)-C(28)	1.399(4)	C(28)-C(29)	1.384(5)
C(28)-H(28)	0.9500	C(29)-C(30)	1.387(6)
C(29)-H(29)	0.9500	C(30)-C(31)	1.379(5)
C(30)-H(30)	0.9500	C(31)-C(32)	1.390(4)
C(31)-H(31)	0.9500	C(32)-H(32)	0.9500
C(33)-C(34)	1.398(5)	C(33)-C(38)	1.403(4)
C(34)-C(35)	1.394(5)	C(34)-H(34)	0.9500
C(35)-C(36)	1.379(5)	C(35)-H(35)	0.9500
C(36)-C(37)	1.379(5)	C(36)-H(36)	0.9500
C(37)-C(38)	1.387(5)	C(37)-H(37)	0.9500
C(38)-H(38)	0.9500	C(39)-C(44)	1.388(4)
C(39)-C(40)	1.395(5)	C(40)-C(41)	1.382(5)
C(40)-H(40)	0.9500	C(41)-C(42)	1.378(5)
C(41)-H(41)	0.9500	C(42)-C(43)	1.372(5)
C(42)-H(42)	0.9500	C(43)-C(44)	1.386(4)
C(43)-H(43)	0.9500	C(44)-H(44)	0.9500
C(45)-C(50)	1.393(4)	C(45)-C(46)	1.394(4)
C(46)-C(47)	1.391(5)	C(46)-H(46)	0.9500
C(47)-C(48)	1.375(5)	C(47)-H(47)	0.9500
C(48)-C(49)	1.396(5)	C(48)-H(48)	0.9500
C(49)-C(50)	1.383(4)	C(49)-H(49)	0.9500
C(50)-H(50)	0.9500	C(51)-C(56)	1.373(5)
C(51)-C(52)	1.408(4)	C(52)-C(53)	1.381(5)
C(52)-H(52)	0.9500	C(53)-C(54)	1.344(6)
C(53)-H(53)	0.9500	C(54)-C(55)	1.379(7)
C(54)-H(54)	0.9500	C(55)-C(56)	1.400(6)
C(55)-H(55)	0.9500	C(56)-H(56)	0.9500
P(5)-F(4)	1.535(4)	P(5)-F(5)	1.543(3)
P(5)-F(3)	1.560(3)	P(5)-F(2)	1.579(4)
P(5)-F(1)	1.595(3)	P(5)-F(6)	1.618(4)
N(1S)-C(1S)	1.308(16)	N(1S)-C(1S)#1	1.308(16)
C(1S)-C(2S)	1.426(18)	C(2S)-H(2SA)	0.9800
C(2S)-H(2SB)	0.9800	C(2S)-H(2SC)	0.9800
P(2)-Rh(1)-P(3)	164.15(3)	P(2)-Rh(1)-P(4)	98.81(3)
P(3)-Rh(1)-P(4)	81.97(3)	P(2)-Rh(1)-P(1)	81.03(2)
P(3)-Rh(1)-P(1)	103.08(3)	P(4)-Rh(1)-P(1)	162.17(3)
C(21)-P(1)-C(1)	101.41(12)	C(21)-P(1)-C(2)	103.49(14)

Table 3-8. (cont'd)

C(1)-P(1)-C(2)	100.30(13)	C(21)-P(1)-Rh(1)	124.58(9)
C(1)-P(1)-Rh(1)	105.83(9)	C(2)-P(1)-Rh(1)	117.46(9)
C(27)-P(2)-C(3)	103.23(13)	C(27)-P(2)-C(4)	100.93(12)
C(3)-P(2)-C(4)	101.76(13)	C(27)-P(2)-Rh(1)	122.06(9)
C(3)-P(2)-Rh(1)	113.73(9)	C(4)-P(2)-Rh(1)	112.56(10)
C(45)-P(3)-C(6)	107.02(14)	C(45)-P(3)-C(7)	100.00(13)
C(6)-P(3)-C(7)	100.33(14)	C(45)-P(3)-Rh(1)	121.80(9)
C(6)-P(3)-Rh(1)	115.83(10)	C(7)-P(3)-Rh(1)	108.55(10)
C(51)-P(4)-C(8)	106.67(14)	C(51)-P(4)-C(5)	101.35(13)
C(8)-P(4)-C(5)	99.18(14)	C(51)-P(4)-Rh(1)	120.82(10)
C(8)-P(4)-Rh(1)	113.93(10)	C(5)-P(4)-Rh(1)	112.08(10)
C(9)-N(1)-C(1)	116.6(2)	C(9)-N(1)-C(3)	114.3(2)
C(1)-N(1)-C(3)	116.8(2)	C(15)-N(2)-C(4)	121.0(2)
C(15)-N(2)-C(2)	117.8(2)	C(4)-N(2)-C(2)	114.3(2)
C(33)-N(3)-C(6)	120.4(3)	C(33)-N(3)-C(5)	119.2(3)
C(6)-N(3)-C(5)	113.3(2)	C(39)-N(4)-C(7)	119.4(2)
C(39)-N(4)-C(8)	118.0(2)	C(7)-N(4)-C(8)	117.2(2)
N(1)-C(1)-P(1)	110.70(18)	N(1)-C(1)-H(1A)	109.5
P(1)-C(1)-H(1A)	109.5	N(1)-C(1)-H(1B)	109.5
P(1)-C(1)-H(1B)	109.5	H(1A)-C(1)-H(1B)	108.1
N(2)-C(2)-P(1)	112.52(19)	N(2)-C(2)-H(2A)	109.1
P(1)-C(2)-H(2A)	109.1	N(2)-C(2)-H(2B)	109.1
P(1)-C(2)-H(2B)	109.1	H(2A)-C(2)-H(2B)	107.8
N(1)-C(3)-P(2)	112.91(18)	N(1)-C(3)-H(3A)	109.0
P(2)-C(3)-H(3A)	109.0	N(1)-C(3)-H(3B)	109.0
P(2)-C(3)-H(3B)	109.0	H(3A)-C(3)-H(3B)	107.8
N(2)-C(4)-P(2)	117.0(2)	N(2)-C(4)-H(4A)	108.0
P(2)-C(4)-H(4A)	108.0	N(2)-C(4)-H(4B)	108.0
P(2)-C(4)-H(4B)	108.0	H(4A)-C(4)-H(4B)	107.3
N(3)-C(5)-P(4)	115.9(2)	N(3)-C(5)-H(5A)	108.3
P(4)-C(5)-H(5A)	108.3	N(3)-C(5)-H(5B)	108.3
P(4)-C(5)-H(5B)	108.3	H(5A)-C(5)-H(5B)	107.4
N(3)-C(6)-P(3)	111.79(19)	N(3)-C(6)-H(6A)	109.3
P(3)-C(6)-H(6A)	109.3	N(3)-C(6)-H(6B)	109.3
P(3)-C(6)-H(6B)	109.3	H(6A)-C(6)-H(6B)	107.9
N(4)-C(7)-P(3)	111.67(19)	N(4)-C(7)-H(7A)	109.3
P(3)-C(7)-H(7A)	109.3	N(4)-C(7)-H(7B)	109.3
P(3)-C(7)-H(7B)	109.3	H(7A)-C(7)-H(7B)	107.9

Table 3-8. (cont'd)

N(4)-C(8)-P(4)	109.0(2)	N(4)-C(8)-H(8A)	109.9
P(4)-C(8)-H(8A)	109.9	N(4)-C(8)-H(8B)	109.9
P(4)-C(8)-H(8B)	109.9	H(8A)-C(8)-H(8B)	108.3
C(14)-C(9)-C(10)	118.8(2)	C(14)-C(9)-N(1)	118.6(2)
C(10)-C(9)-N(1)	122.6(2)	C(11)-C(10)-C(9)	120.0(2)
C(11)-C(10)-H(10)	120.0	C(9)-C(10)-H(10)	120.0
C(12)-C(11)-C(10)	120.9(3)	C(12)-C(11)-H(11)	119.5
C(10)-C(11)-H(11)	119.5	C(11)-C(12)-C(13)	119.3(3)
C(11)-C(12)-H(12)	120.4	C(13)-C(12)-H(12)	120.4
C(14)-C(13)-C(12)	120.3(3)	C(14)-C(13)-H(13)	119.8
C(12)-C(13)-H(13)	119.8	C(13)-C(14)-C(9)	120.7(3)
C(13)-C(14)-H(14)	119.7	C(9)-C(14)-H(14)	119.7
C(20)-C(15)-C(16)	118.2(3)	C(20)-C(15)-N(2)	122.8(3)
C(16)-C(15)-N(2)	118.9(3)	C(17)-C(16)-C(15)	120.8(3)
C(17)-C(16)-H(16)	119.6	C(15)-C(16)-H(16)	119.6
C(16)-C(17)-C(18)	120.4(3)	C(16)-C(17)-H(17)	119.8
C(18)-C(17)-H(17)	119.8	C(19)-C(18)-C(17)	119.3(3)
C(19)-C(18)-H(18)	120.4	C(17)-C(18)-H(18)	120.4
C(18)-C(19)-C(20)	120.9(3)	C(18)-C(19)-H(19)	119.5
C(20)-C(19)-H(19)	119.5	C(15)-C(20)-C(19)	120.4(3)
C(15)-C(20)-H(20)	119.8	C(19)-C(20)-H(20)	119.8
C(22)-C(21)-C(26)	118.3(3)	C(22)-C(21)-P(1)	120.0(2)
C(26)-C(21)-P(1)	121.7(3)	C(21)-C(22)-C(23)	121.4(3)
C(21)-C(22)-H(22)	119.3	C(23)-C(22)-H(22)	119.3
C(24)-C(23)-C(22)	120.0(4)	C(24)-C(23)-H(23)	120.0
C(22)-C(23)-H(23)	120.0	C(23)-C(24)-C(25)	119.4(4)
C(23)-C(24)-H(24)	120.3	C(25)-C(24)-H(24)	120.3
C(24)-C(25)-C(26)	121.9(4)	C(24)-C(25)-H(25)	119.1
C(26)-C(25)-H(25)	119.1	C(21)-C(26)-C(25)	118.9(4)
C(21)-C(26)-H(26)	120.5	C(25)-C(26)-H(26)	120.5
C(32)-C(27)-C(28)	119.3(3)	C(32)-C(27)-P(2)	123.5(2)
C(28)-C(27)-P(2)	117.2(2)	C(29)-C(28)-C(27)	120.0(3)
C(29)-C(28)-H(28)	120.0	C(27)-C(28)-H(28)	120.0
C(28)-C(29)-C(30)	119.9(3)	C(28)-C(29)-H(29)	120.0
C(30)-C(29)-H(29)	120.0	C(31)-C(30)-C(29)	120.7(3)
C(31)-C(30)-H(30)	119.6	C(29)-C(30)-H(30)	119.6
C(30)-C(31)-C(32)	119.5(3)	C(30)-C(31)-H(31)	120.2
C(32)-C(31)-H(31)	120.2	C(31)-C(32)-C(27)	120.5(3)

Table 3-8. (cont'd)

C(31)-C(32)-H(32)	119.8	C(27)-C(32)-H(32)	119.8
C(34)-C(33)-N(3)	121.2(3)	C(34)-C(33)-C(38)	117.0(3)
N(3)-C(33)-C(38)	121.6(3)	C(35)-C(34)-C(33)	120.7(3)
C(35)-C(34)-H(34)	119.7	C(33)-C(34)-H(34)	119.7
C(36)-C(35)-C(34)	121.8(4)	C(36)-C(35)-H(35)	119.1
C(34)-C(35)-H(35)	119.1	C(37)-C(36)-C(35)	118.0(3)
C(37)-C(36)-H(36)	121.0	C(35)-C(36)-H(36)	121.0
C(36)-C(37)-C(38)	121.2(3)	C(36)-C(37)-H(37)	119.4
C(38)-C(37)-H(37)	119.4	C(37)-C(38)-C(33)	121.4(3)
C(37)-C(38)-H(38)	119.3	C(33)-C(38)-H(38)	119.3
C(44)-C(39)-C(40)	117.7(3)	C(44)-C(39)-N(4)	122.8(3)
C(40)-C(39)-N(4)	119.5(3)	C(41)-C(40)-C(39)	121.2(3)
C(41)-C(40)-H(40)	119.4	C(39)-C(40)-H(40)	119.4
C(42)-C(41)-C(40)	120.5(3)	C(42)-C(41)-H(41)	119.7
C(40)-C(41)-H(41)	119.7	C(43)-C(42)-C(41)	118.6(3)
C(43)-C(42)-H(42)	120.7	C(41)-C(42)-H(42)	120.7
C(42)-C(43)-C(44)	121.5(3)	C(42)-C(43)-H(43)	119.2
C(44)-C(43)-H(43)	119.3	C(43)-C(44)-C(39)	120.4(3)
C(43)-C(44)-H(44)	119.8	C(39)-C(44)-H(44)	119.8
C(50)-C(45)-C(46)	119.5(3)	C(50)-C(45)-P(3)	116.2(2)
C(46)-C(45)-P(3)	124.3(2)	C(47)-C(46)-C(45)	119.7(3)
C(47)-C(46)-H(46)	120.1	C(45)-C(46)-H(46)	120.1
C(48)-C(47)-C(46)	120.6(3)	C(48)-C(47)-H(47)	119.7
C(46)-C(47)-H(47)	119.7	C(47)-C(48)-C(49)	119.8(3)
C(47)-C(48)-H(48)	120.1	C(49)-C(48)-H(48)	120.1
C(50)-C(49)-C(48)	119.9(3)	C(50)-C(49)-H(49)	120.0
C(48)-C(49)-H(49)	120.0	C(49)-C(50)-C(45)	120.3(3)
C(49)-C(50)-H(50)	119.8	C(45)-C(50)-H(50)	119.8
C(56)-C(51)-C(52)	119.3(3)	C(56)-C(51)-P(4)	125.1(3)
C(52)-C(51)-P(4)	115.7(2)	C(53)-C(52)-C(51)	120.5(3)
C(53)-C(52)-H(52)	119.7	C(51)-C(52)-H(52)	119.7
C(54)-C(53)-C(52)	119.5(4)	C(54)-C(53)-H(53)	120.3
C(52)-C(53)-H(53)	120.3	C(53)-C(54)-C(55)	121.5(4)
C(53)-C(54)-H(54)	119.2	C(55)-C(54)-H(54)	119.2
C(54)-C(55)-C(56)	120.0(4)	C(54)-C(55)-H(55)	120.0
C(56)-C(55)-H(55)	120.0	C(51)-C(56)-C(55)	119.2(4)
C(51)-C(56)-H(56)	120.4	C(55)-C(56)-H(56)	120.4
F(4)-P(5)-F(5)	95.6(3)	F(4)-P(5)-F(3)	92.8(2)

Table 3-8. (cont'd)

F(5)-P(5)-F(3)	91.3(2)	F(4)-P(5)-F(2)	175.7(3)
F(5)-P(5)-F(2)	88.7(2)	F(3)-P(5)-F(2)	87.7(3)
F(4)-P(5)-F(1)	89.1(2)	F(5)-P(5)-F(1)	90.40(16)
F(3)-P(5)-F(1)	177.3(2)	F(2)-P(5)-F(1)	90.3(2)
F(4)-P(5)-F(6)	90.8(3)	F(5)-P(5)-F(6)	172.3(3)
F(3)-P(5)-F(6)	92.7(2)	F(2)-P(5)-F(6)	84.9(3)
F(1)-P(5)-F(6)	85.40(19)	C(1S)-N(1S)-C(1S)#1	180.000(4)
N(1S)-C(1S)-C(2S)	173.1(13)	C(1S)-C(2S)-H(2SA)	109.5
C(1S)-C(2S)-H(2SB)	109.5	H(2SA)-C(2S)-H(2SB)	109.5
C(1S)-C(2S)-H(2SC)	109.5	H(2SA)-C(2S)-H(2SC)	109.5
H(2SB)-C(2S)-H(2SC)	109.5		

3.6.2 Crystal data for $Rh(P^{Ph}{}_2N^{Bn}{}_2)_2BF_4$ (2)

The data were consistent with the triclinic space group P-1 with Z = 4 and Z' = 2. The asymmetric unit two Rh cations, two uncoordinated tetrafluoroborate ions, and two uncoordinated diethyl ether molecules. All hydrogen atoms were included into the model at geometrically calculated positions and refined using a riding model. One of the benzylic arms of each molecule in the asymmetric unit was disordered over 2 positions. The two parts were found in the difference map are refined as freely rotating fitted hexagons. The BF_4^- groups were also disordered and modeled. The goodness of fit on F^2 was 1.017 with R1(wR2) = 0.0435(0.0896) for [I>2sigma(I)] and with a largest difference peak and hole of 0.696 and -0.631(e.Å-3).

Table 3-9. Crystal data and structure refinement for $Rh(P^{Ph}{}_2N^{Bn}{}_2)_2BF_4$ (**2**)

Identification code	Alyssia18_0m	
Empirical formula	C62 H69 B F4 N4 O0.50 P4 Rh	
Formula weight	1191.81	
Temperature	100.0 K	
Wavelength	0.71073 Å	
Crystal system	Triclinic	
Space group	P-1	
Unit cell dimensions	a = 10.3561(4) Å	α = 78.3650(10)°.
	b = 22.3066(9) Å	β = 88.8020(10)°.
	c = 25.1180(11) Å	γ = 85.9470(10)°.
Volume	5668.9(4) $Å^3$	
Z	4	
Density (calculated)	1.396 Mg/m^3	
Absorption coefficient	0.472 mm^{-1}	
F(000)	2476	
Crystal size	0.44 x 0.21 x 0.05 mm^3	
Theta range for data collection	0.934 to 25.410°.	
Index ranges	-12<=h<=12, -26<=k<=26, -30<=l<=30	
Reflections collected	78721	
Independent reflections	20830 [R(int) = 0.0694]	
Completeness to theta = 25.000°	99.9 %	
Absorption correction	Semi-empirical from equivalents	
Max. and min. transmission	0.7452 and 0.6926	
Refinement method	Full-matrix least-squares on F^2	
Data / restraints / parameters	20830 / 228 / 1489	
Goodness-of-fit on F^2	1.017	
Final R indices [I>2sigma(I)]	R1 = 0.0435, wR2 = 0.0896	
R indices (all data)	R1 = 0.0765, wR2 = 0.1060	
Extinction coefficient	not measured	
Largest diff. peak and hole	0.696 and -0.631 e.Å-3	

Table 3-10. Bond lengths [Å] and angles [°] for $Rh(P^{Ph}{}_2N^{Bn}{}_2)_2BF_4$ (**2**)

Rh(1)-P(1)	2.2877(10)	Rh(1)-P(2)	2.2724(9)
Rh(1)-P(3)	2.2669(10)	Rh(1)-P(4)	2.2819(9)
P(1)-C(1)	1.896(3)	P(1)-C(3)	1.837(3)
P(1)-C(9)	1.819(4)	P(2)-C(2)	1.873(3)
P(2)-C(4)	1.856(3)	P(2)-C(29)	1.834(3)
P(3)-C(5)	1.862(3)	P(3)-C(7)	1.873(3)
P(3)-C(35)	1.832(4)	P(4)-C(6)	1.849(3)
P(4)-C(8)	1.901(3)	P(4)-C(48)	1.817(4)
N(1)-C(1)	1.455(4)	N(1)-C(2)	1.460(4)
N(1)-C(22)	1.468(4)	N(2)-C(3)	1.475(4)
N(2)-C(4)	1.466(4)	N(2)-C(15)	1.490(4)
N(3)-C(5)	1.466(4)	N(3)-C(6)	1.466(4)
N(3)-C(41)	1.478(4)	N(4)-C(7)	1.462(4)
N(4)-C(8)	1.450(4)	N(4)-C(54)	1.468(4)
C(1)-H(1A)	0.9900	C(1)-H(1B)	0.9900
C(2)-H(2A)	0.9900	C(2)-H(2B)	0.9900
C(3)-H(3A)	0.9900	C(3)-H(3B)	0.9900
C(4)-H(4A)	0.9900	C(4)-H(4B)	0.9900
C(5)-H(5A)	0.9900	C(5)-H(5B)	0.9900
C(6)-H(6A)	0.9900	C(6)-H(6B)	0.9900
C(7)-H(7A)	0.9900	C(7)-H(7B)	0.9900
C(8)-H(8A)	0.9900	C(8)-H(8B)	0.9900
C(9)-C(10)	1.393(5)	C(9)-C(14)	1.394(5)
C(10)-H(10)	0.9500	C(10)-C(11)	1.391(5)
C(11)-H(11)	0.9500	C(11)-C(12)	1.393(6)
C(12)-H(12)	0.9500	C(12)-C(13)	1.387(6)
C(13)-H(13)	0.9500	C(13)-C(14)	1.384(5)
C(14)-H(14)	0.9500	C(15)-H(15A)	0.9900
C(15)-H(15B)	0.9900	C(15)-H(15C)	0.9900
C(15)-H(15D)	0.9900	C(15)-C(16)	1.613(5)
C(15)-C(16B)	1.457(9)	C(22)-H(22A)	0.9900
C(22)-H(22B)	0.9900	C(22)-C(23)	1.516(5)
C(23)-C(24)	1.394(5)	C(23)-C(28)	1.386(5)
C(24)-H(24)	0.9500	C(24)-C(25)	1.383(5)
C(25)-H(25)	0.9500	C(25)-C(26)	1.374(5)
C(26)-H(26)	0.9500	C(26)-C(27)	1.387(5)
C(27)-H(27)	0.9500	C(27)-C(28)	1.398(5)
C(28)-H(28)	0.9500	C(29)-C(30)	1.400(5)

Table 3-10. (cont'd)

C(29)-C(34)	1.387(5)	C(30)-H(30)	0.9500
C(30)-C(31)	1.392(5)	C(31)-H(31)	0.9500
C(31)-C(32)	1.384(5)	C(32)-H(32)	0.9500
C(32)-C(33)	1.383(5)	C(33)-H(33)	0.9500
C(33)-C(34)	1.396(5)	C(34)-H(34)	0.9500
C(35)-C(36)	1.392(5)	C(35)-C(40)	1.393(5)
C(36)-H(36)	0.9500	C(36)-C(37)	1.391(5)
C(37)-H(37)	0.9500	C(37)-C(38)	1.387(5)
C(38)-H(38)	0.9500	C(38)-C(39)	1.376(5)
C(39)-H(39)	0.9500	C(39)-C(40)	1.389(5)
C(40)-H(40)	0.9500	C(41)-H(41A)	0.9900
C(41)-H(41B)	0.9900	C(41)-C(42)	1.509(5)
C(42)-C(43)	1.387(5)	C(42)-C(47)	1.393(5)
C(43)-H(43)	0.9500	C(43)-C(44)	1.385(5)
C(44)-H(44)	0.9500	C(44)-C(45)	1.371(6)
C(45)-H(45)	0.9500	C(45)-C(46)	1.382(6)
C(46)-H(46)	0.9500	C(46)-C(47)	1.393(6)
C(47)-H(47)	0.9500	C(48)-C(49)	1.391(5)
C(48)-C(53)	1.398(5)	C(49)-H(49)	0.9500
C(49)-C(50)	1.388(5)	C(50)-H(50)	0.9500
C(50)-C(51)	1.376(5)	C(51)-H(51)	0.9500
C(51)-C(52)	1.388(5)	C(52)-H(52)	0.9500
C(52)-C(53)	1.383(5)	C(53)-H(53)	0.9500
C(54)-H(54A)	0.9900	C(54)-H(54B)	0.9900
C(54)-C(55)	1.511(5)	C(55)-C(56)	1.407(5)
C(55)-C(60)	1.386(5)	C(56)-H(56)	0.9500
C(56)-C(57)	1.386(5)	C(57)-H(57)	0.9500
C(57)-C(58)	1.378(5)	C(58)-H(58)	0.9500
C(58)-C(59)	1.385(5)	C(59)-H(59)	0.9500
C(59)-C(60)	1.394(5)	C(60)-H(60)	0.9500
C(16)-C(17)	1.3900	C(16)-C(21)	1.3900
C(17)-H(17)	0.9500	C(17)-C(18)	1.3900
C(18)-H(18)	0.9500	C(18)-C(19)	1.3900
C(19)-H(19)	0.9500	C(19)-C(20)	1.3900
C(20)-H(20)	0.9500	C(20)-C(21)	1.3900
C(21)-H(21)	0.9500	C(16B)-C(17B)	1.410(12)
C(16B)-C(21B)	1.360(12)	C(17B)-H(17B)	0.9500
C(17B)-C(18B)	1.377(12)	C(18B)-H(18B)	0.9500

Table 3-10. (cont'd)

C(18B)-C(19B)	1.400(13)	C(19B)-H(19B)	0.9500
C(19B)-C(20B)	1.365(14)	C(20B)-H(20B)	0.9500
C(20B)-C(21B)	1.409(13)	C(21B)-H(21B)	0.9500
Rh(1')-P(1')	2.2871(10)	Rh(1')-P(2')	2.2718(9)
Rh(1')-P(3')	2.2658(9)	Rh(1')-P(4')	2.2793(9)
P(1')-C(1')	1.902(4)	P(1')-C(3')	1.836(4)
P(1')-C(9')	1.824(4)	P(2')-C(2')	1.865(3)
P(2')-C(4')	1.864(4)	P(2')-C(29')	1.830(4)
P(3')-C(5')	1.868(3)	P(3')-C(7')	1.875(4)
P(3')-C(35')	1.827(4)	P(4')-C(6')	1.844(3)
P(4')-C(8')	1.902(3)	P(4')-C(48')	1.816(3)
N(1')-C(1')	1.453(4)	N(1')-C(2')	1.462(4)
N(1')-C(22')	1.464(4)	N(2')-C(3')	1.474(4)
N(2')-C(4')	1.469(4)	N(2')-C(15')	1.492(5)
N(3')-C(5')	1.467(4)	N(3')-C(6')	1.473(4)
N(3')-C(41')	1.483(4)	N(4')-C(7')	1.467(4)
N(4')-C(8')	1.452(4)	N(4')-C(54')	1.466(4)
C(1')-H(1'A)	0.9900	C(1')-H(1'B)	0.9900
C(2')-H(2'A)	0.9900	C(2')-H(2'B)	0.9900
C(3')-H(3'A)	0.9900	C(3')-H(3'B)	0.9900
C(4')-H(4'A)	0.9900	C(4')-H(4'B)	0.9900
C(5')-H(5'A)	0.9900	C(5')-H(5'B)	0.9900
C(6')-H(6'A)	0.9900	C(6')-H(6'B)	0.9900
C(7')-H(7'A)	0.9900	C(7')-H(7'B)	0.9900
C(8')-H(8'A)	0.9900	C(8')-H(8'B)	0.9900
C(9')-C(10')	1.397(5)	C(9')-C(14')	1.391(5)
C(10')-H(10')	0.9500	C(10')-C(11')	1.393(5)
C(11')-H(11')	0.9500	C(11')-C(12')	1.385(6)
C(12')-H(12')	0.9500	C(12')-C(13')	1.381(6)
C(13')-H(13')	0.9500	C(13')-C(14')	1.381(5)
C(14')-H(14')	0.9500	C(15')-H(15E)	0.9900
C(15')-H(15F)	0.9900	C(15')-H(15G)	0.9900
C(15')-H(15H)	0.9900	C(15')-C(16')	1.639(10)
C(15')-C(16C)	1.459(5)	C(22')-H(22C)	0.9900
C(22')-H(22D)	0.9900	C(22')-C(23')	1.519(5)
C(23')-C(24')	1.393(5)	C(23')-C(28')	1.384(5)
C(24')-H(24')	0.9500	C(24')-C(25')	1.390(5)
C(25')-H(25')	0.9500	C(25')-C(26')	1.371(6)

Table 3-10. (cont'd)

C(26')-H(26')	0.9500	C(26')-C(27')	1.391(6)
C(27')-H(27')	0.9500	C(27')-C(28')	1.394(6)
C(28')-H(28')	0.9500	C(29')-C(30')	1.386(5)
C(29')-C(34')	1.383(5)	C(30')-H(30')	0.9500
C(30')-C(31')	1.386(6)	C(31')-H(31')	0.9500
C(31')-C(32')	1.386(6)	C(32')-H(32')	0.9500
C(32')-C(33')	1.360(5)	C(33')-H(33')	0.9500
C(33')-C(34')	1.379(5)	C(34')-H(34')	0.9500
C(35')-C(36')	1.390(5)	C(35')-C(40')	1.401(5)
C(36')-H(36')	0.9500	C(36')-C(37')	1.391(5)
C(37')-H(37')	0.9500	C(37')-C(38')	1.377(5)
C(38')-H(38')	0.9500	C(38')-C(39')	1.388(5)
C(39')-H(39')	0.9500	C(39')-C(40')	1.390(5)
C(40')-H(40')	0.9500	C(41')-H(41C)	0.9900
C(41')-H(41D)	0.9900	C(41')-C(42')	1.504(5)
C(42')-C(43')	1.388(5)	C(42')-C(47')	1.395(5)
C(43')-H(43')	0.9500	C(43')-C(44')	1.403(6)
C(44')-H(44')	0.9500	C(44')-C(45')	1.380(6)
C(45')-H(45')	0.9500	C(45')-C(46')	1.378(6)
C(46')-H(46')	0.9500	C(46')-C(47')	1.379(5)
C(47')-H(47')	0.9500	C(48')-C(49')	1.397(5)
C(48')-C(53')	1.396(5)	C(49')-H(49')	0.9500
C(49')-C(50')	1.392(5)	C(50')-H(50')	0.9500
C(50')-C(51')	1.380(5)	C(51')-H(51')	0.9500
C(51')-C(52')	1.387(5)	C(52')-H(52')	0.9500
C(52')-C(53')	1.383(5)	C(53')-H(53')	0.9500
C(54')-H(54C)	0.9900	C(54')-H(54D)	0.9900
C(54')-C(55')	1.512(4)	C(55')-C(56')	1.402(5)
C(55')-C(60')	1.385(5)	C(56')-H(56')	0.9500
C(56')-C(57')	1.394(5)	C(57')-H(57')	0.9500
C(57')-C(58')	1.384(5)	C(58')-H(58')	0.9500
C(58')-C(59')	1.386(5)	C(59')-H(59')	0.9500
C(59')-C(60')	1.397(5)	C(60')-H(60')	0.9500
C(16')-C(21')	1.3900	C(16')-C(17')	1.3900
C(21')-H(21')	0.9500	C(21')-C(20')	1.3900
C(20')-H(20')	0.9500	C(20')-C(19')	1.3900
C(19')-H(19')	0.9500	C(19')-C(18')	1.3900
C(18')-H(18')	0.9500	C(18')-C(17')	1.3900

Table 3-10. (cont'd)

C(17')-H(17')	0.9500	C(16C)-C(21C)	1.3900
C(16C)-C(17C)	1.3900	C(21C)-H(21C)	0.9500
C(21C)-C(20C)	1.3900	C(20C)-H(20C)	0.9500
C(20C)-C(19C)	1.3900	C(19C)-H(19C)	0.9500
C(19C)-C(18C)	1.3900	C(18C)-H(18C)	0.9500
C(18C)-C(17C)	1.3900	C(17C)-H(17C)	0.9500
F(1)-B(1)	1.385(5)	F(2)-B(1)	1.391(5)
F(3)-B(1)	1.368(5)	F(4)-B(1)	1.385(5)
F(5)-B(2)	1.382(5)	F(6)-B(2)	1.369(6)
F(7)-B(2)	1.371(6)	F(8)-B(2)	1.392(5)
O(1S)-C(2S)	1.420(13)	O(1S)-C(3S)	1.417(13)
C(1S)-H(1SA)	0.9800	C(1S)-H(1SB)	0.9800
C(1S)-H(1SC)	0.9800	C(1S)-C(2S)	1.507(14)
C(2S)-H(2SA)	0.9900	C(2S)-H(2SB)	0.9900
C(3S)-H(3SA)	0.9900	C(3S)-H(3SB)	0.9900
C(3S)-C(4S)	1.502(14)	C(4S)-H(4SA)	0.9800
C(4S)-H(4SB)	0.9800	C(4S)-H(4SC)	0.9800
O(2S)-C(6S)	1.414(13)	O(2S)-C(7S)	1.336(13)
C(5S)-H(5SA)	0.9800	C(5S)-H(5SB)	0.9800
C(5S)-H(5SC)	0.9800	C(5S)-C(6S)	1.460(14)
C(6S)-H(6SA)	0.9900	C(6S)-H(6SB)	0.9900
C(7S)-H(7SA)	0.9900	C(7S)-H(7SB)	0.9900
C(7S)-C(8S)	1.570(13)	C(8S)-H(8SA)	0.9800
C(8S)-H(8SB)	0.9800	C(8S)-H(8SC)	0.9800
P(2)-Rh(1)-P(1)	80.02(3)	P(2)-Rh(1)-P(4)	162.89(4)
P(3)-Rh(1)-P(1)	165.57(4)	P(3)-Rh(1)-P(2)	105.36(3)
P(3)-Rh(1)-P(4)	80.79(3)	P(4)-Rh(1)-P(1)	97.94(3)
C(1)-P(1)-Rh(1)	112.81(11)	C(3)-P(1)-Rh(1)	114.49(12)
C(3)-P(1)-C(1)	100.64(16)	C(9)-P(1)-Rh(1)	120.79(12)
C(9)-P(1)-C(1)	99.54(16)	C(9)-P(1)-C(3)	105.82(16)
C(2)-P(2)-Rh(1)	114.48(11)	C(4)-P(2)-Rh(1)	109.03(11)
C(4)-P(2)-C(2)	104.77(16)	C(29)-P(2)-Rh(1)	125.94(12)
C(29)-P(2)-C(2)	104.21(16)	C(29)-P(2)-C(4)	95.10(15)
C(5)-P(3)-Rh(1)	109.99(12)	C(5)-P(3)-C(7)	102.00(16)
C(7)-P(3)-Rh(1)	114.16(11)	C(35)-P(3)-Rh(1)	124.92(12)
C(35)-P(3)-C(5)	99.02(16)	C(35)-P(3)-C(7)	103.59(16)
C(6)-P(4)-Rh(1)	116.27(12)	C(6)-P(4)-C(8)	99.10(16)
C(8)-P(4)-Rh(1)	111.60(11)	C(48)-P(4)-Rh(1)	120.75(11)

Table 3-10. (cont'd)

C(48)-P(4)-C(6)	105.28(16)	C(48)-P(4)-C(8)	100.70(16)
C(1)-N(1)-C(2)	112.9(3)	C(1)-N(1)-C(22)	113.3(3)
C(2)-N(1)-C(22)	115.2(3)	C(3)-N(2)-C(15)	109.1(3)
C(4)-N(2)-C(3)	115.4(3)	C(4)-N(2)-C(15)	106.7(3)
C(5)-N(3)-C(41)	111.5(3)	C(6)-N(3)-C(5)	114.8(3)
C(6)-N(3)-C(41)	114.4(3)	C(7)-N(4)-C(54)	115.7(3)
C(8)-N(4)-C(7)	113.6(3)	C(8)-N(4)-C(54)	111.7(3)
P(1)-C(1)-H(1A)	107.9	P(1)-C(1)-H(1B)	107.9
N(1)-C(1)-P(1)	117.6(2)	N(1)-C(1)-H(1A)	107.9
N(1)-C(1)-H(1B)	107.9	H(1A)-C(1)-H(1B)	107.2
P(2)-C(2)-H(2A)	108.5	P(2)-C(2)-H(2B)	108.5
N(1)-C(2)-P(2)	115.2(2)	N(1)-C(2)-H(2A)	108.5
N(1)-C(2)-H(2B)	108.5	H(2A)-C(2)-H(2B)	107.5
P(1)-C(3)-H(3A)	109.6	P(1)-C(3)-H(3B)	109.6
N(2)-C(3)-P(1)	110.4(2)	N(2)-C(3)-H(3A)	109.6
N(2)-C(3)-H(3B)	109.6	H(3A)-C(3)-H(3B)	108.1
P(2)-C(4)-H(4A)	107.9	P(2)-C(4)-H(4B)	107.9
N(2)-C(4)-P(2)	117.5(2)	N(2)-C(4)-H(4A)	107.9
N(2)-C(4)-H(4B)	107.9	H(4A)-C(4)-H(4B)	107.2
P(3)-C(5)-H(5A)	109.1	P(3)-C(5)-H(5B)	109.1
N(3)-C(5)-P(3)	112.4(2)	N(3)-C(5)-H(5A)	109.1
N(3)-C(5)-H(5B)	109.1	H(5A)-C(5)-H(5B)	107.9
P(4)-C(6)-H(6A)	110.2	P(4)-C(6)-H(6B)	110.2
N(3)-C(6)-P(4)	107.4(2)	N(3)-C(6)-H(6A)	110.2
N(3)-C(6)-H(6B)	110.2	H(6A)-C(6)-H(6B)	108.5
P(3)-C(7)-H(7A)	108.4	P(3)-C(7)-H(7B)	108.4
N(4)-C(7)-P(3)	115.6(2)	N(4)-C(7)-H(7A)	108.4
N(4)-C(7)-H(7B)	108.4	H(7A)-C(7)-H(7B)	107.5
P(4)-C(8)-H(8A)	107.8	P(4)-C(8)-H(8B)	107.8
N(4)-C(8)-P(4)	118.1(2)	N(4)-C(8)-H(8A)	107.8
N(4)-C(8)-H(8B)	107.8	H(8A)-C(8)-H(8B)	107.1
C(10)-C(9)-P(1)	124.1(3)	C(10)-C(9)-C(14)	118.9(3)
C(14)-C(9)-P(1)	116.8(3)	C(9)-C(10)-H(10)	119.8
C(11)-C(10)-C(9)	120.4(4)	C(11)-C(10)-H(10)	119.8
C(10)-C(11)-H(11)	120.0	C(10)-C(11)-C(12)	120.0(4)
C(12)-C(11)-H(11)	120.0	C(11)-C(12)-H(12)	120.0
C(13)-C(12)-C(11)	119.9(4)	C(13)-C(12)-H(12)	120.0
C(12)-C(13)-H(13)	120.1	C(14)-C(13)-C(12)	119.8(4)

Table 3-10. (cont'd)

C(14)-C(13)-H(13)	120.1	C(9)-C(14)-H(14)	119.5
C(13)-C(14)-C(9)	121.0(4)	C(13)-C(14)-H(14)	119.5
N(2)-C(15)-H(15A)	110.7	N(2)-C(15)-H(15B)	110.7
N(2)-C(15)-H(15C)	107.1	N(2)-C(15)-H(15D)	107.1
N(2)-C(15)-C(16)	105.0(3)	H(15A)-C(15)-H(15B)	108.8
H(15C)-C(15)-H(15D)	106.8	C(16)-C(15)-H(15A)	110.7
C(16)-C(15)-H(15B)	110.7	C(16B)-C(15)-N(2)	121.0(4)
C(16B)-C(15)-H(15C)	107.1	C(16B)-C(15)-H(15D)	107.1
N(1)-C(22)-H(22A)	108.9	N(1)-C(22)-H(22B)	108.9
N(1)-C(22)-C(23)	113.3(3)	H(22A)-C(22)-H(22B)	107.7
C(23)-C(22)-H(22A)	108.9	C(23)-C(22)-H(22B)	108.9
C(24)-C(23)-C(22)	121.7(3)	C(28)-C(23)-C(22)	119.6(3)
C(28)-C(23)-C(24)	118.5(3)	C(23)-C(24)-H(24)	119.8
C(25)-C(24)-C(23)	120.5(4)	C(25)-C(24)-H(24)	119.8
C(24)-C(25)-H(25)	119.6	C(26)-C(25)-C(24)	120.8(4)
C(26)-C(25)-H(25)	119.6	C(25)-C(26)-H(26)	120.1
C(25)-C(26)-C(27)	119.7(4)	C(27)-C(26)-H(26)	120.1
C(26)-C(27)-H(27)	120.2	C(26)-C(27)-C(28)	119.6(4)
C(28)-C(27)-H(27)	120.2	C(23)-C(28)-C(27)	120.8(4)
C(23)-C(28)-H(28)	119.6	C(27)-C(28)-H(28)	119.6
C(30)-C(29)-P(2)	120.3(3)	C(34)-C(29)-P(2)	120.1(3)
C(34)-C(29)-C(30)	118.9(3)	C(29)-C(30)-H(30)	120.0
C(31)-C(30)-C(29)	120.1(3)	C(31)-C(30)-H(30)	120.0
C(30)-C(31)-H(31)	119.8	C(32)-C(31)-C(30)	120.4(3)
C(32)-C(31)-H(31)	119.8	C(31)-C(32)-H(32)	120.0
C(33)-C(32)-C(31)	119.9(3)	C(33)-C(32)-H(32)	120.0
C(32)-C(33)-H(33)	120.0	C(32)-C(33)-C(34)	119.9(4)
C(34)-C(33)-H(33)	120.0	C(29)-C(34)-C(33)	120.7(3)
C(29)-C(34)-H(34)	119.6	C(33)-C(34)-H(34)	119.6
C(36)-C(35)-P(3)	120.5(3)	C(36)-C(35)-C(40)	118.5(3)
C(40)-C(35)-P(3)	120.9(3)	C(35)-C(36)-H(36)	119.6
C(37)-C(36)-C(35)	120.8(4)	C(37)-C(36)-H(36)	119.6
C(36)-C(37)-H(37)	120.2	C(38)-C(37)-C(36)	119.6(4)
C(38)-C(37)-H(37)	120.2	C(37)-C(38)-H(38)	119.9
C(39)-C(38)-C(37)	120.2(4)	C(39)-C(38)-H(38)	119.9
C(38)-C(39)-H(39)	119.9	C(38)-C(39)-C(40)	120.1(4)
C(40)-C(39)-H(39)	119.9	C(35)-C(40)-H(40)	119.7
C(39)-C(40)-C(35)	120.7(4)	C(39)-C(40)-H(40)	119.7

Table 3-10. (cont'd)

N(3)-C(41)-H(41A)	109.8	N(3)-C(41)-H(41B)	109.8
N(3)-C(41)-C(42)	109.2(3)	H(41A)-C(41)-H(41B)	108.3
C(42)-C(41)-H(41A)	109.8	C(42)-C(41)-H(41B)	109.8
C(43)-C(42)-C(41)	121.4(4)	C(43)-C(42)-C(47)	117.8(4)
C(47)-C(42)-C(41)	120.5(4)	C(42)-C(43)-H(43)	119.5
C(44)-C(43)-C(42)	121.0(4)	C(44)-C(43)-H(43)	119.5
C(43)-C(44)-H(44)	119.6	C(45)-C(44)-C(43)	120.8(4)
C(45)-C(44)-H(44)	119.6	C(44)-C(45)-H(45)	120.4
C(44)-C(45)-C(46)	119.2(4)	C(46)-C(45)-H(45)	120.4
C(45)-C(46)-H(46)	119.9	C(45)-C(46)-C(47)	120.2(4)
C(47)-C(46)-H(46)	119.9	C(42)-C(47)-H(47)	119.6
C(46)-C(47)-C(42)	120.8(4)	C(46)-C(47)-H(47)	119.6
C(49)-C(48)-P(4)	123.8(3)	C(49)-C(48)-C(53)	118.8(3)
C(53)-C(48)-P(4)	117.4(3)	C(48)-C(49)-H(49)	119.8
C(50)-C(49)-C(48)	120.4(3)	C(50)-C(49)-H(49)	119.8
C(49)-C(50)-H(50)	119.9	C(51)-C(50)-C(49)	120.2(4)
C(51)-C(50)-H(50)	119.9	C(50)-C(51)-H(51)	119.9
C(50)-C(51)-C(52)	120.2(4)	C(52)-C(51)-H(51)	119.9
C(51)-C(52)-H(52)	120.1	C(53)-C(52)-C(51)	119.8(4)
C(53)-C(52)-H(52)	120.1	C(48)-C(53)-H(53)	119.7
C(52)-C(53)-C(48)	120.6(4)	C(52)-C(53)-H(53)	119.7
N(4)-C(54)-H(54A)	108.6	N(4)-C(54)-H(54B)	108.6
N(4)-C(54)-C(55)	114.7(3)	H(54A)-C(54)-H(54B)	107.6
C(55)-C(54)-H(54A)	108.6	C(55)-C(54)-H(54B)	108.6
C(56)-C(55)-C(54)	117.8(3)	C(60)-C(55)-C(54)	123.6(3)
C(60)-C(55)-C(56)	118.5(3)	C(55)-C(56)-H(56)	119.9
C(57)-C(56)-C(55)	120.2(3)	C(57)-C(56)-H(56)	119.9
C(56)-C(57)-H(57)	119.7	C(58)-C(57)-C(56)	120.6(4)
C(58)-C(57)-H(57)	119.7	C(57)-C(58)-H(58)	120.0
C(57)-C(58)-C(59)	120.0(4)	C(59)-C(58)-H(58)	120.0
C(58)-C(59)-H(59)	120.1	C(58)-C(59)-C(60)	119.8(4)
C(60)-C(59)-H(59)	120.1	C(55)-C(60)-C(59)	121.0(3)
C(55)-C(60)-H(60)	119.5	C(59)-C(60)-H(60)	119.5
C(17)-C(16)-C(15)	118.0(3)	C(17)-C(16)-C(21)	120.0
C(21)-C(16)-C(15)	121.9(3)	C(16)-C(17)-H(17)	120.0
C(16)-C(17)-C(18)	120.0	C(18)-C(17)-H(17)	120.0
C(17)-C(18)-H(18)	120.0	C(19)-C(18)-C(17)	120.0
C(19)-C(18)-H(18)	120.0	C(18)-C(19)-H(19)	120.0

Table 3-10. (cont'd)

C(18)-C(19)-C(20)	120.0	C(20)-C(19)-H(19)	120.0
C(19)-C(20)-H(20)	120.0	C(21)-C(20)-C(19)	120.0
C(21)-C(20)-H(20)	120.0	C(16)-C(21)-H(21)	120.0
C(20)-C(21)-C(16)	120.0	C(20)-C(21)-H(21)	120.0
C(17B)-C(16B)-C(15)	123.3(8)	C(21B)-C(16B)-C(15)	117.3(8)
C(21B)-C(16B)-C(17B)	119.2(9)	C(16B)-C(17B)-H(17B)	119.8
C(18B)-C(17B)-C(16B)	120.4(9)	C(18B)-C(17B)-H(17B)	119.8
C(17B)-C(18B)-H(18B)	120.0	C(17B)-C(18B)-C(19B)	119.9(10)
C(19B)-C(18B)-H(18B)	120.0	C(18B)-C(19B)-H(19B)	120.2
C(20B)-C(19B)-C(18B)	119.5(11)	C(20B)-C(19B)-H(19B)	120.2
C(19B)-C(20B)-H(20B)	119.7	C(19B)-C(20B)-C(21B)	120.6(10)
C(21B)-C(20B)-H(20B)	119.7	C(16B)-C(21B)-C(20B)	120.3(9)
C(16B)-C(21B)-H(21B)	119.9	C(20B)-C(21B)-H(21B)	119.9
P(2')-Rh(1')-P(1')	79.43(3)	P(2')-Rh(1')-P(4')	163.16(4)
P(3')-Rh(1')-P(1')	166.44(4)	P(3')-Rh(1')-P(2')	105.20(3)
P(3')-Rh(1')-P(4')	79.96(3)	P(4')-Rh(1')-P(1')	99.29(3)
C(1')-P(1')-Rh(1')	113.04(12)	C(3')-P(1')-Rh(1')	114.60(12)
C(3')-P(1')-C(1')	99.96(17)	C(9')-P(1')-Rh(1')	120.37(12)
C(9')-P(1')-C(1')	99.67(16)	C(9')-P(1')-C(3')	106.38(17)
C(2')-P(2')-Rh(1')	116.01(11)	C(4')-P(2')-Rh(1')	109.86(12)
C(4')-P(2')-C(2')	104.00(16)	C(29')-P(2')-Rh(1')	122.47(12)
C(29')-P(2')-C(2')	105.11(16)	C(29')-P(2')-C(4')	96.28(16)
C(5')-P(3')-Rh(1')	111.75(12)	C(5')-P(3')-C(7')	102.07(16)
C(7')-P(3')-Rh(1')	114.31(11)	C(35')-P(3')-Rh(1')	122.69(12)
C(35')-P(3')-C(5')	99.21(15)	C(35')-P(3')-C(7')	104.02(16)
C(6')-P(4')-Rh(1')	116.17(12)	C(6')-P(4')-C(8')	98.20(16)
C(8')-P(4')-Rh(1')	112.98(11)	C(48')-P(4')-Rh(1')	118.95(11)
C(48')-P(4')-C(6')	106.44(15)	C(48')-P(4')-C(8')	101.19(15)
C(1')-N(1')-C(2')	113.5(3)	C(1')-N(1')-C(22')	113.3(3)
C(2')-N(1')-C(22')	114.5(3)	C(3')-N(2')-C(15')	110.3(3)
C(4')-N(2')-C(3')	114.7(3)	C(4')-N(2')-C(15')	106.4(3)
C(5')-N(3')-C(6')	115.2(3)	C(5')-N(3')-C(41')	110.7(3)
C(6')-N(3')-C(41')	112.0(3)	C(8')-N(4')-C(7')	113.4(3)
C(8')-N(4')-C(54')	111.2(3)	C(54')-N(4')-C(7')	115.6(3)
P(1')-C(1')-H(1'A)	107.7	P(1')-C(1')-H(1'B)	107.7
N(1')-C(1')-P(1')	118.4(2)	N(1')-C(1')-H(1'A)	107.7
N(1')-C(1')-H(1'B)	107.7	H(1'A)-C(1')-H(1'B)	107.1
P(2')-C(2')-H(2'A)	108.6	P(2')-C(2')-H(2'B)	108.6

Table 3-10. (cont'd)

N(1')-C(2')-P(2')	114.7(2)	N(1')-C(2')-H(2'A)	108.6
N(1')-C(2')-H(2'B)	108.6	H(2'A)-C(2')-H(2'B)	107.6
P(1')-C(3')-H(3'A)	109.4	P(1')-C(3')-H(3'B)	109.4
N(2')-C(3')-P(1')	111.1(2)	N(2')-C(3')-H(3'A)	109.4
N(2')-C(3')-H(3'B)	109.4	H(3'A)-C(3')-H(3'B)	108.0
P(2')-C(4')-H(4'A)	107.9	P(2')-C(4')-H(4'B)	107.9
N(2')-C(4')-P(2')	117.4(2)	N(2')-C(4')-H(4'A)	107.9
N(2')-C(4')-H(4'B)	107.9	H(4'A)-C(4')-H(4'B)	107.2
P(3')-C(5')-H(5'A)	108.9	P(3')-C(5')-H(5'B)	108.9
N(3')-C(5')-P(3')	113.5(2)	N(3')-C(5')-H(5'A)	108.9
N(3')-C(5')-H(5'B)	108.9	H(5'A)-C(5')-H(5'B)	107.7
P(4')-C(6')-H(6'A)	110.1	P(4')-C(6')-H(6'B)	110.1
N(3')-C(6')-P(4')	108.1(2)	N(3')-C(6')-H(6'A)	110.1
N(3')-C(6')-H(6'B)	110.1	H(6'A)-C(6')-H(6'B)	108.4
P(3')-C(7')-H(7'A)	108.3	P(3')-C(7')-H(7'B)	108.3
N(4')-C(7')-P(3')	116.1(2)	N(4')-C(7')-H(7'A)	108.3
N(4')-C(7')-H(7'B)	108.3	H(7'A)-C(7')-H(7'B)	107.4
P(4')-C(8')-H(8'A)	107.8	P(4')-C(8')-H(8'B)	107.8
N(4')-C(8')-P(4')	118.1(2)	N(4')-C(8')-H(8'A)	107.8
N(4')-C(8')-H(8'B)	107.8	H(8'A)-C(8')-H(8'B)	107.1
C(10')-C(9')-P(1')	124.2(3)	C(14')-C(9')-P(1')	116.5(3)
C(14')-C(9')-C(10')	119.2(4)	C(9')-C(10')-H(10')	120.0
C(11')-C(10')-C(9')	119.9(4)	C(11')-C(10')-H(10')	120.0
C(10')-C(11')-H(11')	120.2	C(12')-C(11')-C(10')	119.5(4)
C(12')-C(11')-H(11')	120.2	C(11')-C(12')-H(12')	119.5
C(13')-C(12')-C(11')	121.1(4)	C(13')-C(12')-H(12')	119.5
C(12')-C(13')-H(13')	120.4	C(14')-C(13')-C(12')	119.2(4)
C(14')-C(13')-H(13')	120.4	C(9')-C(14')-H(14')	119.5
C(13')-C(14')-C(9')	121.1(4)	C(13')-C(14')-H(14')	119.5
N(2')-C(15')-H(15E)	111.0	N(2')-C(15')-H(15F)	111.0
N(2')-C(15')-H(15G)	108.0	N(2')-C(15')-H(15H)	108.0
N(2')-C(15')-C(16')	104.0(8)	H(15E)-C(15')-H(15F)	109.0
H(15G)-C(15')-H(15H)	107.3	C(16')-C(15')-H(15E)	111.0
C(16')-C(15')-H(15F)	111.0	C(16C)-C(15')-N(2')	117.0(4)
C(16C)-C(15')-H(15G)	108.0	C(16C)-C(15')-H(15H)	108.0
N(1')-C(22')-H(22C)	108.8	N(1')-C(22')-H(22D)	108.8
N(1')-C(22')-C(23')	113.7(3)	H(22C)-C(22')-H(22D)	107.7
C(23')-C(22')-H(22C)	108.8	C(23')-C(22')-H(22D)	108.8

Table 3-10. (cont'd)

C(24')-C(23')-C(22')	121.3(4)	C(28')-C(23')-C(22')	120.0(3)
C(28')-C(23')-C(24')	118.7(4)	C(23')-C(24')-H(24')	119.7
C(25')-C(24')-C(23')	120.6(4)	C(25')-C(24')-H(24')	119.7
C(24')-C(25')-H(25')	119.8	C(26')-C(25')-C(24')	120.3(4)
C(26')-C(25')-H(25')	119.8	C(25')-C(26')-H(26')	120.0
C(25')-C(26')-C(27')	120.0(4)	C(27')-C(26')-H(26')	120.0
C(26')-C(27')-H(27')	120.2	C(26')-C(27')-C(28')	119.5(4)
C(28')-C(27')-H(27')	120.2	C(23')-C(28')-C(27')	120.9(4)
C(23')-C(28')-H(28')	119.6	C(27')-C(28')-H(28')	119.6
C(30')-C(29')-P(2')	124.2(3)	C(34')-C(29')-P(2')	117.8(3)
C(34')-C(29')-C(30')	117.9(3)	C(29')-C(30')-H(30')	120.0
C(31')-C(30')-C(29')	120.0(4)	C(31')-C(30')-H(30')	120.0
C(30')-C(31')-H(31')	119.5	C(30')-C(31')-C(32')	121.0(4)
C(32')-C(31')-H(31')	119.5	C(31')-C(32')-H(32')	120.5
C(33')-C(32')-C(31')	119.1(4)	C(33')-C(32')-H(32')	120.5
C(32')-C(33')-H(33')	119.9	C(32')-C(33')-C(34')	120.1(4)
C(34')-C(33')-H(33')	119.9	C(29')-C(34')-H(34')	119.1
C(33')-C(34')-C(29')	121.9(3)	C(33')-C(34')-H(34')	119.1
C(36')-C(35')-P(3')	119.1(3)	C(36')-C(35')-C(40')	118.8(3)
C(40')-C(35')-P(3')	122.0(3)	C(35')-C(36')-H(36')	119.7
C(35')-C(36')-C(37')	120.6(3)	C(37')-C(36')-H(36')	119.7
C(36')-C(37')-H(37')	119.8	C(38')-C(37')-C(36')	120.4(4)
C(38')-C(37')-H(37')	119.8	C(37')-C(38')-H(38')	120.2
C(37')-C(38')-C(39')	119.6(3)	C(39')-C(38')-H(38')	120.2
C(38')-C(39')-H(39')	119.8	C(38')-C(39')-C(40')	120.5(4)
C(40')-C(39')-H(39')	119.8	C(35')-C(40')-H(40')	120.0
C(39')-C(40')-C(35')	120.1(3)	C(39')-C(40')-H(40')	120.0
N(3')-C(41')-H(41C)	109.2	N(3')-C(41')-H(41D)	109.2
N(3')-C(41')-C(42')	111.9(3)	H(41C)-C(41')-H(41D)	107.9
C(42')-C(41')-H(41C)	109.2	C(42')-C(41')-H(41D)	109.2
C(43')-C(42')-C(41')	120.2(4)	C(43')-C(42')-C(47')	118.5(4)
C(47')-C(42')-C(41')	121.3(3)	C(42')-C(43')-H(43')	119.9
C(42')-C(43')-C(44')	120.2(4)	C(44')-C(43')-H(43')	119.9
C(43')-C(44')-H(44')	119.9	C(45')-C(44')-C(43')	120.3(4)
C(45')-C(44')-H(44')	119.9	C(44')-C(45')-H(45')	120.2
C(46')-C(45')-C(44')	119.6(4)	C(46')-C(45')-H(45')	120.2
C(45')-C(46')-H(46')	119.8	C(45')-C(46')-C(47')	120.5(4)
C(47')-C(46')-H(46')	119.8	C(42')-C(47')-H(47')	119.5

Table 3-10. (cont'd)

C(46')-C(47')-C(42')	121.0(4)	C(46')-C(47')-H(47')	119.5
C(49')-C(48')-P(4')	124.5(3)	C(53')-C(48')-P(4')	116.6(3)
C(53')-C(48')-C(49')	118.9(3)	C(48')-C(49')-H(49')	119.9
C(50')-C(49')-C(48')	120.2(3)	C(50')-C(49')-H(49')	119.9
C(49')-C(50')-H(50')	119.9	C(51')-C(50')-C(49')	120.2(3)
C(51')-C(50')-H(50')	119.9	C(50')-C(51')-H(51')	120.0
C(50')-C(51')-C(52')	120.0(3)	C(52')-C(51')-H(51')	120.0
C(51')-C(52')-H(52')	119.9	C(53')-C(52')-C(51')	120.2(3)
C(53')-C(52')-H(52')	119.9	C(48')-C(53')-H(53')	119.7
C(52')-C(53')-C(48')	120.5(3)	C(52')-C(53')-H(53')	119.7
N(4')-C(54')-H(54C)	108.5	N(4')-C(54')-H(54D)	108.5
N(4')-C(54')-C(55')	115.1(3)	H(54C)-C(54')-H(54D)	107.5
C(55')-C(54')-H(54C)	108.5	C(55')-C(54')-H(54D)	108.5
C(56')-C(55')-C(54')	117.5(3)	C(60')-C(55')-C(54')	123.8(3)
C(60')-C(55')-C(56')	118.7(3)	C(55')-C(56')-H(56')	119.6
C(57')-C(56')-C(55')	120.7(3)	C(57')-C(56')-H(56')	119.6
C(56')-C(57')-H(57')	120.1	C(58')-C(57')-C(56')	119.8(3)
C(58')-C(57')-H(57')	120.1	C(57')-C(58')-H(58')	120.0
C(57')-C(58')-C(59')	120.1(3)	C(59')-C(58')-H(58')	120.0
C(58')-C(59')-H(59')	120.0	C(58')-C(59')-C(60')	120.1(3)
C(60')-C(59')-H(59')	120.0	C(55')-C(60')-C(59')	120.6(3)
C(55')-C(60')-H(60')	119.7	C(59')-C(60')-H(60')	119.7
C(21')-C(16')-C(15')	119.0(10)	C(21')-C(16')-C(17')	120.0
C(17')-C(16')-C(15')	120.7(10)	C(16')-C(21')-H(21')	120.0
C(20')-C(21')-C(16')	120.0	C(20')-C(21')-H(21')	120.0
C(21')-C(20')-H(20')	120.0	C(21')-C(20')-C(19')	120.0
C(19')-C(20')-H(20')	120.0	C(20')-C(19')-H(19')	120.0
C(18')-C(19')-C(20')	120.0	C(18')-C(19')-H(19')	120.0
C(19')-C(18')-H(18')	120.0	C(19')-C(18')-C(17')	120.0
C(17')-C(18')-H(18')	120.0	C(16')-C(17')-H(17')	120.0
C(18')-C(17')-C(16')	120.0	C(18')-C(17')-H(17')	120.0
C(21C)-C(16C)-C(15')	119.8(4)	C(21C)-C(16C)-C(17C)	120.0
C(17C)-C(16C)-C(15')	120.1(4)	C(16C)-C(21C)-H(21C)	120.0
C(20C)-C(21C)-C(16C)	120.0	C(20C)-C(21C)-H(21C)	120.0
C(21C)-C(20C)-H(20C)	120.0	C(19C)-C(20C)-C(21C)	120.0
C(19C)-C(20C)-H(20C)	120.0	C(20C)-C(19C)-H(19C)	120.0
C(20C)-C(19C)-C(18C)	120.0	C(18C)-C(19C)-H(19C)	120.0
C(19C)-C(18C)-H(18C)	120.0	C(17C)-C(18C)-C(19C)	120.0

Table 3-10. (cont'd)

C(17C)-C(18C)-H(18C)	120.0	C(16C)-C(17C)-H(17C)	120.0
C(18C)-C(17C)-C(16C)	120.0	C(18C)-C(17C)-H(17C)	120.0
F(1)-B(1)-F(2)	107.2(4)	F(3)-B(1)-F(1)	108.9(4)
F(3)-B(1)-F(2)	110.1(4)	F(3)-B(1)-F(4)	110.6(4)
F(4)-B(1)-F(1)	109.3(4)	F(4)-B(1)-F(2)	110.6(4)
F(5)-B(2)-F(8)	109.4(4)	F(6)-B(2)-F(5)	108.4(4)
F(6)-B(2)-F(7)	110.4(4)	F(6)-B(2)-F(8)	110.3(4)
F(7)-B(2)-F(5)	108.6(4)	F(7)-B(2)-F(8)	109.7(4)
C(3S)-O(1S)-C(2S)	113.5(6)	H(1SA)-C(1S)-H(1SB)	109.5
H(1SA)-C(1S)-H(1SC)	109.5	H(1SB)-C(1S)-H(1SC)	109.5
C(2S)-C(1S)-H(1SA)	109.5	C(2S)-C(1S)-H(1SB)	109.5
C(2S)-C(1S)-H(1SC)	109.5	O(1S)-C(2S)-C(1S)	108.3(8)
O(1S)-C(2S)-H(2SA)	110.0	O(1S)-C(2S)-H(2SB)	110.0
C(1S)-C(2S)-H(2SA)	110.0	C(1S)-C(2S)-H(2SB)	110.0
H(2SA)-C(2S)-H(2SB)	108.4	O(1S)-C(3S)-H(3SA)	109.7
O(1S)-C(3S)-H(3SB)	109.7	O(1S)-C(3S)-C(4S)	109.6(8)
H(3SA)-C(3S)-H(3SB)	108.2	C(4S)-C(3S)-H(3SA)	109.7
C(4S)-C(3S)-H(3SB)	109.7	C(3S)-C(4S)-H(4SA)	109.5
C(3S)-C(4S)-H(4SB)	109.5	C(3S)-C(4S)-H(4SC)	109.5
H(4SA)-C(4S)-H(4SB)	109.5	H(4SA)-C(4S)-H(4SC)	109.5
H(4SB)-C(4S)-H(4SC)	109.5	C(7S)-O(2S)-C(6S)	117.0(9)
H(5SA)-C(5S)-H(5SB)	109.5	H(5SA)-C(5S)-H(5SC)	109.5
H(5SB)-C(5S)-H(5SC)	109.5	C(6S)-C(5S)-H(5SA)	109.5
C(6S)-C(5S)-H(5SB)	109.5	C(6S)-C(5S)-H(5SC)	109.5
O(2S)-C(6S)-C(5S)	119.2(13)	O(2S)-C(6S)-H(6SA)	107.5
O(2S)-C(6S)-H(6SB)	107.5	C(5S)-C(6S)-H(6SA)	107.5
C(5S)-C(6S)-H(6SB)	107.5	H(6SA)-C(6S)-H(6SB)	107.0
O(2S)-C(7S)-H(7SA)	109.3	O(2S)-C(7S)-H(7SB)	109.3
O(2S)-C(7S)-C(8S)	111.6(11)	H(7SA)-C(7S)-H(7SB)	108.0
C(8S)-C(7S)-H(7SA)	109.3	C(8S)-C(7S)-H(7SB)	109.3
C(7S)-C(8S)-H(8SA)	109.5	C(7S)-C(8S)-H(8SB)	109.5
C(7S)-C(8S)-H(8SC)	109.5	H(8SA)-C(8S)-H(8SB)	109.5
H(8SA)-C(8S)-H(8SC)	109.5	H(8SB)-C(8S)-H(8SC)	109.5

3.6.3 Crystal data for $Rh(P^{Ph}_2N^{PhOMe}_2)_2BF_4$ (3)

The systematic absences in the diffraction data were consistent with monoclinic space group P21/c with Z = 4 and Z' = 1. The asymmetric unit also contains one BF_4^- anion and an uncoordinated acetonitrile. All hydrogen atoms were included into the model at geometrically calculated positions and refined using a riding model. The goodness of fit on F^2 was 1.008 with R1(wR2) = 0.0422(0.0731) for [I>2sigma(I)] and with a largest difference peak and hole of 0.798 and -0.448(e.Å-3).

Table 3-11. Crystal data and structure refinement for $Rh(P^{Ph}{}_2N^{PhOMe}{}_2)_2BF_4$ (**3**)

Identification code		
Empirical formula	C62 H67 B F4 N5 P4 Rh	
Formula weight	1259.81	
Temperature	100(2) K	
Wavelength	0.71073 Å	
Crystal system	Monoclinic	
Space group	$P2_1/c$	
Unit cell dimensions	a = 12.8250(11) Å	α = 90°.
	b = 17.1647(16) Å	β = 94.522(4)°.
	c = 26.185(2) Å	γ = 90°.
Volume	5746.3(9) $Å^3$	
Z	4	
Density (calculated)	1.456 Mg/m^3	
Absorption coefficient	0.475 mm^{-1}	
F(000)	2608	
Crystal size	0.4 x 0.2 x 0.2 mm^3	
Theta range for data collection	2.32 to 26.45°.	
Index ranges	-16<=h<=15, -21<=k<=21, -22<=l<=32	
Reflections collected	94846	
Independent reflections	11794 [R(int) = 0.0992]	
Completeness to theta = 25.00°	99.5 %	
Absorption correction	Semi-empirical from equivalents	
Max. and min. transmission	0.9098 and 0.8307	
Refinement method	Full-matrix least-squares on F^2	
Data / restraints / parameters	11794 / 0 / 735	
Goodness-of-fit on F^2	1.008	
Final R indices [I>2sigma(I)]	R1 = 0.0422, wR2 = 0.0731	
R indices (all data)	R1 = 0.0740, wR2 = 0.0840	
Extinction coefficient	not measured	
Largest diff. peak and hole	0.798 and -0.448 $e.Å^{-3}$	

Table 3-12. Bond lengths [Å] and angles [°] for $Rh(P^{Ph}{}_2N^{PhOMe}{}_2)_2BF_4$ (**3**)

Rh(1)-P(4)	2.2764(8)	Rh(1)-P(1)	2.2784(8)
Rh(1)-P(2)	2.2878(8)	Rh(1)-P(3)	2.2955(8)
P(1)-C(5)	1.826(3)	P(1)-C(11)	1.860(3)
P(1)-C(3)	1.891(3)	P(2)-C(50)	1.822(3)
P(2)-C(32)	1.868(3)	P(2)-C(41)	1.873(3)
P(3)-C(27)	1.836(3)	P(3)-C(13)	1.869(3)
P(3)-C(1)	1.874(3)	P(4)-C(56)	1.829(3)
P(4)-C(4)	1.854(3)	P(4)-C(33)	1.888(3)
O(1)-C(23)	1.374(4)	O(1)-C(24)	1.421(4)
O(2)-C(17)	1.381(3)	O(2)-C(1A)	1.401(4)
O(3)-C(37)	1.375(3)	O(3)-C(38)	1.427(4)
O(5)-C(46)	1.371(3)	O(5)-C(47)	1.432(4)
N(1)-C(20)	1.412(4)	N(1)-C(1)	1.448(4)
N(1)-C(3)	1.450(4)	N(2)-C(34)	1.416(4)
N(2)-C(33)	1.445(3)	N(2)-C(32)	1.459(4)
N(12)-C(14)	1.432(4)	N(12)-C(13)	1.458(4)
N(12)-C(11)	1.462(4)	N(42)-C(43)	1.434(4)
N(42)-C(4)	1.465(4)	N(42)-C(41)	1.465(4)
C(1)-H(1A)	0.9900	C(1)-H(1B)	0.9900
C(1A)-H(1AA)	0.9800	C(1A)-H(1AB)	0.9800
C(1A)-H(1AC)	0.9800	C(1B)-C(30)	1.378(5)
C(1B)-C(31)	1.385(4)	C(1B)-H(1BA)	0.9500
C(3)-H(3A)	0.9900	C(3)-H(3B)	0.9900
C(4)-H(4A)	0.9900	C(4)-H(4B)	0.9900
C(5)-C(6)	1.388(4)	C(5)-C(10)	1.390(4)
C(6)-C(7)	1.386(4)	C(6)-H(6)	0.9500
C(7)-C(8)	1.372(4)	C(7)-H(7)	0.9500
C(8)-C(9)	1.382(4)	C(8)-H(8)	0.9500
C(9)-C(10)	1.386(4)	C(9)-H(9)	0.9500
C(10)-H(10)	0.9500	C(11)-H(11A)	0.9900
C(11)-H(11B)	0.9900	C(13)-H(13A)	0.9900
C(13)-H(13B)	0.9900	C(14)-C(19)	1.386(4)
C(14)-C(15)	1.403(4)	C(15)-C(16)	1.378(4)
C(15)-H(15)	0.9500	C(16)-C(17)	1.390(4)
C(16)-H(16)	0.9500	C(17)-C(18)	1.379(4)
C(18)-C(19)	1.399(4)	C(18)-H(18)	0.9500
C(19)-H(19)	0.9500	C(20)-C(26)	1.396(4)
C(20)-C(21)	1.401(4)	C(21)-C(22)	1.390(4)

Table 3-12. (cont'd)

C(21)-H(21)	0.9500	C(22)-C(23)	1.384(4)
C(22)-H(22)	0.9500	C(23)-C(25)	1.388(4)
C(24)-H(24A)	0.9800	C(24)-H(24B)	0.9800
C(24)-H(24C)	0.9800	C(25)-C(26)	1.378(4)
C(25)-H(25)	0.9500	C(26)-H(26)	0.9500
C(27)-C(28)	1.391(4)	C(27)-C(31)	1.395(4)
C(28)-C(29)	1.390(4)	C(28)-H(28)	0.9500
C(29)-C(30)	1.381(5)	C(29)-H(29)	0.9500
C(30)-H(30)	0.9500	C(31)-H(31)	0.9500
C(32)-H(32A)	0.9900	C(32)-H(32B)	0.9900
C(33)-H(33A)	0.9900	C(33)-H(33B)	0.9900
C(34)-C(35)	1.397(4)	C(34)-C(40)	1.404(4)
C(35)-C(36)	1.393(4)	C(35)-H(35)	0.9500
C(36)-C(37)	1.383(4)	C(36)-H(36)	0.9500
C(37)-C(39)	1.382(4)	C(38)-H(38A)	0.9800
C(38)-H(38B)	0.9800	C(38)-H(38C)	0.9800
C(39)-C(40)	1.386(4)	C(39)-H(39)	0.9500
C(40)-H(40)	0.9500	C(41)-H(41A)	0.9900
C(41)-H(41B)	0.9900	C(43)-C(49)	1.383(4)
C(43)-C(44)	1.398(4)	C(44)-C(45)	1.388(4)
C(44)-H(44)	0.9500	C(45)-C(46)	1.397(4)
C(45)-H(45)	0.9500	C(46)-C(48)	1.387(4)
C(47)-H(47A)	0.9800	C(47)-H(47B)	0.9800
C(47)-H(47C)	0.9800	C(48)-C(49)	1.401(4)
C(48)-H(48)	0.9500	C(49)-H(49)	0.9500
C(50)-C(55)	1.394(4)	C(50)-C(51)	1.395(4)
C(51)-C(52)	1.386(4)	C(51)-H(51)	0.9500
C(52)-C(53)	1.386(4)	C(52)-H(52)	0.9500
C(53)-C(54)	1.382(4)	C(53)-H(53)	0.9500
C(54)-C(55)	1.387(4)	C(54)-H(54)	0.9500
C(55)-H(55)	0.9500	C(56)-C(61)	1.388(4)
C(56)-C(57)	1.400(4)	C(57)-C(58)	1.381(4)
C(57)-H(57)	0.9500	C(58)-C(59)	1.381(4)
C(58)-H(58)	0.9500	C(59)-C(60)	1.378(4)
C(59)-H(59)	0.9500	C(60)-C(61)	1.384(4)
C(60)-H(60)	0.9500	C(61)-H(61)	0.9500
F(6)-B(2)	1.392(5)	F(62)-B(2)	1.399(5)
F(63)-B(2)	1.364(5)	F(64)-B(2)	1.375(5)

Table 3-12. (cont'd)

N(65)-C(66)	1.135(5)	C(66)-C(67)	1.463(6)
C(67)-H(67A)	0.9800	C(67)-H(67B)	0.9800
C(67)-H(67C)	0.9800	P(4)-Rh(1)-P(1)	98.63(3)
P(4)-Rh(1)-P(2)	82.01(3)	P(1)-Rh(1)-P(2)	169.03(3)
P(4)-Rh(1)-P(3)	161.97(3)	P(1)-Rh(1)-P(3)	81.69(3)
P(2)-Rh(1)-P(3)	101.13(3)	C(5)-P(1)-C(11)	103.77(13)
C(5)-P(1)-C(3)	100.44(13)	C(11)-P(1)-C(3)	100.83(14)
C(5)-P(1)-Rh(1)	123.46(9)	C(11)-P(1)-Rh(1)	113.41(10)
C(3)-P(1)-Rh(1)	111.96(9)	C(50)-P(2)-C(32)	106.14(13)
C(50)-P(2)-C(41)	98.35(13)	C(32)-P(2)-C(41)	100.05(13)
C(50)-P(2)-Rh(1)	125.38(9)	C(32)-P(2)-Rh(1)	112.94(9)
C(41)-P(2)-Rh(1)	110.26(10)	C(27)-P(3)-C(13)	101.05(13)
C(27)-P(3)-C(1)	101.97(13)	C(13)-P(3)-C(1)	99.98(13)
C(27)-P(3)-Rh(1)	126.87(9)	C(13)-P(3)-Rh(1)	107.90(10)
C(1)-P(3)-Rh(1)	115.17(10)	C(56)-P(4)-C(4)	102.33(13)
C(56)-P(4)-C(33)	100.73(13)	C(4)-P(4)-C(33)	99.07(13)
C(56)-P(4)-Rh(1)	124.89(10)	C(4)-P(4)-Rh(1)	116.40(10)
C(33)-P(4)-Rh(1)	109.50(9)	C(23)-O(1)-C(24)	117.0(2)
C(17)-O(2)-C(1A)	118.1(3)	C(37)-O(3)-C(38)	116.9(2)
C(46)-O(5)-C(47)	117.1(2)	C(20)-N(1)-C(1)	117.9(2)
C(20)-N(1)-C(3)	119.3(2)	C(1)-N(1)-C(3)	113.4(2)
C(34)-N(2)-C(33)	119.4(2)	C(34)-N(2)-C(32)	119.3(2)
C(33)-N(2)-C(32)	113.2(2)	C(14)-N(12)-C(13)	116.9(2)
C(14)-N(12)-C(11)	115.2(2)	C(13)-N(12)-C(11)	117.0(2)
C(43)-N(42)-C(4)	115.4(2)	C(43)-N(42)-C(41)	117.2(2)
C(4)-N(42)-C(41)	115.4(2)	N(1)-C(1)-P(3)	113.09(19)
N(1)-C(1)-H(1A)	109.0	P(3)-C(1)-H(1A)	109.0
N(1)-C(1)-H(1B)	109.0	P(3)-C(1)-H(1B)	109.0
H(1A)-C(1)-H(1B)	107.8	O(2)-C(1A)-H(1AA)	109.5
O(2)-C(1A)-H(1AB)	109.5	H(1AA)-C(1A)-H(1AB)	109.5
O(2)-C(1A)-H(1AC)	109.5	H(1AA)-C(1A)-H(1AC)	109.5
H(1AB)-C(1A)-H(1AC)	109.5	C(30)-C(1B)-C(31)	119.7(3)
C(30)-C(1B)-H(1BA)	120.1	C(31)-C(1B)-H(1BA)	120.1
N(1)-C(3)-P(1)	116.05(19)	N(1)-C(3)-H(3A)	108.3
P(1)-C(3)-H(3A)	108.3	N(1)-C(3)-H(3B)	108.3
P(1)-C(3)-H(3B)	108.3	H(3A)-C(3)-H(3B)	107.4
N(42)-C(4)-P(4)	110.22(19)	N(42)-C(4)-H(4A)	109.6
P(4)-C(4)-H(4A)	109.6	N(42)-C(4)-H(4B)	109.6

Table 3-12. (cont'd)

P(4)-C(4)-H(4B)	109.6	H(4A)-C(4)-H(4B)	108.1
C(6)-C(5)-C(10)	118.8(3)	C(6)-C(5)-P(1)	122.8(2)
C(10)-C(5)-P(1)	118.3(2)	C(7)-C(6)-C(5)	120.3(3)
C(7)-C(6)-H(6)	119.9	C(5)-C(6)-H(6)	119.9
C(8)-C(7)-C(6)	120.3(3)	C(8)-C(7)-H(7)	119.9
C(6)-C(7)-H(7)	119.9	C(7)-C(8)-C(9)	120.3(3)
C(7)-C(8)-H(8)	119.9	C(9)-C(8)-H(8)	119.9
C(8)-C(9)-C(10)	119.5(3)	C(8)-C(9)-H(9)	120.2
C(10)-C(9)-H(9)	120.2	C(9)-C(10)-C(5)	120.8(3)
C(9)-C(10)-H(10)	119.6	C(5)-C(10)-H(10)	119.6
N(12)-C(11)-P(1)	111.44(19)	N(12)-C(11)-H(11A)	109.3
P(1)-C(11)-H(11A)	109.3	N(12)-C(11)-H(11B)	109.3
P(1)-C(11)-H(11B)	109.3	H(11A)-C(11)-H(11B)	108.0
N(12)-C(13)-P(3)	110.95(19)	N(12)-C(13)-H(13A)	109.4
P(3)-C(13)-H(13A)	109.4	N(12)-C(13)-H(13B)	109.4
P(3)-C(13)-H(13B)	109.4	H(13A)-C(13)-H(13B)	108.0
C(19)-C(14)-C(15)	118.2(3)	C(19)-C(14)-N(12)	123.4(3)
C(15)-C(14)-N(12)	118.3(3)	C(16)-C(15)-C(14)	121.0(3)
C(16)-C(15)-H(15)	119.5	C(14)-C(15)-H(15)	119.5
C(15)-C(16)-C(17)	120.3(3)	C(15)-C(16)-H(16)	119.9
C(17)-C(16)-H(16)	119.9	C(18)-C(17)-O(2)	124.9(3)
C(18)-C(17)-C(16)	119.5(3)	O(2)-C(17)-C(16)	115.5(3)
C(17)-C(18)-C(19)	120.2(3)	C(17)-C(18)-H(18)	119.9
C(19)-C(18)-H(18)	119.9	C(14)-C(19)-C(18)	120.7(3)
C(14)-C(19)-H(19)	119.6	C(18)-C(19)-H(19)	119.6
C(26)-C(20)-C(21)	117.3(3)	C(26)-C(20)-N(1)	122.8(3)
C(21)-C(20)-N(1)	119.8(3)	C(22)-C(21)-C(20)	121.4(3)
C(22)-C(21)-H(21)	119.3	C(20)-C(21)-H(21)	119.3
C(23)-C(22)-C(21)	120.2(3)	C(23)-C(22)-H(22)	119.9
C(21)-C(22)-H(22)	119.9	O(1)-C(23)-C(22)	125.0(3)
O(1)-C(23)-C(25)	116.1(3)	C(22)-C(23)-C(25)	118.8(3)
O(1)-C(24)-H(24A)	109.5	O(1)-C(24)-H(24B)	109.5
H(24A)-C(24)-H(24B)	109.5	O(1)-C(24)-H(24C)	109.5
H(24A)-C(24)-H(24C)	109.5	H(24B)-C(24)-H(24C)	109.5
C(26)-C(25)-C(23)	121.1(3)	C(26)-C(25)-H(25)	119.5
C(23)-C(25)-H(25)	119.5	C(25)-C(26)-C(20)	121.2(3)
C(25)-C(26)-H(26)	119.4	C(20)-C(26)-H(26)	119.4
C(28)-C(27)-C(31)	118.7(3)	C(28)-C(27)-P(3)	120.2(2)

Table 3-12. (cont'd)

C(31)-C(27)-P(3)	121.1(2)	C(29)-C(28)-C(27)	120.3(3)
C(29)-C(28)-H(28)	119.9	C(27)-C(28)-H(28)	119.9
C(30)-C(29)-C(28)	120.2(3)	C(30)-C(29)-H(29)	119.9
C(28)-C(29)-H(29)	119.9	C(1B)-C(30)-C(29)	120.2(3)
C(1B)-C(30)-H(30)	119.9	C(29)-C(30)-H(30)	119.9
C(1B)-C(31)-C(27)	120.9(3)	C(1B)-C(31)-H(31)	119.5
C(27)-C(31)-H(31)	119.5	N(2)-C(32)-P(2)	112.22(19)
N(2)-C(32)-H(32A)	109.2	P(2)-C(32)-H(32A)	109.2
N(2)-C(32)-H(32B)	109.2	P(2)-C(32)-H(32B)	109.2
H(32A)-C(32)-H(32B)	107.9	N(2)-C(33)-P(4)	115.88(19)
N(2)-C(33)-H(33A)	108.3	P(4)-C(33)-H(33A)	108.3
N(2)-C(33)-H(33B)	108.3	P(4)-C(33)-H(33B)	108.3
H(33A)-C(33)-H(33B)	107.4	C(35)-C(34)-C(40)	116.7(3)
C(35)-C(34)-N(2)	121.6(3)	C(40)-C(34)-N(2)	121.3(3)
C(36)-C(35)-C(34)	122.1(3)	C(36)-C(35)-H(35)	118.9
C(34)-C(35)-H(35)	118.9	C(37)-C(36)-C(35)	120.1(3)
C(37)-C(36)-H(36)	119.9	C(35)-C(36)-H(36)	119.9
O(3)-C(37)-C(39)	116.5(3)	O(3)-C(37)-C(36)	124.8(3)
C(39)-C(37)-C(36)	118.6(3)	O(3)-C(38)-H(38A)	109.5
O(3)-C(38)-H(38B)	109.5	H(38A)-C(38)-H(38B)	109.5
O(3)-C(38)-H(38C)	109.5	H(38A)-C(38)-H(38C)	109.5
H(38B)-C(38)-H(38C)	109.5	C(37)-C(39)-C(40)	121.5(3)
C(37)-C(39)-H(39)	119.2	C(40)-C(39)-H(39)	119.2
C(39)-C(40)-C(34)	120.8(3)	C(39)-C(40)-H(40)	119.6
C(34)-C(40)-H(40)	119.6	N(42)-C(41)-P(2)	111.60(19)
N(42)-C(41)-H(41A)	109.3	P(2)-C(41)-H(41A)	109.3
N(42)-C(41)-H(41B)	109.3	P(2)-C(41)-H(41B)	109.3
H(41A)-C(41)-H(41B)	108.0	C(49)-C(43)-C(44)	118.0(3)
C(49)-C(43)-N(42)	123.5(3)	C(44)-C(43)-N(42)	118.4(3)
C(45)-C(44)-C(43)	121.3(3)	C(45)-C(44)-H(44)	119.4
C(43)-C(44)-H(44)	119.4	C(44)-C(45)-C(46)	120.0(3)
C(44)-C(45)-H(45)	120.0	C(46)-C(45)-H(45)	120.0
O(5)-C(46)-C(48)	124.9(3)	O(5)-C(46)-C(45)	115.7(3)
C(48)-C(46)-C(45)	119.4(3)	O(5)-C(47)-H(47A)	109.5
O(5)-C(47)-H(47B)	109.5	H(47A)-C(47)-H(47B)	109.5
O(5)-C(47)-H(47C)	109.5	H(47A)-C(47)-H(47C)	109.5
H(47B)-C(47)-H(47C)	109.5	C(46)-C(48)-C(49)	119.8(3)
C(46)-C(48)-H(48)	120.1	C(49)-C(48)-H(48)	120.1

Table 3-12. (cont'd)

C(43)-C(49)-C(48)	121.5(3)	C(43)-C(49)-H(49)	119.3
C(48)-C(49)-H(49)	119.3	C(55)-C(50)-C(51)	118.6(3)
C(55)-C(50)-P(2)	118.1(2)	C(51)-C(50)-P(2)	123.3(2)
C(52)-C(51)-C(50)	120.6(3)	C(52)-C(51)-H(51)	119.7
C(50)-C(51)-H(51)	119.7	C(53)-C(52)-C(51)	120.0(3)
C(53)-C(52)-H(52)	120.0	C(51)-C(52)-H(52)	120.0
C(54)-C(53)-C(52)	120.2(3)	C(54)-C(53)-H(53)	119.9
C(52)-C(53)-H(53)	119.9	C(53)-C(54)-C(55)	119.7(3)
C(53)-C(54)-H(54)	120.1	C(55)-C(54)-H(54)	120.1
C(54)-C(55)-C(50)	120.9(3)	C(54)-C(55)-H(55)	119.6
C(50)-C(55)-H(55)	119.6	C(61)-C(56)-C(57)	117.9(3)
C(61)-C(56)-P(4)	124.0(2)	C(57)-C(56)-P(4)	118.1(2)
C(58)-C(57)-C(56)	121.2(3)	C(58)-C(57)-H(57)	119.4
C(56)-C(57)-H(57)	119.4	C(59)-C(58)-C(57)	120.1(3)
C(59)-C(58)-H(58)	119.9	C(57)-C(58)-H(58)	119.9
C(60)-C(59)-C(58)	119.3(3)	C(60)-C(59)-H(59)	120.3
C(58)-C(59)-H(59)	120.3	C(59)-C(60)-C(61)	120.8(3)
C(59)-C(60)-H(60)	119.6	C(61)-C(60)-H(60)	119.6
C(60)-C(61)-C(56)	120.7(3)	C(60)-C(61)-H(61)	119.7
C(56)-C(61)-H(61)	119.7	F(63)-B(2)-F(64)	112.7(4)
F(63)-B(2)-F(6)	108.9(3)	F(64)-B(2)-F(6)	109.9(3)
F(63)-B(2)-F(62)	108.6(3)	F(64)-B(2)-F(62)	107.7(3)
F(6)-B(2)-F(62)	108.8(3)	N(65)-C(66)-C(67)	178.2(4)
C(66)-C(67)-H(67A)	109.5	C(66)-C(67)-H(67B)	109.5
H(67A)-C(67)-H(67B)	109.5	C(66)-C(67)-H(67C)	109.5
H(67A)-C(67)-H(67C)	109.5	H(67B)-C(67)-H(67C)	109.5

3.6.4 Crystal data for $Rh(P^{Cy}{}_2N^{Ph}{}_2)_2BF_4$ (4)

The data were consistent with the monoclinic space group P21/n with Z = 4 and Z' = 1. All hydrogen atoms were included into the model at geometrically calculated positions and refined using a riding model and all non-hydrogen atoms were refined anisotropically. The goodness of fit on F^2 was 1.030 with R1(wR2) = 0.0955 (0.1378) for [I>2sigma(I)] and with a largest difference peak and hole of 0.1539 and -0.695(e.Å-3).

Table 3-13. Crystal data and structure refinement for $Rh(P^{Cy}{}_2N^{Ph}{}_2)_2BF_4$ (**4**)

Identification code	alyssia07_0m	
Empirical formula	C56 H80 B F4 N4 P4 Rh	
Formula weight	1122.84	
Temperature	100(2) K	
Wavelength	0.71073 Å	
Crystal system	Monoclinic	
Space group	$P2_1/n$	
Unit cell dimensions	a = 10.0583(10) Å	α = 90°.
	b = 23.787(3) Å	β = 93.350(2)°.
	c = 23.004(2) Å	γ = 90°.
Volume	5494.4(10) $Å^3$	
Z	4	
Density (calculated)	1.357 Mg/m^3	
Absorption coefficient	0.482 mm^{-1}	
F(000)	2360	
Crystal size	0.4 x 0.2 x 0.2 mm^3	
Theta range for data collection	1.23 to 28.32°.	
Index ranges	-13<=h<=12, -31<=k<=29, -30<=l<=29	
Reflections collected	37318	
Independent reflections	12462 [R(int) = 0.0685]	
Completeness to theta = 25.00°	99.7 %	
Absorption correction	Semi-empirical from equivalents	
Max. and min. transmission	0.9098 and 0.8307	
Refinement method	Full-matrix least-squares on F^2	
Data / restraints / parameters	12462 / 0 / 631	
Goodness-of-fit on F^2	1.031	
Final R indices [I>2sigma(I)]	R1 = 0.0577, wR2 = 0.1167	
R indices (all data)	R1 = 0.0955, wR2 = 0.1378	
Extinction coefficient	not measured	
Largest diff. peak and hole	1.539 and -0.655 e.$Å^{-3}$	

Table 3-14. Bond lengths [Å] and angles [°] for $Rh(P^{Cy}{}_2N^{Ph}{}_2)_2BF_4$ (**4**)

Rh(1)-P(1)	2.2908(9)	Rh(1)-P(3)	2.2927(11)
Rh(1)-P(2)	2.2931(11)	Rh(1)-P(4)	2.3166(10)
P(1)-C(9)	1.852(4)	P(1)-C(3)	1.861(4)
P(1)-C(1)	1.867(4)	P(2)-C(2)	1.852(4)
P(2)-C(21)	1.864(4)	P(2)-C(4)	1.886(4)
P(3)-C(45)	1.843(4)	P(3)-C(8)	1.854(4)
P(3)-C(6)	1.872(4)	P(4)-C(33)	1.859(4)
P(4)-C(7)	1.871(4)	P(4)-C(5)	1.888(4)
N(1)-C(15)	1.434(5)	N(1)-C(1)	1.452(5)
N(1)-C(2)	1.465(5)	N(2)-C(27)	1.401(5)
N(2)-C(4)	1.445(5)	N(2)-C(3)	1.458(5)
N(3)-C(39)	1.407(5)	N(3)-C(5)	1.446(5)
N(3)-C(6)	1.454(5)	N(4)-C(51)	1.440(5)
N(4)-C(7)	1.451(5)	N(4)-C(8)	1.467(4)
C(1)-H(1A)	0.9900	C(1)-H(1B)	0.9900
C(2)-H(2A)	0.9900	C(2)-H(2B)	0.9900
C(3)-H(3A)	0.9900	C(3)-H(3B)	0.9900
C(4)-H(4A)	0.9900	C(4)-H(4B)	0.9900
C(5)-H(5A)	0.9900	C(5)-H(5B)	0.9900
C(6)-H(6A)	0.9900	C(6)-H(6B)	0.9900
C(7)-H(7A)	0.9900	C(7)-H(7B)	0.9900
C(8)-H(8A)	0.9900	C(8)-H(8B)	0.9900
C(9)-C(10)	1.529(5)	C(9)-C(14)	1.533(5)
C(9)-H(9)	1.0000	C(10)-C(11)	1.519(6)
C(10)-H(10A)	0.9900	C(10)-H(10B)	0.9900
C(11)-C(12)	1.531(6)	C(11)-H(11A)	0.9900
C(11)-H(11B)	0.9900	C(12)-C(13)	1.531(6)
C(12)-H(12A)	0.9900	C(12)-H(12B)	0.9900
C(13)-C(14)	1.526(6)	C(13)-H(13A)	0.9900
C(13)-H(13B)	0.9900	C(14)-H(14A)	0.9900
C(14)-H(14B)	0.9900	C(15)-C(16)	1.392(6)
C(15)-C(20)	1.401(6)	C(16)-C(17)	1.399(6)
C(16)-H(16)	0.9500	C(17)-C(18)	1.371(7)

Table 3-14. (cont'd)

C(17)-H(17)	0.9500	C(18)-C(19)	1.389(7)
C(18)-H(18)	0.9500	C(19)-C(20)	1.386(6)
C(19)-H(19)	0.9500	C(20)-H(20)	0.9500
C(21)-C(26)	1.530(5)	C(21)-C(22)	1.536(5)
C(21)-H(21)	1.0000	C(22)-C(23)	1.531(5)
C(22)-H(22A)	0.9900	C(22)-H(22B)	0.9900
C(23)-C(24)	1.525(6)	C(23)-H(23A)	0.9900
C(23)-H(23B)	0.9900	C(24)-C(25)	1.523(6)
C(24)-H(24A)	0.9900	C(24)-H(24B)	0.9900
C(25)-C(26)	1.523(5)	C(25)-H(25A)	0.9900
C(25)-H(25B)	0.9900	C(26)-H(26A)	0.9900
C(26)-H(26B)	0.9900	C(27)-C(28)	1.391(5)
C(27)-C(32)	1.408(5)	C(28)-C(29)	1.400(6)
C(28)-H(28)	0.9500	C(29)-C(30)	1.380(6)
C(29)-H(29)	0.9500	C(30)-C(31)	1.387(6)
C(30)-H(30)	0.9500	C(31)-C(32)	1.387(6)
C(31)-H(31)	0.9500	C(32)-H(32)	0.9500
C(33)-C(38)	1.540(5)	C(33)-C(34)	1.543(5)
C(33)-H(33)	1.0000	C(34)-C(35)	1.526(5)
C(34)-H(34A)	0.9900	C(34)-H(34B)	0.9900
C(35)-C(36)	1.525(5)	C(35)-H(35A)	0.9900
C(35)-H(35B)	0.9900	C(36)-C(37)	1.521(6)
C(36)-H(36A)	0.9900	C(36)-H(36B)	0.9900
C(37)-C(38)	1.523(5)	C(37)-H(37A)	0.9900
C(37)-H(37B)	0.9900	C(38)-H(38A)	0.9900
C(38)-H(38B)	0.9900	C(39)-C(44)	1.396(5)
C(39)-C(40)	1.399(6)	C(40)-C(41)	1.388(6)
C(40)-H(40)	0.9500	C(41)-C(42)	1.388(6)
C(41)-H(41)	0.9500	C(42)-C(43)	1.397(7)
C(42)-H(42)	0.9500	C(43)-C(44)	1.389(6)
C(43)-H(43)	0.9500	C(44)-H(44)	0.9500
C(45)-C(50)	1.529(5)	C(45)-C(46)	1.545(6)
C(45)-H(45)	1.0000	C(46)-C(47)	1.527(6)

Table 3-14. (cont'd)

C(46)-H(46A)	0.9900	C(46)-H(46B)	0.9900
C(47)-C(48)	1.524(7)	C(47)-H(47A)	0.9900
C(47)-H(47B)	0.9900	C(48)-C(49)	1.516(7)
C(48)-H(48A)	0.9900	C(48)-H(48B)	0.9900
C(49)-C(50)	1.533(6)	C(49)-H(49A)	0.9900
C(49)-H(49B)	0.9900	C(50)-H(50A)	0.9900
C(50)-H(50B)	0.9900	C(51)-C(52)	1.384(6)
C(51)-C(56)	1.386(6)	C(52)-C(53)	1.390(6)
C(52)-H(52)	0.9500	C(53)-C(54)	1.387(7)
C(53)-H(53)	0.9500	C(54)-C(55)	1.371(7)
C(54)-H(54)	0.9500	C(55)-C(56)	1.391(6)
C(55)-H(55)	0.9500	C(56)-H(56)	0.9500
F(1)-B(1)	1.381(6)	F(2)-B(1)	1.437(7)
F(3)-B(1)	1.380(5)	F(4)-B(1)	1.362(6)
P(1)-Rh(1)-P(3)	99.82(4)	P(1)-Rh(1)-P(2)	80.70(4)
P(3)-Rh(1)-P(2)	164.83(4)	P(1)-Rh(1)-P(4)	164.71(4)
P(3)-Rh(1)-P(4)	80.69(4)	P(2)-Rh(1)-P(4)	102.83(4)
C(9)-P(1)-C(3)	102.48(17)	C(9)-P(1)-C(1)	100.01(18)
C(3)-P(1)-C(1)	102.52(18)	C(9)-P(1)-Rh(1)	124.67(12)
C(3)-P(1)-Rh(1)	116.72(13)	C(1)-P(1)-Rh(1)	107.23(12)
C(2)-P(2)-C(21)	101.72(18)	C(2)-P(2)-C(4)	101.09(18)
C(21)-P(2)-C(4)	101.05(18)	C(2)-P(2)-Rh(1)	113.27(14)
C(21)-P(2)-Rh(1)	124.71(12)	C(4)-P(2)-Rh(1)	111.90(13)
C(45)-P(3)-C(8)	99.30(18)	C(45)-P(3)-C(6)	102.82(18)
C(8)-P(3)-C(6)	104.44(17)	C(45)-P(3)-Rh(1)	126.18(13)
C(8)-P(3)-Rh(1)	105.75(14)	C(6)-P(3)-Rh(1)	115.40(13)
C(33)-P(4)-C(7)	101.95(17)	C(33)-P(4)-C(5)	100.87(18)
C(7)-P(4)-C(5)	101.27(18)	C(33)-P(4)-Rh(1)	124.88(13)
C(7)-P(4)-Rh(1)	115.01(12)	C(5)-P(4)-Rh(1)	109.66(11)
C(15)-N(1)-C(1)	114.8(3)	C(15)-N(1)-C(2)	114.5(3)
C(1)-N(1)-C(2)	115.0(3)	C(27)-N(2)-C(4)	119.7(3)
C(27)-N(2)-C(3)	117.9(3)	C(4)-N(2)-C(3)	115.3(3)
C(39)-N(3)-C(5)	120.2(3)	C(39)-N(3)-C(6)	119.5(3)

Table 3-14. (cont'd)

C(5)-N(3)-C(6)	114.3(3)	C(51)-N(4)-C(7)	116.8(3)
C(51)-N(4)-C(8)	110.8(3)	C(7)-N(4)-C(8)	113.3(3)
N(1)-C(1)-P(1)	112.7(3)	N(1)-C(1)-H(1A)	109.1
P(1)-C(1)-H(1A)	109.1	N(1)-C(1)-H(1B)	109.1
P(1)-C(1)-H(1B)	109.1	H(1A)-C(1)-H(1B)	107.8
N(1)-C(2)-P(2)	113.0(3)	N(1)-C(2)-H(2A)	109.0
P(2)-C(2)-H(2A)	109.0	N(1)-C(2)-H(2B)	109.0
P(2)-C(2)-H(2B)	109.0	H(2A)-C(2)-H(2B)	107.8
N(2)-C(3)-P(1)	113.1(2)	N(2)-C(3)-H(3A)	109.0
P(1)-C(3)-H(3A)	109.0	N(2)-C(3)-H(3B)	109.0
P(1)-C(3)-H(3B)	109.0	H(3A)-C(3)-H(3B)	107.8
N(2)-C(4)-P(2)	117.6(3)	N(2)-C(4)-H(4A)	107.9
P(2)-C(4)-H(4A)	107.9	N(2)-C(4)-H(4B)	107.9
P(2)-C(4)-H(4B)	107.9	H(4A)-C(4)-H(4B)	107.2
N(3)-C(5)-P(4)	117.7(2)	N(3)-C(5)-H(5A)	107.9
P(4)-C(5)-H(5A)	107.9	N(3)-C(5)-H(5B)	107.9
P(4)-C(5)-H(5B)	107.9	H(5A)-C(5)-H(5B)	107.2
N(3)-C(6)-P(3)	111.8(3)	N(3)-C(6)-H(6A)	109.2
P(3)-C(6)-H(6A)	109.2	N(3)-C(6)-H(6B)	109.2
P(3)-C(6)-H(6B)	109.2	H(6A)-C(6)-H(6B)	107.9
N(4)-C(7)-P(4)	110.3(3)	N(4)-C(7)-H(7A)	109.6
P(4)-C(7)-H(7A)	109.6	N(4)-C(7)-H(7B)	109.6
P(4)-C(7)-H(7B)	109.6	H(7A)-C(7)-H(7B)	108.1
N(4)-C(8)-P(3)	112.8(3)	N(4)-C(8)-H(8A)	109.0
P(3)-C(8)-H(8A)	109.0	N(4)-C(8)-H(8B)	109.0
P(3)-C(8)-H(8B)	109.0	H(8A)-C(8)-H(8B)	107.8
C(10)-C(9)-C(14)	110.7(3)	C(10)-C(9)-P(1)	109.9(3)
C(14)-C(9)-P(1)	115.8(3)	C(10)-C(9)-H(9)	106.7
C(14)-C(9)-H(9)	106.7	P(1)-C(9)-H(9)	106.7
C(11)-C(10)-C(9)	112.1(3)	C(11)-C(10)-H(10A)	109.2
C(9)-C(10)-H(10A)	109.2	C(11)-C(10)-H(10B)	109.2
C(9)-C(10)-H(10B)	109.2	H(10A)-C(10)-H(10B)	107.9
C(10)-C(11)-C(12)	111.7(4)	C(10)-C(11)-H(11A)	109.3

Table 3-14. (cont'd)

C(12)-C(11)-H(11A)	109.3	C(10)-C(11)-H(11B)	109.3
C(12)-C(11)-H(11B)	109.3	H(11A)-C(11)-H(11B)	107.9
C(13)-C(12)-C(11)	110.5(3)	C(13)-C(12)-H(12A)	109.5
C(11)-C(12)-H(12A)	109.5	C(13)-C(12)-H(12B)	109.5
C(11)-C(12)-H(12B)	109.5	H(12A)-C(12)-H(12B)	108.1
C(14)-C(13)-C(12)	111.3(3)	C(14)-C(13)-H(13A)	109.4
C(12)-C(13)-H(13A)	109.4	C(14)-C(13)-H(13B)	109.4
C(12)-C(13)-H(13B)	109.4	H(13A)-C(13)-H(13B)	108.0
C(13)-C(14)-C(9)	110.4(3)	C(13)-C(14)-H(14A)	109.6
C(9)-C(14)-H(14A)	109.6	C(13)-C(14)-H(14B)	109.6
C(9)-C(14)-H(14B)	109.6	H(14A)-C(14)-H(14B)	108.1
C(16)-C(15)-C(20)	118.6(4)	C(16)-C(15)-N(1)	122.5(4)
C(20)-C(15)-N(1)	118.9(4)	C(15)-C(16)-C(17)	120.2(4)
C(15)-C(16)-H(16)	119.9	C(17)-C(16)-H(16)	119.9
C(18)-C(17)-C(16)	120.8(5)	C(18)-C(17)-H(17)	119.6
C(16)-C(17)-H(17)	119.6	C(17)-C(18)-C(19)	119.4(4)
C(17)-C(18)-H(18)	120.3	C(19)-C(18)-H(18)	120.3
C(20)-C(19)-C(18)	120.7(5)	C(20)-C(19)-H(19)	119.7
C(18)-C(19)-H(19)	119.7	C(19)-C(20)-C(15)	120.3(5)
C(19)-C(20)-H(20)	119.8	C(15)-C(20)-H(20)	119.8
C(26)-C(21)-C(22)	109.1(3)	C(26)-C(21)-P(2)	111.5(3)
C(22)-C(21)-P(2)	116.0(2)	C(26)-C(21)-H(21)	106.6
C(22)-C(21)-H(21)	106.6	P(2)-C(21)-H(21)	106.6
C(23)-C(22)-C(21)	111.1(3)	C(23)-C(22)-H(22A)	109.4
C(21)-C(22)-H(22A)	109.4	C(23)-C(22)-H(22B)	109.4
C(21)-C(22)-H(22B)	109.4	H(22A)-C(22)-H(22B)	108.0
C(24)-C(23)-C(22)	112.5(4)	C(24)-C(23)-H(23A)	109.1
C(22)-C(23)-H(23A)	109.1	C(24)-C(23)-H(23B)	109.1
C(22)-C(23)-H(23B)	109.1	H(23A)-C(23)-H(23B)	107.8
C(25)-C(24)-C(23)	110.7(4)	C(25)-C(24)-H(24A)	109.5
C(23)-C(24)-H(24A)	109.5	C(25)-C(24)-H(24B)	109.5
C(23)-C(24)-H(24B)	109.5	H(24A)-C(24)-H(24B)	108.1
C(24)-C(25)-C(26)	110.9(3)	C(24)-C(25)-H(25A)	109.5

Table 3-14. (cont'd)

C(26)-C(25)-H(25A)	109.5	C(24)-C(25)-H(25B)	109.5
C(26)-C(25)-H(25B)	109.5	H(25A)-C(25)-H(25B)	108.1
C(25)-C(26)-C(21)	111.4(3)	C(25)-C(26)-H(26A)	109.4
C(21)-C(26)-H(26A)	109.4	C(25)-C(26)-H(26B)	109.4
C(21)-C(26)-H(26B)	109.4	H(26A)-C(26)-H(26B)	108.0
C(28)-C(27)-N(2)	122.9(4)	C(28)-C(27)-C(32)	117.9(4)
N(2)-C(27)-C(32)	119.0(3)	C(27)-C(28)-C(29)	120.7(4)
C(27)-C(28)-H(28)	119.7	C(29)-C(28)-H(28)	119.7
C(30)-C(29)-C(28)	121.0(4)	C(30)-C(29)-H(29)	119.5
C(28)-C(29)-H(29)	119.5	C(29)-C(30)-C(31)	118.5(4)
C(29)-C(30)-H(30)	120.8	C(31)-C(30)-H(30)	120.8
C(32)-C(31)-C(30)	121.3(4)	C(32)-C(31)-H(31)	119.3
C(30)-C(31)-H(31)	119.3	C(31)-C(32)-C(27)	120.5(4)
C(31)-C(32)-H(32)	119.7	C(27)-C(32)-H(32)	119.7
C(38)-C(33)-C(34)	108.7(3)	C(38)-C(33)-P(4)	115.1(3)
C(34)-C(33)-P(4)	112.0(2)	C(38)-C(33)-H(33)	106.9
C(34)-C(33)-H(33)	106.9	P(4)-C(33)-H(33)	106.9
C(35)-C(34)-C(33)	110.2(3)	C(35)-C(34)-H(34A)	109.6
C(33)-C(34)-H(34A)	109.6	C(35)-C(34)-H(34B)	109.6
C(33)-C(34)-H(34B)	109.6	H(34A)-C(34)-H(34B)	108.1
C(36)-C(35)-C(34)	110.0(3)	C(36)-C(35)-H(35A)	109.7
C(34)-C(35)-H(35A)	109.7	C(36)-C(35)-H(35B)	109.7
C(34)-C(35)-H(35B)	109.7	H(35A)-C(35)-H(35B)	108.2
C(37)-C(36)-C(35)	111.5(3)	C(37)-C(36)-H(36A)	109.3
C(35)-C(36)-H(36A)	109.3	C(37)-C(36)-H(36B)	109.3
C(35)-C(36)-H(36B)	109.3	H(36A)-C(36)-H(36B)	108.0
C(36)-C(37)-C(38)	112.0(3)	C(36)-C(37)-H(37A)	109.2
C(38)-C(37)-H(37A)	109.2	C(36)-C(37)-H(37B)	109.2
C(38)-C(37)-H(37B)	109.2	H(37A)-C(37)-H(37B)	107.9
C(37)-C(38)-C(33)	110.6(3)	C(37)-C(38)-H(38A)	109.5
C(33)-C(38)-H(38A)	109.5	C(37)-C(38)-H(38B)	109.5
C(33)-C(38)-H(38B)	109.5	H(38A)-C(38)-H(38B)	108.1
C(44)-C(39)-C(40)	118.2(4)	C(44)-C(39)-N(3)	119.4(4)

Table 3-14. (cont'd)

C(40)-C(39)-N(3)	122.4(4)	C(41)-C(40)-C(39)	120.9(4)
C(41)-C(40)-H(40)	119.6	C(39)-C(40)-H(40)	119.6
C(40)-C(41)-C(42)	121.0(4)	C(40)-C(41)-H(41)	119.5
C(42)-C(41)-H(41)	119.5	C(41)-C(42)-C(43)	118.3(4)
C(41)-C(42)-H(42)	120.9	C(43)-C(42)-H(42)	120.9
C(44)-C(43)-C(42)	121.0(4)	C(44)-C(43)-H(43)	119.5
C(42)-C(43)-H(43)	119.5	C(43)-C(44)-C(39)	120.6(4)
C(43)-C(44)-H(44)	119.7	C(39)-C(44)-H(44)	119.7
C(50)-C(45)-C(46)	111.3(3)	C(50)-C(45)-P(3)	110.1(3)
C(46)-C(45)-P(3)	113.5(3)	C(50)-C(45)-H(45)	107.2
C(46)-C(45)-H(45)	107.2	P(3)-C(45)-H(45)	107.2
C(47)-C(46)-C(45)	110.1(3)	C(47)-C(46)-H(46A)	109.6
C(45)-C(46)-H(46A)	109.6	C(47)-C(46)-H(46B)	109.6
C(45)-C(46)-H(46B)	109.6	H(46A)-C(46)-H(46B)	108.2
C(48)-C(47)-C(46)	111.1(4)	C(48)-C(47)-H(47A)	109.4
C(46)-C(47)-H(47A)	109.4	C(48)-C(47)-H(47B)	109.4
C(46)-C(47)-H(47B)	109.4	H(47A)-C(47)-H(47B)	108.0
C(49)-C(48)-C(47)	111.7(4)	C(49)-C(48)-H(48A)	109.3
C(47)-C(48)-H(48A)	109.3	C(49)-C(48)-H(48B)	109.3
C(47)-C(48)-H(48B)	109.3	H(48A)-C(48)-H(48B)	107.9
C(48)-C(49)-C(50)	110.4(4)	C(48)-C(49)-H(49A)	109.6
C(50)-C(49)-H(49A)	109.6	C(48)-C(49)-H(49B)	109.6
C(50)-C(49)-H(49B)	109.6	H(49A)-C(49)-H(49B)	108.1
C(45)-C(50)-C(49)	111.0(4)	C(45)-C(50)-H(50A)	109.4
C(49)-C(50)-H(50A)	109.4	C(45)-C(50)-H(50B)	109.4
C(49)-C(50)-H(50B)	109.4	H(50A)-C(50)-H(50B)	108.0
C(52)-C(51)-C(56)	119.6(4)	C(52)-C(51)-N(4)	116.8(4)
C(56)-C(51)-N(4)	123.5(4)	C(51)-C(52)-C(53)	120.3(4)
C(51)-C(52)-H(52)	119.9	C(53)-C(52)-H(52)	119.9
C(54)-C(53)-C(52)	119.8(5)	C(54)-C(53)-H(53)	120.1
C(52)-C(53)-H(53)	120.1	C(55)-C(54)-C(53)	119.9(4)
C(55)-C(54)-H(54)	120.1	C(53)-C(54)-H(54)	120.1
C(54)-C(55)-C(56)	120.6(4)	C(54)-C(55)-H(55)	119.7

Table 3-14. (cont'd)

C(56)-C(55)-H(55)	119.7	C(51)-C(56)-C(55)	119.8(4)
C(51)-C(56)-H(56)	120.1	C(55)-C(56)-H(56)	120.1
F(4)-B(1)-F(3)	112.5(4)	F(4)-B(1)-F(1)	113.7(4)
F(3)-B(1)-F(1)	111.3(4)	F(4)-B(1)-F(2)	105.5(4)
F(3)-B(1)-F(2)	107.3(4)	F(1)-B(1)-F(2)	106.0(4)

3.6.5 Crystal data for $Rh(P^{Cy}{}_2N^{PhOMe}{}_2)_2BF_4$ (5)

The data were consistent with the monoclinic space group *C*2/*c* with half a molecule in the asymmetric unit, $Z' = 0.5$ and $Z = 4$. The asymmetric unit also contains an uncoordinated acetonitrile ligand and half a tetrafluoroborate anion. All hydrogen atoms were included into the model at geometrically calculated positions and refined using a riding model. The goodness of fit on F^2 was 1.027 with R1(wR2) = 0.0543 (0.0867) for [I>2sigma(I)] and with a largest difference peak and hole of 0.853 and -0.625(e.Å-3).

Table 3-15. Crystal data and structure refinement for $Rh(P^{Cy}{}_2N^{PhOMe}{}_2)_2BF_4$ (**4**)

Identification code	P15037	
Empirical formula	C64 H94 B F4 N6 O4 P4 Rh	
Formula weight	1325.05	
Temperature	100(2) K	
Wavelength	0.71073 Å	
Crystal system	Monoclinic	
Space group	C2/c	
Unit cell dimensions	a = 22.7509(9) Å	α = 90°.
	b = 13.4975(6) Å	β =109.6649(15)°.
	c = 22.3982(9) Å	γ = 90°.
Volume	6476.9(5) $Å^3$	
Z	4	
Density (calculated)	1.359 Mg/m^3	
Absorption coefficient	0.425 mm^{-1}	
F(000)	2792	
Crystal size	0.2 x 0.1 x 0.1 mm^3	
Theta range for data collection	2.207 to 36.394°.	
Index ranges	-37<=h<=37, -22<=k<=22, -37<=l<=37	
Reflections collected	93916	
Independent reflections	15651 [R(int) = 0.0944]	
Completeness to theta = 25.00°	99.9 %	
Absorption correction	Semi-empirical from equivalents	
Max. and min. transmission	0.7471 and 0.7036	
Refinement method	Full-matrix least-squares on F^2	
Data / restraints / parameters	15651 / 0 / 383	
Goodness-of-fit on F^2	1.027	
Final R indices [I>2sigma(I)]	R1 = 0.0543, wR2 = 0.0867	
R indices (all data)	R1 = 0.1046, wR2 = 0.0984	
Extinction coefficient	not measured	
Largest diff. peak and hole	0.853 and -0.625 e.$Å^{-3}$	

Table 3-16. Bond lengths [Å] and angles [°] for $Rh(P^{Cy}{}_2N^{PhOMe}{}_2)_2BF_4$ (**4**)

Rh(1)-P(1)#1	2.2781(4)	Rh(1)-P(1)	2.2782(4)
Rh(1)-P(3)	2.2828(4)	Rh(1)-P(3)#1	2.2829(4)
P(1)-C(11)	1.8526(16)	P(1)-C(1)	1.8817(16)
P(1)-C(2)#1	1.8889(16)	C(11)-C(16)	1.532(2)
C(11)-C(12)	1.540(2)	C(11)-H(11)	1.0000
C(12)-C(13)	1.531(2)	C(12)-H(12A)	0.9900
C(12)-H(12B)	0.9900	C(13)-C(14)	1.535(3)
C(13)-H(13A)	0.9900	C(13)-H(13B)	0.9900
C(14)-C(15)	1.526(3)	C(14)-H(14A)	0.9900
C(14)-H(14B)	0.9900	C(15)-C(16)	1.534(2)
C(15)-H(15A)	0.9900	C(15)-H(15B)	0.9900
C(16)-H(16A)	0.9900	C(16)-H(16B)	0.9900
C(1)-N(1)	1.450(2)	C(1)-H(1A)	0.9900
C(1)-H(1B)	0.9900	N(1)-C(21)	1.425(2)
N(1)-C(2)	1.456(2)	C(21)-C(22)	1.391(2)
C(21)-C(26)	1.402(2)	C(22)-C(23)	1.400(2)
C(22)-H(22)	0.9500	C(23)-C(24)	1.389(2)
C(23)-H(23)	0.9500	C(24)-O(1)	1.381(2)
C(24)-C(25)	1.392(2)	O(1)-C(27)	1.424(2)
C(27)-H(27A)	0.9800	C(27)-H(27B)	0.9800
C(27)-H(27C)	0.9800	C(25)-C(26)	1.385(2)
C(25)-H(25)	0.9500	C(26)-H(26)	0.9500
C(2)-P(1)#1	1.8889(16)	C(2)-H(2A)	0.9900
C(2)-H(2B)	0.9900	P(3)-C(31)	1.8528(15)
P(3)-C(5)	1.8593(16)	P(3)-C(6)#1	1.8630(16)
C(31)-C(32)	1.526(2)	C(31)-C(36)	1.541(2)
C(31)-H(31)	1.0000	C(32)-C(33)	1.531(2)
C(32)-H(32A)	0.9900	C(32)-H(32B)	0.9900
C(33)-C(34)	1.531(2)	C(33)-H(33A)	0.9900
C(33)-H(33B)	0.9900	C(34)-C(35)	1.523(3)
C(34)-H(34A)	0.9900	C(34)-H(34B)	0.9900
C(35)-C(36)	1.532(2)	C(35)-H(35A)	0.9900
C(35)-H(35B)	0.9900	C(36)-H(36A)	0.9900

Table 3-16. (cont'd)

C(36)-H(36B)	0.9900	C(5)-N(3)	1.467(2)
C(5)-H(5A)	0.9900	C(5)-H(5B)	0.9900
N(3)-C(41)	1.427(2)	N(3)-C(6)	1.460(2)
C(41)-C(46)	1.387(2)	C(41)-C(42)	1.405(2)
C(42)-C(43)	1.379(2)	C(42)-H(42)	0.9500
C(43)-C(44)	1.393(2)	C(43)-H(43)	0.9500
C(44)-O(3)	1.377(2)	C(44)-C(45)	1.379(2)
O(3)-C(47)	1.421(2)	C(47)-H(47A)	0.9800
C(47)-H(47B)	0.9800	C(47)-H(47C)	0.9800
C(45)-C(46)	1.403(2)	C(45)-H(45)	0.9500
C(46)-H(46)	0.9500	C(6)-P(3)#1	1.8630(16)
C(6)-H(6A)	0.9900	C(6)-H(6B)	0.9900
B(1)-F(2)	1.379(2)	B(1)-F(2)#2	1.379(2)
B(1)-F(1)#2	1.383(2)	B(1)-F(1)	1.383(2)
N(1S)-C(1S)	1.115(3)	C(1S)-C(2S)	1.458(4)
C(2S)-H(2S1)	0.9800	C(2S)-H(2S2)	0.9800
C(2S)-H(2S3)	0.9800	P(1)#1-Rh(1)-P(1)	79.81(2)
P(1)#1-Rh(1)-P(3)	104.161(14)	P(1)-Rh(1)-P(3)	159.494(15)
P(1)#1-Rh(1)-P(3)#1	159.493(15)	P(1)-Rh(1)-P(3)#1	104.160(14)
P(3)-Rh(1)-P(3)#1	79.30(2)	C(11)-P(1)-C(1)	99.33(7)
C(11)-P(1)-C(2)#1	102.84(7)	C(1)-P(1)-C(2)#1	103.27(7)
C(11)-P(1)-Rh(1)	123.70(5)	C(1)-P(1)-Rh(1)	109.70(5)
C(2)#1-P(1)-Rh(1)	115.23(5)	C(16)-C(11)-C(12)	109.42(14)
C(16)-C(11)-P(1)	111.84(11)	C(12)-C(11)-P(1)	114.86(11)
C(16)-C(11)-H(11)	106.7	C(12)-C(11)-H(11)	106.7
P(1)-C(11)-H(11)	106.7	C(13)-C(12)-C(11)	109.82(14)
C(13)-C(12)-H(12A)	109.7	C(11)-C(12)-H(12A)	109.7
C(13)-C(12)-H(12B)	109.7	C(11)-C(12)-H(12B)	109.7
H(12A)-C(12)-H(12B)	108.2	C(12)-C(13)-C(14)	111.03(15)
C(12)-C(13)-H(13A)	109.4	C(14)-C(13)-H(13A)	109.4
C(12)-C(13)-H(13B)	109.4	C(14)-C(13)-H(13B)	109.4
H(13A)-C(13)-H(13B)	108.0	C(15)-C(14)-C(13)	111.78(15)
C(15)-C(14)-H(14A)	109.3	C(13)-C(14)-H(14A)	109.3

Table 3-16. (cont'd)

C(15)-C(14)-H(14B)	109.3	C(13)-C(14)-H(14B)	109.3
H(14A)-C(14)-H(14B)	107.9	C(14)-C(15)-C(16)	110.84(15)
C(14)-C(15)-H(15A)	109.5	C(16)-C(15)-H(15A)	109.5
C(14)-C(15)-H(15B)	109.5	C(16)-C(15)-H(15B)	109.5
H(15A)-C(15)-H(15B)	108.1	C(11)-C(16)-C(15)	110.30(14)
C(11)-C(16)-H(16A)	109.6	C(15)-C(16)-H(16A)	109.6
C(11)-C(16)-H(16B)	109.6	C(15)-C(16)-H(16B)	109.6
H(16A)-C(16)-H(16B)	108.1	N(1)-C(1)-P(1)	119.40(11)
N(1)-C(1)-H(1A)	107.5	P(1)-C(1)-H(1A)	107.5
N(1)-C(1)-H(1B)	107.5	P(1)-C(1)-H(1B)	107.5
H(1A)-C(1)-H(1B)	107.0	C(21)-N(1)-C(1)	118.75(13)
C(21)-N(1)-C(2)	118.04(13)	C(1)-N(1)-C(2)	114.53(13)
C(22)-C(21)-C(26)	118.40(15)	C(22)-C(21)-N(1)	123.34(14)
C(26)-C(21)-N(1)	118.19(14)	C(21)-C(22)-C(23)	121.20(14)
C(21)-C(22)-H(22)	119.4	C(23)-C(22)-H(22)	119.4
C(24)-C(23)-C(22)	119.48(15)	C(24)-C(23)-H(23)	120.3
C(22)-C(23)-H(23)	120.3	O(1)-C(24)-C(23)	124.24(16)
O(1)-C(24)-C(25)	115.95(14)	C(23)-C(24)-C(25)	119.81(15)
C(24)-O(1)-C(27)	116.29(14)	O(1)-C(27)-H(27A)	109.5
O(1)-C(27)-H(27B)	109.5	H(27A)-C(27)-H(27B)	109.5
O(1)-C(27)-H(27C)	109.5	H(27A)-C(27)-H(27C)	109.5
H(27B)-C(27)-H(27C)	109.5	C(26)-C(25)-C(24)	120.38(15)
C(26)-C(25)-H(25)	119.8	C(24)-C(25)-H(25)	119.8
C(25)-C(26)-C(21)	120.67(15)	C(25)-C(26)-H(26)	119.7
C(21)-C(26)-H(26)	119.7	N(1)-C(2)-P(1)#1	113.81(10)
N(1)-C(2)-H(2A)	108.8	P(1)#1-C(2)-H(2A)	108.8
N(1)-C(2)-H(2B)	108.8	P(1)#1-C(2)-H(2B)	108.8
H(2A)-C(2)-H(2B)	107.7	C(31)-P(3)-C(5)	100.74(7)
C(31)-P(3)-C(6)#1	100.19(7)	C(5)-P(3)-C(6)#1	104.16(7)
C(31)-P(3)-Rh(1)	125.10(5)	C(5)-P(3)-Rh(1)	114.07(5)
C(6)#1-P(3)-Rh(1)	110.03(5)	C(32)-C(31)-C(36)	109.35(13)
C(32)-C(31)-P(3)	112.72(11)	C(36)-C(31)-P(3)	114.93(11)
C(32)-C(31)-H(31)	106.4	C(36)-C(31)-H(31)	106.4

Table 3-16. (cont'd)

P(3)-C(31)-H(31)	106.4	C(31)-C(32)-C(33)	110.59(13)
C(31)-C(32)-H(32A)	109.5	C(33)-C(32)-H(32A)	109.5
C(31)-C(32)-H(32B)	109.5	C(33)-C(32)-H(32B)	109.5
H(32A)-C(32)-H(32B)	108.1	C(34)-C(33)-C(32)	109.95(14)
C(34)-C(33)-H(33A)	109.7	C(32)-C(33)-H(33A)	109.7
C(34)-C(33)-H(33B)	109.7	C(32)-C(33)-H(33B)	109.7
H(33A)-C(33)-H(33B)	108.2	C(35)-C(34)-C(33)	111.78(14)
C(35)-C(34)-H(34A)	109.3	C(33)-C(34)-H(34A)	109.3
C(35)-C(34)-H(34B)	109.3	C(33)-C(34)-H(34B)	109.3
H(34A)-C(34)-H(34B)	107.9	C(34)-C(35)-C(36)	111.56(14)
C(34)-C(35)-H(35A)	109.3	C(36)-C(35)-H(35A)	109.3
C(34)-C(35)-H(35B)	109.3	C(36)-C(35)-H(35B)	109.3
H(35A)-C(35)-H(35B)	108.0	C(35)-C(36)-C(31)	109.90(14)
C(35)-C(36)-H(36A)	109.7	C(31)-C(36)-H(36A)	109.7
C(35)-C(36)-H(36B)	109.7	C(31)-C(36)-H(36B)	109.7
H(36A)-C(36)-H(36B)	108.2	N(3)-C(5)-P(3)	111.43(10)
N(3)-C(5)-H(5A)	109.3	P(3)-C(5)-H(5A)	109.3
N(3)-C(5)-H(5B)	109.3	P(3)-C(5)-H(5B)	109.3
H(5A)-C(5)-H(5B)	108.0	C(41)-N(3)-C(6)	115.83(13)
C(41)-N(3)-C(5)	114.65(12)	C(6)-N(3)-C(5)	113.28(13)
C(46)-C(41)-C(42)	117.54(15)	C(46)-C(41)-N(3)	123.87(15)
C(42)-C(41)-N(3)	118.51(14)	C(43)-C(42)-C(41)	121.55(15)
C(43)-C(42)-H(42)	119.2	C(41)-C(42)-H(42)	119.2
C(42)-C(43)-C(44)	120.08(16)	C(42)-C(43)-H(43)	120.0
C(44)-C(43)-H(43)	120.0	O(3)-C(44)-C(45)	125.25(16)
O(3)-C(44)-C(43)	115.23(15)	C(45)-C(44)-C(43)	119.52(16)
C(44)-O(3)-C(47)	116.61(15)	O(3)-C(47)-H(47A)	109.5
O(3)-C(47)-H(47B)	109.5	H(47A)-C(47)-H(47B)	109.5
O(3)-C(47)-H(47C)	109.5	H(47A)-C(47)-H(47C)	109.5
H(47B)-C(47)-H(47C)	109.5	C(44)-C(45)-C(46)	120.08(16)
C(44)-C(45)-H(45)	120.0	C(46)-C(45)-H(45)	120.0
C(41)-C(46)-C(45)	121.22(16)	C(41)-C(46)-H(46)	119.4
C(45)-C(46)-H(46)	119.4	N(3)-C(6)-P(3)#1	113.68(11)

Table 3-16. (cont'd)

N(3)-C(6)-H(6A)	108.8	P(3)#1-C(6)-H(6A)	108.8
N(3)-C(6)-H(6B)	108.8	P(3)#1-C(6)-H(6B)	108.8
H(6A)-C(6)-H(6B)	107.7	F(2)-B(1)-F(2)#2	108.8(3)
F(2)-B(1)-F(1)#2	109.52(10)	F(2)#2-B(1)-F(1)#2	110.02(10)
F(2)-B(1)-F(1)	110.03(10)	F(2)#2-B(1)-F(1)	109.52(10)
F(1)#2-B(1)-F(1)	108.9(2)	N(1S)-C(1S)-C(2S)	177.6(3)
C(1S)-C(2S)-H(2S1)	109.5	C(1S)-C(2S)-H(2S2)	109.5
H(2S1)-C(2S)-H(2S2)	109.5	C(1S)-C(2S)-H(2S3)	109.5
H(2S1)-C(2S)-H(2S3)	109.5	H(2S2)-C(2S)-H(2S3)	109.5

3.6.6 Crystal data for $HRh(P^{Ph}{}_2N^{Bn}{}_2)_2$ (7)

The systematic absences in the diffraction data were consistent with the monoclinic space group P-1 with Z = 2 and Z' = 1. All hydrogen atoms, with the exception of the hydride ligand, were included into the model at geometrically calculated positions and refined using a riding model. The coordinates for the hydrogen atom bound to Rh1 were located in the difference map and refined freely. The goodness of fit on F^2 was 1.030 with R1(wR2) = 0.0306(0.0704) for [I>2sigma(I)] and with a largest difference peak and hole of 0.825 and -0.482(e.Å-^{3}).

Table 3-17. Crystal data and structure refinement for $HRh(P^{Ph}{}_2N^{Bn}{}_2)_2$ (**7**)

Identification code	A14441	
Empirical formula	C60 H65 N4 P4 Rh	
Formula weight	1068.95	
Temperature	100(2) K	
Wavelength	0.71073 Å	
Crystal system	Triclinic	
Space group	P-1	
Unit cell dimensions	a = 10.0163(7) Å	α = 96.498(2)°.
	b = 14.2416(9) Å	β = 90.811(3)°.
	c = 18.7726(12) Å	γ = 100.226(3)°.
Volume	2616.8(3) $Å^3$	
Z	2	
Density (calculated)	1.357 Mg/m^3	
Absorption coefficient	0.492 mm^{-1}	
F(000)	1116	
Crystal size	0.350 x 0.250 x 0.100 mm^3	
Theta range for data collection	1.463 to 36.387°.	
Index ranges	-16<=h<=16, -23<=k<=23, -31<=l<=31	
Reflections collected	159545	
Independent reflections	25463 [R(int) = 0.0478]	
Completeness to theta = 25.00°	100.0 %	
Absorption correction	Semi-empirical from equivalents	
Max. and min. transmission	0.7471 and 0.6868	
Refinement method	Full-matrix least-squares on F^2	
Data / restraints / parameters	25463 / 0 / 625	
Goodness-of-fit on F^2	1.030	
Final R indices [I>2sigma(I)]	R1 = 0.0306, wR2 = 0.0704	
R indices (all data)	R1 = 0.0420, wR2 = 0.0749	
Extinction coefficient	not measured	
Largest diff. peak and hole	0.825 and -0.482 $e.Å^{-3}$	

Table 3-18. Bond lengths [Å] and angles [°] for $HRh(P^{Ph}{}_2N^{Bn}{}_2)_2$ (**7**)

Rh(1)-P(3)	2.2246(3)	Rh(1)-P(1)	2.2538(3)
Rh(1)-P(4)	2.2803(3)	Rh(1)-P(2)	2.3186(3)
Rh(1)-H(1)	1.587(15)	P(1)-C(11)	1.8341(11)
P(1)-C(4)	1.8593(11)	P(1)-C(1)	1.8659(11)
C(11)-C(12)	1.3939(16)	C(11)-C(16)	1.3985(17)
C(12)-C(13)	1.3930(17)	C(12)-H(12)	0.9500
C(13)-C(14)	1.381(2)	C(13)-H(13)	0.9500
C(14)-C(15)	1.390(2)	C(14)-H(14)	0.9500
C(15)-C(16)	1.3905(19)	C(15)-H(15)	0.9500
C(16)-H(16)	0.9500	C(1)-N(1)	1.4615(14)
C(1)-H(1A)	0.9900	C(1)-H(1B)	0.9900
N(1)-C(2)	1.4633(14)	N(1)-C(5)	1.4739(14)
C(5)-C(21)	1.5160(16)	C(5)-H(5A)	0.9900
C(5)-H(5B)	0.9900	C(21)-C(22)	1.3956(17)
C(21)-C(26)	1.3958(17)	C(22)-C(23)	1.3907(19)
C(22)-H(22)	0.9500	C(23)-C(24)	1.381(2)
C(23)-H(23)	0.9500	C(24)-C(25)	1.383(2)
C(24)-H(24)	0.9500	C(25)-C(26)	1.3939(18)
C(25)-H(25)	0.9500	C(26)-H(26)	0.9500
C(2)-P(2)	1.8703(11)	C(2)-H(2A)	0.9900
C(2)-H(2B)	0.9900	P(2)-C(31)	1.8319(11)
P(2)-C(3)	1.8707(11)	C(31)-C(32)	1.4004(16)
C(31)-C(36)	1.4009(16)	C(32)-C(33)	1.3912(16)
C(32)-H(32)	0.9500	C(33)-C(34)	1.3876(18)
C(33)-H(33)	0.9500	C(34)-C(35)	1.3868(19)
C(34)-H(34)	0.9500	C(35)-C(36)	1.3944(17)
C(35)-H(35)	0.9500	C(36)-H(36)	0.9500
C(3)-N(2)	1.4666(14)	C(3)-H(3A)	0.9900
C(3)-H(3B)	0.9900	N(2)-C(4)	1.4618(14)
N(2)-C(6)	1.4745(15)	C(6)-C(41)	1.5126(17)
C(6)-H(6A)	0.9900	C(6)-H(6B)	0.9900
C(41)-C(42)	1.3913(17)	C(41)-C(46)	1.3967(18)
C(42)-C(43)	1.3957(18)	C(42)-H(42)	0.9500

Table 3-18. (cont'd)

C(43)-C(44)	1.384(2)	C(43)-H(43)	0.9500
C(44)-C(45)	1.390(2)	C(44)-H(44)	0.9500
C(45)-C(46)	1.3932(19)	C(45)-H(45)	0.9500
C(46)-H(46)	0.9500	C(4)-H(4A)	0.9900
C(4)-H(4B)	0.9900	P(3)-C(61)	1.8313(11)
P(3)-C(51)	1.8679(11)	P(3)-C(54)	1.8774(11)
C(61)-C(66)	1.3949(15)	C(61)-C(62)	1.4055(15)
C(62)-C(63)	1.3942(16)	C(62)-H(62)	0.9500
C(63)-C(64)	1.3923(17)	C(63)-H(63)	0.9500
C(64)-C(65)	1.3894(17)	C(64)-H(64)	0.9500
C(65)-C(66)	1.3970(15)	C(65)-H(65)	0.9500
C(66)-H(66)	0.9500	C(51)-N(3)	1.4584(14)
C(51)-H(51A)	0.9900	C(51)-H(51B)	0.9900
N(3)-C(55)	1.4528(14)	N(3)-C(52)	1.4597(14)
C(71)-C(72)	1.3905(16)	C(71)-C(76)	1.3990(15)
C(71)-C(55)	1.5221(16)	C(72)-C(73)	1.4013(16)
C(72)-H(72)	0.9500	C(73)-C(74)	1.3845(18)
C(73)-H(73)	0.9500	C(74)-C(75)	1.386(2)
C(74)-H(74)	0.9500	C(75)-C(76)	1.3905(18)
C(75)-H(75)	0.9500	C(76)-H(76)	0.9500
C(55)-H(55A)	0.9900	C(55)-H(55B)	0.9900
C(52)-P(4)	1.8689(11)	C(52)-H(52A)	0.9900
C(52)-H(52B)	0.9900	P(4)-C(81)	1.8311(11)
P(4)-C(53)	1.8959(11)	C(81)-C(86)	1.4025(15)
C(81)-C(82)	1.4026(15)	C(82)-C(83)	1.3953(16)
C(82)-H(82)	0.9500	C(83)-C(84)	1.3877(18)
C(83)-H(83)	0.9500	C(84)-C(85)	1.3969(18)
C(84)-H(84)	0.9500	C(85)-C(86)	1.3902(16)
C(85)-H(85)	0.9500	C(86)-H(86)	0.9500
C(53)-N(4)	1.4589(14)	C(53)-H(53A)	0.9900
C(53)-H(53B)	0.9900	N(4)-C(54)	1.4613(14)
N(4)-C(56)	1.4645(15)	C(56)-C(91)	1.5207(16)
C(56)-H(56A)	0.9900	C(56)-H(56B)	0.9900

Table 3-18. (cont'd)

C(91)-C(92)	1.3850(17)	C(91)-C(96)	1.3899(17)
C(92)-C(93)	1.399(2)	C(92)-H(92)	0.9500
C(93)-C(94)	1.388(2)	C(93)-H(93)	0.9500
C(94)-C(95)	1.383(2)	C(94)-H(94)	0.9500
C(95)-C(96)	1.3891(19)	C(95)-H(95)	0.9500
C(96)-H(96)	0.9500	C(54)-H(54A)	0.9900
C(54)-H(54B)	0.9900	P(3)-Rh(1)-P(1)	161.632(11)
P(3)-Rh(1)-P(4)	81.254(11)	P(1)-Rh(1)-P(4)	104.897(11)
P(3)-Rh(1)-P(2)	113.779(10)	P(1)-Rh(1)-P(2)	80.811(10)
P(4)-Rh(1)-P(2)	110.040(11)	P(3)-Rh(1)-H(1)	87.3(5)
P(1)-Rh(1)-H(1)	80.0(5)	P(4)-Rh(1)-H(1)	154.4(5)
P(2)-Rh(1)-H(1)	95.5(5)	C(11)-P(1)-C(4)	97.11(5)
C(11)-P(1)-C(1)	102.44(5)	C(4)-P(1)-C(1)	100.25(5)
C(11)-P(1)-Rh(1)	126.22(4)	C(4)-P(1)-Rh(1)	111.72(4)
C(1)-P(1)-Rh(1)	114.95(3)	C(12)-C(11)-C(16)	118.76(10)
C(12)-C(11)-P(1)	117.42(9)	C(16)-C(11)-P(1)	123.73(9)
C(13)-C(12)-C(11)	120.87(12)	C(13)-C(12)-H(12)	119.6
C(11)-C(12)-H(12)	119.6	C(14)-C(13)-C(12)	119.85(13)
C(14)-C(13)-H(13)	120.1	C(12)-C(13)-H(13)	120.1
C(13)-C(14)-C(15)	119.93(12)	C(13)-C(14)-H(14)	120.0
C(15)-C(14)-H(14)	120.0	C(14)-C(15)-C(16)	120.31(14)
C(14)-C(15)-H(15)	119.8	C(16)-C(15)-H(15)	119.8
C(15)-C(16)-C(11)	120.20(13)	C(15)-C(16)-H(16)	119.9
C(11)-C(16)-H(16)	119.9	N(1)-C(1)-P(1)	112.87(7)
N(1)-C(1)-H(1A)	109.0	P(1)-C(1)-H(1A)	109.0
N(1)-C(1)-H(1B)	109.0	P(1)-C(1)-H(1B)	109.0
H(1A)-C(1)-H(1B)	107.8	C(1)-N(1)-C(2)	115.95(9)
C(1)-N(1)-C(5)	113.26(8)	C(2)-N(1)-C(5)	111.50(8)
N(1)-C(5)-C(21)	115.67(9)	N(1)-C(5)-H(5A)	108.4
C(21)-C(5)-H(5A)	108.4	N(1)-C(5)-H(5B)	108.4
C(21)-C(5)-H(5B)	108.4	H(5A)-C(5)-H(5B)	107.4
C(22)-C(21)-C(26)	117.91(11)	C(22)-C(21)-C(5)	121.74(11)
C(26)-C(21)-C(5)	120.29(10)	C(23)-C(22)-C(21)	120.57(12)

Table 3-18. (cont'd)

C(23)-C(22)-H(22)	119.7	C(21)-C(22)-H(22)	119.7
C(24)-C(23)-C(22)	120.78(13)	C(24)-C(23)-H(23)	119.6
C(22)-C(23)-H(23)	119.6	C(23)-C(24)-C(25)	119.58(12)
C(23)-C(24)-H(24)	120.2	C(25)-C(24)-H(24)	120.2
C(24)-C(25)-C(26)	119.73(13)	C(24)-C(25)-H(25)	120.1
C(26)-C(25)-H(25)	120.1	C(25)-C(26)-C(21)	121.40(12)
C(25)-C(26)-H(26)	119.3	C(21)-C(26)-H(26)	119.3
N(1)-C(2)-P(2)	112.82(7)	N(1)-C(2)-H(2A)	109.0
P(2)-C(2)-H(2A)	109.0	N(1)-C(2)-H(2B)	109.0
P(2)-C(2)-H(2B)	109.0	H(2A)-C(2)-H(2B)	107.8
C(31)-P(2)-C(2)	99.85(5)	C(31)-P(2)-C(3)	99.90(5)
C(2)-P(2)-C(3)	97.53(5)	C(31)-P(2)-Rh(1)	127.51(4)
C(2)-P(2)-Rh(1)	114.12(3)	C(3)-P(2)-Rh(1)	113.08(4)
C(32)-C(31)-C(36)	117.93(10)	C(32)-C(31)-P(2)	119.96(8)
C(36)-C(31)-P(2)	122.06(9)	C(33)-C(32)-C(31)	121.13(11)
C(33)-C(32)-H(32)	119.4	C(31)-C(32)-H(32)	119.4
C(34)-C(33)-C(32)	120.35(11)	C(34)-C(33)-H(33)	119.8
C(32)-C(33)-H(33)	119.8	C(35)-C(34)-C(33)	119.18(11)
C(35)-C(34)-H(34)	120.4	C(33)-C(34)-H(34)	120.4
C(34)-C(35)-C(36)	120.76(12)	C(34)-C(35)-H(35)	119.6
C(36)-C(35)-H(35)	119.6	C(35)-C(36)-C(31)	120.59(11)
C(35)-C(36)-H(36)	119.7	C(31)-C(36)-H(36)	119.7
N(2)-C(3)-P(2)	111.38(7)	N(2)-C(3)-H(3A)	109.4
P(2)-C(3)-H(3A)	109.4	N(2)-C(3)-H(3B)	109.4
P(2)-C(3)-H(3B)	109.4	H(3A)-C(3)-H(3B)	108.0
C(4)-N(2)-C(3)	114.14(9)	C(4)-N(2)-C(6)	110.06(9)
C(3)-N(2)-C(6)	110.05(9)	N(2)-C(6)-C(41)	112.30(10)
N(2)-C(6)-H(6A)	109.1	C(41)-C(6)-H(6A)	109.1
N(2)-C(6)-H(6B)	109.1	C(41)-C(6)-H(6B)	109.1
H(6A)-C(6)-H(6B)	107.9	C(42)-C(41)-C(46)	118.56(11)
C(42)-C(41)-C(6)	120.99(11)	C(46)-C(41)-C(6)	120.45(11)
C(41)-C(42)-C(43)	120.94(12)	C(41)-C(42)-H(42)	119.5
C(43)-C(42)-H(42)	119.5	C(44)-C(43)-C(42)	120.01(12)

Table 3-18. (cont'd)

C(44)-C(43)-H(43)	120.0	C(42)-C(43)-H(43)	120.0
C(43)-C(44)-C(45)	119.66(12)	C(43)-C(44)-H(44)	120.2
C(45)-C(44)-H(44)	120.2	C(44)-C(45)-C(46)	120.25(13)
C(44)-C(45)-H(45)	119.9	C(46)-C(45)-H(45)	119.9
C(45)-C(46)-C(41)	120.56(12)	C(45)-C(46)-H(46)	119.7
C(41)-C(46)-H(46)	119.7	N(2)-C(4)-P(1)	113.74(7)
N(2)-C(4)-H(4A)	108.8	P(1)-C(4)-H(4A)	108.8
N(2)-C(4)-H(4B)	108.8	P(1)-C(4)-H(4B)	108.8
H(4A)-C(4)-H(4B)	107.7	C(61)-P(3)-C(51)	98.16(5)
C(61)-P(3)-C(54)	104.88(5)	C(51)-P(3)-C(54)	98.57(5)
C(61)-P(3)-Rh(1)	122.30(4)	C(51)-P(3)-Rh(1)	112.66(4)
C(54)-P(3)-Rh(1)	116.37(4)	C(66)-C(61)-C(62)	119.08(10)
C(66)-C(61)-P(3)	119.26(8)	C(62)-C(61)-P(3)	121.35(8)
C(63)-C(62)-C(61)	120.52(10)	C(63)-C(62)-H(62)	119.7
C(61)-C(62)-H(62)	119.7	C(64)-C(63)-C(62)	119.75(10)
C(64)-C(63)-H(63)	120.1	C(62)-C(63)-H(63)	120.1
C(65)-C(64)-C(63)	120.18(10)	C(65)-C(64)-H(64)	119.9
C(63)-C(64)-H(64)	119.9	C(64)-C(65)-C(66)	120.17(10)
C(64)-C(65)-H(65)	119.9	C(66)-C(65)-H(65)	119.9
C(61)-C(66)-C(65)	120.29(10)	C(61)-C(66)-H(66)	119.9
C(65)-C(66)-H(66)	119.9	N(3)-C(51)-P(3)	110.91(7)
N(3)-C(51)-H(51A)	109.5	P(3)-C(51)-H(51A)	109.5
N(3)-C(51)-H(51B)	109.5	P(3)-C(51)-H(51B)	109.5
H(51A)-C(51)-H(51B)	108.0	C(55)-N(3)-C(51)	115.98(9)
C(55)-N(3)-C(52)	116.64(9)	C(51)-N(3)-C(52)	117.92(9)
C(72)-C(71)-C(76)	118.54(10)	C(72)-C(71)-C(55)	123.53(10)
C(76)-C(71)-C(55)	117.92(10)	C(71)-C(72)-C(73)	120.57(11)
C(71)-C(72)-H(72)	119.7	C(73)-C(72)-H(72)	119.7
C(74)-C(73)-C(72)	120.15(12)	C(74)-C(73)-H(73)	119.9
C(72)-C(73)-H(73)	119.9	C(73)-C(74)-C(75)	119.72(12)
C(73)-C(74)-H(74)	120.1	C(75)-C(74)-H(74)	120.1
C(74)-C(75)-C(76)	120.18(12)	C(74)-C(75)-H(75)	119.9
C(76)-C(75)-H(75)	119.9	C(75)-C(76)-C(71)	120.80(12)

Table 3-18. (cont'd)

C(75)-C(76)-H(76)	119.6	C(71)-C(76)-H(76)	119.6
N(3)-C(55)-C(71)	119.10(9)	N(3)-C(55)-H(55A)	107.5
C(71)-C(55)-H(55A)	107.5	N(3)-C(55)-H(55B)	107.5
C(71)-C(55)-H(55B)	107.5	H(55A)-C(55)-H(55B)	107.0
N(3)-C(52)-P(4)	109.59(7)	N(3)-C(52)-H(52A)	109.8
P(4)-C(52)-H(52A)	109.8	N(3)-C(52)-H(52B)	109.8
P(4)-C(52)-H(52B)	109.8	H(52A)-C(52)-H(52B)	108.2
C(81)-P(4)-C(52)	102.90(5)	C(81)-P(4)-C(53)	100.46(5)
C(52)-P(4)-C(53)	97.48(5)	C(81)-P(4)-Rh(1)	123.85(4)
C(52)-P(4)-Rh(1)	114.02(4)	C(53)-P(4)-Rh(1)	114.19(3)
C(86)-C(81)-C(82)	118.40(10)	C(86)-C(81)-P(4)	116.97(8)
C(82)-C(81)-P(4)	124.62(8)	C(83)-C(82)-C(81)	120.61(10)
C(83)-C(82)-H(82)	119.7	C(81)-C(82)-H(82)	119.7
C(84)-C(83)-C(82)	120.38(11)	C(84)-C(83)-H(83)	119.8
C(82)-C(83)-H(83)	119.8	C(83)-C(84)-C(85)	119.57(11)
C(83)-C(84)-H(84)	120.2	C(85)-C(84)-H(84)	120.2
C(86)-C(85)-C(84)	120.18(11)	C(86)-C(85)-H(85)	119.9
C(84)-C(85)-H(85)	119.9	C(85)-C(86)-C(81)	120.84(10)
C(85)-C(86)-H(86)	119.6	C(81)-C(86)-H(86)	119.6
N(4)-C(53)-P(4)	117.64(7)	N(4)-C(53)-H(53A)	107.9
P(4)-C(53)-H(53A)	107.9	N(4)-C(53)-H(53B)	107.9
P(4)-C(53)-H(53B)	107.9	H(53A)-C(53)-H(53B)	107.2
C(53)-N(4)-C(54)	115.63(9)	C(53)-N(4)-C(56)	113.84(9)
C(54)-N(4)-C(56)	115.23(9)	N(4)-C(56)-C(91)	111.66(9)
N(4)-C(56)-H(56A)	109.3	C(91)-C(56)-H(56A)	109.3
N(4)-C(56)-H(56B)	109.3	C(91)-C(56)-H(56B)	109.3
H(56A)-C(56)-H(56B)	107.9	C(92)-C(91)-C(96)	118.82(11)
C(92)-C(91)-C(56)	120.44(11)	C(96)-C(91)-C(56)	120.71(11)
C(91)-C(92)-C(93)	120.59(13)	C(91)-C(92)-H(92)	119.7
C(93)-C(92)-H(92)	119.7	C(94)-C(93)-C(92)	120.07(13)
C(94)-C(93)-H(93)	120.0	C(92)-C(93)-H(93)	120.0
C(95)-C(94)-C(93)	119.40(13)	C(95)-C(94)-H(94)	120.3
C(93)-C(94)-H(94)	120.3	C(94)-C(95)-C(96)	120.34(14)

Table 3-18. (cont'd)

C(94)-C(95)-H(95)	119.8	C(96)-C(95)-H(95)	119.8
C(95)-C(96)-C(91)	120.77(13)	C(95)-C(96)-H(96)	119.6
C(91)-C(96)-H(96)	119.6	N(4)-C(54)-P(3)	116.73(7)
N(4)-C(54)-H(54A)	108.1	P(3)-C(54)-H(54A)	108.1
N(4)-C(54)-H(54B)	108.1	P(3)-C(54)-H(54B)	108.1
H(54A)-C(54)-H(54B)	107.3		

3.6.7 Crystal data for $HRh(P^{Ph}{}_2N^{PhOMe}{}_2)_2$ (9)

The systematic absences in the diffraction data were consistent with the monoclinic space group P1 21 1 with Z = 4 and Z' = 2. The asymmetric unit contains two Rh molecules and an uncoordinated THF molecule. The data was refined as a twin with scales of 0.541(14) and 0.459(14). All hydrogen atoms, with the exception of the hydride ligands, were included in the model at geometrically calculated positions and refined using a riding model. The coordinates for the hydrogen atom bound to Rh1 and Rh1' were located in the difference map. One of the hydrogens was refined freely, while the other was restrained to a distance of 1.6 with sigma of 0.02. Included in the asymmetric unit were two THF molecules, one of which was modeled as being disordered over two positions. The goodness of fit on F^2 was 1.081 with R1(wR2) = 0.0257(0.0582) for [I>2sigma(I)] and with a largest difference peak and hole of 0.466 and -0.375(e.Å-3).

Table 3-19. Crystal data and structure refinement for $HRh(P^{Ph}{}_2N^{PhOMe}{}_2)$ (**8**)

Identification code	a14403_a	
Empirical formula	C64 H73 N4 O5 P4 Rh	
Formula weight	1205.05	
Temperature	100(2) K	
Wavelength	0.71073 Å	
Crystal system	Monoclinic	
Space group	P 1 21 1	
Unit cell dimensions	a = 9.9890(2) Å	α = 90°.
	b = 12.8422(3) Å	β = 112.6250(10)°.
	c = 12.8422(3) Å	γ = 90°.
Volume	5717.9(2) $Å^3$	
Z	4	
Density (calculated)	1.400 Mg/m^3	
Absorption coefficient	0.465 mm^{-1}	
F(000)	2520	
Crystal size	0.21 x 0.15 x 0.11 mm^3	
Theta range for data collection	1.687 to 26.000°.	
Index ranges	-12<=h<=12, -59<=k<=59, -15<=l<=15	
Reflections collected	99820	
Independent reflections	22483 [R(int) = 0.0294]	
Completeness to theta = 25.00°	100.0 %	
Absorption correction	Semi-empirical from equivalents	
Max. and min. transmission	0.1138 and 0.0657	
Refinement method	Full-matrix least-squares on F^2	
Data / restraints / parameters	22483 / 13 / 1413	
Goodness-of-fit on F^2	1.081	
Final R indices [I>2sigma(I)]	R1 = 0.0250, wR2 = 0.0578	
R indices (all data)	R1 = 0.0257, wR2 = 0.0582	
Extinction coefficient	not measured	
Largest diff. peak and hole	0.466 and -0.375 $e.Å^{-3}$	

Table 3-20. Bond lengths [Å] and angles [°] for $HRh(P^{Ph}{}_2N^{PhOMe}{}_2)_2$ (**8**)

Rh(1)-H	1.59(3)	Rh(1)-P(1)	2.2831(9)
Rh(1)-P(2)	2.2879(9)	Rh(1)-P(3)	2.2420(9)
Rh(1)-P(4)	2.2841(9)	P(1)-C(1)	1.890(4)
P(1)-C(3)	1.863(4)	P(1)-C(9)	1.840(4)
P(2)-C(2)	1.893(4)	P(2)-C(4)	1.869(4)
P(2)-C(29)	1.839(4)	P(3)-C(5)	1.866(3)
P(3)-C(6)	1.892(4)	P(3)-C(35)	1.834(4)
P(4)-C(7)	1.895(4)	P(4)-C(8)	1.860(4)
P(4)-C(55)	1.845(4)	O(1)-C(18)	1.383(4)
O(1)-C(21)	1.427(4)	O(2)-C(25)	1.384(5)
O(2)-C(28)	1.427(5)	O(3)-C(44)	1.384(4)
O(3)-C(47)	1.424(5)	O(4)-C(51)	1.376(5)
O(4)-C(54)	1.423(5)	N(1)-C(1)	1.457(4)
N(1)-C(2)	1.455(5)	N(1)-C(22)	1.404(5)
N(2)-C(3)	1.472(4)	N(2)-C(4)	1.473(4)
N(2)-C(15)	1.452(4)	N(3)-C(5)	1.464(5)
N(3)-C(7)	1.458(5)	N(3)-C(41)	1.417(5)
N(4)-C(6)	1.458(4)	N(4)-C(8)	1.461(5)
N(4)-C(48)	1.414(5)	C(1)-H(1A)	0.9900
C(1)-H(1B)	0.9900	C(2)-H(2A)	0.9900
C(2)-H(2B)	0.9900	C(3)-H(3A)	0.9900
C(3)-H(3B)	0.9900	C(4)-H(4A)	0.9900
C(4)-H(4B)	0.9900	C(5)-H(5A)	0.9900
C(5)-H(5B)	0.9900	C(6)-H(6A)	0.9900
C(6)-H(6B)	0.9900	C(7)-H(7A)	0.9900
C(7)-H(7B)	0.9900	C(8)-H(8A)	0.9900
C(8)-H(8B)	0.9900	C(9)-C(10)	1.394(5)
C(9)-C(14)	1.402(5)	C(10)-H(10)	0.9500
C(10)-C(11)	1.394(5)	C(11)-H(11)	0.9500
C(11)-C(12)	1.381(6)	C(12)-H(12)	0.9500
C(12)-C(13)	1.393(6)	C(13)-H(13)	0.9500
C(13)-C(14)	1.390(5)	C(14)-H(14)	0.9500
C(15)-C(16)	1.386(5)	C(15)-C(20)	1.381(5)

Table 3-20. (cont'd)

C(16)-H(16)	0.9500	C(16)-C(17)	1.383(6)
C(17)-H(17)	0.9500	C(17)-C(18)	1.382(5)
C(18)-C(19)	1.387(5)	C(19)-H(19)	0.9500
C(19)-C(20)	1.390(5)	C(20)-H(20)	0.9500
C(21)-H(21A)	0.9800	C(21)-H(21B)	0.9800
C(21)-H(21C)	0.9800	C(22)-C(23)	1.403(5)
C(22)-C(27)	1.403(5)	C(23)-H(23)	0.9500
C(23)-C(24)	1.395(5)	C(24)-H(24)	0.9500
C(24)-C(25)	1.380(6)	C(25)-C(26)	1.389(6)
C(26)-H(26)	0.9500	C(26)-C(27)	1.383(6)
C(27)-H(27)	0.9500	C(28)-H(28A)	0.9800
C(28)-H(28B)	0.9800	C(28)-H(28C)	0.9800
C(29)-C(30)	1.406(5)	C(29)-C(34)	1.395(5)
C(30)-H(30)	0.9500	C(30)-C(31)	1.389(5)
C(31)-H(31)	0.9500	C(31)-C(32)	1.388(5)
C(32)-H(32)	0.9500	C(32)-C(33)	1.391(6)
C(33)-H(33)	0.9500	C(33)-C(34)	1.393(5)
C(34)-H(34)	0.9500	C(35)-C(36)	1.391(5)
C(35)-C(40)	1.405(5)	C(36)-H(36)	0.9500
C(36)-C(37)	1.392(5)	C(37)-H(37)	0.9500
C(37)-C(38)	1.390(6)	C(38)-H(38)	0.9500
C(38)-C(39)	1.390(6)	C(39)-H(39)	0.9500
C(39)-C(40)	1.388(5)	C(40)-H(40)	0.9500
C(41)-C(42)	1.400(5)	C(41)-C(46)	1.395(5)
C(42)-H(42)	0.9500	C(42)-C(43)	1.390(5)
C(43)-H(43)	0.9500	C(43)-C(44)	1.387(5)
C(44)-C(45)	1.379(5)	C(45)-H(45)	0.9500
C(45)-C(46)	1.400(5)	C(46)-H(46)	0.9500
C(47)-H(47A)	0.9800	C(47)-H(47B)	0.9800
C(47)-H(47C)	0.9800	C(48)-C(49)	1.402(5)
C(48)-C(53)	1.396(5)	C(49)-H(49)	0.9500
C(49)-C(50)	1.390(5)	C(50)-H(50)	0.9500
C(50)-C(51)	1.388(5)	C(51)-C(52)	1.383(5)

Table 3-20. (cont'd)

C(52)-H(52)	0.9500	C(52)-C(53)	1.389(5)
C(53)-H(53)	0.9500	C(54)-H(54A)	0.9800
C(54)-H(54B)	0.9800	C(54)-H(54C)	0.9800
C(55)-C(56)	1.400(5)	C(55)-C(60)	1.397(5)
C(56)-H(56)	0.9500	C(56)-C(57)	1.393(5)
C(57)-H(57)	0.9500	C(57)-C(58)	1.378(6)
C(58)-H(58)	0.9500	C(58)-C(59)	1.393(6)
C(59)-H(59)	0.9500	C(59)-C(60)	1.388(5)
C(60)-H(60)	0.9500	Rh(1')-HA	1.61(3)
Rh(1')-P(1')	2.2812(9)	Rh(1')-P(2')	2.3024(9)
Rh(1')-P(3')	2.2389(9)	Rh(1')-P(4')	2.2779(9)
P(1')-C(1')	1.898(4)	P(1')-C(3')	1.872(4)
P(1')-C(9')	1.839(4)	P(2')-C(2')	1.901(4)
P(2')-C(4')	1.880(4)	P(2')-C(29')	1.845(4)
P(3')-C(5')	1.896(4)	P(3')-C(6')	1.881(4)
P(3')-C(35')	1.835(4)	P(4')-C(7')	1.860(3)
P(4')-C(8')	1.891(3)	P(4')-C(55')	1.834(4)
O(1')-C(18')	1.378(4)	O(1')-C(21')	1.418(5)
O(2')-C(25')	1.383(5)	O(2')-C(28')	1.424(5)
O(3')-C(44')	1.376(5)	O(3')-C(47')	1.420(5)
O(4')-C(51')	1.389(4)	O(4')-C(54')	1.423(5)
N(1')-C(1')	1.453(5)	N(1')-C(2')	1.451(5)
N(1')-C(22')	1.410(5)	N(2')-C(3')	1.471(4)
N(2')-C(4')	1.467(4)	N(2')-C(15')	1.439(5)
N(3')-C(5')	1.469(4)	N(3')-C(7')	1.448(5)
N(3')-C(41')	1.420(5)	N(4')-C(6')	1.463(5)
N(4')-C(8')	1.460(4)	N(4')-C(48')	1.414(5)
C(1')-H(1'A)	0.9900	C(1')-H(1'B)	0.9900
C(2')-H(2'A)	0.9900	C(2')-H(2'B)	0.9900
C(3')-H(3'A)	0.9900	C(3')-H(3'B)	0.9900
C(4')-H(4'A)	0.9900	C(4')-H(4'B)	0.9900
C(5')-H(5'A)	0.9900	C(5')-H(5'B)	0.9900
C(6')-H(6'A)	0.9900	C(6')-H(6'B)	0.9900

Table 3-20. (cont'd)

C(7')-H(7'A)	0.9900	C(7')-H(7'B)	0.9900
C(8')-H(8'A)	0.9900	C(8')-H(8'B)	0.9900
C(9')-C(10')	1.385(5)	C(9')-C(14')	1.406(5)
C(10')-H(10')	0.9500	C(10')-C(11')	1.395(6)
C(11')-H(11')	0.9500	C(11')-C(12')	1.382(6)
C(12')-H(12')	0.9500	C(12')-C(13')	1.387(6)
C(13')-H(13')	0.9500	C(13')-C(14')	1.381(6)
C(14')-H(14')	0.9500	C(15')-C(16')	1.390(5)
C(15')-C(20')	1.397(5)	C(16')-H(16')	0.9500
C(16')-C(17')	1.387(5)	C(17')-H(17')	0.9500
C(17')-C(18')	1.384(5)	C(18')-C(19')	1.392(5)
C(19')-H(19')	0.9500	C(19')-C(20')	1.391(5)
C(20')-H(20')	0.9500	C(21')-H(21D)	0.9800
C(21')-H(21E)	0.9800	C(21')-H(21F)	0.9800
C(22')-C(23')	1.408(5)	C(22')-C(27')	1.399(5)
C(23')-H(23')	0.9500	C(23')-C(24')	1.383(6)
C(24')-H(24')	0.9500	C(24')-C(25')	1.391(6)
C(25')-C(26')	1.382(6)	C(26')-H(26')	0.9500
C(26')-C(27')	1.383(6)	C(27')-H(27')	0.9500
C(28')-H(28D)	0.9800	C(28')-H(28E)	0.9800
C(28')-H(28F)	0.9800	C(29')-C(30')	1.399(5)
C(29')-C(34')	1.394(5)	C(30')-H(30')	0.9500
C(30')-C(31')	1.398(5)	C(31')-H(31')	0.9500
C(31')-C(32')	1.388(6)	C(32')-H(32')	0.9500
C(32')-C(33')	1.385(6)	C(33')-H(33')	0.9500
C(33')-C(34')	1.395(5)	C(34')-H(34')	0.9500
C(35')-C(36')	1.393(5)	C(35')-C(40')	1.406(5)
C(36')-H(36')	0.9500	C(36')-C(37')	1.398(5)
C(37')-H(37')	0.9500	C(37')-C(38')	1.394(5)
C(38')-H(38')	0.9500	C(38')-C(39')	1.384(6)
C(39')-H(39')	0.9500	C(39')-C(40')	1.385(5)
C(40')-H(40')	0.9500	C(41')-C(42')	1.399(5)
C(41')-C(46')	1.402(5)	C(42')-H(42')	0.9500

Table 3-20. (cont'd)

C(42')-C(43')	1.392(5)	C(43')-H(43')	0.9500
C(43')-C(44')	1.385(5)	C(44')-C(45')	1.387(5)
C(45')-H(45')	0.9500	C(45')-C(46')	1.396(5)
C(46')-H(46')	0.9500	C(47')-H(47D)	0.9800
C(47')-H(47E)	0.9800	C(47')-H(47F)	0.9800
C(48')-C(49')	1.407(5)	C(48')-C(53')	1.396(5)
C(49')-H(49')	0.9500	C(49')-C(50')	1.396(5)
C(50')-H(50')	0.9500	C(50')-C(51')	1.384(5)
C(51')-C(52')	1.380(5)	C(52')-H(52')	0.9500
C(52')-C(53')	1.389(5)	C(53')-H(53')	0.9500
C(54')-H(54D)	0.9800	C(54')-H(54E)	0.9800
C(54')-H(54F)	0.9800	C(55')-C(56')	1.399(5)
C(55')-C(60')	1.390(5)	C(56')-H(56')	0.9500
C(56')-C(57')	1.388(5)	C(57')-H(57')	0.9500
C(57')-C(58')	1.379(6)	C(58')-H(58')	0.9500
C(58')-C(59')	1.393(6)	C(59')-H(59')	0.9500
C(59')-C(60')	1.396(5)	C(60')-H(60')	0.9500
O(1S)-C(1S)	1.425(5)	O(1S)-C(4S)	1.423(5)
C(1S)-H(1SA)	0.9900	C(1S)-H(1SB)	0.9900
C(1S)-C(2S)	1.527(7)	C(2S)-H(2SA)	0.9900
C(2S)-H(2SB)	0.9900	C(2S)-C(3S)	1.537(7)
C(3S)-H(3SA)	0.9900	C(3S)-H(3SB)	0.9900
C(3S)-C(4S)	1.514(7)	C(4S)-H(4SA)	0.9900
C(4S)-H(4SB)	0.9900	O(2S)-C(5S)	1.288(7)
O(2S)-C(8S)	1.451(10)	O(2SB)-C(6S)	1.401(10)
O(2SB)-C(7SB)	1.395(18)	O(2SC)-C(5S)	1.719(11)
O(2SC)-C(7SC)	1.38(4)	C(5S)-H(5SA)	0.9900
C(5S)-H(5SB)	0.9900	C(5S)-H(5SC)	0.9900
C(5S)-H(5SD)	0.9900	C(5S)-H(5SE)	0.9900
C(5S)-H(5SF)	0.9900	C(5S)-C(6S)	1.492(6)
C(5S)-C(8SB)	1.719(12)	C(6S)-H(6SA)	0.9900
C(6S)-H(6SB)	0.9900	C(6S)-H(6SC)	0.9900
C(6S)-H(6SD)	0.9900	C(6S)-H(6SE)	0.9900

Table 3-20. (cont'd)

C(6S)-H(6SF)	0.9900	C(6S)-C(7S)	1.591(9)
C(6S)-C(8SC)	1.401(10)	C(7S)-H(7SA)	0.9900
C(7S)-H(7SB)	0.9900	C(7S)-C(8S)	1.545(10)
C(8S)-H(8SA)	0.9900	C(8S)-H(8SB)	0.9900
C(7SB)-H(7SC)	0.9900	C(7SB)-H(7SD)	0.9900
C(7SB)-C(8SB)	1.590(18)	C(8SB)-H(8SC)	0.9900
C(8SB)-H(8SD)	0.9900	C(7SC)-H(7SE)	0.9900
C(7SC)-H(7SF)	0.9900	C(7SC)-C(8SC)	1.58(3)
C(8SC)-H(8SE)	0.9900	C(8SC)-H(8SF)	0.9900
P(1)-Rh(1)-H	84(2)	P(1)-Rh(1)-P(2)	82.89(3)
P(1)-Rh(1)-P(4)	104.08(3)	P(2)-Rh(1)-H	87(2)
P(3)-Rh(1)-H	85(2)	P(3)-Rh(1)-P(1)	139.13(3)
P(3)-Rh(1)-P(2)	135.55(3)	P(3)-Rh(1)-P(4)	78.94(3)
P(4)-Rh(1)-H	162(2)	P(4)-Rh(1)-P(2)	109.05(3)
C(1)-P(1)-Rh(1)	113.12(11)	C(3)-P(1)-Rh(1)	111.82(12)
C(3)-P(1)-C(1)	98.87(16)	C(9)-P(1)-Rh(1)	127.70(12)
C(9)-P(1)-C(1)	103.72(16)	C(9)-P(1)-C(3)	97.02(16)
C(2)-P(2)-Rh(1)	113.17(12)	C(4)-P(2)-Rh(1)	113.14(12)
C(4)-P(2)-C(2)	95.65(16)	C(29)-P(2)-Rh(1)	128.99(12)
C(29)-P(2)-C(2)	102.56(16)	C(29)-P(2)-C(4)	97.54(16)
C(5)-P(3)-Rh(1)	114.40(12)	C(5)-P(3)-C(6)	99.49(16)
C(6)-P(3)-Rh(1)	115.67(11)	C(35)-P(3)-Rh(1)	124.71(12)
C(35)-P(3)-C(5)	97.05(16)	C(35)-P(3)-C(6)	101.29(16)
C(7)-P(4)-Rh(1)	114.68(12)	C(8)-P(4)-Rh(1)	112.86(12)
C(8)-P(4)-C(7)	97.92(16)	C(55)-P(4)-Rh(1)	126.09(11)
C(55)-P(4)-C(7)	100.20(16)	C(55)-P(4)-C(8)	100.69(16)
C(18)-O(1)-C(21)	116.5(3)	C(25)-O(2)-C(28)	116.6(3)
C(44)-O(3)-C(47)	116.5(3)	C(51)-O(4)-C(54)	116.6(3)
C(2)-N(1)-C(1)	115.0(3)	C(22)-N(1)-C(1)	121.8(3)
C(22)-N(1)-C(2)	120.2(3)	C(3)-N(2)-C(4)	117.0(3)
C(15)-N(2)-C(3)	112.0(3)	C(15)-N(2)-C(4)	110.7(3)
C(7)-N(3)-C(5)	114.5(3)	C(41)-N(3)-C(5)	117.7(3)
C(41)-N(3)-C(7)	118.2(3)	C(6)-N(4)-C(8)	116.8(3)

Table 3-20. (cont'd)

C(48)-N(4)-C(6)	117.2(3)	C(48)-N(4)-C(8)	116.1(3)
P(1)-C(1)-H(1A)	108.5	P(1)-C(1)-H(1B)	108.5
N(1)-C(1)-P(1)	115.1(2)	N(1)-C(1)-H(1A)	108.5
N(1)-C(1)-H(1B)	108.5	H(1A)-C(1)-H(1B)	107.5
P(2)-C(2)-H(2A)	108.4	P(2)-C(2)-H(2B)	108.4
N(1)-C(2)-P(2)	115.4(2)	N(1)-C(2)-H(2A)	108.4
N(1)-C(2)-H(2B)	108.4	H(2A)-C(2)-H(2B)	107.5
P(1)-C(3)-H(3A)	108.9	P(1)-C(3)-H(3B)	108.9
N(2)-C(3)-P(1)	113.5(2)	N(2)-C(3)-H(3A)	108.9
N(2)-C(3)-H(3B)	108.9	H(3A)-C(3)-H(3B)	107.7
P(2)-C(4)-H(4A)	109.1	P(2)-C(4)-H(4B)	109.1
N(2)-C(4)-P(2)	112.5(2)	N(2)-C(4)-H(4A)	109.1
N(2)-C(4)-H(4B)	109.1	H(4A)-C(4)-H(4B)	107.8
P(3)-C(5)-H(5A)	109.2	P(3)-C(5)-H(5B)	109.2
N(3)-C(5)-P(3)	112.2(2)	N(3)-C(5)-H(5A)	109.2
N(3)-C(5)-H(5B)	109.2	H(5A)-C(5)-H(5B)	107.9
P(3)-C(6)-H(6A)	108.9	P(3)-C(6)-H(6B)	108.9
N(4)-C(6)-P(3)	113.4(2)	N(4)-C(6)-H(6A)	108.9
N(4)-C(6)-H(6B)	108.9	H(6A)-C(6)-H(6B)	107.7
P(4)-C(7)-H(7A)	108.7	P(4)-C(7)-H(7B)	108.7
N(3)-C(7)-P(4)	114.4(2)	N(3)-C(7)-H(7A)	108.7
N(3)-C(7)-H(7B)	108.7	H(7A)-C(7)-H(7B)	107.6
P(4)-C(8)-H(8A)	109.1	P(4)-C(8)-H(8B)	109.1
N(4)-C(8)-P(4)	112.5(2)	N(4)-C(8)-H(8A)	109.1
N(4)-C(8)-H(8B)	109.1	H(8A)-C(8)-H(8B)	107.8
C(10)-C(9)-P(1)	117.4(3)	C(10)-C(9)-C(14)	118.9(3)
C(14)-C(9)-P(1)	123.7(3)	C(9)-C(10)-H(10)	119.7
C(11)-C(10)-C(9)	120.6(4)	C(11)-C(10)-H(10)	119.7
C(10)-C(11)-H(11)	120.0	C(12)-C(11)-C(10)	120.0(4)
C(12)-C(11)-H(11)	120.0	C(11)-C(12)-H(12)	119.9
C(11)-C(12)-C(13)	120.1(4)	C(13)-C(12)-H(12)	119.9
C(12)-C(13)-H(13)	120.0	C(14)-C(13)-C(12)	120.1(4)
C(14)-C(13)-H(13)	120.0	C(9)-C(14)-H(14)	119.9

Table 3-20. (cont'd)

C(13)-C(14)-C(9)	120.3(3)	C(13)-C(14)-H(14)	119.9
C(16)-C(15)-N(2)	122.7(3)	C(20)-C(15)-N(2)	118.3(3)
C(20)-C(15)-C(16)	119.0(3)	C(15)-C(16)-H(16)	119.4
C(17)-C(16)-C(15)	121.1(4)	C(17)-C(16)-H(16)	119.4
C(16)-C(17)-H(17)	120.3	C(18)-C(17)-C(16)	119.5(4)
C(18)-C(17)-H(17)	120.3	O(1)-C(18)-C(19)	115.5(3)
C(17)-C(18)-O(1)	124.4(3)	C(17)-C(18)-C(19)	120.1(3)
C(18)-C(19)-H(19)	120.1	C(18)-C(19)-C(20)	119.8(3)
C(20)-C(19)-H(19)	120.1	C(15)-C(20)-C(19)	120.5(3)
C(15)-C(20)-H(20)	119.7	C(19)-C(20)-H(20)	119.7
O(1)-C(21)-H(21A)	109.5	O(1)-C(21)-H(21B)	109.5
O(1)-C(21)-H(21C)	109.5	H(21A)-C(21)-H(21B)	109.5
H(21A)-C(21)-H(21C)	109.5	H(21B)-C(21)-H(21C)	109.5
C(23)-C(22)-N(1)	122.2(3)	C(23)-C(22)-C(27)	115.7(3)
C(27)-C(22)-N(1)	122.0(3)	C(22)-C(23)-H(23)	118.8
C(24)-C(23)-C(22)	122.3(4)	C(24)-C(23)-H(23)	118.8
C(23)-C(24)-H(24)	119.8	C(25)-C(24)-C(23)	120.4(4)
C(25)-C(24)-H(24)	119.8	O(2)-C(25)-C(26)	116.3(3)
C(24)-C(25)-O(2)	125.3(4)	C(24)-C(25)-C(26)	118.4(4)
C(25)-C(26)-H(26)	119.5	C(27)-C(26)-C(25)	121.1(4)
C(27)-C(26)-H(26)	119.5	C(22)-C(27)-H(27)	119.0
C(26)-C(27)-C(22)	122.0(4)	C(26)-C(27)-H(27)	119.0
O(2)-C(28)-H(28A)	109.5	O(2)-C(28)-H(28B)	109.5
O(2)-C(28)-H(28C)	109.5	H(28A)-C(28)-H(28B)	109.5
H(28A)-C(28)-H(28C)	109.5	H(28B)-C(28)-H(28C)	109.5
C(30)-C(29)-P(2)	124.0(3)	C(34)-C(29)-P(2)	117.4(3)
C(34)-C(29)-C(30)	118.5(3)	C(29)-C(30)-H(30)	119.7
C(31)-C(30)-C(29)	120.6(3)	C(31)-C(30)-H(30)	119.7
C(30)-C(31)-H(31)	119.9	C(32)-C(31)-C(30)	120.2(3)
C(32)-C(31)-H(31)	119.9	C(31)-C(32)-H(32)	120.0
C(31)-C(32)-C(33)	120.0(4)	C(33)-C(32)-H(32)	120.0
C(32)-C(33)-H(33)	120.0	C(32)-C(33)-C(34)	119.9(4)
C(34)-C(33)-H(33)	120.0	C(29)-C(34)-H(34)	119.6

Table 3-20. (cont'd)

C(33)-C(34)-C(29)	120.8(3)	C(33)-C(34)-H(34)	119.6
C(36)-C(35)-P(3)	120.2(3)	C(36)-C(35)-C(40)	119.0(3)
C(40)-C(35)-P(3)	120.7(3)	C(35)-C(36)-H(36)	119.6
C(35)-C(36)-C(37)	120.7(4)	C(37)-C(36)-H(36)	119.6
C(36)-C(37)-H(37)	120.1	C(38)-C(37)-C(36)	119.9(4)
C(38)-C(37)-H(37)	120.1	C(37)-C(38)-H(38)	120.0
C(37)-C(38)-C(39)	119.9(3)	C(39)-C(38)-H(38)	120.0
C(38)-C(39)-H(39)	119.8	C(40)-C(39)-C(38)	120.4(4)
C(40)-C(39)-H(39)	119.8	C(35)-C(40)-H(40)	120.0
C(39)-C(40)-C(35)	120.1(3)	C(39)-C(40)-H(40)	120.0
C(42)-C(41)-N(3)	121.8(3)	C(46)-C(41)-N(3)	121.1(3)
C(46)-C(41)-C(42)	117.0(3)	C(41)-C(42)-H(42)	119.4
C(43)-C(42)-C(41)	121.1(3)	C(43)-C(42)-H(42)	119.4
C(42)-C(43)-H(43)	119.6	C(44)-C(43)-C(42)	120.8(3)
C(44)-C(43)-H(43)	119.6	O(3)-C(44)-C(43)	116.3(3)
C(45)-C(44)-O(3)	124.4(3)	C(45)-C(44)-C(43)	119.4(3)
C(44)-C(45)-H(45)	120.2	C(44)-C(45)-C(46)	119.7(4)
C(46)-C(45)-H(45)	120.2	C(41)-C(46)-C(45)	122.1(4)
C(41)-C(46)-H(46)	119.0	C(45)-C(46)-H(46)	119.0
O(3)-C(47)-H(47A)	109.5	O(3)-C(47)-H(47B)	109.5
O(3)-C(47)-H(47C)	109.5	H(47A)-C(47)-H(47B)	109.5
H(47A)-C(47)-H(47C)	109.5	H(47B)-C(47)-H(47C)	109.5
C(49)-C(48)-N(4)	120.1(3)	C(53)-C(48)-N(4)	122.8(3)
C(53)-C(48)-C(49)	117.0(3)	C(48)-C(49)-H(49)	119.0
C(50)-C(49)-C(48)	122.1(3)	C(50)-C(49)-H(49)	119.0
C(49)-C(50)-H(50)	120.2	C(51)-C(50)-C(49)	119.6(3)
C(51)-C(50)-H(50)	120.2	O(4)-C(51)-C(50)	124.8(3)
O(4)-C(51)-C(52)	115.8(3)	C(52)-C(51)-C(50)	119.3(3)
C(51)-C(52)-H(52)	119.6	C(51)-C(52)-C(53)	120.8(3)
C(53)-C(52)-H(52)	119.6	C(48)-C(53)-H(53)	119.4
C(52)-C(53)-C(48)	121.2(4)	C(52)-C(53)-H(53)	119.4
O(4)-C(54)-H(54A)	109.5	O(4)-C(54)-H(54B)	109.5
O(4)-C(54)-H(54C)	109.5	H(54A)-C(54)-H(54B)	109.5

Table 3-20. (cont'd)

H(54A)-C(54)-H(54C)	109.5	H(54B)-C(54)-H(54C)	109.5
C(56)-C(55)-P(4)	123.7(3)	C(60)-C(55)-P(4)	118.2(3)
C(60)-C(55)-C(56)	117.9(3)	C(55)-C(56)-H(56)	119.7
C(57)-C(56)-C(55)	120.6(3)	C(57)-C(56)-H(56)	119.7
C(56)-C(57)-H(57)	119.6	C(58)-C(57)-C(56)	120.7(3)
C(58)-C(57)-H(57)	119.6	C(57)-C(58)-H(58)	120.2
C(57)-C(58)-C(59)	119.6(3)	C(59)-C(58)-H(58)	120.2
C(58)-C(59)-H(59)	120.1	C(60)-C(59)-C(58)	119.8(4)
C(60)-C(59)-H(59)	120.1	C(55)-C(60)-H(60)	119.3
C(59)-C(60)-C(55)	121.5(3)	C(59)-C(60)-H(60)	119.3
P(1')-Rh(1')-HA	82.4(19)	P(1')-Rh(1')-P(2')	82.07(3)
P(2')-Rh(1')-HA	84.5(19)	P(3')-Rh(1')-HA	88.0(19)
P(3')-Rh(1')-P(1')	137.74(3)	P(3')-Rh(1')-P(2')	137.93(3)
P(3')-Rh(1')-P(4')	78.34(3)	P(4')-Rh(1')-HA	166(2)
P(4')-Rh(1')-P(1')	107.77(3)	P(4')-Rh(1')-P(2')	105.55(3)
C(1')-P(1')-Rh(1')	113.46(12)	C(3')-P(1')-Rh(1')	114.55(11)
C(3')-P(1')-C(1')	95.50(16)	C(9')-P(1')-Rh(1')	127.89(13)
C(9')-P(1')-C(1')	103.32(16)	C(9')-P(1')-C(3')	96.42(16)
C(2')-P(2')-Rh(1')	112.50(11)	C(4')-P(2')-Rh(1')	111.83(12)
C(4')-P(2')-C(2')	99.28(17)	C(29')-P(2')-Rh(1')	129.49(12)
C(29')-P(2')-C(2')	102.93(16)	C(29')-P(2')-C(4')	95.96(16)
C(5')-P(3')-Rh(1')	115.24(12)	C(6')-P(3')-Rh(1')	115.52(12)
C(6')-P(3')-C(5')	98.80(16)	C(35')-P(3')-Rh(1')	125.28(12)
C(35')-P(3')-C(5')	101.52(17)	C(35')-P(3')-C(6')	95.90(16)
C(7')-P(4')-Rh(1')	112.66(12)	C(7')-P(4')-C(8')	98.79(16)
C(8')-P(4')-Rh(1')	115.53(11)	C(55')-P(4')-Rh(1')	124.54(12)
C(55')-P(4')-C(7')	102.53(17)	C(55')-P(4')-C(8')	98.95(16)
C(18')-O(1')-C(21')	117.1(3)	C(25')-O(2')-C(28')	116.6(3)
C(44')-O(3')-C(47')	116.6(3)	C(51')-O(4')-C(54')	117.2(3)
C(2')-N(1')-C(1')	115.1(3)	C(22')-N(1')-C(1')	120.0(3)
C(22')-N(1')-C(2')	121.8(3)	C(4')-N(2')-C(3')	115.7(3)
C(15')-N(2')-C(3')	110.8(3)	C(15')-N(2')-C(4')	113.1(3)
C(7')-N(3')-C(5')	116.5(3)	C(41')-N(3')-C(5')	116.8(3)

Table 3-20. (cont'd)

C(41')-N(3')-C(7')	116.9(3)	C(8')-N(4')-C(6')	113.7(3)
C(48')-N(4')-C(6')	117.1(3)	C(48')-N(4')-C(8')	117.3(3)
P(1')-C(1')-H(1'A)	108.6	P(1')-C(1')-H(1'B)	108.6
N(1')-C(1')-P(1')	114.7(2)	N(1')-C(1')-H(1'A)	108.6
N(1')-C(1')-H(1'B)	108.6	H(1'A)-C(1')-H(1'B)	107.6
P(2')-C(2')-H(2'A)	108.5	P(2')-C(2')-H(2'B)	108.5
N(1')-C(2')-P(2')	115.1(2)	N(1')-C(2')-H(2'A)	108.5
N(1')-C(2')-H(2'B)	108.5	H(2'A)-C(2')-H(2'B)	107.5
P(1')-C(3')-H(3'A)	108.8	P(1')-C(3')-H(3'B)	108.8
N(2')-C(3')-P(1')	113.8(2)	N(2')-C(3')-H(3'A)	108.8
N(2')-C(3')-H(3'B)	108.8	H(3'A)-C(3')-H(3'B)	107.7
P(2')-C(4')-H(4'A)	109.0	P(2')-C(4')-H(4'B)	109.0
N(2')-C(4')-P(2')	113.0(2)	N(2')-C(4')-H(4'A)	109.0
N(2')-C(4')-H(4'B)	109.0	H(4'A)-C(4')-H(4'B)	107.8
P(3')-C(5')-H(5'A)	109.1	P(3')-C(5')-H(5'B)	109.1
N(3')-C(5')-P(3')	112.7(2)	N(3')-C(5')-H(5'A)	109.1
N(3')-C(5')-H(5'B)	109.1	H(5'A)-C(5')-H(5'B)	107.8
P(3')-C(6')-H(6'A)	109.2	P(3')-C(6')-H(6'B)	109.2
N(4')-C(6')-P(3')	112.0(2)	N(4')-C(6')-H(6'A)	109.2
N(4')-C(6')-H(6'B)	109.2	H(6'A)-C(6')-H(6'B)	107.9
P(4')-C(7')-H(7'A)	109.3	P(4')-C(7')-H(7'B)	109.3
N(3')-C(7')-P(4')	111.5(2)	N(3')-C(7')-H(7'A)	109.3
N(3')-C(7')-H(7'B)	109.3	H(7'A)-C(7')-H(7'B)	108.0
P(4')-C(8')-H(8'A)	108.5	P(4')-C(8')-H(8'B)	108.5
N(4')-C(8')-P(4')	115.1(2)	N(4')-C(8')-H(8'A)	108.5
N(4')-C(8')-H(8'B)	108.5	H(8'A)-C(8')-H(8'B)	107.5
C(10')-C(9')-P(1')	117.6(3)	C(10')-C(9')-C(14')	119.1(3)
C(14')-C(9')-P(1')	123.3(3)	C(9')-C(10')-H(10')	119.5
C(9')-C(10')-C(11')	121.0(4)	C(11')-C(10')-H(10')	119.5
C(10')-C(11')-H(11')	120.3	C(12')-C(11')-C(10')	119.5(4)
C(12')-C(11')-H(11')	120.3	C(11')-C(12')-H(12')	120.0
C(11')-C(12')-C(13')	119.9(4)	C(13')-C(12')-H(12')	120.0
C(12')-C(13')-H(13')	119.6	C(14')-C(13')-C(12')	120.9(4)

Table 3-20. (cont'd)

C(14')-C(13')-H(13')	119.6	C(9')-C(14')-H(14')	120.2
C(13')-C(14')-C(9')	119.6(4)	C(13')-C(14')-H(14')	120.2
C(16')-C(15')-N(2')	123.6(3)	C(16')-C(15')-C(20')	117.7(3)
C(20')-C(15')-N(2')	118.8(3)	C(15')-C(16')-H(16')	119.6
C(17')-C(16')-C(15')	120.9(3)	C(17')-C(16')-H(16')	119.6
C(16')-C(17')-H(17')	119.6	C(18')-C(17')-C(16')	120.8(3)
C(18')-C(17')-H(17')	119.6	O(1')-C(18')-C(17')	116.0(3)
O(1')-C(18')-C(19')	124.5(3)	C(17')-C(18')-C(19')	119.5(3)
C(18')-C(19')-H(19')	120.4	C(20')-C(19')-C(18')	119.2(3)
C(20')-C(19')-H(19')	120.4	C(15')-C(20')-H(20')	119.0
C(19')-C(20')-C(15')	122.0(3)	C(19')-C(20')-H(20')	119.0
O(1')-C(21')-H(21D)	109.5	O(1')-C(21')-H(21E)	109.5
O(1')-C(21')-H(21F)	109.5	H(21D)-C(21')-H(21E)	109.5
H(21D)-C(21')-H(21F)	109.5	H(21E)-C(21')-H(21F)	109.5
C(23')-C(22')-N(1')	121.9(3)	C(27')-C(22')-N(1')	122.1(3)
C(27')-C(22')-C(23')	115.8(3)	C(22')-C(23')-H(23')	119.0
C(24')-C(23')-C(22')	121.9(4)	C(24')-C(23')-H(23')	119.0
C(23')-C(24')-H(24')	119.6	C(23')-C(24')-C(25')	120.9(4)
C(25')-C(24')-H(24')	119.6	O(2')-C(25')-C(24')	116.2(3)
C(26')-C(25')-O(2')	125.7(4)	C(26')-C(25')-C(24')	118.1(4)
C(25')-C(26')-H(26')	119.5	C(25')-C(26')-C(27')	121.1(4)
C(27')-C(26')-H(26')	119.5	C(22')-C(27')-H(27')	118.9
C(26')-C(27')-C(22')	122.2(4)	C(26')-C(27')-H(27')	118.9
O(2')-C(28')-H(28D)	109.5	O(2')-C(28')-H(28E)	109.5
O(2')-C(28')-H(28F)	109.5	H(28D)-C(28')-H(28E)	109.5
H(28D)-C(28')-H(28F)	109.5	H(28E)-C(28')-H(28F)	109.5
C(30')-C(29')-P(2')	123.2(3)	C(34')-C(29')-P(2')	117.4(3)
C(34')-C(29')-C(30')	119.2(3)	C(29')-C(30')-H(30')	119.9
C(31')-C(30')-C(29')	120.2(3)	C(31')-C(30')-H(30')	119.9
C(30')-C(31')-H(31')	120.0	C(32')-C(31')-C(30')	120.0(4)
C(32')-C(31')-H(31')	120.0	C(31')-C(32')-H(32')	120.0
C(33')-C(32')-C(31')	120.0(4)	C(33')-C(32')-H(32')	120.0
C(32')-C(33')-H(33')	119.9	C(32')-C(33')-C(34')	120.3(4)

Table 3-20. (cont'd)

C(34')-C(33')-H(33')	119.9	C(29')-C(34')-C(33')	120.3(4)
C(29')-C(34')-H(34')	119.9	C(33')-C(34')-H(34')	119.9
C(36')-C(35')-P(3')	119.6(3)	C(36')-C(35')-C(40')	119.3(3)
C(40')-C(35')-P(3')	120.9(3)	C(35')-C(36')-H(36')	119.7
C(35')-C(36')-C(37')	120.6(3)	C(37')-C(36')-H(36')	119.7
C(36')-C(37')-H(37')	120.2	C(38')-C(37')-C(36')	119.6(4)
C(38')-C(37')-H(37')	120.2	C(37')-C(38')-H(38')	120.1
C(39')-C(38')-C(37')	119.8(3)	C(39')-C(38')-H(38')	120.1
C(38')-C(39')-H(39')	119.5	C(38')-C(39')-C(40')	121.1(4)
C(40')-C(39')-H(39')	119.5	C(35')-C(40')-H(40')	120.2
C(39')-C(40')-C(35')	119.6(4)	C(39')-C(40')-H(40')	120.2
C(42')-C(41')-N(3')	120.5(3)	C(42')-C(41')-C(46')	117.5(3)
C(46')-C(41')-N(3')	121.9(3)	C(41')-C(42')-H(42')	119.0
C(43')-C(42')-C(41')	121.9(3)	C(43')-C(42')-H(42')	119.0
C(42')-C(43')-H(43')	120.1	C(44')-C(43')-C(42')	119.7(3)
C(44')-C(43')-H(43')	120.1	O(3')-C(44')-C(43')	125.0(3)
O(3')-C(44')-C(45')	115.5(3)	C(43')-C(44')-C(45')	119.5(3)
C(44')-C(45')-H(45')	119.6	C(44')-C(45')-C(46')	120.7(3)
C(46')-C(45')-H(45')	119.6	C(41')-C(46')-H(46')	119.7
C(45')-C(46')-C(41')	120.6(3)	C(45')-C(46')-H(46')	119.7
O(3')-C(47')-H(47D)	109.5	O(3')-C(47')-H(47E)	109.5
O(3')-C(47')-H(47F)	109.5	H(47D)-C(47')-H(47E)	109.5
H(47D)-C(47')-H(47F)	109.5	H(47E)-C(47')-H(47F)	109.5
C(49')-C(48')-N(4')	122.8(3)	C(53')-C(48')-N(4')	120.4(3)
C(53')-C(48')-C(49')	116.7(3)	C(48')-C(49')-H(49')	119.5
C(50')-C(49')-C(48')	120.9(3)	C(50')-C(49')-H(49')	119.5
C(49')-C(50')-H(50')	119.7	C(51')-C(50')-C(49')	120.6(3)
C(51')-C(50')-H(50')	119.7	C(50')-C(51')-O(4')	116.3(3)
C(52')-C(51')-O(4')	124.1(3)	C(52')-C(51')-C(50')	119.6(3)
C(51')-C(52')-H(52')	120.2	C(51')-C(52')-C(53')	119.6(3)
C(53')-C(52')-H(52')	120.2	C(48')-C(53')-H(53')	118.7
C(52')-C(53')-C(48')	122.6(4)	C(52')-C(53')-H(53')	118.7
O(4')-C(54')-H(54D)	109.5	O(4')-C(54')-H(54E)	109.5

Table 3-20. (cont'd)

O(4')-C(54')-H(54F)	109.5	H(54D)-C(54')-H(54E)	109.5
H(54D)-C(54')-H(54F)	109.5	H(54E)-C(54')-H(54F)	109.5
C(56')-C(55')-P(4')	117.0(3)	C(60')-C(55')-P(4')	124.0(3)
C(60')-C(55')-C(56')	118.6(3)	C(55')-C(56')-H(56')	119.5
C(57')-C(56')-C(55')	121.0(3)	C(57')-C(56')-H(56')	119.5
C(56')-C(57')-H(57')	120.0	C(58')-C(57')-C(56')	120.0(4)
C(58')-C(57')-H(57')	120.0	C(57')-C(58')-H(58')	120.0
C(57')-C(58')-C(59')	119.9(4)	C(59')-C(58')-H(58')	120.0
C(58')-C(59')-H(59')	119.9	C(58')-C(59')-C(60')	120.1(4)
C(60')-C(59')-H(59')	119.9	C(55')-C(60')-C(59')	120.4(4)
C(55')-C(60')-H(60')	119.8	C(59')-C(60')-H(60')	119.8
C(4S)-O(1S)-C(1S)	105.6(3)	O(1S)-C(1S)-H(1SA)	110.3
O(1S)-C(1S)-H(1SB)	110.3	O(1S)-C(1S)-C(2S)	106.9(4)
H(1SA)-C(1S)-H(1SB)	108.6	C(2S)-C(1S)-H(1SA)	110.3
C(2S)-C(1S)-H(1SB)	110.3	C(1S)-C(2S)-H(2SA)	111.0
C(1S)-C(2S)-H(2SB)	111.0	C(1S)-C(2S)-C(3S)	103.7(4)
H(2SA)-C(2S)-H(2SB)	109.0	C(3S)-C(2S)-H(2SA)	111.0
C(3S)-C(2S)-H(2SB)	111.0	C(2S)-C(3S)-H(3SA)	111.1
C(2S)-C(3S)-H(3SB)	111.1	H(3SA)-C(3S)-H(3SB)	109.0
C(4S)-C(3S)-C(2S)	103.4(4)	C(4S)-C(3S)-H(3SA)	111.1
C(4S)-C(3S)-H(3SB)	111.1	O(1S)-C(4S)-C(3S)	105.0(4)
O(1S)-C(4S)-H(4SA)	110.7	O(1S)-C(4S)-H(4SB)	110.7
C(3S)-C(4S)-H(4SA)	110.7	C(3S)-C(4S)-H(4SB)	110.7
H(4SA)-C(4S)-H(4SB)	108.8	C(5S)-O(2S)-C(8S)	102.5(5)
C(7SB)-O(2SB)-C(6S)	101.0(11)	C(7SC)-O(2SC)-C(5S)	110.3(16)
O(2S)-C(5S)-H(5SA)	108.8	O(2S)-C(5S)-H(5SB)	108.8
O(2S)-C(5S)-C(6S)	113.8(5)	O(2SC)-C(5S)-H(5SE)	113.0
O(2SC)-C(5S)-H(5SF)	113.0	H(5SA)-C(5S)-H(5SB)	107.7
H(5SC)-C(5S)-H(5SD)	110.4	H(5SE)-C(5S)-H(5SF)	110.4
C(6S)-C(5S)-O(2SC)	93.8(5)	C(6S)-C(5S)-H(5SA)	108.8
C(6S)-C(5S)-H(5SB)	108.8	C(6S)-C(5S)-H(5SC)	113.0
C(6S)-C(5S)-H(5SD)	113.0	C(6S)-C(5S)-H(5SE)	113.0
C(6S)-C(5S)-H(5SF)	113.0	C(6S)-C(5S)-C(8SB)	93.8(5)

Table 3-20. (cont'd)

C(8SB)-C(5S)-H(5SC)	113.0	C(8SB)-C(5S)-H(5SD)	113.0
O(2SB)-C(6S)-C(5S)	117.0(5)	O(2SB)-C(6S)-H(6SC)	108.0
O(2SB)-C(6S)-H(6SD)	108.0	C(5S)-C(6S)-H(6SA)	112.4
C(5S)-C(6S)-H(6SB)	112.4	C(5S)-C(6S)-H(6SC)	108.0
C(5S)-C(6S)-H(6SD)	108.0	C(5S)-C(6S)-H(6SE)	108.0
C(5S)-C(6S)-H(6SF)	108.0	C(5S)-C(6S)-C(7S)	96.9(4)
H(6SA)-C(6S)-H(6SB)	109.9	H(6SC)-C(6S)-H(6SD)	107.3
H(6SE)-C(6S)-H(6SF)	107.3	C(7S)-C(6S)-H(6SA)	112.4
C(7S)-C(6S)-H(6SB)	112.4	C(8SC)-C(6S)-C(5S)	117.0(5)
C(8SC)-C(6S)-H(6SE)	108.0	C(8SC)-C(6S)-H(6SF)	108.0
C(6S)-C(7S)-H(7SA)	111.3	C(6S)-C(7S)-H(7SB)	111.3
H(7SA)-C(7S)-H(7SB)	109.2	C(8S)-C(7S)-C(6S)	102.6(6)
C(8S)-C(7S)-H(7SA)	111.3	C(8S)-C(7S)-H(7SB)	111.3
O(2S)-C(8S)-C(7S)	107.0(7)	O(2S)-C(8S)-H(8SA)	110.3
O(2S)-C(8S)-H(8SB)	110.3	C(7S)-C(8S)-H(8SA)	110.3
C(7S)-C(8S)-H(8SB)	110.3	H(8SA)-C(8S)-H(8SB)	108.6
O(2SB)-C(7SB)-H(7SC)	111.2	O(2SB)-C(7SB)-H(7SD)	111.2
O(2SB)-C(7SB)-C(8SB)	102.6(13)	H(7SC)-C(7SB)-H(7SD)	109.2
C(8SB)-C(7SB)-H(7SC)	111.2	C(8SB)-C(7SB)-H(7SD)	111.2
C(5S)-C(8SB)-H(8SC)	111.5	C(5S)-C(8SB)-H(8SD)	111.5
C(7SB)-C(8SB)-C(5S)	101.2(10)	C(7SB)-C(8SB)-H(8SC)	111.5
C(7SB)-C(8SB)-H(8SD)	111.5	H(8SC)-C(8SB)-H(8SD)	109.4
O(2SC)-C(7SC)-H(7SE)	111.0	O(2SC)-C(7SC)-H(7SF)	111.0
O(2SC)-C(7SC)-C(8SC)	104(2)	H(7SE)-C(7SC)-H(7SF)	109.0
C(8SC)-C(7SC)-H(7SE)	111.0	C(8SC)-C(7SC)-H(7SF)	111.0
C(6S)-C(8SC)-C(7SC)	107.2(15)	C(6S)-C(8SC)-H(8SE)	110.3
C(6S)-C(8SC)-H(8SF)	110.3	C(7SC)-C(8SC)-H(8SE)	110.3
C(7SC)-C(8SC)-H(8SF)	110.3	H(8SE)-C(8SC)-H(8SF)	108.5

3.6.8 Crystal data for $HRh(P^{Cy}{}_2N^{Ph}{}_2)_2$ (9)

The systematic absences in the diffraction data were consistent with the tetragonal space group I-4 with $Z = 8$ and $Z' = 1$. The data was refined as a twinned

data set with scales of 0.55(3) and 0.45(3). All hydrogen atoms, with the exception of the hydride ligand, were included into the model at geometrically calculated positions and refined using a riding model. The coordinates for the hydrogen atom bound to Rh1was located in the difference map. The goodness of fit on F^2 was 1.035 with R1(wR2) = 0.0573(0.1034) for [I>2sigma(I)] and with a largest difference peak and hole of 1.254 and -0.745(e.Å-3).

Table 3-21. Crystal data and structure refinement for $HRh(P^{Cy}{}_2N^{Ph}{}_2)_2$ (**9**)

Identification code	mo_p14016_0m	
Empirical formula	C56 H81 N4 P4 Rh	
Formula weight	1037.03	
Temperature	100(2) K	
Wavelength	0.71073 Å	
Crystal system	Tetragonal	
Space group	I-4	
Unit cell dimensions	a = 22.7640(7) Å	α = 90°.
	b = 22.7640(7) Å	β = 90°.
	c = 20.1397(5) Å	γ = 90°.
Volume	10436.4(7) $Å^3$	
Z	8	
Density (calculated)	1.320 Mg/m^3	
Absorption coefficient	0.491 mm^{-1}	
F(000)	4400	
Crystal size	0.28 x 0.14 x 0.13 mm^3	
Theta range for data collection	1.463 to 36.387°.	
Index ranges	-29<=h<=26, -29<=k<=29, -25<=l<=26	
Reflections collected	76059	
Independent reflections	11992 [R(int) = 0.0487]	
Completeness to theta = 25.00°	99.9 %	
Absorption correction	Semi-empirical from equivalents	
Max. and min. transmission	0.0942 and 0.0691	
Refinement method	Full-matrix least-squares on F^2	
Data / restraints / parameters	11992 / 0 / 591	
Goodness-of-fit on F^2	1.063	
Final R indices [I>2sigma(I)]	R1 = 0.0446, wR2 = 0.0972	
R indices (all data)	R1 = 0.0573, wR2 = 0.1035	
Extinction coefficient	not measured	
Largest diff. peak and hole	1.254 and -0.745 $e.Å^{-3}$	

Table 3-22. Bond lengths [Å] and angles [°] for $HRh(P^{Cy}{}_2N^{Ph}{}_2)_2$ (**9**)

Rh(1)-H	1.64(7)	Rh(1)-P(1)	2.2621(13)
Rh(1)-P(2)	2.2598(14)	Rh(1)-P(3)	2.1967(14)
Rh(1)-P(4)	2.2683(14)	P(1)-C(1)	1.864(5)
P(1)-C(3)	1.881(6)	P(1)-C(9)	1.867(5)
P(2)-C(2)	1.867(6)	P(2)-C(4)	1.875(6)
P(2)-C(27)	1.851(5)	P(3)-C(5)	1.845(7)
P(3)-C(7)	1.867(7)	P(3)-C(33)	1.844(5)
P(4)-C(6)	1.847(6)	P(4)-C(8)	1.889(6)
P(4)-C(51)	1.875(6)	N(1)-C(1)	1.452(7)
N(1)-C(2)	1.465(8)	N(1)-C(21)	1.374(8)
N(2)-C(3)	1.476(7)	N(2)-C(4)	1.470(7)
N(2)-C(15)	1.397(7)	N(3)-C(5)	1.457(8)
N(3)-C(6)	1.450(7)	N(3)-C(39)	1.399(7)
N(4)-C(7)	1.458(8)	N(4)-C(8)	1.434(8)
N(4)-C(45)	1.406(7)	C(1)-H(1A)	0.9900
C(1)-H(1B)	0.9900	C(2)-H(2A)	0.9900
C(2)-H(2B)	0.9900	C(3)-H(3A)	0.9900
C(3)-H(3B)	0.9900	C(4)-H(4A)	0.9900
C(4)-H(4B)	0.9900	C(5)-H(5A)	0.9900
C(5)-H(5B)	0.9900	C(6)-H(6A)	0.9900
C(6)-H(6B)	0.9900	C(7)-H(7A)	0.9900
C(7)-H(7B)	0.9900	C(8)-H(8A)	0.9900
C(8)-H(8B)	0.9900	C(9)-H(9)	1.0000
C(9)-C(10)	1.543(7)	C(9)-C(14)	1.534(8)
C(10)-H(10A)	0.9900	C(10)-H(10B)	0.9900
C(10)-C(11)	1.528(8)	C(11)-H(11A)	0.9900
C(11)-H(11B)	0.9900	C(11)-C(12)	1.513(8)
C(12)-H(12A)	0.9900	C(12)-H(12B)	0.9900
C(12)-C(13)	1.534(9)	C(13)-H(13A)	0.9900
C(13)-H(13B)	0.9900	C(13)-C(14)	1.533(7)
C(14)-H(14A)	0.9900	C(14)-H(14B)	0.9900
C(15)-C(16)	1.406(8)	C(15)-C(20)	1.408(8)
C(16)-H(16)	0.9500	C(16)-C(17)	1.386(9)

Table 3-22. (cont'd)

C(17)-H(17)	0.9500	C(17)-C(18)	1.364(10)
C(18)-H(18)	0.9500	C(18)-C(19)	1.374(10)
C(19)-H(19)	0.9500	C(19)-C(20)	1.392(9)
C(20)-H(20)	0.9500	C(21)-C(22)	1.420(8)
C(21)-C(26)	1.416(8)	C(22)-H(22)	0.9500
C(22)-C(23)	1.355(9)	C(23)-H(23)	0.9500
C(23)-C(24)	1.411(10)	C(24)-H(24)	0.9500
C(24)-C(25)	1.373(10)	C(25)-H(25)	0.9500
C(25)-C(26)	1.385(9)	C(26)-H(26)	0.9500
C(27)-H(27)	1.0000	C(27)-C(28)	1.533(8)
C(27)-C(32)	1.532(8)	C(28)-H(28A)	0.9900
C(28)-H(28B)	0.9900	C(28)-C(29)	1.534(8)
C(29)-H(29A)	0.9900	C(29)-H(29B)	0.9900
C(29)-C(30)	1.504(9)	C(30)-H(30A)	0.9900
C(30)-H(30B)	0.9900	C(30)-C(31)	1.500(10)
C(31)-H(31A)	0.9900	C(31)-H(31B)	0.9900
C(31)-C(32)	1.532(8)	C(32)-H(32A)	0.9900
C(32)-H(32B)	0.9900	C(33)-H(33)	1.0000
C(33)-C(34)	1.520(8)	C(33)-C(38)	1.528(8)
C(34)-H(34A)	0.9900	C(34)-H(34B)	0.9900
C(34)-C(35)	1.529(8)	C(35)-H(35A)	0.9900
C(35)-H(35B)	0.9900	C(35)-C(36)	1.516(9)
C(36)-H(36A)	0.9900	C(36)-H(36B)	0.9900
C(36)-C(37)	1.503(10)	C(37)-H(37A)	0.9900
C(37)-H(37B)	0.9900	C(37)-C(38)	1.534(9)
C(38)-H(38A)	0.9900	C(38)-H(38B)	0.9900
C(39)-C(40)	1.406(8)	C(39)-C(44)	1.387(8)
C(40)-H(40)	0.9500	C(40)-C(41)	1.361(10)
C(41)-H(41)	0.9500	C(41)-C(42)	1.380(11)
C(42)-H(42)	0.9500	C(42)-C(43)	1.373(11)
C(43)-H(43)	0.9500	C(43)-C(44)	1.389(10)
C(44)-H(44)	0.9500	C(45)-C(46)	1.408(9)
C(45)-C(50)	1.401(9)	C(46)-H(46)	0.9500

Table 3-22. (cont'd)

C(46)-C(47)	1.372(9)	C(47)-H(47)	0.9500
C(47)-C(48)	1.373(11)	C(48)-H(48)	0.9500
C(48)-C(49)	1.349(12)	C(49)-H(49)	0.9500
C(49)-C(50)	1.402(10)	C(50)-H(50)	0.9500
C(51)-H(51)	1.0000	C(51)-C(52)	1.531(9)
C(51)-C(56)	1.532(8)	C(52)-H(52A)	0.9900
C(52)-H(52B)	0.9900	C(52)-C(53)	1.520(9)
C(53)-H(53A)	0.9900	C(53)-H(53B)	0.9900
C(53)-C(54)	1.555(10)	C(54)-H(54A)	0.9900
C(54)-H(54B)	0.9900	C(54)-C(55)	1.500(9)
C(55)-H(55A)	0.9900	C(55)-H(55B)	0.9900
C(55)-C(56)	1.514(8)	C(56)-H(56A)	0.9900
C(56)-H(56B)	0.9900	P(1)-Rh(1)-H	83(2)
P(1)-Rh(1)-P(4)	113.62(5)	P(2)-Rh(1)-H	79(2)
P(2)-Rh(1)-P(1)	81.72(5)	P(2)-Rh(1)-P(4)	115.66(5)
P(3)-Rh(1)-H	79(2)	P(3)-Rh(1)-P(1)	138.66(5)
P(3)-Rh(1)-P(2)	129.84(6)	P(3)-Rh(1)-P(4)	79.32(5)
P(4)-Rh(1)-H	158(2)	C(1)-P(1)-Rh(1)	112.54(18)
C(1)-P(1)-C(3)	97.2(3)	C(1)-P(1)-C(9)	100.7(2)
C(3)-P(1)-Rh(1)	113.4(2)	C(9)-P(1)-Rh(1)	127.65(18)
C(9)-P(1)-C(3)	100.5(2)	C(2)-P(2)-Rh(1)	113.4(2)
C(2)-P(2)-C(4)	96.0(3)	C(4)-P(2)-Rh(1)	117.36(19)
C(27)-P(2)-Rh(1)	125.95(18)	C(27)-P(2)-C(2)	100.0(3)
C(27)-P(2)-C(4)	98.8(3)	C(5)-P(3)-Rh(1)	119.1(2)
C(5)-P(3)-C(7)	96.4(4)	C(7)-P(3)-Rh(1)	115.5(3)
C(33)-P(3)-Rh(1)	121.99(18)	C(33)-P(3)-C(5)	101.8(3)
C(33)-P(3)-C(7)	97.2(3)	C(6)-P(4)-Rh(1)	116.92(19)
C(6)-P(4)-C(8)	98.6(3)	C(6)-P(4)-C(51)	96.4(3)
C(8)-P(4)-Rh(1)	111.8(2)	C(51)-P(4)-Rh(1)	130.7(2)
C(51)-P(4)-C(8)	96.6(3)	C(1)-N(1)-C(2)	113.2(5)
C(21)-N(1)-C(1)	123.0(5)	C(21)-N(1)-C(2)	122.8(5)
C(4)-N(2)-C(3)	118.1(4)	C(15)-N(2)-C(3)	115.2(4)
C(15)-N(2)-C(4)	114.4(4)	C(6)-N(3)-C(5)	112.2(6)

Table 3-22. (cont'd)

C(39)-N(3)-C(5)	120.3(5)	C(39)-N(3)-C(6)	118.2(5)
C(8)-N(4)-C(7)	122.4(5)	C(45)-N(4)-C(7)	113.6(5)
C(45)-N(4)-C(8)	113.9(5)	P(1)-C(1)-H(1A)	108.3
P(1)-C(1)-H(1B)	108.3	N(1)-C(1)-P(1)	116.0(4)
N(1)-C(1)-H(1A)	108.3	N(1)-C(1)-H(1B)	108.3
H(1A)-C(1)-H(1B)	107.4	P(2)-C(2)-H(2A)	108.7
P(2)-C(2)-H(2B)	108.7	N(1)-C(2)-P(2)	114.2(4)
N(1)-C(2)-H(2A)	108.7	N(1)-C(2)-H(2B)	108.7
H(2A)-C(2)-H(2B)	107.6	P(1)-C(3)-H(3A)	108.5
P(1)-C(3)-H(3B)	108.5	N(2)-C(3)-P(1)	115.1(4)
N(2)-C(3)-H(3A)	108.5	N(2)-C(3)-H(3B)	108.5
H(3A)-C(3)-H(3B)	107.5	P(2)-C(4)-H(4A)	108.6
P(2)-C(4)-H(4B)	108.6	N(2)-C(4)-P(2)	114.7(4)
N(2)-C(4)-H(4A)	108.6	N(2)-C(4)-H(4B)	108.6
H(4A)-C(4)-H(4B)	107.6	P(3)-C(5)-H(5A)	108.2
P(3)-C(5)-H(5B)	108.2	N(3)-C(5)-P(3)	116.3(4)
N(3)-C(5)-H(5A)	108.2	N(3)-C(5)-H(5B)	108.2
H(5A)-C(5)-H(5B)	107.4	P(4)-C(6)-H(6A)	108.0
P(4)-C(6)-H(6B)	108.0	N(3)-C(6)-P(4)	117.2(4)
N(3)-C(6)-H(6A)	108.0	N(3)-C(6)-H(6B)	108.0
H(6A)-C(6)-H(6B)	107.2	P(3)-C(7)-H(7A)	108.1
P(3)-C(7)-H(7B)	108.1	N(4)-C(7)-P(3)	116.9(5)
N(4)-C(7)-H(7A)	108.1	N(4)-C(7)-H(7B)	108.1
H(7A)-C(7)-H(7B)	107.3	P(4)-C(8)-H(8A)	107.9
P(4)-C(8)-H(8B)	107.9	N(4)-C(8)-P(4)	117.7(4)
N(4)-C(8)-H(8A)	107.9	N(4)-C(8)-H(8B)	107.9
H(8A)-C(8)-H(8B)	107.2	P(1)-C(9)-H(9)	109.0
C(10)-C(9)-P(1)	108.9(4)	C(10)-C(9)-H(9)	109.0
C(14)-C(9)-P(1)	110.6(4)	C(14)-C(9)-H(9)	109.0
C(14)-C(9)-C(10)	110.2(4)	C(9)-C(10)-H(10A)	109.2
C(9)-C(10)-H(10B)	109.2	H(10A)-C(10)-H(10B)	107.9
C(11)-C(10)-C(9)	112.2(5)	C(11)-C(10)-H(10A)	109.2
C(11)-C(10)-H(10B)	109.2	C(10)-C(11)-H(11A)	109.3

Table 3-22. (cont'd)

C(10)-C(11)-H(11B)	109.3	H(11A)-C(11)-H(11B)	108.0
C(12)-C(11)-C(10)	111.6(5)	C(12)-C(11)-H(11A)	109.3
C(12)-C(11)-H(11B)	109.3	C(11)-C(12)-H(12A)	109.6
C(11)-C(12)-H(12B)	109.6	C(11)-C(12)-C(13)	110.1(5)
H(12A)-C(12)-H(12B)	108.2	C(13)-C(12)-H(12A)	109.6
C(13)-C(12)-H(12B)	109.6	C(12)-C(13)-H(13A)	109.5
C(12)-C(13)-H(13B)	109.5	H(13A)-C(13)-H(13B)	108.1
C(14)-C(13)-C(12)	110.6(5)	C(14)-C(13)-H(13A)	109.5
C(14)-C(13)-H(13B)	109.5	C(9)-C(14)-H(14A)	109.1
C(9)-C(14)-H(14B)	109.1	C(13)-C(14)-C(9)	112.4(5)
C(13)-C(14)-H(14A)	109.1	C(13)-C(14)-H(14B)	109.1
H(14A)-C(14)-H(14B)	107.9	N(2)-C(15)-C(16)	121.4(5)
N(2)-C(15)-C(20)	123.1(5)	C(16)-C(15)-C(20)	115.4(5)
C(15)-C(16)-H(16)	119.3	C(17)-C(16)-C(15)	121.4(6)
C(17)-C(16)-H(16)	119.3	C(16)-C(17)-H(17)	118.8
C(18)-C(17)-C(16)	122.4(6)	C(18)-C(17)-H(17)	118.8
C(17)-C(18)-H(18)	121.2	C(17)-C(18)-C(19)	117.6(6)
C(19)-C(18)-H(18)	121.2	C(18)-C(19)-H(19)	119.3
C(18)-C(19)-C(20)	121.5(7)	C(20)-C(19)-H(19)	119.3
C(15)-C(20)-H(20)	119.2	C(19)-C(20)-C(15)	121.6(6)
C(19)-C(20)-H(20)	119.2	N(1)-C(21)-C(22)	122.0(5)
N(1)-C(21)-C(26)	122.9(5)	C(26)-C(21)-C(22)	115.1(6)
C(21)-C(22)-H(22)	118.6	C(23)-C(22)-C(21)	122.7(6)
C(23)-C(22)-H(22)	118.6	C(22)-C(23)-H(23)	119.5
C(22)-C(23)-C(24)	120.9(6)	C(24)-C(23)-H(23)	119.5
C(23)-C(24)-H(24)	121.1	C(25)-C(24)-C(23)	117.9(6)
C(25)-C(24)-H(24)	121.1	C(24)-C(25)-H(25)	119.3
C(24)-C(25)-C(26)	121.5(6)	C(26)-C(25)-H(25)	119.3
C(21)-C(26)-H(26)	119.1	C(25)-C(26)-C(21)	121.8(6)
C(25)-C(26)-H(26)	119.1	P(2)-C(27)-H(27)	108.9
C(28)-C(27)-P(2)	110.7(4)	C(28)-C(27)-H(27)	108.9
C(32)-C(27)-P(2)	110.8(4)	C(32)-C(27)-H(27)	108.9
C(32)-C(27)-C(28)	108.5(5)	C(27)-C(28)-H(28A)	109.2

Table 3-22. (cont'd)

C(27)-C(28)-H(28B)	109.2	C(27)-C(28)-C(29)	112.1(5)
H(28A)-C(28)-H(28B)	107.9	C(29)-C(28)-H(28A)	109.2
C(29)-C(28)-H(28B)	109.2	C(28)-C(29)-H(29A)	109.4
C(28)-C(29)-H(29B)	109.4	H(29A)-C(29)-H(29B)	108.0
C(30)-C(29)-C(28)	111.3(5)	C(30)-C(29)-H(29A)	109.4
C(30)-C(29)-H(29B)	109.4	C(29)-C(30)-H(30A)	109.2
C(29)-C(30)-H(30B)	109.2	H(30A)-C(30)-H(30B)	107.9
C(31)-C(30)-C(29)	111.9(6)	C(31)-C(30)-H(30A)	109.2
C(31)-C(30)-H(30B)	109.2	C(30)-C(31)-H(31A)	109.1
C(30)-C(31)-H(31B)	109.1	C(30)-C(31)-C(32)	112.4(5)
H(31A)-C(31)-H(31B)	107.8	C(32)-C(31)-H(31A)	109.1
C(32)-C(31)-H(31B)	109.1	C(27)-C(32)-C(31)	111.1(5)
C(27)-C(32)-H(32A)	109.4	C(27)-C(32)-H(32B)	109.4
C(31)-C(32)-H(32A)	109.4	C(31)-C(32)-H(32B)	109.4
H(32A)-C(32)-H(32B)	108.0	P(3)-C(33)-H(33)	108.0
C(34)-C(33)-P(3)	112.3(4)	C(34)-C(33)-H(33)	108.0
C(34)-C(33)-C(38)	108.0(5)	C(38)-C(33)-P(3)	112.3(4)
C(38)-C(33)-H(33)	108.0	C(33)-C(34)-H(34A)	109.3
C(33)-C(34)-H(34B)	109.3	C(33)-C(34)-C(35)	111.8(5)
H(34A)-C(34)-H(34B)	107.9	C(35)-C(34)-H(34A)	109.3
C(35)-C(34)-H(34B)	109.3	C(34)-C(35)-H(35A)	109.4
C(34)-C(35)-H(35B)	109.4	H(35A)-C(35)-H(35B)	108.0
C(36)-C(35)-C(34)	111.3(5)	C(36)-C(35)-H(35A)	109.4
C(36)-C(35)-H(35B)	109.4	C(35)-C(36)-H(36A)	109.6
C(35)-C(36)-H(36B)	109.6	H(36A)-C(36)-H(36B)	108.1
C(37)-C(36)-C(35)	110.5(5)	C(37)-C(36)-H(36A)	109.6
C(37)-C(36)-H(36B)	109.6	C(36)-C(37)-H(37A)	109.4
C(36)-C(37)-H(37B)	109.4	C(36)-C(37)-C(38)	111.2(6)
H(37A)-C(37)-H(37B)	108.0	C(38)-C(37)-H(37A)	109.4
C(38)-C(37)-H(37B)	109.4	C(33)-C(38)-C(37)	110.3(5)
C(33)-C(38)-H(38A)	109.6	C(33)-C(38)-H(38B)	109.6
C(37)-C(38)-H(38A)	109.6	C(37)-C(38)-H(38B)	109.6
H(38A)-C(38)-H(38B)	108.1	N(3)-C(39)-C(40)	121.8(5)

Table 3-22. (cont'd)

C(44)-C(39)-N(3)	122.8(5)	C(44)-C(39)-C(40)	115.4(6)
C(39)-C(40)-H(40)	118.6	C(41)-C(40)-C(39)	122.7(6)
C(41)-C(40)-H(40)	118.6	C(40)-C(41)-H(41)	119.6
C(40)-C(41)-C(42)	120.8(6)	C(42)-C(41)-H(41)	119.6
C(41)-C(42)-H(42)	120.9	C(43)-C(42)-C(41)	118.2(7)
C(43)-C(42)-H(42)	120.9	C(42)-C(43)-H(43)	119.5
C(42)-C(43)-C(44)	120.9(7)	C(44)-C(43)-H(43)	119.5
C(39)-C(44)-C(43)	121.9(6)	C(39)-C(44)-H(44)	119.1
C(43)-C(44)-H(44)	119.1	N(4)-C(45)-C(46)	121.0(6)
C(50)-C(45)-N(4)	122.7(6)	C(50)-C(45)-C(46)	116.3(6)
C(45)-C(46)-H(46)	119.3	C(47)-C(46)-C(45)	121.3(7)
C(47)-C(46)-H(46)	119.3	C(46)-C(47)-H(47)	119.1
C(46)-C(47)-C(48)	121.8(7)	C(48)-C(47)-H(47)	119.1
C(47)-C(48)-H(48)	120.9	C(49)-C(48)-C(47)	118.1(7)
C(49)-C(48)-H(48)	120.9	C(48)-C(49)-H(49)	118.9
C(48)-C(49)-C(50)	122.2(8)	C(50)-C(49)-H(49)	118.9
C(45)-C(50)-C(49)	120.3(7)	C(45)-C(50)-H(50)	119.9
C(49)-C(50)-H(50)	119.9	P(4)-C(51)-H(51)	108.7
C(52)-C(51)-P(4)	110.4(4)	C(52)-C(51)-H(51)	108.7
C(52)-C(51)-C(56)	110.3(5)	C(56)-C(51)-P(4)	109.9(4)
C(56)-C(51)-H(51)	108.7	C(51)-C(52)-H(52A)	108.8
C(51)-C(52)-H(52B)	108.8	H(52A)-C(52)-H(52B)	107.7
C(53)-C(52)-C(51)	113.7(5)	C(53)-C(52)-H(52A)	108.8
C(53)-C(52)-H(52B)	108.8	C(52)-C(53)-H(53A)	110.0
C(52)-C(53)-H(53B)	110.0	C(52)-C(53)-C(54)	108.3(6)
H(53A)-C(53)-H(53B)	108.4	C(54)-C(53)-H(53A)	110.0
C(54)-C(53)-H(53B)	110.0	C(53)-C(54)-H(54A)	109.8
C(53)-C(54)-H(54B)	109.8	H(54A)-C(54)-H(54B)	108.3
C(55)-C(54)-C(53)	109.2(6)	C(55)-C(54)-H(54A)	109.8
C(55)-C(54)-H(54B)	109.8	C(54)-C(55)-H(55A)	109.1
C(54)-C(55)-H(55B)	109.1	C(54)-C(55)-C(56)	112.4(6)
H(55A)-C(55)-H(55B)	107.8	C(56)-C(55)-H(55A)	109.1
C(56)-C(55)-H(55B)	109.1	C(51)-C(56)-H(56A)	109.2

Table 3-22. (cont'd)

C(51)-C(56)-H(56B)	109.2	C(55)-C(56)-C(51)	112.0(5)
C(55)-C(56)-H(56A)	109.2	C(55)-C(56)-H(56B)	109.2
H(56A)-C(56)-H(56B)	107.9		

3.6.9 Copyright note

Much of the material in this chapter comes from a manuscript entitled "Incorporation of pendant bases into Rh(diphosphine)$_2$ complexes: Synthesis, thermodynamic studies, and catalytic CO_2 hydrogenation activity of $[Rh(P_2N_2)_2]^+$ complexes," by Alyssia M. Lilio, Mark H. Reineke, Curtis E. Moore, Arnold L Rheingold, Michael K. Takase, and Clifford P. Kubiak. The dissertation author is the primary author of this manuscript.

Chapter 4

Studies of electrocatalytic reduction of CO_2 with $[Rh(P_2N_2)_2]^+$ complexes

4.1 Introduction

Along with being active for CO_2 hydrogenation to formate, rhodium bis-diphosphine complexes are active for the electrochemical reduction of CO_2 to formate. We initially set out to synthesize $Rh(P_2N_2)_2$ complexes not for studies of their hydrogenation chemistry, but to look at how the addition of the proton-relay-containing ligand affected their electrochemical CO_2 reduction activity, hoping that the proton concentrating P_2N_2 ligands would enhance the electrochemical CO_2 reduction activity of the Rh bis-diphosphine platform. The first record of CO_2 reduction to formate by rhodium bis-diphosphine complexes was reported in 1984 (diphosphine = dppe).[1] Since that report, rhodium bis-diphosphine complexes have not received any more study for CO_2 electro-reduction, likely because the less than optimal faradaic efficiencies of 50%, the large overpotentials, and the cost of rhodium, which would prevent a

catalyst that was not exceptionally active to be used for any kind of large scale conversion of CO_2. Despite this, we decided it was worth trying to improve this system with proton-relay-containing ligands. Currently, even though there is great interest in the enhancement of electrocatalytic reactivity in homogeneous catalysts for CO_2 reduction through co-operative second coordination sphere interactions, there are few examples where a catalysts for CO_2 reduction has been significantly improved though modifications in the second coordination sphere. Some of these examples have been discussed in Chapter 1. We hoped through our studies of the $[Rh(P_2N_2)_2]^+$ system, we might be able to add to these.

In this chapter, we explored the electrochemical reactivity of several of the $Rh(P_2N_2)_2$ complexes described in the previous chapter. Unfortunately, the rhodium complexes are not stable under electrolysis conditions, making it difficult to determine the products of their reduction in the presence of the substrates. Because of this we were also not able to determine whether the addition of the proton-relaying ligand improved CO_2 reduction with the $[Rh(P_2N_2)_2]^+$ complexes.

4.2 Experimental

Materials and Methods

Unless otherwise noted, all reactions were carried out under a N_2 atmosphere using standard Schlenk and glovebox techniques. Acetone was dried over 4Å molecular sieves and degassed prior to use. All other solvents used were dried over activated molecular sieves and alumina and degassed prior to use. Tetrabutylammonium hexafluorophosphate (NBu_4PF_6) was recrystallized from methanol prior to use. All other chemicals were obtained from commercial suppliers and used without further purification. All Rh complexes were synthesized as described in the previous chapter.

General Electrochemical Experiments

All solvents used were dried over activated molecular sieves and alumina and degassed prior to use. Electrochemical experiments were performed using a BAS Epsilon potentiostat. Initial cyclic voltammograms (CV's) were performed under nitrogen in a one compartment cell using a glassy carbon BASi working electrode, a glassy carbon rod counter electrode, and a non-aqueous Ag pseudo reference electrode from BASi (silver wire in a 0.2 M TBAH and 1mM $AgNO_3$ acetonitrile solution separated from the working compartment by porous Vycor (4mm). All experiments were performed in dry acetonitrile using 0.2 M NBu_4PF_6 as the supporting electrolyte. The CV's were carried out using 7 mL volumes of electrolyte solution with 1 mM catalysts concentrations. Initial CV's were taken under an inert N_2 atmosphere. For CO_2 CV's, these solutions were sparged with CO_2 prior to the addition of aliquots of TFE. For control studies, aliquots of TFE were added to solutions under a N_2 atmosphere.

4.3 Results and Discussion

4.3.1 Electrochemical reactivity with CO_2

In Chapter 3 we showed that the $[Rh(P_2N_2)_2]^+$ complexes show reversible two electron reductions under an inert atmosphere corresponding to the Rh(I/–I) couple. They also show an irreversible oxidation that occurs near 500 mV, which is assigned to the Rh(I/II) couple (**Figure 4-1**). Four of these Rh complexes, $[Rh(P^{Ph}{}_2N^{Ph}{}_2)_2]^+$ (**1**), $[Rh(P^{Ph}{}_2N^{Bn}{}_2)_2]^+$ (**2**), $[Rh(P^{Ph}{}_2N^{PhOMe}{}_2)_2]^+$ (**3**), $[Rh(P^{Cy}{}_2N^{Ph}{}_2)_2]^+$ (**4**), were tested for their reactivity with CO_2 with and without an added proton source. Based on the previous report of CO_2 reduction to formate with $[Rh(dppe)_2]^+$, we expected all complexes would show catalytic current under CO_2 without protons, but that we would see significantly more current when a proton source was added. We planned to compare these CV's to those of another $[Rh(diphosphine)_2]^+$ complex with ligands that have no proton relays.

1mM solutions of complexes **1**–**4** were sparged with CO_2 for 5 minutes and CV's were taken to confirm reactivity with CO_2. All complexes showed changes in their CV's after the solutions were sparged with CO_2. For complexes **1-3**, the phenylphosphine analogues, there was no change in current at the Rh(I/–I) couple, but there was a new irreversible peak that closely followed and a loss of reversibility of the Rh(I/–I) couple, indicating a reaction with CO_2 and the formation of a new complex. After scanning through the new peak and then scanning back to the oxidation assigned to the Rh I/II couple, the position of the oxidation has become more positive, indicating that a new species was now being oxidized. When the solution was then sparged with N_2, the original CV returned. For complex **4**, $[Rh(P^{Cy}{}_2N^{Ph}{}_2)_2]^+$, there is a significant current enhancement around the Rh(I/–I) couple, resembling the electrochemistry of the previously reported CO_2 reduction catalysts, $[Rh(dppe)_2]^+$.

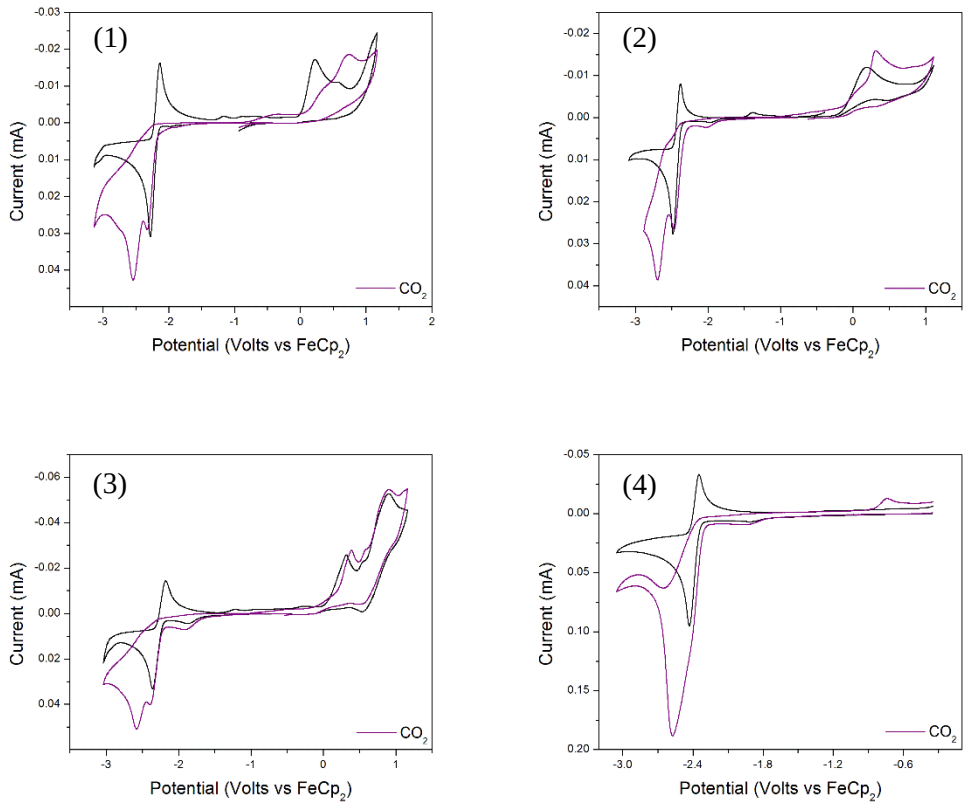

Figure 4-1. CV's of 1 mM solutions of $(Rh(P^{Ph}{}_2N^{Ph}{}_2)_2]^+$ (**1**), $(Rh(P^{Ph}{}_2{}^{Bn}{}_2)_2]^+$ (**2**), $(Rh(P^{Ph}{}_2N^{PhOMe}{}_2)_2]^+$ (**3**) and $(Rh(P^{Cy}{}_2N^{Ph}{}_2)_2]^+$ (**4**) under an N_2 atmosphere (black) and a CO_2 atmosphere (purple).

4.3.2 Reactivity with an added proton source

Next, varying concentrations of a proton source were added. 2,2,2-triflouroethanol,TFE (p*K*a = 12.5), was chosen as the proton source because the potentials at which the Rh complexes are reduced is fairly negative and when experiments were attempted with stronger proton sources, background reduction of protons by the electrode dominated the CV's. For further studies, we chose to focus on two of the complexes, complex **1** which showed a new reduction peak after CO_2 was added, and **4** which showed catalytic current around the Rh(I/–I) couple when CO_2 was added. We also expected that these complexes should be able

to reduce protons to make H_2, so we compared their CO_2 and TFE activity with their activity when only TFE was added.

For the first case, $[Rh(P^{Ph}{}_2N^{Ph}{}_2)_2]^+$ (**1**), there is a significant enhancement around the second reduction peak when TFE is added, and the catalytic current continued to increase as more TFE was added, leveling off after 125 uL. When the experiment was repeated in the absence of CO_2, there was also a significant enhancement in current, which is attributed to proton reduction. The amplitude of the catalytic current was significantly larger than when CO_2 was present for the same amount of added TFE. This could be indicative of CO_2 reduction dominating over protons and inhibiting proton reduction. There is also a difference in the shape if the catalytic CV's when CO_2 is and is not present, which could be indicative of a different mechanism for catalysis under the two conditions.

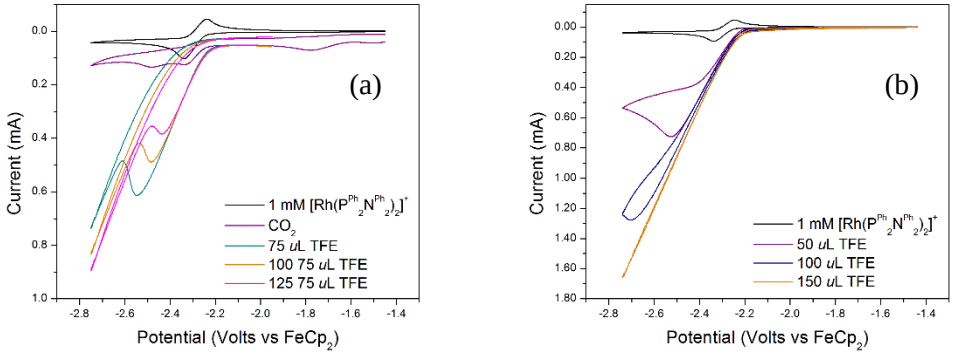

Figure 4-2. CV's showing the responses of complex **1** with CO_2 and increasing amounts of TFE (a) and complex **1** with increasing amounts of TFE under N_2 (b).

The CV's with complex **4**, $[Rh(P^{Cy}{}_2N^{Ph}{}_2)_2]^+$, under a CO_2 atmosphere with added TFE show a significant current increase that starts near the Rh(I/–I) reduction potential, which is further increased as more TFE is added. The catalytic current begins to level off as 200 uL of TFE is added. When the experiment was repeated without the addition of CO_2, there was also a large increase in current at the Rh(I/–I) reduction potential, but like the previous complex,

the catalytic current is significantly larger when no CO_2 was added and the shapes of the catalytic voltammograms are very different than when CO_2 is present.

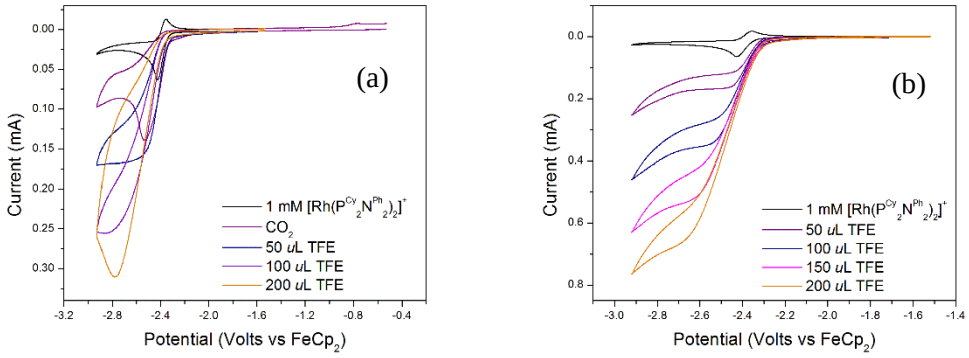

Figure 4-3. CV's showing the responses of complex **4** with CO_2 and increasing amounts of TFE (a) and complex **4** with increasing amounts of TFE under N_2 (b).

The enhancements in current under CO_2 and TFE and differences in the shapes of the CV's and the amounts of catalytic current when compared to the CV's where only protons were present was promising, but to determine if the current enhancement is due to anything more than just proton reduction, the products of the reduction need to be observed and quantified. To do this, we attempted bulk electrolysis of both complexes **1** and **4** to generate products for analysis and quantification.

Controlled potential electrolysis on 1mM solutions of complexes **1** and **4** were attempted under a CO_2 atmosphere and under a CO_2 atmosphere with 30 equivalents to TFE. Unfortunately, these complex are unstable under bulk electrolysis conditions. When the potential is held just negative of the reduction potentials for prolonged periods of time, the current significantly diminishes quickly (current is near background current after 10 min of electrolysis), and we were unable to pass enough charge to generate any significant build-up of products in order to identify and quantify them. We did not further explore what the Rh complexes were degrading to under electrolysis conditions.

4.4 Conclusions

The preliminary results for the electrochemical reduction of CO_2 in the presence of the $[Rh(P_2N_2)_2]^+$ were promising. For the cyclohexyl phosphine containing complex, there is a significant enhancement in current at the potential of the Rh(I/–I) couple, and that current is further enhanced in the presence of a weak proton source. For the phenyl phosphine containing complexes, there is also reactivity with CO_2. When scanning cathodically, and a new peak appears that may be due to a CO_2 bound species, but there is no significant enhancement in current until a proton source is added. These complexes also reduce protons at similar potentials, but comparisons of the CV's in the presence of CO_2 and protons to the CV's with only added protons indicant that there is a difference in the rates of catalysis which may show some preference for CO_2 reduction over proton reduction. Unfortunately, these complexes are unstable under electrolysis conditions, preventing us from determining and quantifying the reduction products in the presence of substrate and from conducting further studies to determine whether these complexes are any better at reduction CO_2 than non-pendant-amine-containing analogues.

4.5 References

(1) Slater, S.; Wagenknecht, J. H. *J. Am. Chem. Soc.* , **1984**, *106*, 5367-5368.

Chapter 5

Investigation of the redox reactivity of Ru and Fe pincer complexes

5.1 Introduction

In our group's 2009 review of homogeneous CO_2 reduction catalysis, we recommended that the best way to achieve CO_2 reduction beyond the usual $2e^-$ reduction products to the methanol oxidation state may be to use several catalysts in series.[1] A panel of catalysts, either for the electrochemical reduction or for the hydrogenation of CO_2, optimized for a series of sequential $2e^-$ reductions, could provide a means to efficiently and selectively take CO_2 to methanol. This method would likely be much easier than finding one catalyst that could handle the reduction to CO_2 all the way to methanol, although it should be noted that there has been a recent report of this happening at a single homogeneous catalyst site. Leitner and co-workers recently reported the direct hydrogenation of CO_2 to methanol by a single Ru(II) complex [(triphos)Ru(trimethylenemethane)$_2$] in the presence of organic acids showing

turnover numbers up to 221.[2] At the present, this is the only homogeneous single site catalysts for the reduction of CO_2 to methanol.

In 2011, the Sanford group successfully used a panel catalysis method to sequentially convert CO_2 to methanol.[3] The system consisted of 3 homogenous catalysts (**1**-**3**) that operate in tandem as shown in **Scheme 5-1** to hydrogenate CO_2 to methanol. For the first catalyst the well-known Jessop's Ru catalyst was used for the hydrogenation of CO_2 to formic acid. The second catalysts was a lewis acid to catalyze the esterification of formic acid to yield methylformate. The final catalyst used was one of the RuPNN catalysts (shown in **Scheme 5-1** as catalysts **3a** and **3b**) developed by Milstein and co-workers,[4,5] which were shown to be effective for the hydrogenation of methylformate to methanol in this publication and in a report from Milstein and co-workers that was published around the same time.[6] These Ru complexes are very interesting because they represent the only homogeneous catalysts reported to date that can hydrogenate alkylformates. Their unique mode of reactivity is discussed in the next paragraph. This cascade catalysis system provided support for the viability of the panel catalysis method that we had hoped to implement for the electrochemical reduction CO_2 to methanol, got us interested in methylformate as an activated form of formic acid to reduce, and also sparked our interest in the unique activity in Milstein's RuPNN catalysts.

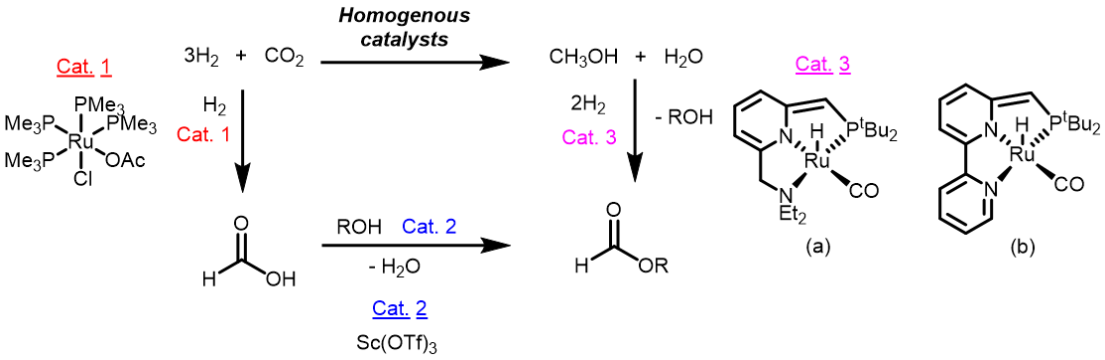

Scheme 5-1. Cascade catalysis scheme for the hydrogenation of CO_2 to methanol.

The Ru pincer complexes **3a** and **3b** shown in **Scheme 5-1** are capable of catalyzing the conversion of alcohols to esters,[7] the conversion of esters to alcohols,[5] the dehydrogenation of amines to amides,[8] and the hydrogenation of amides.[4] As mentioned previously, they are also capable of the hydrogenation of formates, as well as organic carbamates and carbonates[6] and the hydrogenation of CO_2 to formate.[9] After the reports of the unique activity of these complexes, there were reports of analogous Ru complexes with CNN ligands in which the phosphines of complexes **3a** and **3b** have been replaced with N-heterocyclic carbenes. These complexes were shown to hydrogenate un-activated esters under mild conditions.[10,11] The proposed mechanisms of reactivity in these complexes involves the ability of the catalysts to be de-protonated at the methylene "arm" of the ligand leading to de-aromatization of the pyridine rings. In the hydrogenation catalysis mechanisms, the de-aromatized complexes react with H_2, adding it across the metal center and the methylene arm to make the dihydrogen complexes that are the active species in catalysis. The re-protonated methylene arm can then serve as a proton donor to substrates that have inserted into the Ru–H bond to help stabilize intermediates through hydrogen bonding interactions or to transfer a proton to the substrate. The proposed mechanism for methylformate hydrogenation by RuPNN complexes, shown in **Scheme 5-2**, exhibits this kind of reactivity. This new type of metal-ligand co-operation involving de-aromatization/aromatization is now receiving extensive study in the development of bi-functional hydrogenation catalysts and has been reviewed recently.[12,13] This new cooperativity has not yet been explored in electrochemical catalysis.

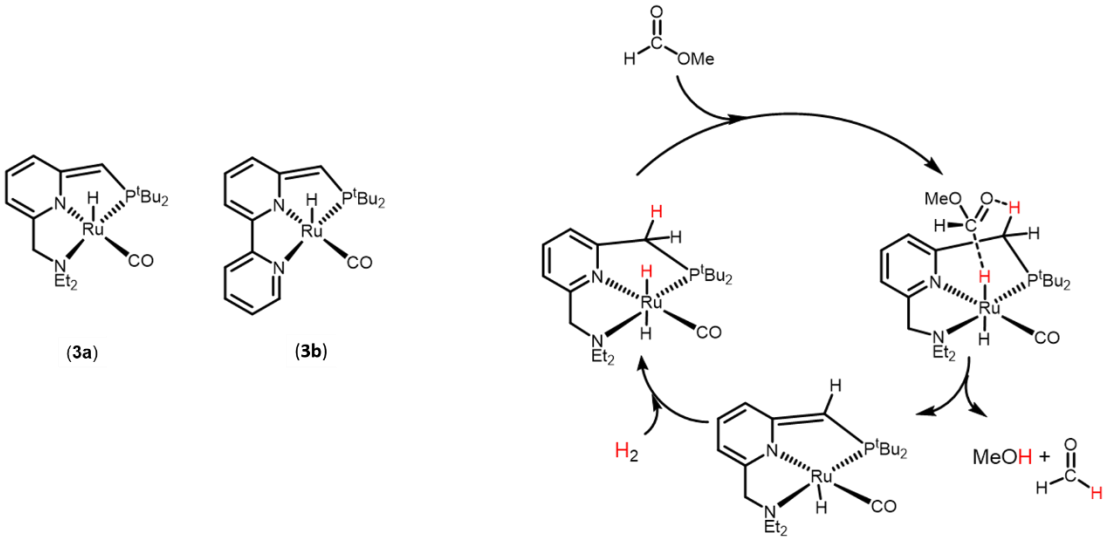

Scheme 5-2. Mechanism of the hydrogenation of methylformate by RuPNN complexes.

Currently, there is great interest in transforming traditional thermal hydrogenation catalysts into electrocatalysts. Having the reducing equivalents delivered as protons and electrons instead of pressurized H_2 gas would help remove or lessen two of the bottlenecks that often slow down thermal catalysts, H_2 activation and the release of the reduction product. Despite this growing interests, there are few electrocatalytic mechanisms for CO_2 reduction that involve metal hydrides, and none for the reduction of formates, to our knowledge. In a report by Deronzier and co-workers, Ir and Rh complexes that were known hydrogenation catalysts were used to reduce CO_2 to formate through electrochemically generated hydride complexes, albeit with low efficiencies.[14] A major difficulty in the implementation of this strategy is in generating a metal hydride that is sufficiently hydridic for substrate insertion, but is able to coexist in the presence of an excess of a proton source for hydride regeneration, without the generation of significant amounts of H_2. This makes obtaining selective catalysts under these conditions difficult. In 2012, Brookhart and Meyer were the first to demonstrate the feasibility of adapting a hydrogenation catalysts for the selective electrochemical reduction

of CO_2 to HCOOH. Catalysis happens though an electrochemically generated Ir dihydride complex that is stable in the presence or water, but is able to insert CO_2. Since this report, there have likely been several similar attempts at converting CO_2 hydrogenation catalysts into electrocatalysts, but to our knowledge there have not been any other successful reports.

We hoped that electrochemical studies of Milstein's Ru complexes would produce similar results as the Ir pincer system discussed above, and that the acidic methylene protons might be able to have stabilizing interactions with an inserted substrate, as is seen in the hydrogenation mechanisms. We decided to study these complexes for electrocatalytic methylformate and CO_2 reduction. Being that our main interest is electrocatalytic reductions, we focused on the Ru pincer complexes that have redox active ligands. This could produce metal complexes able to accept multiple electrons at favorable potentials and would hopefully produce catalysts that could operate via $2e^-$ reduction pathways with low overpotentials.

We were also interested in exploring both the thermal hydrogenation activity and the electrochemical reactivity of iron analogues of these complexes. Ruthenium is a rare and expensive metal and the extension of this kind of hydrogenation activity to inexpensive and abundant first row metals is of great interest. Recently, there has been progress in the development of Fe complexes for the hydrogenation of polar bonds. In 2007, Casey et al. reported the bi-functional complex [{2,5-$(SiMe_3)_2$-3,4-$(CH_2)_4$(η^5-C_4COH)}$Fe(CO)_2H$], which catalyzes the hydrogenation of ketones under mild conditions. [15] In 2009, Morris et al. reported the hydrogenation of acetophenone by diiminodiphosphine and diaminodiphosphine iron complexes under high pressures.[16] In 2011, Milstein published a lutidine based diphosphine PNP pincer system that was capable of hydrogenating ketones under mild conditions,[17] and active for the hydrogenation of CO_2, the most active Fe catalysts that had been reported for CO_2 hydrogenation to date.[18] Both mechanisms are thought to involve bi-functional metal-ligand co-operative activity as is invoked in the mechanisms for hydrogenation by the RuPNN

complexes discussed previously. Since these reports, there have been several similar reports of the hydrogenation of polar bonds with Fe complexes of pincer ligands, with high turnover numbers.[19-22] Still, Fe complexes that are able to hydrogenate CO_2 are rare and Fe complexes able to hydrogenate formates remain elusive. Some common features of most of the Fe catalysts mentioned above are that they contain strongly donating ligands that are able to have some bi-functional activity with the metal, and in the catalytic mechanisms a *trans* dihydride species is the active species for substrate insertion into the metal hydride. Despite the interesting activity of Milstein's RuPNN complexes, and the recent successes with hydrogenations catalyzed by similar Fe pincer complexes, there had not been any reports of the synthesis of FePNN analogues and their hydrogenation activity when we decided to start working on this system. It should be noted that as we were working on this project, there was a report of the synthesis of $FePNNCl_2$ complexes and their use as precatalysts in the hydroboration of alkenes with pinacolborane.[23,24]

In this chapter, we investigate the electrochemical reactivity of two previously reported Ru pincer hydrogenation catalyst with methylformate and CO_2. We also worked on the synthesis of Fe analogues of Milstein's Ru pincer complexes and looked at their electrochemical reactivity with methylformate and CO_2.

5.2 Experimental

Materials and Methods

Unless otherwise noted, all reactions were carried out under a N_2 atmosphere using standard Schlenk and glovebox techniques. Acetone was dried over 4Å molecular sieves and degassed prior to use. All other solvents used were dried over activated molecular sieves and alumina and degassed prior to use. Tetrabutylammonium hexafluorophosphate (NBu_4PF_6) was recrystallized from methanol prior to use. The ligand, *t*Bu-PNN ligand 6-((di-

tertbutylphosphino)methyl)-2,2'-bipyridine (PNN) and the RuPNN complex (**3b**) were synthesized as previously reported.[4] The RuCNN complex (**4**) was also synthesized as previously reported.[11] All other chemicals were obtained from commercial suppliers and used without further purification. ^{1}H and $^{31}P\{^{1}H\}$ NMR spectra were recorded using 300MHz or 500MHz Varian spectrometers. ^{1}H NMR chemical shifts were referenced against the residual solvent signal and are reported in ppm downfield of tetramethylsilane ($\delta = 0$). $^{31}P\{^{1}H\}$ NMR chemical shifts were externally referenced to 85 % phosphoric acid ($\delta = 0$). Mass spectrometry data was collected on a Finnagan LCQDECA in ESI positive ion mode. Elemental analyses were performed by Midwest Microlabs, LLC. in Indianapolis, Indiana.

General Electrochemical Experiments

All solvents used were dried over activated molecular sieves and alumina and degassed prior to use. NBu_4PF_6 was recrystallized from methanol prior to use. All other chemicals were obtained from commercial suppliers and used without further purification. Electrochemical experiments were performed using a BAS Epsilon potentiostat. Cyclic voltammograms (CV's) were performed under nitrogen in a one compartment cell using a glassy carbon BASi working electrode, a glassy carbon rod counter electrode, and a non-aqueous Ag pseudo reference electrode from BASi (silver wire in a 0.2 M NBu_4PF_6 and 1mM $AgNO_3$ acetonitrile solution separated from the working compartment by porous Vycor (4mm). All experiments were performed in dry acetonitrile using 0.2 M NBu_4PF_6 as the supporting electrolyte. Cp^*_2Fe was added as an internal reference and was then used to reference the reduction potentials of the complexes to the Cp_2Fe^+/Cp_2Fe couple. For CV's taken under CO_2 atmospheres, the solutions were sparged with CO_2 for 10 minutes before taking the CV's.

Bulk electrolysis experiments

Bulk electrolysis experiments were conducted at 1atm CO_2 pressure in a glass 2-chamber Hcell. One chamber of the Hcell contained the working electrode (a 6 cm × 1 cm ×

0.3 cm glassy carbon plate) and the reference electrode (a $Ag/AgNO_3$ (1 mM)/acetonitrile reference electrode separated from the solution by a Vycor frit and contained 0.1 M NBu_4PF_6. The other chamber contained the auxillary electrode (a nichrome wire coiled). The two champers were separated by a fine glass frit. The both compartments were filled with 0.1 M NBu_4PF_6 acetonitrile solutions so that the total volume in the cell was 45 mL. For the Ru bulk electrolysis, the acetonitrile solutions also contained 2.5% H_2O as the proton source. For the Fe bulk electrolysis experiments, the acetonitrile solutions contained 1% 2,2,2-trifluoroethanol (TFE) as the proton source. To the working electrode compartment, catalyst added so the concentration of the catalyst in that compartment was 0.5 mM. The Hcell was prepared in a glovebox with dry and degassed acetonitrile. Both compartments of the cell were sparged with CO_2 and then sealed before the electrolysis and then the cell was taken out of the box to run the electrolysis. Carbon monoxide and H_2 were quantified using an Agilent 7890A gas chromatograph with a thermal conductivity detector. Formate was detected (8.11 ppm in the ^1H NMR spectra) after an acidic workup of the working electrode electrolysis solution, dilution with CD_3CN, and the addition of benzene as an internal standard for formate quantification.

Synthesis of (*t*Bu-PNN)Fe(CO)$_2$ (5)

0.505 g (1.60 mmol) *t*Bu-PNN was dissolved in 10 mL toluene in a schlenk tube with a stir bar. $Fe(CO)_5$ (0.211 mL, 1.60 mmol) was added via syringe and the flask was closed and heated to reflux for 5 days. The dark purple solution was evaporated to yield a purple solid. The characterization of this complex matches what was previously reported.[25]

Synthesis of [HFe(*t*Bu-PNN)(CO)$_2$]BF$_4$ (6)

0.120 g (0.282 mmol) (*t*Bu-PNN)$Fe(CO)_2$ was dissolved in ca 5 mL THF in a vial with a stir bar. The vial was set to stir in the cold well, which was cooled with a dry ice/ isopropanol bath. 50 uL (0.364 mmol) HBF_4 Et_2O complex was added via syringe. The solution immediately changed from purple to light green. The solution was left to stir in cold well for

20 min, and after 20 min, a light green precipitate had formed. Solution was filtered and the precipitate was washed with 5 mL THF and 2 x 5 mL pentane. Complex **6** was dried in under vacuum to yield 0.136g (93%) of a light green powder. ^{1}H NMR (500 MHz, Acetonitrile-d_3) δ 9.01 (d, *J* = 5.6 Hz, 1H, Ar*H*), 8.32 (d, *J* = 8.3 Hz, 1H, Ar*H*), 8.23 (d, *J* = 8.1 Hz, 1H, Ar*H*), 8.12 (m, 2H, Ar*H*), 4.05 – 3.75 (m, 2H, CH_2), 1.46 (d, *J* = 14.4 Hz, 9H, CH_3), 1.29 (d, *J* = 14.0 Hz, 9H, CH_3), -4.87 (d, *J* = 55.0 Hz, 1H, Fe–*H*). ^{31}P{^{1}H} NMR (121 MHz, Acetonitrie-d_3): δ 121.07 (d, *J* = 18.7 Hz). $\nu_{(CO)}$ = 2035 cm^{-1}, 1971 cm^{-1}.

Synthesis of [Fe(*t*Bu-PNN)(CO)$_2$ACN](BF$_4$)$_2$ (7)

0.100 g (0.235 mmol) of 3 was weighted in a vial and a stir bar was added along with 10 mL acetonitrile. To the stirred purple solution, 0.110 g (0.470 mmol) $AgBF_4$ was added and the solution was allowed to stir for 30 min. The color changed to an orange/red with a suspended brown precipitate. The solution was evaporated to dryness and dissolved 5 mL methylene chloride. This solution was filtered again though a plug of celite and layered with pentane to induce the precipitation of the product. The next day, the orange powder that had precipitated out was collected by filtration and dried to yield 0.098 g product (82%). ^{1}H NMR (300 MHz, Acetonitrile-d_3) δ 9.15 (d, *J* = 5.6 Hz, 1H, Ar*H*), 8.58 – 8.47 (m, 2H, Ar*H*), 8.45–8.36 (m, 2H, Ar*H*), 8.03 (d, *J* = 7.6 Hz, 1H, Ar*H*), 7.96 – 7.89 (m, 1H, Ar*H*), 4.19 (qd, *J* = 18.0, 11.3 Hz, 2H, CH_2), 1.98 (s, 3H,CH_3CN), 1.46 (dd, *J* = 15.0, 11.8 Hz, 18H, CH_3-*t*Bu). ^{31}P NMR (121 MHz, Acetonitrile-d_3) δ 105.91.

5.3 Results and Discussion

5.3.1 Electrochemistry of Ru pincer complexes

For our electrochemical studies with Ru pincer complexes, we decided to focus on complexes **3b** and **4**, shown in **Scheme 5-3**. Both complexes were developed by the Milstein group. Complex **3b** is one of the RuPNN complexes extensively studied as a hydrogenation catalyst for the hydrogenation of amides, carbamates, carbonates, and alkylformates. Complex **4** contains an N-heterocylic carbene instead of a phosphine ligand and is active for the hydrogenation of un-activated esters. Both complexes were synthesized as previously reported.[4,11] The complexes contain bipyridine backbones and were chosen for study as electrocatalyts because of the ability of bipyridine ligands to generally accept electrons at lower potentials than metal centers, allowing the complexes to easily access multiple oxidation states. They also contain the methylene arm that has the ability to have favorable proton donating interactions with a metal-bound substrate.

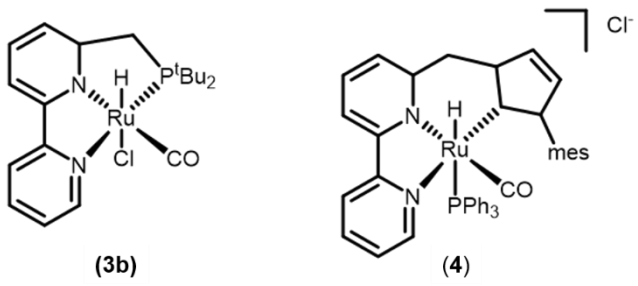

Scheme 5-3. RuPNN (**3b**) and RuCNN (**4**) pincer complexes investigated as electrocatalysts.

Electrochemistry of Complex 3b (RuPNN)

The cyclic voltammogram (CV) of the Ru complex **3b** has not been reported. Under an N_2 atmosphere, complex **3b** shows two reversible 1 e^- reductions ($E_{1/2}$ = –1.87 and $E_{1/2}$ = –1.97 V vs $FeCp_2$) when scanning negatively and several oxidative events when scanning positively. The one electron nature of the reductions is evident in the splitting of the cathodic and anodic peaks, which is 61mV for both peaks. The two reductions are diffusion controlled, as indicated by the linear plots of the current against the square root of the scan rate.

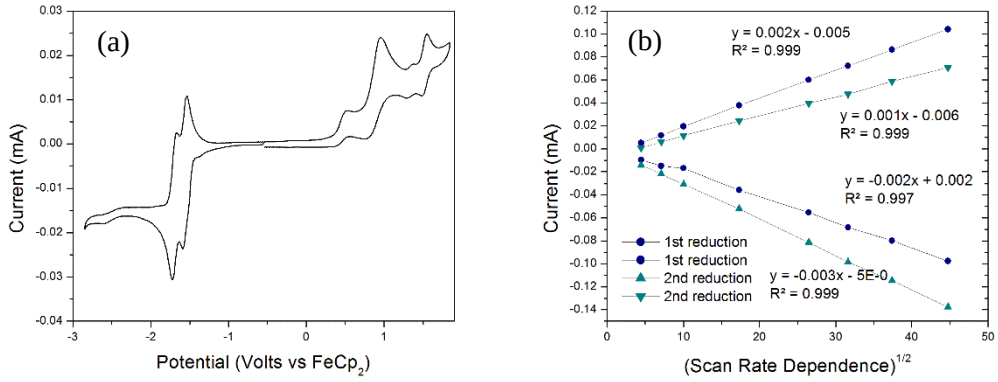

Figure 5-1. CV of complex **3b** under an atmopshere of N_2 (a) and scanrate dependence of the two reductions (b).

Table 5-1. Reduction potentials of complex **3b** (Volts vs $FeCp_2$)

$Ec_{1/2}$ =	–1.83 (ΔE = 61 mV)	Ea =	0.53
$Ec_{1/2}$ =	–1.97(ΔE = 61 mV)	Ea =	0.96
		$Ea_{1/2}$ =	1.51 (ΔE = 61 mV)

When increasing amounts of methylformate are added, no changes in the CV's occurred. Since the reduction of methylformate requires protons, we added H_2O or methanol as proton sources, but the CV's still remained unchanged. Complex **3b** does however show reactivity with CO_2. Under a CO_2 atmosphere, the position of the second reduction shifts positively so that the two reductions overlap and a new peak is observed further negative (–

2.29 V vs $FeCp_2$) that corresponds to the reduction of, and possibly catalytic reactivity of a new species (**Figure 5-2**). On the return scan, the reoxidation peaks corresponding to the two reduction are missing, indicating that the reduced species have been consumed and are not available to be reoxidized. The positive shift of the potentials of the first two reductions and the lack of reversibility are likely indicative of irreversible CO_2 binding. As increasing amounts of water or methanol are added as a proton source, the current at the new peak continues to grow and begins to level after 3M H_2O has been added (14x current increase). A control study with just added methanol or water shows that this complex does not show any new peaks or any catalytic current due to proton reduction under these conditions. The CV does show that the position of the first reduction moves slightly more positive, an indication that H_2O is likely substituting the chloride ligand as the H_2O concentration is increased. When a stronger proton source is used ([HDBU]BF_4, pK_a ~ 12, DBU = 1,8-Diazabicyclo[5.4.0]undec-7-ene)), proton reduction does occur, but it happens around the potential of the first two reductions. This all supports that the new peak observed in the CV (a) is related to CO_2 addition and the increase in current when water is added is likely due to proton dependent CO_2 reduction catalysis.

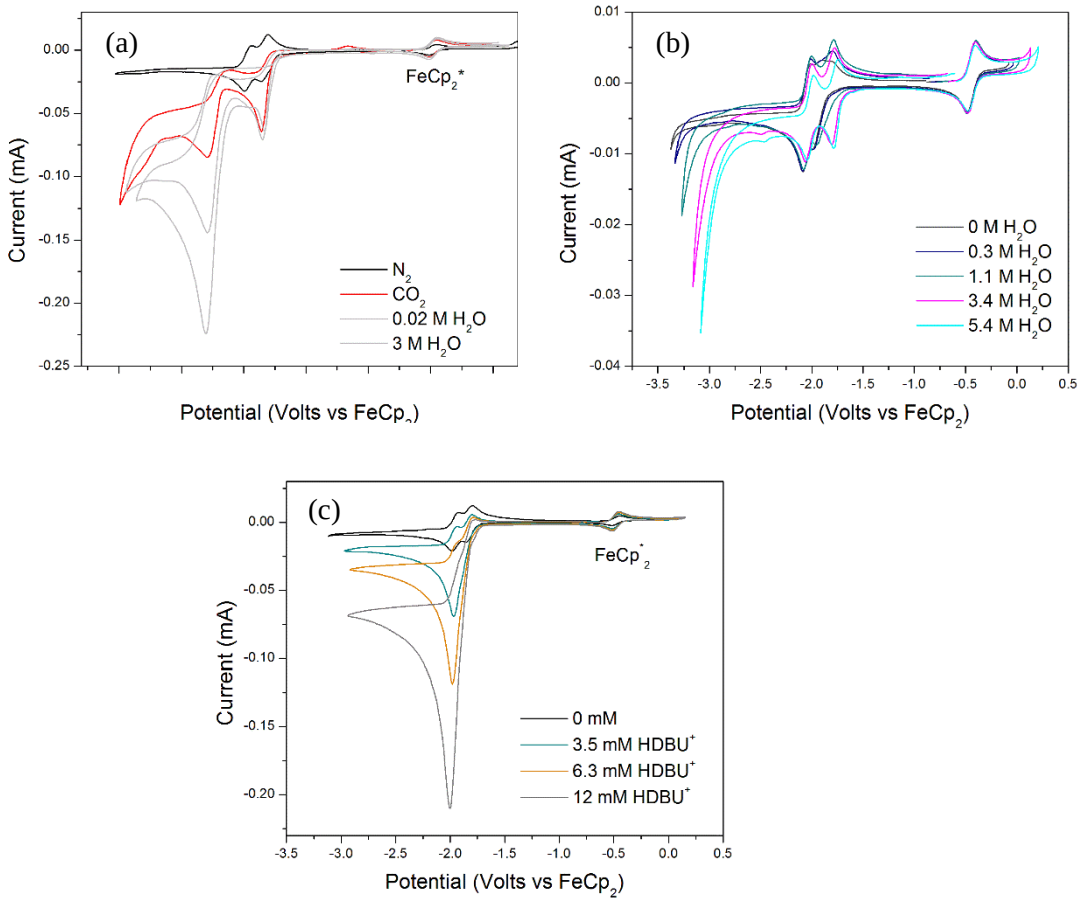

Figure 5-2. CV showing the electrochemical response of complex **3b** in the presence of CO_2 with increasing amounts of H_2O (a), CV showing the electrochemical response of complex **3b** in the presence of H_2O (b), CV showing the electrochemical response of complex **3b** in the presence of $[HDBU]BF_4$ (c).

Electrochemistry of complex 4 (RuCNN)

The electrochemistry of complex 4 has also not been previously reported. Under an atmosphere of N_2, complex 4 shows a reversible reduction at –1.82 V (vs $FeCp_2$) and an irreversible reduction at –2.36 V. The reversible nature of the first reduction are evident in the between the cathodic and anodic peak (ΔE = 71 mV) and the complexes are freely diffusing in solution, shown by the linear plots of the current against the square root of the scan rate.

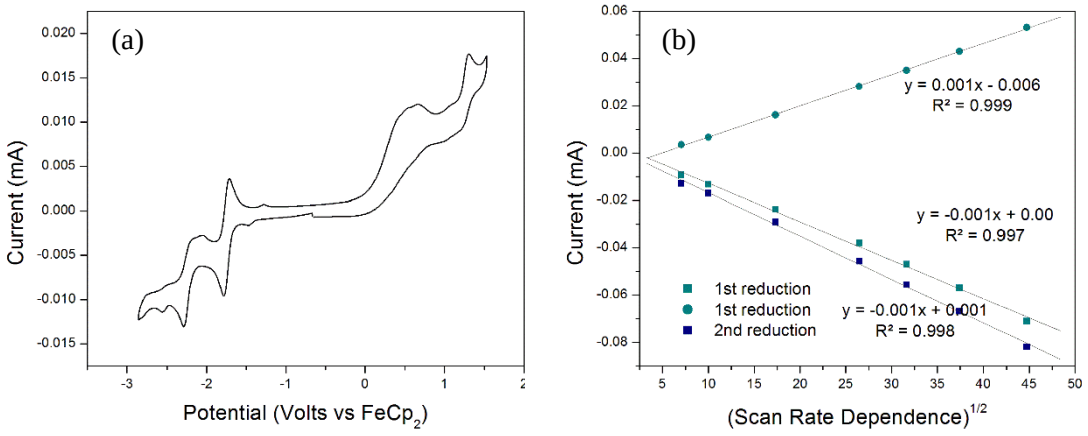

Figure 5-3. CV of complex **4** under an atmopshere of N_2 (a) and scanrate dependence of the reduction peak (b).

Table 5-2. Reduction potentials of complex **4** (Volts vs $FeCp_2$)

$Ec_{1/2}$ =	–1.82 (ΔE = 71 mV)	Ea =	0.59
Ec =	–2.36	Ea =	1.37

When increasing amounts of methylformate are added, no changes in the CV's occurred, even when an excess of water or methanol was added as a proton source. Complex **4** does show reactivity with CO_2. Under a CO_2 atmosphere, there is a significant increase in current at the first reduction (2x) and an even larger increase in current at the second reduction (4x). The current at both reductions is further enhanced when a proton source (H_2O) is added

and levels off after 3 M H_2O has been added (5x for the first reduction and 10x for the second). In the absence of CO_2 and with the same amounts of H_2O added, the CV remains unchanged, indicating that the current enhancement in the experiments with CO_2 and H_2O is not related to proton reduction. CV's with a stronger proton source, $[HDBU]BF_4$ shows that this complex does reduce protons around the potential of the 2nd reduction, but when CO_2 and H_2O are present, the catalytic current seems to be due to proton dependent CO_2 reduction.

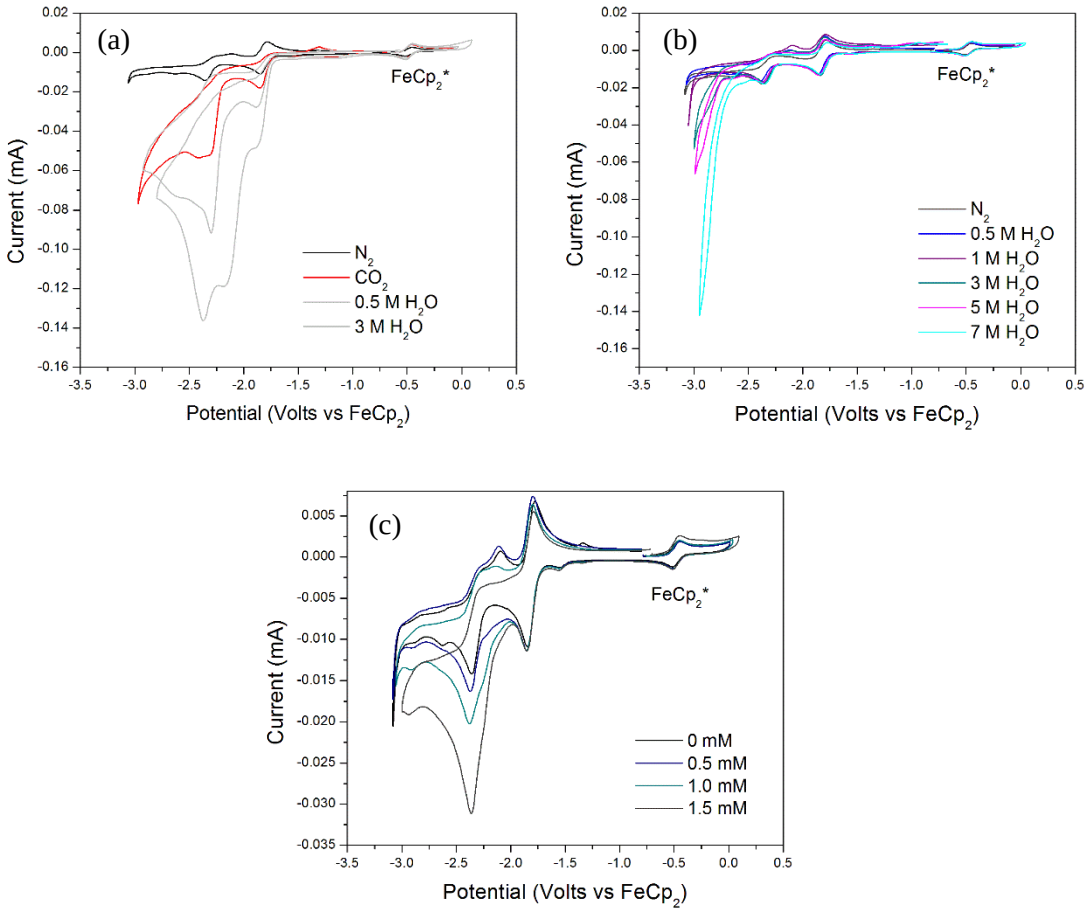

Figure 5-4. CV showing the electrochemical response of complex **4** in the presence of CO_2 with increasing amounts of H_2O (a), CV showing the electrochemical response of complex **4** in the presence of H_2O (b), CV showing the electrochemical response of complex **4** in the presence of $[HDBU]BF_4$ (c).

Preliminary bulk electrolysis experiments for the reductions of complexes **3b** and **4** in the presence of CO_2 and H_2O revealed that CO and formate are major products of the

electrolysis and H_2 is a minor product, although there was a large amount of variation in the efficiencies for the formation of these products and not all of the current passed in the electrolysis experiments could be accounted for. Due to lack of time, I was unable to trouble-shoot these experiments enough to produce publication quality results, but the preliminary results confirm that these complexes are electrochemically reducing CO_2 to produce mainly CO and formate, with H_2 as a minor product.

5.3.2 Fe pincer complexes

Synthesis

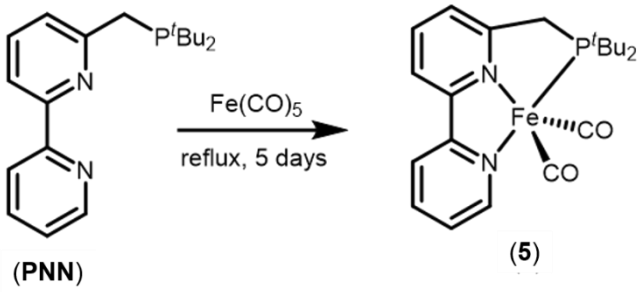

Scheme 5-4. Synthesis of (*t*Bu-PNN)Fe(CO)$_2$ (**5**)

We tried various different methods to synthesize analogous Fe complexes to Milstein's RuPNN bipyridine system. Previous Fe(II) pincer complexes of a similar type have been synthesized starting from $FeCl_2$, adding the pincer ligand and a CO ligand, and then reacting with a borohydride reagent to make the mono or dihydride complex.[18] Several attempts at making complexes with the *t*Bu-PNN ligand using this route failed. We also tried to start from $[Fe(ACN)_6](BF_4)_2$ and add the pincer ligand and a CO ligand, but this also did not work. What ultimately worked was to start from Fe(0) with $Fe(CO)_5$. Refluxing the *t*Bu-PNN ligand with $Fe(CO)_5$ in toluene results in the formation of the diamagnetic five coordinate iron complex (*t*Bu-PNN)Fe(CO)$_2$ (**5**). The $^{31}P\{^1H\}$ NMR spectrum shows a single resonance at 137.9 ppm.

The "arm" of the methylene protons appear up as one resonance, a doublet ($^1J_{P\text{-}H}$ = 12.7 Hz) and there is one set of resonances for the substituents on the phosphine moiety. The IR spectra shows two CO stretching vibrations at 1891 cm^{-1} and 1834 cm^{-1}, consistent with *cis* CO ligands.

The molecular structure of **5**, determined by X-ray diffraction, can best be described as square pyramidal around the Fe center (**Figure 5-5**). The PNN ligand coordinates in a meridional fashion with one carbonyl ligand forming the base of the pyramid and the other carbonyl at the apical position. The phosphorous atom is slightly twisted out of the plane of the PNN ligand. Selected bond lengths and angles are listed in **Table 5-3**. This complex was then later reported by Milstein, and was obtained using a similar synthesis.[25]

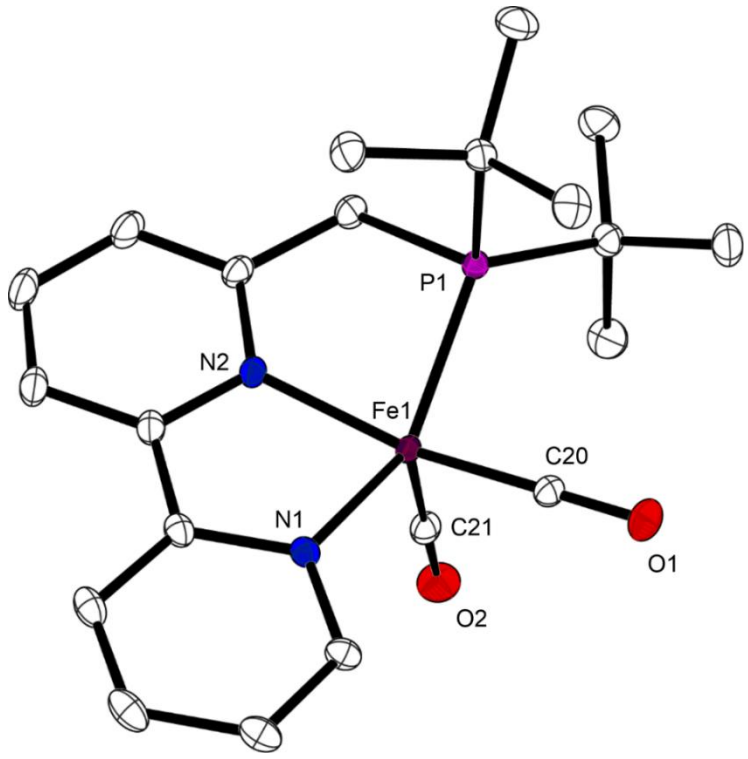

Figure 5-5. Molecular structure of (*t*Bu-PNN)Fe$(CO)_2$ (**5)** shown at the 50% probability level. Hydrogens have been omitted for clarity.

Table 5-3. Selected bond lengths [Å] and angles [°] for complex **5**

Bond length [Å]		Bond angles [°]	
Fe(1)-C(20)	1.7521(12)	N(1)-Fe(1)-P(1)	145.88(3)
Fe(1)-C(21)	1.7763(12)	C(20)-Fe(1)-C(21)	97.96(5)
Fe(1)-N(2)	1.9355(10)	C(20)-Fe(1)-N(2)	160.57(5)
Fe(1)-N(1)	1.9437(10)	C(21)-Fe(1)-N(2)	101.43(5)
C(20)-O(1)	1.1636(14)	C(21)-Fe(1)-P(1)	105.28(4)
C(21)-O(2)	1.1621(15)	C(21)-Fe(1)-N(1)	106.64(5)

Complex **5** can be protonated with HBF_4 or HBArF to form the Fe(II) complex **6**, [HFe(*t*Bu-PNN)$(CO)_2$]BArF or BF_4. The $^{31}P\{^1H\}$ NMR spectrum shows a single resonance at 120.1 ppm. In the ^1H NMR spectra, the hydride resonance appears as a doublet at –4.86 ($J_{P–H}$ = 55.0 Hz). The "arm" of the methylene protons give rise to signals at 4.0 and 3.83 ppm ($^2J_{H\text{-}H}$ = 17.1 Hz and $^2J_{P\text{-}H}$ = 13.6 Hz). The IR spectra of this complex shows two CO stretching vibrations at 1891 cm^{-1} and 1834 cm^{-1}.

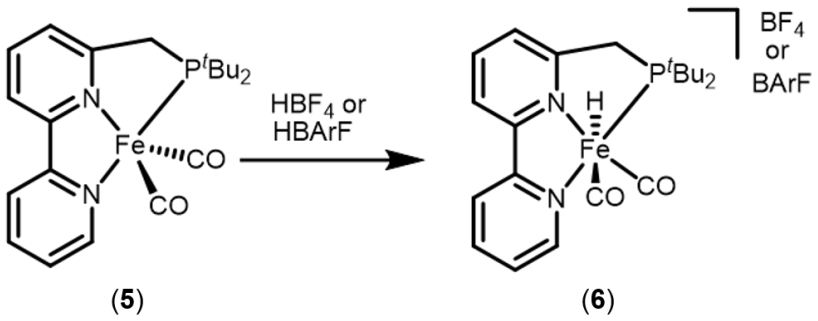

(**5**) (**6**)

Scheme 5-5. Synthesis [HFe(*t*Bu-PNN)$(CO)_2$]BF_4 or BArF (**6**)

Suitable crystals for X-ray diffraction of the **6** BArF complex were grown by the diffusion of pentane into a THF solution. The molecular structure shows complex **6** is six coordinate octahedral with a CO ligand *trans* to the central nitrogen of the pincer ligand and the hydride ligand *trans* to the other CO (**Figure 5-6**). The CO opposite of the hydride shows a Fe–C distance of 1.838 while the other shows a distance of 1.768, a result of the strong *trans*

effect of the hydride ligand. The phosphorus atom is slightly twisted out of the plane of the pincer ligand.

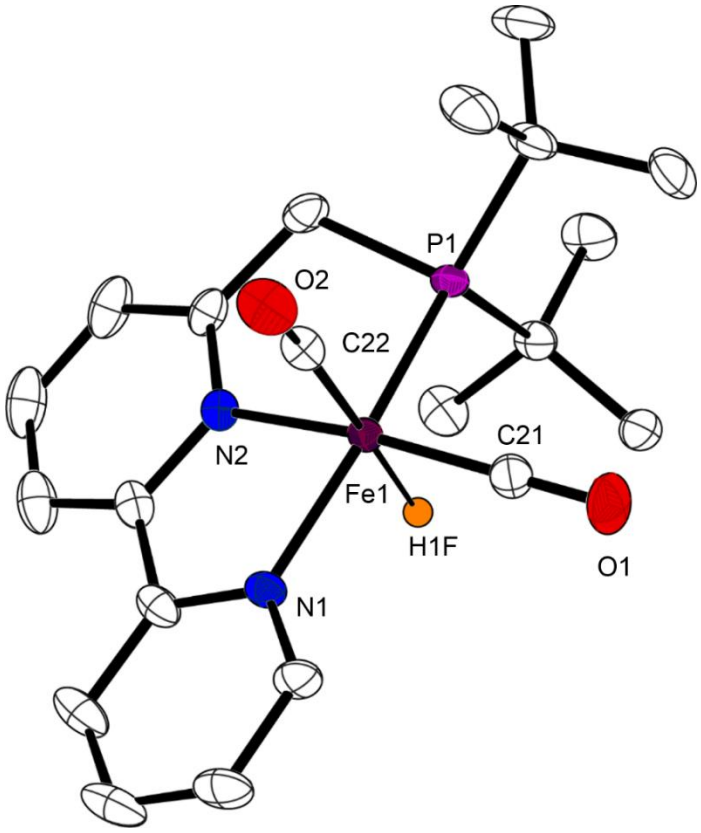

Figure 5-6. Molecular structure of [HFe(*t*Bu-PNN)$(CO)_2$]BArF (**6**) shown at the 50% probability level. Hydrogens and uncoordinated $BArF^-$ anion have been omitted for clarity.

Table 5-4. Selected bond lengths [Å] and angles [°] for complex **6**

Bond length [Å]		Bond angles [°]	
Fe(1)-C(21)	1.768(2)	C(21)-Fe(1)-N(2)	167.75(8)
Fe(1)-C(22)	1.8377(19)	N(2)-Fe(1)-H(1F)	87.0(12)
Fe(1)-N(2)	1.9746(15)	C(22)-Fe(1)-H(1F)	172.9(11)
Fe(1)-N(1)	1.9866(15)	N(1)-Fe(1)-P(1)	159.92(5)
Fe(1)-P(1)	2.2327(4)		
Fe(1)-H(1F)	1.44(3)		
C(21)-O(1)	1.144(3)		
C(22)-O(2)	1.139(2)		

Complex **6** can be oxidized with 2 equivalents of $AgBF_4$ to form [Fe(*t*Bu-PNN)$(CO)_2(CH_3CN)](BF_4)_2$ (**7**). The complex shows a single resonance in the $^{31}P\{^1H\}$ NMR at 105.9 ppm. The methylene protons appear two resonances at 4.25 and 4.13 ppm ($^2J_{HH}$ = 18.0 Hz and $^2J_{PH}$ = 11.7 Hz).

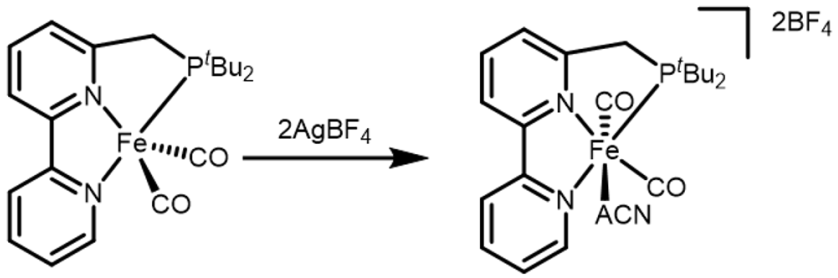

(**5**) (**7**)

Scheme 5-6. Scheme for the synthesis [Fe(*t*Bu-PNN)$(CO)_2(CH_3CN)](BF_4)_2$ (**7**)

Crystals for x-ray diffraction of **7** were grown from the vapor diffusion of diethylether into a saturated methylene chloride solution. The structure exhibits octahedral geometry with the PNN ligand meridionally coordinated to the Fe center, two carbonyl ligands *cis* to each other, an acetonitrile ligand *trans* to one of the carbonyls, and two uncoordinated BF_4 anions (**Figure 5-7**). The asymmetric unit contains two Fe molecules, along with four molecules of BF_4^- and 2.5 molecules of dichloromethane. Selected bond lengths and angles for complex **5** can be found in **Table 5-5**.

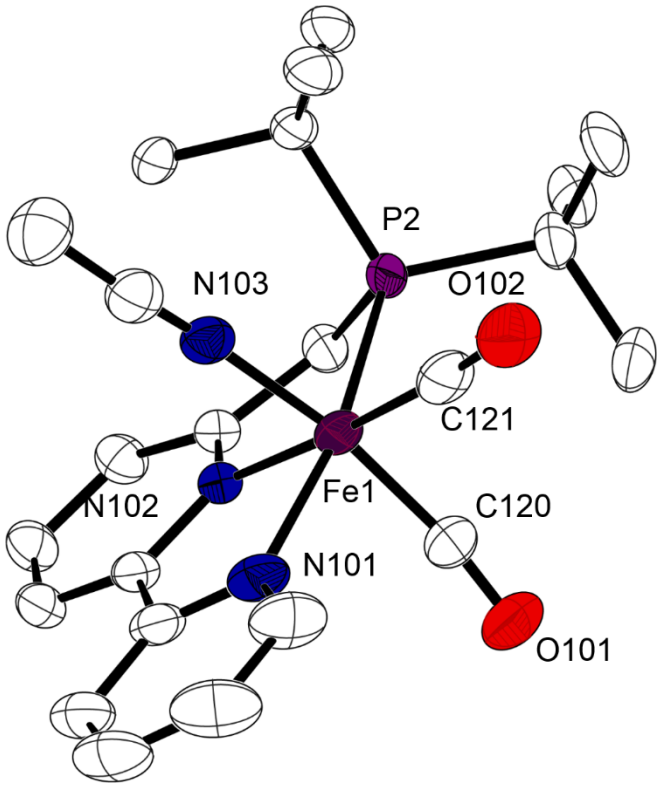

Figure 5-7. Molecular structure of [Fe(*t*Bu-PNN)$(CO)_2(CH_3CN)](BF_4)_2$ (**7**) shown at the 50% probability level. Hydrogens, uncoordinated BF_4^- anions, and co-crystallized methylene chlorides have been omitted for clarity.

Table 5-5. Selected bond lengths [Å] and angles [°] for complex (**7**)

Molecule 1			
Bond length [Å]		Bond angles [°]	
Fe(1)-C(21)	1.796(3)	N(1)-Fe(1)-N(2)	80.55(9)
Fe(1)-C(20)	1.819(3)	N(2)-Fe(1)-C(20)	175.72(11)
Fe(1)-N(3)	1.957(2)	N(3)-Fe(1)-C(21)	88.47(11)
Fe(1)-N(2)	1.974(2)	N(2)-Fe(1)-P(1)	83.17(7)
Fe(1)-N(1)	2.012(2)	N(1)-Fe(1)-P(1)	162.69(7)
Fe(1)-P(1)	2.3102(8)		
N(3)-C(22)	1.130(4)		
C(20)-O(1)	1.134(3)		
C(21)-O(2)	1.129(3)		
Molecule 2			
Bond length [Å]		Bond angles [°]	
Fe(2)-C(120)	1.805(3)	N(102)-Fe(2)-N(101)	82.64(10)
Fe(2)-C1(21)	1.817(3)	C(120)-Fe(2)-N(103)	169.36(12)
Fe(2)-N(103)	1.952(3)	N(101)-Fe(2)-P(2)	164.00(8)
Fe(2)-N(102)	1.973(2)	N(102)-Fe(2)-P(2)	83.63(7)
Fe(2)-N(101)	1.998(8)	C(121)-Fe(2)-N(102)	176.69(11)
Fe(2)-(P2)	2.2896(8)		
C(120)-O(101)	1.128(4)		
C(121)-O(102)	1.131(4)		
N(103)-C(122)	1.130(4)		

Complex **6** can also be de-protonated with K*t*BuO in THF-d_8 to form the de-aromatized complex **8** as the only product by NMR. This complex is unstable at room temperature and could not be further isolated, but we were able to obtain a ^{1}H and ^{31}P{^{1}H} NMR. The ^{31}P{^{1}H} spectra shows a doublet at 112.8 ppm ($^{1}J_{P\text{-}H}$ = 26.3 Hz). In the ^{1}H NMR, the hydride ligand appears as a doublet at –5.15 (J = 52.4 Hz) and the methylene arm, which initially appeared as a two multiplets in complex **6** integrating to two protons, now appears as a broad singlet with an integration of one proton. The three de-aromatized protons from the ring can be seen at 6.21, 6.25, and 6.64 ppm. We were not able to get a good enough ^{13}C spectrum or IR data to

be able to tell if the both carbonyls were still coordinated, or if one had dissociated, but it is likely that both carbonyl ligands remain coordinated.

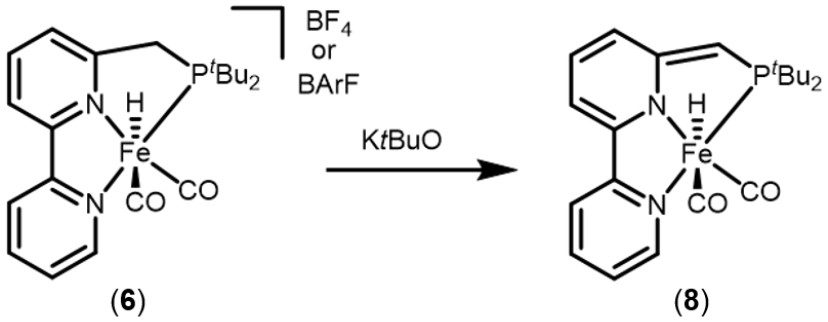

(**6**) (**8**)

Scheme 5-7. Synthesis of de-aromatized Fe complex (**8**)

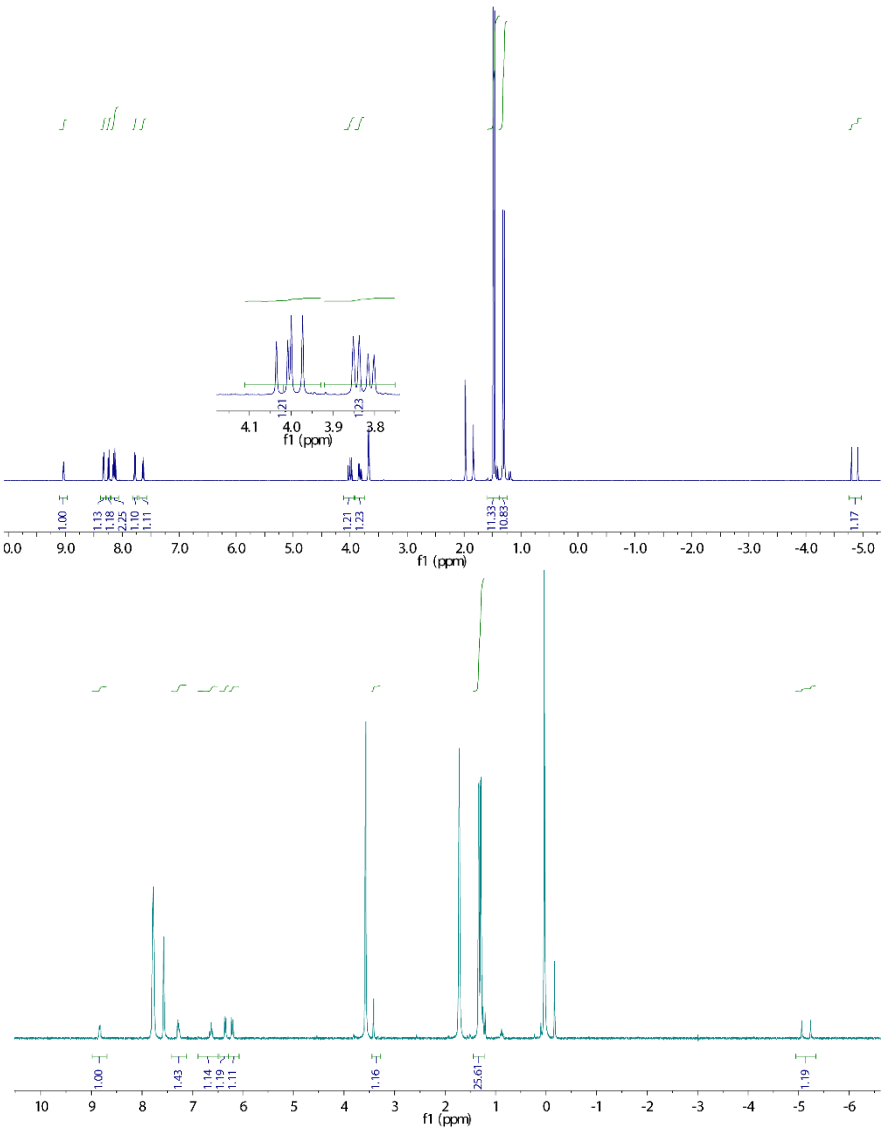

Figure 5-8. ^{1}H NMR showing the spectra of the aromatized complex (**6**) on the top and the de-aromatized complex (**8**) in the bottom.

Attempts were made to activate H_2 across the metal center and the methylene arm to make the *trans* dihyidride complex, which is the active species in most Fe pincer hydrogenation catalysts. Reaction complex **8** with H_2 seemed to lead mostly to the regeneration of the (*t*Bu-PNN)Fe(CO)$_2$ complex (**5**). Attempts to make a dihydride complex by adding an excess of borohydride reagent to **7** also led to the formation of the initial Fe(0) complex. This may be

due to the fact that the second carbonyl ligand remains coordinated upon de-protonation of complex **6**, so there would not be an open site for the coordination of the second hydride ligand. A key similarity between the Fe based hydrogenation catalysts reported so far is that they have a *trans* dihydride active species, since the strong *trans* effect of the hydride makes the other hyride more unstable (more hydridic). Although we were unable make a *trans* dihydride Fe complex with the PNN ligand, this may not be a problem for hydrogenation catalysis. Carbonyl ligands also exerts a strong *trans* effect, and the de-protonated hydride complex may be hydridic enough to transfer a hydride to a substrate. Preliminary attempts to try to transfer the hydride from **8** to CO_2 failed. I was unable to explore the stoichiometric chemistry of this Fe system further, but some obvious experiments to do would be to see if the de-protonated hydride complex is able to transfer a hydride to any substrate under certain conditions. Another experiment would be to take complex **5**, de-protonate the methylene arm, and see if hydrogen can be activated across the metal center and the methylene are to regenerate the Fe–H complex, **4**. This could provide another example of bi-functional metal-ligand H_2 activation and provide a potential entrance into a hydrogenation cycle.

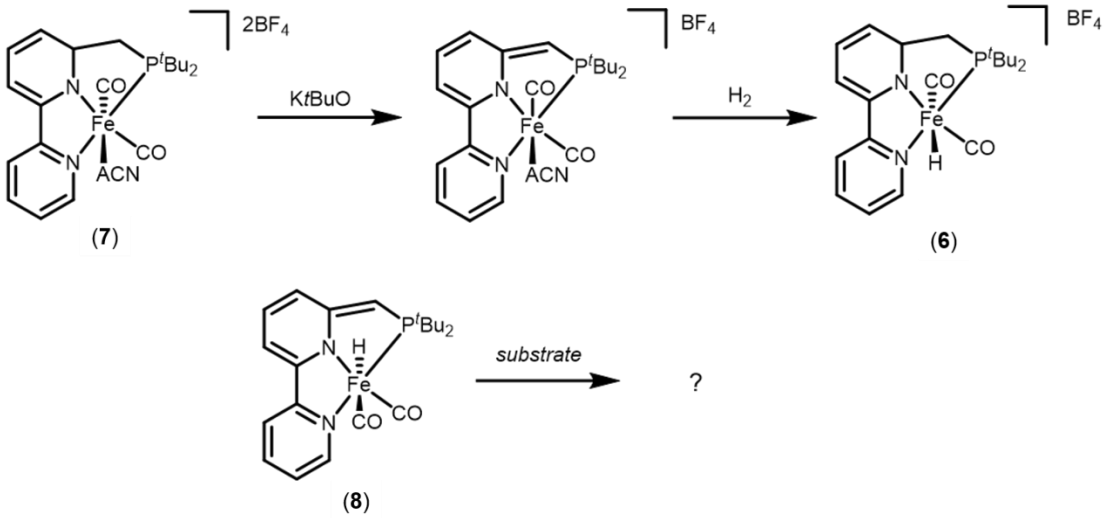

(**7**) (**6**) (**8**)

Scheme 5-8. Other experiments to try to explore possible hydrogenation chemistry of the FePNN system.

Electrochemistry of [HFe(*t*Bu-PNN)(CO)$_2$]BF$_4$ (6)

Given that we saw interesting electrochemistry with the Ru pincer bipyridine complexes and given the similarity between those and the Fe complex **6**, we decided to look at its electrochemical reactivity. Under a N_2 atmosphere, complex **6** shows two reductions, one irreversible reduction at 1.81 V and a reversible one at 2.45 V (ΔE = 71 mV). Scanning anodically, there is a reversible oxidation at –1.03 V (ΔE = 72 mV). The peak separations indicate that these are one electron processes and that linear plots of the current versus the square root of the scan rate shows these complexes are freely diffusing in solution.

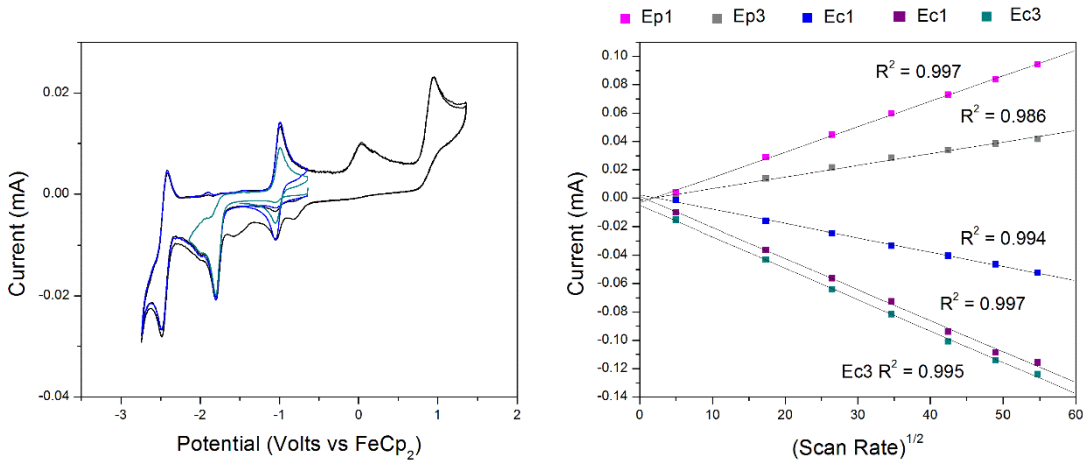

Figure 5-9. CV of complex **6** under an atmopshere of N_2 (a) and scanrate dependence of the two reductions (b).

Table 5-6. Reduction potentials of complex **6** (Volts vs $FeCp_2$)

$Ec_{1/2}$ =	–1.82	$Ea_{1/2}$=	–1.01 (ΔE = 72 mV)
$Ec_{1/2}$ =	–2.45(ΔE = 72 mV)	Ea =	0.03
		$Ea_{1/2}$ =	0.95

When increasing amounts of methylformate are added, there is no current response in the CV. Under an atmosphere of CO_2, complex **6** does show a modest increase in current (2.5x) at the second reduction and a loss of reversibility on the return oxidation. When increasing amounts 2,2,2- trifluoroethanol (TFE) are added as a proton source, the current at the potential

of the second reduction significantly increases and maxes out at 7.5x the current of the original CV. When the increasing amounts of trifluoroethanol are added and CO_2 is not present, there is no significant change in the appearance of the CV, indicating that the increases in current are not related to proton reduction.

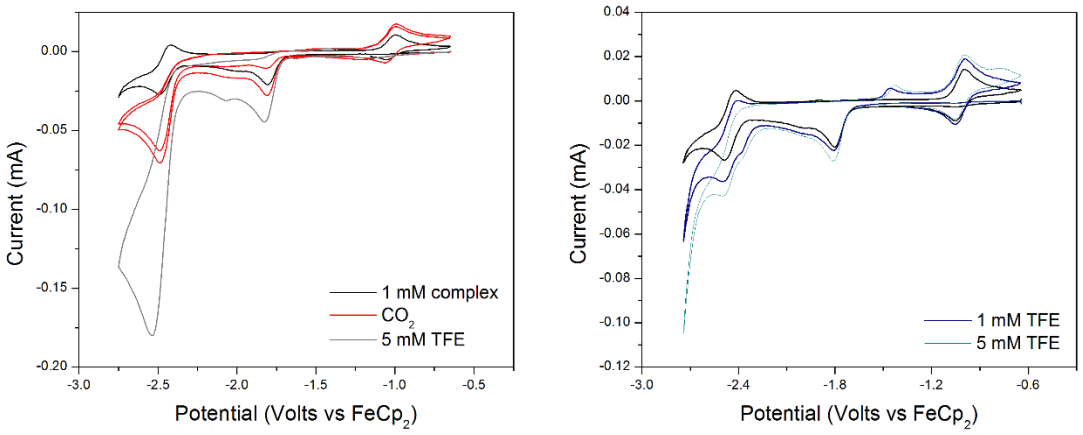

Figure 5-10. CV showing the electrochemical response of complex **6** in the presence of CO_2 and TFE (a), CV showing the electrochemical response of complex **6** in the presence of TFE (b).

Similar to the Ru complexes **3b** and **4**, preliminary bulk electrolysis experiments also showed that CO and formate are major products of the reduction of CO_2, although these experiments also need much more work to get publication quality efficiencies for the formation of these products.

5.4 Conclusions

In this chapter, the electrochemistry of the previously reported Ru complexes **3b** and **4** is reported. Complexes **3b** and **4** are known to catalyze the hydrogenation of various un-activated esters, including some alkylformates, but they are not active for the electrochemical reduction of methylformate. They also do not show any new features when reduced in the

presence of a weak acid, indicating we are not electrochemically generating the dihydride species that are active for hydrogenations. They do show indications of irreversible CO_2 binding and increased in current in the presence of CO_2, which is further enhanced when a proton source is added. These CV's are indicative of proton dependent CO_2 reduction. Initial bulk electrolysis studies show that H_2, CO, and formate are all products of the electrochemical reduction of CO_2, although further experiments need to be done to determine the faradic efficiencies for the formation of each product. I was unable to finish the studies of these complexes as electrocatalysts, but I hope that future Kubiak group members will continue to study these complexes and fully characterize their electrocatalytic activity with CO_2. Regardless of whether these complexes are primarily electrochemically "hydrogenating" CO_2 to make formate as we had hoped or if they are primarily making CO as the major product, it is interesting that known hydrogenation catalysts show significant electrochemical reactivity at all, and at potentials that are comparable to other CO_2 reduction catalysts. Further characterization of these systems would add to the growing, but still small, list of complexes able to electrocatalytically reduce CO_2. At that point, mechanistic studies should be conducted to better understand how catalysis is occurring.

We also synthesized several Fe complexes with the bipyridine containing PNN ligand and began to explore their stoichiometric and electrochemical reactivity. We were not able to make Fe dihydride complexes, which are the active species in most Fe hydrogenation catalysts, but further study of the monohydride Fe species may prove that they are able transfer a hydride to a substrate, and if they are, they may be able to be used in a hydrogenation scheme. Similar to the Ru pincer complexes, the Fe complex **6**, [HFe(*t*Bu-PNN)$(CO)_2$]BF_4, showed catalytic current under a CO_2 atmosphere, and the current is further enhanced when a proton source is present. Preliminary bulk electrolysis experiments also show that formate and CO are major products of the electrochemical reduction of these complexes in the presence of a proton

source. The potential that this complex operates at is similar to the potentials of the Ru complexes. Further studies need to be conducted to properly quantify the products of CO_2 reduction. This system is also ripe for further studies by the Kubiak group.

5.5 References

(1) Benson, E. E.; Kubiak, C. P.; Sathrum, A. J.; Smieja, J. M. *Chem. Soc. Rev.* , **2009**, *38*, 89-99.

(2) Wesselbaum, S.; vom Stein, T.; Klankermayer, J.; Leitner, W. *Angew. Chem., Int. Ed.* , **2012**, *51*, 7499-7502.

(3) Huff, C. A.; Sanford, M. S. *J. Am. Chem. Soc.*, **2011**, *133*, 18122-18125.

(4) Balaraman, E.; Gnanaprakasam, B.; Shimon, L. J. W.; Milstein, D. *J. Am. Chem. Soc.*, **2010**, *132*, 16756-16758.

(5) Zhang, J.; Leitus, G.; Ben-David, Y.; Milstein, D. *Angew. Chem., Int. Ed.*, **2006**, *45*, 1113-1115.

(6) Balaraman, E.; Gunanathan, C.; Zhang, J.; Shimon, L. J. W.; Milstein, D. *Nat. Chem.*, **2011**, *3*, 609-614.

(7) Zhang, J.; Leitus, G.; Ben-David, Y.; Milstein, D. *J. Am. Chem. Soc.*, **2005**, *127*, 10840-10841.

(8) Gunanathan, C.; Ben-David, Y.; Milstein, D. *Science*, **2007**, *317*, 790-792.

(9) Huff, C. A.; Sanford, M. S. *ACS Cat.*, **2013**, *3*, 2412-2416.

(10) Sun, Y.; Koehler, C.; Tan, R.; Annibale, V. T.; Song, D. *Chem. Comm.*, **2011**, *47*, 8349-8351.

(11) Fogler, E.; Balaraman, E.; Ben-David, Y.; Leitus, G.; Shimon, L. J. W.; Milstein, D. *Organometallics*, **2011**, *30*, 3826-3833.

(12) Gunanathan, C.; Milstein, D. *Chem. Rev.* , **2014**, *114*, 12024-12087.

(13) Annibale, V. T.; Song, D. *R. Soc. Chem. Adv.*, **2013**, *3*, 11432-11449.

(14) Caix, C.; Chardon-Noblat, S.; Deronzier, A. *J. Electroanal. Chem.* , **1997**, *434*, 163-170.

(15) Casey, C. P.; Guan, H. *J. Am. Chem. Soc.* , **2007**, *129*, 5816-5817.

(16) Sui-Seng, C.; Haque, F. N.; Hadzovic, A.; Pütz, A.-M.; Reuss, V.; Meyer, N.; Lough, A. J.; Zimmer-De Iuliis, M.; Morris, R. H. *Inorg. Chem.* , **2009**, *48*, 735-743.

(17) Langer, R.; Leitus, G.; Ben-David, Y.; Milstein, D. *Angew. Chem., Int. Ed.* , **2011**, *50*, 2120-2124.

(18) Langer, R.; Diskin-Posner, Y.; Leitus, G.; Shimon, L. J. W.; Ben-David, Y.; Milstein, D. *Angew. Chem., Int. Ed.* , **2011**, *50*, 9948-9952.

(19) Lagaditis, P. O.; Sues, P. E.; Sonnenberg, J. F.; Wan, K. Y.; Lough, A. J.; Morris, R. H. *J. Am. Chem. Soc.* , **2014**, *136*, 1367-1380.

(20) Alberico, E.; Sponholz, P.; Cordes, C.; Nielsen, M.; Drexler, H.-J.; Baumann, W.; Junge, H.; Beller, M. *Angew. Chem., Int. Ed.* , **2013**, *52*, 14162-14166.

(21) Gorgas, N.; Stöger, B.; Veiros, L. F.; Pittenauer, E.; Allmaier, G.; Kirchner, K. *Organometallics*, **2014**, *33*, 6905-6914.

(22) Chakraborty, S.; Dai, H.; Bhattacharya, P.; Fairweather, N. T.; Gibson, M. S.; Krause, J. A.; Guan, H. *J. Am. Chem. Soc.*, **2014**, *136*, 7869-7872.

(23) Zell, T.; Langer, R.; Iron, M. A.; Konstantinovski, L.; Shimon, L. J. W.; Diskin-Posner, Y.; Leitus, G.; Balaraman, E.; Ben-David, Y.; Milstein, D. *Inorg. Chem.* , **2013**, *52*, 9636-9649.

(24) Zhang, L.; Peng, D.; Leng, X.; Huang, Z. *Angew. Chem., Int. Ed.* , **2013**, *52*, 3676-3680.

(25) Zell, T.; Milko, P.; Fillman, K. L.; Diskin-Posner, Y.; Bendikov, T.; Iron, M. A.; Leitus, G.; Ben-David, Y.; Neidig, M. L.; Milstein, D. *Chem. Eur. J.* , **2014**, *20*, 4403-4413.

(26) Kaljurand, I.; Kütt, A.; Sooväli, L.; Rodima, T.; Mäemets, V.; Leito, I.; Koppel, I. A. *J. Org. Chem.* , **2005**, *70*, 1019-1028.

5.6 Appendix

5.6.1 Crystal data for (*t*Bu-PNN)Fe(CO)$_2$ (5)

Compound A14290 crystallizes in the triclinic space group $P\bar{1}$ with one molecule in the asymmetric unit, Z' = 1 and Z = 2. All hydrogen atoms were included into the model at geometrically calculated positions and refined using a riding model. The goodness of fit on F^2 was 1.030 with R1(wR2) = 0.0316(0.0748) for [I>2sigma(I)] and with a largest difference peak and hole of 0.468 and -0.405(e.Å-3).

Table 5-7. Crystal data and structure refinement for (*t*Bu-PNN)Fe(CO)$_2$ (**5**)

Identification code	A14389	
Empirical formula	C21 H27 Fe N2 O2 P	
Formula weight	426.26	
Temperature	100.0 K	
Wavelength	0.71073 Å	
Crystal system	Triclinic	
Space group	P-1	
Unit cell dimensions	a = 8.2855(7) Å	α = 103.429(5)°.
	b = 10.6223(9) Å	β = 101.870(5)°.
	c = 12.2121(11) Å	γ = 98.165(5)°.
Volume	1002.52(15) Å^3	
Z	2	
Density (calculated)	1.412 Mg/m^3	
Absorption coefficient	0.850 mm^{-1}	
F(000)	448	
Crystal size	0.250 x 0.100 x 0.100 mm^3	
Theta range for data collection	1.770 to 36.480°.	
Index ranges	-13<=h<=13, -17<=k<=17, -20<=l<=20	
Reflections collected	48243	
Independent reflections	9777 [R(int) = 0.0448]	
Completeness to theta = 25.000°	99.8 %	
Absorption correction	Semi-empirical from equivalents	
Max. and min. transmission	0.7471 and 0.7028	
Refinement method	Full-matrix least-squares on F^2	
Data / restraints / parameters	9777 / 0 / 250	
Goodness-of-fit on F^2	1.030	
Final R indices [I>2sigma(I)]	R1 = 0.0316, wR2 = 0.0748	
R indices (all data)	R1 = 0.0418, wR2 = 0.0792	
Extinction coefficient	not measured	
Largest diff. peak and hole	0.568 and -0.405 e.Å-3	

Table 5-8. Bond lengths [Å] and angles [°] for (*t*Bu-PNN)Fe(CO)$_2$ (**5**)

Fe(1)-C(20)	1.7521(10)	Fe(1)-C(21)	1.7758(10)
Fe(1)-N(2)	1.9395(8)	Fe(1)-N(1)	1.9438(9)
Fe(1)-P(1)	2.2145(3)	N(1)-C(1)	1.3690(13)
N(1)-C(5)	1.3770(13)	C(1)-C(2)	1.3724(14)
C(1)-H(1)	0.9500	C(2)-C(3)	1.4063(16)
C(2)-H(2)	0.9500	C(3)-C(4)	1.3735(16)
C(3)-H(3)	0.9500	C(4)-C(5)	1.4080(14)
C(4)-H(4)	0.9500	C(5)-C(6)	1.4311(15)
C(6)-N(2)	1.3728(13)	C(6)-C(7)	1.4081(14)
N(2)-C(10)	1.3719(13)	C(7)-C(8)	1.3739(17)
C(7)-H(7)	0.9500	C(8)-C(9)	1.4085(17)
C(8)-H(8)	0.9500	C(9)-C(10)	1.3736(14)
C(9)-H(9)	0.9500	C(10)-C(11)	1.5023(14)
C(11)-P(1)	1.8458(10)	C(11)-H(11A)	0.9900
C(11)-H(11B)	0.9900	P(1)-C(16)	1.8903(10)
P(1)-C(12)	1.8947(10)	C(12)-C(13)	1.5379(15)
C(12)-C(14)	1.5383(15)	C(12)-C(15)	1.5420(14)
C(13)-H(13A)	0.9800	C(13)-H(13B)	0.9800
C(13)-H(13C)	0.9800	C(14)-H(14A)	0.9800
C(14)-H(14B)	0.9800	C(14)-H(14C)	0.9800
C(15)-H(15A)	0.9800	C(15)-H(15B)	0.9800
C(15)-H(15C)	0.9800	C(16)-C(17)	1.5398(15)
C(16)-C(18)	1.5406(14)	C(16)-C(19)	1.5409(15)
C(17)-H(17A)	0.9800	C(17)-H(17B)	0.9800
C(17)-H(17C)	0.9800	C(18)-H(18A)	0.9800
C(18)-H(18B)	0.9800	C(18)-H(18C)	0.9800
C(19)-H(19A)	0.9800	C(19)-H(19B)	0.9800
C(19)-H(19C)	0.9800	C(20)-O(1)	1.1665(12)
C(21)-O(2)	1.1632(13)	C(20)-Fe(1)-C(21)	97.98(5)
C(20)-Fe(1)-N(2)	160.62(4)	C(21)-Fe(1)-N(2)	101.35(4)
C(20)-Fe(1)-N(1)	95.45(4)	C(21)-Fe(1)-N(1)	106.73(4)
N(2)-Fe(1)-N(1)	80.22(4)	C(20)-Fe(1)-P(1)	91.75(3)
C(21)-Fe(1)-P(1)	105.17(3)	N(2)-Fe(1)-P(1)	82.05(3)
N(1)-Fe(1)-P(1)	145.91(3)	C(1)-N(1)-C(5)	116.78(8)
C(1)-N(1)-Fe(1)	126.49(7)	C(5)-N(1)-Fe(1)	116.41(7)
N(1)-C(1)-C(2)	123.50(10)	N(1)-C(1)-H(1)	118.3
C(2)-C(1)-H(1)	118.3	C(1)-C(2)-C(3)	119.40(10)
C(1)-C(2)-H(2)	120.3	C(3)-C(2)-H(2)	120.3

Table 5-8. (cont'd)

C(4)-C(3)-C(2)	118.56(10)	C(4)-C(3)-H(3)	120.7
C(2)-C(3)-H(3)	120.7	C(3)-C(4)-C(5)	119.91(10)
C(3)-C(4)-H(4)	120.0	C(5)-C(4)-H(4)	120.0
N(1)-C(5)-C(4)	121.85(9)	N(1)-C(5)-C(6)	113.11(8)
C(4)-C(5)-C(6)	125.03(9)	N(2)-C(6)-C(7)	121.12(10)
N(2)-C(6)-C(5)	112.71(8)	C(7)-C(6)-C(5)	126.18(9)
C(10)-N(2)-C(6)	118.59(8)	C(10)-N(2)-Fe(1)	124.49(7)
C(6)-N(2)-Fe(1)	116.87(7)	C(8)-C(7)-C(6)	119.52(10)
C(8)-C(7)-H(7)	120.2	C(6)-C(7)-H(7)	120.2
C(7)-C(8)-C(9)	119.07(9)	C(7)-C(8)-H(8)	120.5
C(9)-C(8)-H(8)	120.5	C(10)-C(9)-C(8)	119.79(10)
C(10)-C(9)-H(9)	120.1	C(8)-C(9)-H(9)	120.1
N(2)-C(10)-C(9)	121.70(10)	N(2)-C(10)-C(11)	114.96(8)
C(9)-C(10)-C(11)	123.33(9)	C(10)-C(11)-P(1)	107.95(7)
C(10)-C(11)-H(11A)	110.1	P(1)-C(11)-H(11A)	110.1
C(10)-C(11)-H(11B)	110.1	P(1)-C(11)-H(11B)	110.1
H(11A)-C(11)-H(11B)	108.4	C(11)-P(1)-C(16)	102.77(5)
C(11)-P(1)-C(12)	105.04(5)	C(16)-P(1)-C(12)	110.23(4)
C(11)-P(1)-Fe(1)	100.07(3)	C(16)-P(1)-Fe(1)	122.37(3)
C(12)-P(1)-Fe(1)	113.59(3)	C(13)-C(12)-C(14)	109.81(9)
C(13)-C(12)-C(15)	108.24(9)	C(14)-C(12)-C(15)	107.12(9)
C(13)-C(12)-P(1)	114.87(7)	C(14)-C(12)-P(1)	109.26(7)
C(15)-C(12)-P(1)	107.22(7)	C(12)-C(13)-H(13A)	109.5
C(12)-C(13)-H(13B)	109.5	H(13A)-C(13)-H(13B)	109.5
C(12)-C(13)-H(13C)	109.5	H(13A)-C(13)-H(13C)	109.5
H(13B)-C(13)-H(13C)	109.5	C(12)-C(14)-H(14A)	109.5
C(12)-C(14)-H(14B)	109.5	H(14A)-C(14)-H(14B)	109.5
C(12)-C(14)-H(14C)	109.5	H(14A)-C(14)-H(14C)	109.5
H(14B)-C(14)-H(14C)	109.5	C(12)-C(15)-H(15A)	109.5
C(12)-C(15)-H(15B)	109.5	H(15A)-C(15)-H(15B)	109.5
C(12)-C(15)-H(15C)	109.5	H(15A)-C(15)-H(15C)	109.5
H(15B)-C(15)-H(15C)	109.5	C(17)-C(16)-C(18)	109.47(9)
C(17)-C(16)-C(19)	107.45(9)	C(18)-C(16)-C(19)	107.90(9)
C(17)-C(16)-P(1)	112.59(7)	C(18)-C(16)-P(1)	111.30(7)
C(19)-C(16)-P(1)	107.94(7)	C(16)-C(17)-H(17A)	109.5
C(16)-C(17)-H(17B)	109.5	H(17A)-C(17)-H(17B)	109.5
C(16)-C(17)-H(17C)	109.5	H(17A)-C(17)-H(17C)	109.5
H(17B)-C(17)-H(17C)	109.5	C(16)-C(18)-H(18A)	109.5

Table 5-8. (cont'd)

C(16)-C(18)-H(18B)	109.5	H(18A)-C(18)-H(18B)	109.5
C(16)-C(18)-H(18C)	109.5	H(18A)-C(18)-H(18C)	109.5
H(18B)-C(18)-H(18C)	109.5	C(16)-C(19)-H(19A)	109.5
C(16)-C(19)-H(19B)	109.5	H(19A)-C(19)-H(19B)	109.5
C(16)-C(19)-H(19C)	109.5	H(19A)-C(19)-H(19C)	109.5
H(19B)-C(19)-H(19C)	109.5	O(1)-C(20)-Fe(1)	178.81(10)
O(2)-C(21)-Fe(1)	176.07(9)		

5.6.2 Crystal data for [HFe(*t*Bu-PNN)(CO)$_2$]BF$_4$ (6)

Compound A14339 crystallizes in the monoclinic space group $P2_1$ with one molecule in the asymmetric unit along with one molecule of pentane (Z' = 1 and Z = 2). Two of the CF_3 groups were modeled as two component disorders. All hydrogen atoms were included into the model at geometrically calculated positions and refined using a riding model. The isotropic displacement parameters of all hydrogen atoms were fixed to 1.2 times the *U* value of the atoms they are linked to (1.5 times for methyl groups). All disordered atoms were refined with the help of similarity restraints on the 1,2- and 1,3-distances and displacement parameters as well as rigid bond and enhanced rigid bond restraints for anisotropic displacement parameters.

Table 5-9. Crystal data and structure refinement for [HFe(*t*Bu-PNN)$(CO)_2$]BArF (**6**)

Identification code	A14339	
Empirical formula	C58 H52 B F24 Fe N2 O2 P	
Formula weight	1362.62	
Temperature	100.0 K	
Wavelength	0.71073 Å	
Crystal system	Monoclinic	
Space group	$P2_1$	
Unit cell dimensions	a = 12.2132(7) Å	α = 90°.
	b = 16.0809(9) Å	β = 90.173(3)°.
	c = 15.3134(9) Å	γ = 90°.
Volume	3007.5(3) $Å^3$	
Z	2	
Density (calculated)	1.505 Mg/m^3	
Absorption coefficient	0.395 mm^{-1}	
F(000)	1384	
Crystal size	0.550 x 0.400 x 0.150 mm^3	
Theta range for data collection	1.667 to 36.515°.	
Index ranges	-20<=h<=20, -26<=k<=26, -25<=l<=25	
Reflections collected	145002	
Independent reflections	29329 [R(int) = 0.0399]	
Completeness to theta = 25.000°	99.9 %	
Absorption correction	Semi-empirical from equivalents	
Max. and min. transmission	0.7471 and 0.6877	
Refinement method	Full-matrix least-squares on F^2	
Data / restraints / parameters	29329 / 377 / 887	
Goodness-of-fit on F^2	1.026	
Final R indices [I>2sigma(I)]	R1 = 0.0411, wR2 = 0.1026	
R indices (all data)	R1 = 0.0525, wR2 = 0.1090	
Extinction coefficient	not measured	
Largest diff. peak and hole	0.618 and -0.368 e.Å-3	

Table 5-10. Bond lengths [Å] and angles [°] for [HFe(*t*Bu-PNN)$(CO)_2$]BArF (**6**)

Fe(1)-C(21)	1.768(2)	Fe(1)-C(22)	1.8377(19)
Fe(1)-N(2)	1.9746(15)	Fe(1)-N(1)	1.9866(15)
Fe(1)-P(1)	2.2327(4)	Fe(1)-H(1F)	1.44(3)
C(21)-O(1)	1.144(3)	C(22)-O(2)	1.139(2)
N(1)-C(1)	1.348(2)	N(1)-C(5)	1.357(3)
C(1)-C(2)	1.390(3)	C(1)-H(1)	0.9500
C(2)-C(3)	1.379(4)	C(2)-H(2)	0.9500
C(3)-C(4)	1.394(4)	C(3)-H(3)	0.9500
C(4)-C(5)	1.398(3)	C(4)-H(4)	0.9500
C(5)-C(6)	1.463(3)	N(2)-C(10)	1.347(2)
N(2)-C(6)	1.359(2)	C(6)-C(7)	1.390(3)
C(7)-C(8)	1.382(4)	C(7)-H(7)	0.9500
C(8)-C(9)	1.377(4)	C(8)-H(8)	0.9500
C(9)-C(10)	1.399(3)	C(9)-H(9)	0.9500
C(10)-C(11)	1.499(3)	C(11)-P(1)	1.8465(19)
C(11)-H(11A)	0.9900	C(11)-H(11B)	0.9900
P(1)-C(12)	1.8811(18)	P(1)-C(16)	1.8886(18)
C(12)-C(15)	1.533(3)	C(12)-C(13)	1.542(3)
C(12)-C(14)	1.550(3)	C(13)-H(13A)	0.9800
C(13)-H(13B)	0.9800	C(13)-H(13C)	0.9800
C(14)-H(14A)	0.9800	C(14)-H(14B)	0.9800
C(14)-H(14C)	0.9800	C(15)-H(15A)	0.9800
C(15)-H(15B)	0.9800	C(15)-H(15C)	0.9800
C(16)-C(18)	1.539(3)	C(16)-C(19)	1.540(3)
C(16)-C(17)	1.542(3)	C(17)-H(17A)	0.9800
C(17)-H(17B)	0.9800	C(17)-H(17C)	0.9800
C(18)-H(18A)	0.9800	C(18)-H(18B)	0.9800
C(18)-H(18C)	0.9800	C(19)-H(19A)	0.9800
C(19)-H(19B)	0.9800	C(19)-H(19C)	0.9800
B(1)-C(31)	1.635(2)	B(1)-C(41)	1.642(3)
B(1)-C(51)	1.643(2)	B(1)-C(61)	1.643(2)
C(31)-C(36)	1.403(2)	C(31)-C(32)	1.408(2)
C(32)-C(33)	1.393(2)	C(32)-H(32)	0.9500
C(33)-C(34)	1.390(2)	C(33)-C(37)	1.502(3)
C(37)-F(2)	1.328(3)	C(37)-F(3)	1.330(2)
C(37)-F(1)	1.349(3)	C(34)-C(35)	1.393(3)
C(34)-H(34)	0.9500	C(35)-C(36)	1.400(2)
C(35)-C(38)	1.498(3)	C(38)-F(5)	1.332(3)

Table 5-10. (cont'd)

C(38)-F(4)	1.332(3)	C(38)-F(6)	1.337(3)
C(36)-H(36)	0.9500	C(41)-C(46)	1.402(2)
C(41)-C(42)	1.406(2)	C(42)-C(43)	1.390(2)
C(42)-H(42)	0.9500	C(43)-C(44)	1.392(2)
C(43)-C(47)	1.496(2)	C(47)-F(9)	1.334(2)
C(47)-F(7)	1.341(2)	C(47)-F(8)	1.342(2)
C(44)-C(45)	1.393(2)	C(44)-H(44)	0.9500
C(45)-C(46)	1.395(3)	C(45)-C(48)	1.498(3)
C(48)-F(12)	1.336(2)	C(48)-F(10)	1.340(3)
C(48)-F(11)	1.340(3)	C(46)-H(46)	0.9500
C(51)-C(56)	1.396(2)	C(51)-C(52)	1.404(2)
C(52)-C(53)	1.395(2)	C(52)-H(52)	0.9500
C(53)-C(54)	1.392(3)	C(53)-C(57)	1.503(3)
C(57)-F(14)	1.322(3)	C(57)-F(13)	1.333(2)
C(57)-F(15)	1.334(2)	C(54)-C(55)	1.383(3)
C(54)-H(54)	0.9500	C(55)-C(56)	1.399(3)
C(55)-C(58)	1.497(7)	C(55)-C(58A)	1.527(10)
C(58)-F(17)	1.322(8)	C(58)-F(18)	1.332(7)
C(58)-F(16)	1.346(7)	C(58A)-F(17A)	1.316(10)
C(58A)-F(16A)	1.333(11)	C(58A)-F(18A)	1.350(10)
C(56)-H(56)	0.9500	C(61)-C(66)	1.405(2)
C(61)-C(62)	1.406(2)	C(62)-C(63)	1.390(2)
C(62)-H(62)	0.9500	C(63)-C(64)	1.392(3)
C(63)-C(67)	1.500(3)	C(67)-F(20)	1.309(3)
C(67)-F(21)	1.327(3)	C(67)-F(19)	1.333(3)
C(64)-C(65)	1.394(3)	C(64)-H(64)	0.9500
C(65)-C(66)	1.395(3)	C(65)-C(68A)	1.469(18)
C(65)-C(68)	1.502(5)	C(68)-F(23)	1.307(5)
C(68)-F(24)	1.317(5)	C(68)-F(22)	1.329(5)
C(68A)-F(22A)	1.278(18)	C(68A)-F(24A)	1.288(18)
C(68A)-F(23A)	1.294(18)	C(66)-H(66)	0.9500
C(1S)-C(2S)	1.561(6)	C(1S)-H(1S1)	0.9800
C(1S)-H(1S2)	0.9800	C(1S)-H(1S3)	0.9800
C(2S)-C(3S)	1.499(7)	C(2S)-H(2S1)	0.9900
C(2S)-H(2S2)	0.9900	C(3S)-C(4S)	1.552(6)
C(3S)-H(3S1)	0.9900	C(3S)-H(3S2)	0.9900
C(4S)-C(5S)	1.494(7)	C(4S)-H(4S1)	0.9900
C(4S)-H(4S2)	0.9900	C(5S)-H(5S1)	0.9800

Table 5-10. (cont'd)

C(5S)-H(5S2)	0.9800	C(5S)-H(5S3)	0.9800
C(21)-Fe(1)-C(22)	94.31(9)	C(21)-Fe(1)-N(2)	167.75(8)
C(22)-Fe(1)-N(2)	97.93(7)	C(21)-Fe(1)-N(1)	98.75(8)
C(22)-Fe(1)-N(1)	91.68(7)	N(2)-Fe(1)-N(1)	80.45(6)
C(21)-Fe(1)-P(1)	94.09(6)	C(22)-Fe(1)-P(1)	102.72(6)
N(2)-Fe(1)-P(1)	83.73(4)	N(1)-Fe(1)-P(1)	159.92(5)
C(21)-Fe(1)-H(1F)	80.7(12)	C(22)-Fe(1)-H(1F)	172.9(11)
N(2)-Fe(1)-H(1F)	87.0(12)	N(1)-Fe(1)-H(1F)	84.1(11)
P(1)-Fe(1)-H(1F)	82.8(11)	O(1)-C(21)-Fe(1)	177.6(2)
O(2)-C(22)-Fe(1)	171.65(18)	C(1)-N(1)-C(5)	118.77(16)
C(1)-N(1)-Fe(1)	125.52(14)	C(5)-N(1)-Fe(1)	115.69(12)
N(1)-C(1)-C(2)	122.3(2)	N(1)-C(1)-H(1)	118.9
C(2)-C(1)-H(1)	118.9	C(3)-C(2)-C(1)	119.2(2)
C(3)-C(2)-H(2)	120.4	C(1)-C(2)-H(2)	120.4
C(2)-C(3)-C(4)	119.30(19)	C(2)-C(3)-H(3)	120.4
C(4)-C(3)-H(3)	120.4	C(3)-C(4)-C(5)	118.8(2)
C(3)-C(4)-H(4)	120.6	C(5)-C(4)-H(4)	120.6
N(1)-C(5)-C(4)	121.64(19)	N(1)-C(5)-C(6)	113.86(15)
C(4)-C(5)-C(6)	124.50(19)	C(10)-N(2)-C(6)	119.98(16)
C(10)-N(2)-Fe(1)	123.81(12)	C(6)-N(2)-Fe(1)	116.05(12)
N(2)-C(6)-C(7)	121.21(19)	N(2)-C(6)-C(5)	113.70(15)
C(7)-C(6)-C(5)	125.08(18)	C(8)-C(7)-C(6)	119.0(2)
C(8)-C(7)-H(7)	120.5	C(6)-C(7)-H(7)	120.5
C(9)-C(8)-C(7)	119.64(19)	C(9)-C(8)-H(8)	120.2
C(7)-C(8)-H(8)	120.2	C(8)-C(9)-C(10)	119.6(2)
C(8)-C(9)-H(9)	120.2	C(10)-C(9)-H(9)	120.2
N(2)-C(10)-C(9)	120.53(19)	N(2)-C(10)-C(11)	115.91(15)
C(9)-C(10)-C(11)	123.56(18)	C(10)-C(11)-P(1)	109.22(12)
C(10)-C(11)-H(11A)	109.8	P(1)-C(11)-H(11A)	109.8
C(10)-C(11)-H(11B)	109.8	P(1)-C(11)-H(11B)	109.8
H(11A)-C(11)-H(11B)	108.3	C(11)-P(1)-C(12)	103.35(9)
C(11)-P(1)-C(16)	104.33(9)	C(12)-P(1)-C(16)	111.41(9)
C(11)-P(1)-Fe(1)	99.23(6)	C(12)-P(1)-Fe(1)	122.00(7)
C(16)-P(1)-Fe(1)	113.43(6)	C(15)-C(12)-C(13)	108.1(2)
C(15)-C(12)-C(14)	110.10(19)	C(13)-C(12)-C(14)	107.46(18)
C(15)-C(12)-P(1)	110.13(14)	C(13)-C(12)-P(1)	107.98(13)
C(14)-C(12)-P(1)	112.91(16)	C(12)-C(13)-H(13A)	109.5
C(12)-C(13)-H(13B)	109.5	H(13A)-C(13)-H(13B)	109.5

Table 5-10. (cont'd)

C(12)-C(13)-H(13C)	109.5	H(13A)-C(13)-H(13C)	109.5
H(13B)-C(13)-H(13C)	109.5	C(12)-C(14)-H(14A)	109.5
C(12)-C(14)-H(14B)	109.5	H(14A)-C(14)-H(14B)	109.5
C(12)-C(14)-H(14C)	109.5	H(14A)-C(14)-H(14C)	109.5
H(14B)-C(14)-H(14C)	109.5	C(12)-C(15)-H(15A)	109.5
C(12)-C(15)-H(15B)	109.5	H(15A)-C(15)-H(15B)	109.5
C(12)-C(15)-H(15C)	109.5	H(15A)-C(15)-H(15C)	109.5
H(15B)-C(15)-H(15C)	109.5	C(18)-C(16)-C(19)	108.43(16)
C(18)-C(16)-C(17)	107.01(17)	C(19)-C(16)-C(17)	109.20(16)
C(18)-C(16)-P(1)	108.28(13)	C(19)-C(16)-P(1)	110.72(13)
C(17)-C(16)-P(1)	113.03(13)	C(16)-C(17)-H(17A)	109.5
C(16)-C(17)-H(17B)	109.5	H(17A)-C(17)-H(17B)	109.5
C(16)-C(17)-H(17C)	109.5	H(17A)-C(17)-H(17C)	109.5
H(17B)-C(17)-H(17C)	109.5	C(16)-C(18)-H(18A)	109.5
C(16)-C(18)-H(18B)	109.5	H(18A)-C(18)-H(18B)	109.5
C(16)-C(18)-H(18C)	109.5	H(18A)-C(18)-H(18C)	109.5
H(18B)-C(18)-H(18C)	109.5	C(16)-C(19)-H(19A)	109.5
C(16)-C(19)-H(19B)	109.5	H(19A)-C(19)-H(19B)	109.5
C(16)-C(19)-H(19C)	109.5	H(19A)-C(19)-H(19C)	109.5
H(19B)-C(19)-H(19C)	109.5	C(31)-B(1)-C(41)	104.60(13)
C(31)-B(1)-C(51)	113.99(13)	C(41)-B(1)-C(51)	112.36(13)
C(31)-B(1)-C(61)	110.89(13)	C(41)-B(1)-C(61)	111.62(13)
C(51)-B(1)-C(61)	103.60(13)	C(36)-C(31)-C(32)	115.36(15)
C(36)-C(31)-B(1)	125.09(15)	C(32)-C(31)-B(1)	119.35(14)
C(33)-C(32)-C(31)	122.77(15)	C(33)-C(32)-H(32)	118.6
C(31)-C(32)-H(32)	118.6	C(34)-C(33)-C(32)	120.81(17)
C(34)-C(33)-C(37)	120.80(16)	C(32)-C(33)-C(37)	118.38(15)
F(2)-C(37)-F(3)	108.42(19)	F(2)-C(37)-F(1)	105.13(18)
F(3)-C(37)-F(1)	105.38(18)	F(2)-C(37)-C(33)	112.45(18)
F(3)-C(37)-C(33)	113.13(16)	F(1)-C(37)-C(33)	111.77(16)
C(33)-C(34)-C(35)	117.68(16)	C(33)-C(34)-H(34)	121.2
C(35)-C(34)-H(34)	121.2	C(34)-C(35)-C(36)	121.25(15)
C(34)-C(35)-C(38)	120.15(17)	C(36)-C(35)-C(38)	118.48(17)
F(5)-C(38)-F(4)	106.0(2)	F(5)-C(38)-F(6)	106.9(2)
F(4)-C(38)-F(6)	106.2(2)	F(5)-C(38)-C(35)	112.2(2)
F(4)-C(38)-C(35)	113.63(19)	F(6)-C(38)-C(35)	111.40(19)
C(35)-C(36)-C(31)	122.00(16)	C(35)-C(36)-H(36)	119.0
C(31)-C(36)-H(36)	119.0	C(46)-C(41)-C(42)	115.94(15)

Table 5-10. (cont'd)

C(46)-C(41)-B(1)	123.46(14)	C(42)-C(41)-B(1)	120.38(14)
C(43)-C(42)-C(41)	122.01(15)	C(43)-C(42)-H(42)	119.0
C(41)-C(42)-H(42)	119.0	C(42)-C(43)-C(44)	121.46(15)
C(42)-C(43)-C(47)	119.95(15)	C(44)-C(43)-C(47)	118.57(16)
F(9)-C(47)-F(7)	106.83(17)	F(9)-C(47)-F(8)	106.22(18)
F(7)-C(47)-F(8)	105.80(16)	F(9)-C(47)-C(43)	112.37(16)
F(7)-C(47)-C(43)	112.61(16)	F(8)-C(47)-C(43)	112.52(15)
C(43)-C(44)-C(45)	117.30(16)	C(43)-C(44)-H(44)	121.4
C(45)-C(44)-H(44)	121.4	C(44)-C(45)-C(46)	121.33(15)
C(44)-C(45)-C(48)	118.64(16)	C(46)-C(45)-C(48)	119.93(15)
F(12)-C(48)-F(10)	106.76(19)	F(12)-C(48)-F(11)	106.17(18)
F(10)-C(48)-F(11)	105.77(19)	F(12)-C(48)-C(45)	112.88(17)
F(10)-C(48)-C(45)	112.03(17)	F(11)-C(48)-C(45)	112.71(16)
C(45)-C(46)-C(41)	121.94(15)	C(45)-C(46)-H(46)	119.0
C(41)-C(46)-H(46)	119.0	C(56)-C(51)-C(52)	116.11(15)
C(56)-C(51)-B(1)	122.63(15)	C(52)-C(51)-B(1)	121.03(14)
C(53)-C(52)-C(51)	122.16(16)	C(53)-C(52)-H(52)	118.9
C(51)-C(52)-H(52)	118.9	C(54)-C(53)-C(52)	120.73(17)
C(54)-C(53)-C(57)	120.15(16)	C(52)-C(53)-C(57)	119.12(16)
F(14)-C(57)-F(13)	108.39(19)	F(14)-C(57)-F(15)	106.05(19)
F(13)-C(57)-F(15)	105.71(19)	F(14)-C(57)-C(53)	112.59(18)
F(13)-C(57)-C(53)	111.96(18)	F(15)-C(57)-C(53)	111.73(15)
C(55)-C(54)-C(53)	117.83(16)	C(55)-C(54)-H(54)	121.1
C(53)-C(54)-H(54)	121.1	C(54)-C(55)-C(56)	121.40(16)
C(54)-C(55)-C(58)	115.6(3)	C(56)-C(55)-C(58)	122.7(3)
C(54)-C(55)-C(58A)	125.4(4)	C(56)-C(55)-C(58A)	113.1(4)
F(17)-C(58)-F(18)	106.3(5)	F(17)-C(58)-F(16)	107.1(7)
F(18)-C(58)-F(16)	105.3(6)	F(17)-C(58)-C(55)	112.2(6)
F(18)-C(58)-C(55)	116.2(5)	F(16)-C(58)-C(55)	109.1(4)
F(17A)-C(58A)-F(16A)	108.2(8)	F(17A)-C(58A)-F(18A)	105.6(8)
F(16A)-C(58A)-F(18A)	104.3(8)	F(17A)-C(58A)-C(55)	110.8(7)
F(16A)-C(58A)-C(55)	109.8(8)	F(18A)-C(58A)-C(55)	117.7(6)
C(51)-C(56)-C(55)	121.71(17)	C(51)-C(56)-H(56)	119.1
C(55)-C(56)-H(56)	119.1	C(66)-C(61)-C(62)	116.29(15)
C(66)-C(61)-B(1)	121.83(14)	C(62)-C(61)-B(1)	121.61(15)
C(63)-C(62)-C(61)	121.72(16)	C(63)-C(62)-H(62)	119.1
C(61)-C(62)-H(62)	119.1	C(62)-C(63)-C(64)	121.39(16)
C(62)-C(63)-C(67)	120.64(17)	C(64)-C(63)-C(67)	117.96(17)

Table 5-10. (cont'd)

F(20)-C(67)-F(21)	108.4(2)	F(20)-C(67)-F(19)	104.8(3)
F(21)-C(67)-F(19)	105.0(2)	F(20)-C(67)-C(63)	113.04(19)
F(21)-C(67)-C(63)	113.92(17)	F(19)-C(67)-C(63)	111.02(19)
C(63)-C(64)-C(65)	117.79(16)	C(63)-C(64)-H(64)	121.1
C(65)-C(64)-H(64)	121.1	C(64)-C(65)-C(66)	120.92(17)
C(64)-C(65)-C(68A)	118.7(8)	C(66)-C(65)-C(68A)	120.4(8)
C(64)-C(65)-C(68)	118.4(2)	C(66)-C(65)-C(68)	120.7(2)
F(23)-C(68)-F(24)	106.1(4)	F(23)-C(68)-F(22)	105.5(5)
F(24)-C(68)-F(22)	105.6(4)	F(23)-C(68)-C(65)	114.2(3)
F(24)-C(68)-C(65)	112.7(4)	F(22)-C(68)-C(65)	111.9(3)
F(22A)-C(68A)-F(24A)	111.5(19)	F(22A)-C(68A)-F(23A)	109.3(19)
F(24A)-C(68A)-F(23A)	96.3(16)	F(22A)-C(68A)-C(65)	111.2(13)
F(24A)-C(68A)-C(65)	111.8(14)	F(23A)-C(68A)-C(65)	115.9(15)
C(65)-C(66)-C(61)	121.88(15)	C(65)-C(66)-H(66)	119.1
C(61)-C(66)-H(66)	119.1	C(2S)-C(1S)-H(1S1)	109.5
C(2S)-C(1S)-H(1S2)	109.5	H(1S1)-C(1S)-H(1S2)	109.5
C(2S)-C(1S)-H(1S3)	109.5	H(1S1)-C(1S)-H(1S3)	109.5
H(1S2)-C(1S)-H(1S3)	109.5	C(3S)-C(2S)-C(1S)	112.6(4)
C(3S)-C(2S)-H(2S1)	109.1	C(1S)-C(2S)-H(2S1)	109.1
C(3S)-C(2S)-H(2S2)	109.1	C(1S)-C(2S)-H(2S2)	109.1
H(2S1)-C(2S)-H(2S2)	107.8	C(2S)-C(3S)-C(4S)	114.9(3)
C(2S)-C(3S)-H(3S1)	108.5	C(4S)-C(3S)-H(3S1)	108.5
C(2S)-C(3S)-H(3S2)	108.5	C(4S)-C(3S)-H(3S2)	108.5
H(3S1)-C(3S)-H(3S2)	107.5	C(5S)-C(4S)-C(3S)	113.7(3)
C(5S)-C(4S)-H(4S1)	108.8	C(3S)-C(4S)-H(4S1)	108.8
C(5S)-C(4S)-H(4S2)	108.8	C(3S)-C(4S)-H(4S2)	108.8
H(4S1)-C(4S)-H(4S2)	107.7	C(4S)-C(5S)-H(5S1)	109.5
C(4S)-C(5S)-H(5S2)	109.5	H(5S1)-C(5S)-H(5S2)	109.5
C(4S)-C(5S)-H(5S3)	109.5	H(5S1)-C(5S)-H(5S3)	109.5
H(5S2)-C(5S)-H(5S3)	109.5		

5.6.3 Crystal data for [Fe(*t*Bu-PNN)(CO)$_2$ACN](BF$_4$)$_2$ (7)

Compound P15038 crystallizes in the triclinic space group *P*-1 with two molecules in the asymmetric unit along with four molecules of BF_4^- and 2.5 molecules of dichloromethane. All BF_4^- anions and dichloromethane molecules were disordered over two positions. One of the

dichloromethane molecules was located near a crystallographic inversion center. All hydrogen atoms were included into the model at geometrically calculated positions and refined using a riding model. The isotropic displacement parameters of all hydrogen atoms were fixed to 1.2 times the *U* value of the atoms they are linked to (1.5 times for methyl groups). All disordered atoms were refined with the help of similarity restraints on the 1,2- and 1,3-distances and displacement parameters as well as enhanced rigid bond restraints for anisotropic displacement parameters.

Table 5-11. Crystal data and structure refinement for [Fe(*t*Bu-PNN)(CO)$_2$ACN](BF$_4$)$_2$ (**7**)

Identification code	P15038	
Empirical formula	C24.25 H32.50 B2 Cl2.50 F8 Fe N3 O2 P	
Formula weight	747.10	
Temperature	100.0 K	
Wavelength	0.71073 Å	
Crystal system	Triclinic	
Space group	P-1	
Unit cell dimensions	a = 11.4402(8) Å	α = 112.280(2)°.
	b = 17.2140(13) Å	β = 99.602(2)°.
	c = 18.5907(14) Å	γ = 101.707(2)°.
Volume	3159.0(4) Å^3	
Z	4	
Density (calculated)	1.553 Mg/m^3	
Absorption coefficient	0.807 mm^{-1}	
F(000)	1522	
Crystal size	0.200 x 0.200 x 0.100 mm^3	
Theta range for data collection	2.196 to 30.508°.	
Index ranges	-16<=h<=16, -24<=k<=24, -26<=l<=26	
Reflections collected	152098	
Independent reflections	19509 [R(int) = 0.0439]	
Completeness to theta = 25.000°	99.8 %	
Absorption correction	Semi-empirical from equivalents	
Max. and min. transmission	0.7465 and 0.6860	
Refinement method	Full-matrix least-squares on F^2	
Data / restraints / parameters	19509 / 2111 / 1056	
Goodness-of-fit on F^2	1.039	
Final R indices [I>2sigma(I)]	R1 = 0.0656, wR2 = 0.1716	
R indices (all data)	R1 = 0.0884, wR2 = 0.1866	
Extinction coefficient	not measured	
Largest diff. peak and hole	1.557 and -1.054 e.Å-3	

Table 5-12. Bond lengths [Å] and angles [°] for [Fe(*t*Bu-PNN)$(CO)_2$ACN]$(BF_4)_2$ (**7**)

Fe(1)-C(21)	1.796(3)	Fe(1)-C(20)	1.819(3)
Fe(1)-N(3)	1.957(2)	Fe(1)-N(2)	1.974(2)
Fe(1)-N(1)	2.012(2)	Fe(1)-P(1)	2.3102(8)
N(1)-C(1)	1.339(4)	N(1)-C(5)	1.355(3)
C(1)-C(2)	1.399(5)	C(1)-H(1)	0.9500
C(2)-C(3)	1.371(6)	C(2)-H(2)	0.9500
C(3)-C(4)	1.367(5)	C(3)-H(3)	0.9500
C(4)-C(5)	1.388(4)	C(4)-H(4)	0.9500
C(5)-C(6)	1.465(4)	C(6)-N(2)	1.348(4)
C(6)-C(7)	1.387(4)	N(2)-C(10)	1.349(4)
C(7)-C(8)	1.378(6)	C(7)-H(7)	0.9500
C(8)-C(9)	1.376(6)	C(8)-H(8)	0.9500
C(9)-C(10)	1.387(5)	C(9)-H(9)	0.9500
C(10)-C(11)	1.492(5)	C(11)-P(1)	1.829(4)
C(11)-H(11A)	0.9900	C(11)-H(11B)	0.9900
P(1)-C(12)	1.876(3)	P(1)-C(16)	1.890(3)
C(12)-C(15)	1.527(5)	C(12)-C(14)	1.528(6)
C(12)-C(13)	1.549(6)	C(13)-H(13A)	0.9800
C(13)-H(13B)	0.9800	C(13)-H(13C)	0.9800
C(14)-H(14A)	0.9800	C(14)-H(14B)	0.9800
C(14)-H(14C)	0.9800	C(15)-H(15A)	0.9800
C(15)-H(15B)	0.9800	C(15)-H(15C)	0.9800
C(16)-C(19)	1.537(6)	C(16)-C(17)	1.543(5)
C(16)-C(18)	1.544(6)	C(17)-H(17A)	0.9800
C(17)-H(17B)	0.9800	C(17)-H(17C)	0.9800
C(18)-H(18A)	0.9800	C(18)-H(18B)	0.9800
C(18)-H(18C)	0.9800	C(19)-H(19A)	0.9800
C(19)-H(19B)	0.9800	C(19)-H(19C)	0.9800
O(1)-C(20)	1.134(4)	O(2)-C(21)	1.129(3)
N(3)-C(22)	1.130(4)	C(22)-C(23)	1.459(4)
C(23)-H(23A)	0.9800	C(23)-H(23B)	0.9800
C(23)-H(23C)	0.9800	Fe(2)-C(120)	1.805(3)
Fe(2)-C(121)	1.817(3)	Fe(2)-N(103)	1.952(3)
Fe(2)-N(102)	1.973(2)	Fe(2)-N(101)	1.998(3)
Fe(2)-P(2)	2.2896(8)	N(101)-C(101)	1.343(4)
N(101)-C(105)	1.352(4)	C(101)-C(102)	1.370(6)
C(101)-H(101)	0.9500	C(102)-C(103)	1.368(7)
C(102)-H(102)	0.9500	C(103)-C(104)	1.390(5)

Table 5-12. (cont'd)

C(103)-H(103)	0.9500	C(104)-C(105)	1.391(4)
C(104)-H(104)	0.9500	C(105)-C(106)	1.466(4)
C(106)-N(102)	1.360(3)	C(106)-C(107)	1.378(4)
N(102)-C(110)	1.343(3)	C(107)-C(108)	1.386(4)
C(107)-H(107)	0.9500	C(108)-C(109)	1.387(4)
C(108)-H(108)	0.9500	C(109)-C(110)	1.384(4)
C(109)-H(109)	0.9500	C(110)-C(111)	1.499(4)
C(111)-P(2)	1.831(3)	C(111)-H(11C)	0.9900
C(111)-H(11D)	0.9900	P(2)-C(112)	1.878(3)
P(2)-C(116)	1.882(3)	C(112)-C(114)	1.534(4)
C(112)-C(115)	1.546(4)	C(112)-C(113)	1.548(4)
C(113)-H(11E)	0.9800	C(113)-H(11F)	0.9800
C(113)-H(11G)	0.9800	C(114)-H(11H)	0.9800
C(114)-H(11I)	0.9800	C(114)-H(11J)	0.9800
C(115)-H(11K)	0.9800	C(115)-H(11L)	0.9800
C(115)-H(11M)	0.9800	C(116)-C(117)	1.539(5)
C(116)-C(118)	1.540(5)	C(116)-C(119)	1.540(5)
C(117)-H(11N)	0.9800	C(117)-H(11O)	0.9800
C(117)-H(11P)	0.9800	C(118)-H(11Q)	0.9800
C(118)-H(11R)	0.9800	C(118)-H(11S)	0.9800
C(119)-H(11T)	0.9800	C(119)-H(11U)	0.9800
C(119)-H(11V)	0.9800	O(101)-C(120)	1.128(4)
O(102)-C(121)	1.131(4)	N(103)-C(122)	1.130(4)
C(122)-C(123)	1.446(5)	C(123)-H(12A)	0.9800
C(123)-H(12B)	0.9800	C(123)-H(12C)	0.9800
B(1)-F(11)	1.375(7)	B(1)-F(13)	1.383(7)
B(1)-F(14)	1.390(8)	B(1)-F(12)	1.392(8)
B(1A)-F(14A)	1.358(12)	B(1A)-F(12A)	1.359(12)
B(1A)-F(11A)	1.360(12)	B(1A)-F(13A)	1.360(12)
B(2)-F(24)	1.372(9)	B(2)-F(21)	1.375(9)
B(2)-F(22)	1.391(8)	B(2)-F(23)	1.394(8)
B(2A)-F(21A)	1.351(12)	B(2A)-F(24A)	1.358(11)
B(2A)-F(22A)	1.376(12)	B(2A)-F(23A)	1.383(12)
B(3)-F(34)	1.362(6)	B(3)-F(31)	1.378(6)
B(3)-F(32)	1.387(6)	B(3)-F(33)	1.387(7)
B(3A)-F(34A)	1.368(12)	B(3A)-F(32A)	1.375(12)
B(3A)-F(33A)	1.376(12)	B(3A)-F(31A)	1.378(12)
B(4)-F(43)	1.317(9)	B(4)-F(44)	1.383(9)

Table 5-12. (cont'd)

B(4)-F(42)	1.387(8)	B(4)-F(41)	1.393(7)
B(4A)-F(44A)	1.340(10)	B(4A)-F(41A)	1.363(11)
B(4A)-F(43A)	1.375(9)	B(4A)-F(42A)	1.384(12)
C(1S)-Cl(2S)	1.702(12)	C(1S)-Cl(1S)	1.741(12)
C(1S)-H(1S1)	0.9900	C(1S)-H(1S2)	0.9900
C(1T)-Cl(2T)	1.721(10)	C(1T)-Cl(1T)	1.794(13)
C(1T)-H(1T1)	0.9900	C(1T)-H(1T2)	0.9900
C(2S)-Cl(4S)	1.639(9)	C(2S)-Cl(3S)	1.719(8)
C(2S)-H(2S1)	0.9900	C(2S)-H(2S2)	0.9900
C(2T)-Cl(3T)	1.767(15)	C(2T)-Cl(4T)	1.797(15)
C(2T)-H(2T1)	0.9900	C(2T)-H(2T2)	0.9900
C(3S)-Cl(6S)	1.691(8)	C(3S)-Cl(5S)	1.725(8)
C(3S)-H(3S1)	0.9900	C(3S)-H(3S2)	0.9900
C(21)-Fe(1)-C(20)	91.78(12)	C(21)-Fe(1)-N(3)	172.25(10)
C(20)-Fe(1)-N(3)	88.47(11)	C(21)-Fe(1)-N(2)	83.94(10)
C(20)-Fe(1)-N(2)	175.72(11)	N(3)-Fe(1)-N(2)	95.77(10)
C(21)-Fe(1)-N(1)	90.33(10)	C(20)-Fe(1)-N(1)	99.56(11)
N(3)-Fe(1)-N(1)	81.99(9)	N(2)-Fe(1)-N(1)	80.55(9)
C(21)-Fe(1)-P(1)	93.80(8)	C(20)-Fe(1)-P(1)	97.11(10)
N(3)-Fe(1)-P(1)	93.86(7)	N(2)-Fe(1)-P(1)	83.17(7)
N(1)-Fe(1)-P(1)	162.69(7)	C(1)-N(1)-C(5)	118.3(2)
C(1)-N(1)-Fe(1)	126.9(2)	C(5)-N(1)-Fe(1)	113.91(17)
N(1)-C(1)-C(2)	121.0(3)	N(1)-C(1)-H(1)	119.5
C(2)-C(1)-H(1)	119.5	C(3)-C(2)-C(1)	120.3(3)
C(3)-C(2)-H(2)	119.9	C(1)-C(2)-H(2)	119.9
C(4)-C(3)-C(2)	119.0(3)	C(4)-C(3)-H(3)	120.5
C(2)-C(3)-H(3)	120.5	C(3)-C(4)-C(5)	118.8(3)
C(3)-C(4)-H(4)	120.6	C(5)-C(4)-H(4)	120.6
N(1)-C(5)-C(4)	122.7(3)	N(1)-C(5)-C(6)	114.3(2)
C(4)-C(5)-C(6)	123.0(3)	N(2)-C(6)-C(7)	121.7(3)
N(2)-C(6)-C(5)	113.8(2)	C(7)-C(6)-C(5)	124.3(3)
C(6)-N(2)-C(10)	120.3(3)	C(6)-N(2)-Fe(1)	116.20(18)
C(10)-N(2)-Fe(1)	122.9(2)	C(8)-C(7)-C(6)	118.1(3)
C(8)-C(7)-H(7)	121.0	C(6)-C(7)-H(7)	121.0
C(9)-C(8)-C(7)	120.3(3)	C(9)-C(8)-H(8)	119.9
C(7)-C(8)-H(8)	119.9	C(8)-C(9)-C(10)	119.6(3)
C(8)-C(9)-H(9)	120.2	C(10)-C(9)-H(9)	120.2
N(2)-C(10)-C(9)	120.1(3)	N(2)-C(10)-C(11)	117.2(3)

Table 5-12. (cont'd)

C(9)-C(10)-C(11)	122.5(3)	C(10)-C(11)-P(1)	110.9(2)
C(10)-C(11)-H(11A)	109.5	P(1)-C(11)-H(11A)	109.5
C(10)-C(11)-H(11B)	109.5	P(1)-C(11)-H(11B)	109.5
H(11A)-C(11)-H(11B)	108.0	C(11)-P(1)-C(12)	105.33(17)
C(11)-P(1)-C(16)	104.83(18)	C(12)-P(1)-C(16)	111.06(16)
C(11)-P(1)-Fe(1)	97.25(11)	C(12)-P(1)-Fe(1)	119.39(12)
C(16)-P(1)-Fe(1)	116.12(10)	C(15)-C(12)-C(14)	106.4(3)
C(15)-C(12)-C(13)	108.6(4)	C(14)-C(12)-C(13)	110.5(3)
C(15)-C(12)-P(1)	108.6(2)	C(14)-C(12)-P(1)	112.6(3)
C(13)-C(12)-P(1)	110.0(2)	C(12)-C(13)-H(13A)	109.5
C(12)-C(13)-H(13B)	109.5	H(13A)-C(13)-H(13B)	109.5
C(12)-C(13)-H(13C)	109.5	H(13A)-C(13)-H(13C)	109.5
H(13B)-C(13)-H(13C)	109.5	C(12)-C(14)-H(14A)	109.5
C(12)-C(14)-H(14B)	109.5	H(14A)-C(14)-H(14B)	109.5
C(12)-C(14)-H(14C)	109.5	H(14A)-C(14)-H(14C)	109.5
H(14B)-C(14)-H(14C)	109.5	C(12)-C(15)-H(15A)	109.5
C(12)-C(15)-H(15B)	109.5	H(15A)-C(15)-H(15B)	109.5
C(12)-C(15)-H(15C)	109.5	H(15A)-C(15)-H(15C)	109.5
H(15B)-C(15)-H(15C)	109.5	C(19)-C(16)-C(17)	106.5(4)
C(19)-C(16)-C(18)	111.6(3)	C(17)-C(16)-C(18)	108.8(4)
C(19)-C(16)-P(1)	106.6(3)	C(17)-C(16)-P(1)	112.1(3)
C(18)-C(16)-P(1)	111.2(3)	C(16)-C(17)-H(17A)	109.5
C(16)-C(17)-H(17B)	109.5	H(17A)-C(17)-H(17B)	109.5
C(16)-C(17)-H(17C)	109.5	H(17A)-C(17)-H(17C)	109.5
H(17B)-C(17)-H(17C)	109.5	C(16)-C(18)-H(18A)	109.5
C(16)-C(18)-H(18B)	109.5	H(18A)-C(18)-H(18B)	109.5
C(16)-C(18)-H(18C)	109.5	H(18A)-C(18)-H(18C)	109.5
H(18B)-C(18)-H(18C)	109.5	C(16)-C(19)-H(19A)	109.5
C(16)-C(19)-H(19B)	109.5	H(19A)-C(19)-H(19B)	109.5
C(16)-C(19)-H(19C)	109.5	H(19A)-C(19)-H(19C)	109.5
H(19B)-C(19)-H(19C)	109.5	O(1)-C(20)-Fe(1)	178.7(3)
O(2)-C(21)-Fe(1)	173.2(2)	C(22)-N(3)-Fe(1)	171.2(2)
N(3)-C(22)-C(23)	177.7(3)	C(22)-C(23)-H(23A)	109.5
C(22)-C(23)-H(23B)	109.5	H(23A)-C(23)-H(23B)	109.5
C(22)-C(23)-H(23C)	109.5	H(23A)-C(23)-H(23C)	109.5
H(23B)-C(23)-H(23C)	109.5	C(120)-Fe(2)-C(121)	93.02(15)
C(120)-Fe(2)-N(103)	169.36(12)	C(121)-Fe(2)-N(103)	87.21(13)
C(120)-Fe(2)-N(102)	89.36(12)	C(121)-Fe(2)-N(102)	176.69(11)

Table 5-12. (cont'd)

N(103)-Fe(2)-N(102)	90.87(9)	C(120)-Fe(2)-N(101)	86.91(12)
C(121)-Fe(2)-N(101)	101.85(13)	N(103)-Fe(2)-N(101)	82.64(10)
N(102)-Fe(2)-N(101)	80.56(10)	C(120)-Fe(2)-P(2)	95.44(10)
C(121)-Fe(2)-P(2)	93.85(11)	N(103)-Fe(2)-P(2)	95.16(7)
N(102)-Fe(2)-P(2)	83.63(7)	N(101)-Fe(2)-P(2)	164.00(8)
C(101)-N(101)-C(105)	119.6(3)	C(101)-N(101)-Fe(2)	125.4(3)
C(105)-N(101)-Fe(2)	114.55(19)	N(101)-C(101)-C(102)	121.3(4)
N(101)-C(101)-H(101)	119.4	C(102)-C(101)-H(101)	119.4
C(103)-C(102)-C(101)	120.1(4)	C(103)-C(102)-H(102)	119.9
C(101)-C(102)-H(102)	119.9	C(102)-C(103)-C(104)	119.4(3)
C(102)-C(103)-H(103)	120.3	C(104)-C(103)-H(103)	120.3
C(103)-C(104)-C(105)	118.2(3)	C(103)-C(104)-H(104)	120.9
C(105)-C(104)-H(104)	120.9	N(101)-C(105)-C(104)	121.4(3)
N(101)-C(105)-C(106)	114.7(2)	C(104)-C(105)-C(106)	124.0(3)
N(102)-C(106)-C(107)	121.0(3)	N(102)-C(106)-C(105)	113.2(2)
C(107)-C(106)-C(105)	125.8(2)	C(110)-N(102)-C(106)	120.4(2)
C(110)-N(102)-Fe(2)	123.59(17)	C(106)-N(102)-Fe(2)	115.94(18)
C(106)-C(107)-C(108)	118.8(2)	C(106)-C(107)-H(107)	120.6
C(108)-C(107)-H(107)	120.6	C(107)-C(108)-C(109)	119.6(3)
C(107)-C(108)-H(108)	120.2	C(109)-C(108)-H(108)	120.2
C(110)-C(109)-C(108)	119.4(3)	C(110)-C(109)-H(109)	120.3
C(108)-C(109)-H(109)	120.3	N(102)-C(110)-C(109)	120.4(2)
N(102)-C(110)-C(111)	116.0(2)	C(109)-C(110)-C(111)	123.5(2)
C(110)-C(111)-P(2)	109.82(19)	C(110)-C(111)-H(11C)	109.7
P(2)-C(111)-H(11C)	109.7	C(110)-C(111)-H(11D)	109.7
P(2)-C(111)-H(11D)	109.7	H(11C)-C(111)-H(11D)	108.2
C(111)-P(2)-C(112)	104.52(12)	C(111)-P(2)-C(116)	105.29(16)
C(112)-P(2)-C(116)	111.00(14)	C(111)-P(2)-Fe(2)	97.78(9)
C(112)-P(2)-Fe(2)	116.06(10)	C(116)-P(2)-Fe(2)	119.36(10)
C(114)-C(112)-C(115)	108.2(2)	C(114)-C(112)-C(113)	105.9(2)
C(115)-C(112)-C(113)	111.0(3)	C(114)-C(112)-P(2)	113.1(2)
C(115)-C(112)-P(2)	110.73(18)	C(113)-C(112)-P(2)	107.74(17)
C(112)-C(113)-H(11E)	109.5	C(112)-C(113)-H(11F)	109.5
H(11E)-C(113)-H(11F)	109.5	C(112)-C(113)-H(11G)	109.5
H(11E)-C(113)-H(11G)	109.5	H(11F)-C(113)-H(11G)	109.5
C(112)-C(114)-H(11H)	109.5	C(112)-C(114)-H(11I)	109.5
H(11H)-C(114)-H(11I)	109.5	C(112)-C(114)-H(11J)	109.5
H(11H)-C(114)-H(11J)	109.5	H(11I)-C(114)-H(11J)	109.5

Table 5-12. (cont'd)

C(112)-C(115)-H(11K)	109.5	C(112)-C(115)-H(11L)	109.5
H(11K)-C(115)-H(11L)	109.5	C(112)-C(115)-H(11M)	109.5
H(11K)-C(115)-H(11M)	109.5	H(11L)-C(115)-H(11M)	109.5
C(117)-C(116)-C(118)	107.5(3)	C(117)-C(116)-C(119)	111.4(3)
C(118)-C(116)-C(119)	107.1(3)	C(117)-C(116)-P(2)	109.7(3)
C(118)-C(116)-P(2)	109.7(2)	C(119)-C(116)-P(2)	111.3(2)
C(116)-C(117)-H(11N)	109.5	C(116)-C(117)-H(11O)	109.5
H(11N)-C(117)-H(11O)	109.5	C(116)-C(117)-H(11P)	109.5
H(11N)-C(117)-H(11P)	109.5	H(11O)-C(117)-H(11P)	109.5
C(116)-C(118)-H(11Q)	109.5	C(116)-C(118)-H(11R)	109.5
H(11Q)-C(118)-H(11R)	109.5	C(116)-C(118)-H(11S)	109.5
H(11Q)-C(118)-H(11S)	109.5	H(11R)-C(118)-H(11S)	109.5
C(116)-C(119)-H(11T)	109.5	C(116)-C(119)-H(11U)	109.5
H(11T)-C(119)-H(11U)	109.5	C(116)-C(119)-H(11V)	109.5
H(11T)-C(119)-H(11V)	109.5	H(11U)-C(119)-H(11V)	109.5
O(101)-C(120)-Fe(2)	171.8(3)	O(102)-C(121)-Fe(2)	175.6(3)
C(122)-N(103)-Fe(2)	172.0(2)	N(103)-C(122)-C(123)	175.9(3)
C(122)-C(123)-H(12A)	109.5	C(122)-C(123)-H(12B)	109.5
H(12A)-C(123)-H(12B)	109.5	C(122)-C(123)-H(12C)	109.5
H(12A)-C(123)-H(12C)	109.5	H(12B)-C(123)-H(12C)	109.5
F(11)-B(1)-F(13)	110.7(7)	F(11)-B(1)-F(14)	107.0(7)
F(13)-B(1)-F(14)	106.4(6)	F(11)-B(1)-F(12)	105.7(7)
F(13)-B(1)-F(12)	104.4(6)	F(14)-B(1)-F(12)	122.4(7)
F(14A)-B(1A)-F(12A)	92.5(12)	F(14A)-B(1A)-F(11A)	105.1(11)
F(12A)-B(1A)-F(11A)	125.1(15)	F(14A)-B(1A)-F(13A)	113.6(12)
F(12A)-B(1A)-F(13A)	110.8(13)	F(11A)-B(1A)-F(13A)	108.5(12)
F(24)-B(2)-F(21)	103.7(9)	F(24)-B(2)-F(22)	108.9(8)
F(21)-B(2)-F(22)	116.3(10)	F(24)-B(2)-F(23)	103.4(9)
F(21)-B(2)-F(23)	113.1(9)	F(22)-B(2)-F(23)	110.4(9)
F(21A)-B(2A)-F(24A)	118.9(14)	F(21A)-B(2A)-F(22A)	98.3(13)
F(24A)-B(2A)-F(22A)	108.4(11)	F(21A)-B(2A)-F(23A)	107.7(13)
F(24A)-B(2A)-F(23A)	114.7(14)	F(22A)-B(2A)-F(23A)	107.1(13)
F(34)-B(3)-F(31)	109.5(5)	F(34)-B(3)-F(32)	109.4(5)
F(31)-B(3)-F(32)	108.8(5)	F(34)-B(3)-F(33)	110.0(5)
F(31)-B(3)-F(33)	109.4(5)	F(32)-B(3)-F(33)	109.7(5)
F(34A)-B(3A)-F(32A)	110.1(10)	F(34A)-B(3A)-F(33A)	109.9(11)
F(32A)-B(3A)-F(33A)	111.4(10)	F(34A)-B(3A)-F(31A)	105.8(11)
F(32A)-B(3A)-F(31A)	110.7(11)	F(33A)-B(3A)-F(31A)	108.8(10)

Table 5-12. (cont'd)

F(43)-B(4)-F(44)	115.1(8)	F(43)-B(4)-F(42)	109.6(8)
F(44)-B(4)-F(42)	104.9(6)	F(43)-B(4)-F(41)	109.9(8)
F(44)-B(4)-F(41)	109.0(7)	F(42)-B(4)-F(41)	107.9(6)
F(44A)-B(4A)-F(41A)	113.7(11)	F(44A)-B(4A)-F(43A)	114.4(8)
F(41A)-B(4A)-F(43A)	111.5(10)	F(44A)-B(4A)-F(42A)	102.2(9)
F(41A)-B(4A)-F(42A)	107.9(11)	F(43A)-B(4A)-F(42A)	106.3(9)
Cl(2S)-C(1S)-Cl(1S)	105.7(8)	Cl(2S)-C(1S)-H(1S1)	110.6
Cl(1S)-C(1S)-H(1S1)	110.6	Cl(2S)-C(1S)-H(1S2)	110.6
Cl(1S)-C(1S)-H(1S2)	110.6	H(1S1)-C(1S)-H(1S2)	108.7
Cl(2T)-C(1T)-Cl(1T)	110.7(9)	Cl(2T)-C(1T)-H(1T1)	109.5
Cl(1T)-C(1T)-H(1T1)	109.5	Cl(2T)-C(1T)-H(1T2)	109.5
Cl(1T)-C(1T)-H(1T2)	109.5	H(1T1)-C(1T)-H(1T2)	108.1
Cl(4S)-C(2S)-Cl(3S)	106.2(5)	Cl(4S)-C(2S)-H(2S1)	110.5
Cl(3S)-C(2S)-H(2S1)	110.5	Cl(4S)-C(2S)-H(2S2)	110.5
Cl(3S)-C(2S)-H(2S2)	110.5	H(2S1)-C(2S)-H(2S2)	108.7
Cl(3T)-C(2T)-Cl(4T)	108.7(11)	Cl(3T)-C(2T)-H(2T1)	110.0
Cl(4T)-C(2T)-H(2T1)	110.0	Cl(3T)-C(2T)-H(2T2)	110.0
Cl(4T)-C(2T)-H(2T2)	110.0	H(2T1)-C(2T)-H(2T2)	108.3
Cl(6S)-C(3S)-Cl(5S)	117.5(6)	Cl(6S)-C(3S)-H(3S1)	107.9
Cl(5S)-C(3S)-H(3S1)	107.9	Cl(6S)-C(3S)-H(3S2)	107.9
Cl(5S)-C(3S)-H(3S2)	107.9	H(3S1)-C(3S)-H(3S2)	107.2